

**Summary Report
of the Annual Clay Minerals Society Meeting
Santa Fe, New Mexico
June 2–7, 2007**

Report Number DOE/ER/15873

The annual Clay Minerals Society meeting was back on US soil this year, after a very successful visit to France in June of 2006. Randall Cygan and his team (George Guthrie Jeffery Greathouse, and Dewey Moore) hosted the 44th annual meeting, with some 180 delegates, in beautiful Santa Fe, an historic city which lies about an hour north of Albuquerque in New Mexico. Santa Fe and La Fonda, the hotel where the conference was held, have long histories dating back to the early Spanish settlers. There has been a hostelry of some shape or form on the La Fonda site since the early 17th century, and Santa Fe is the oldest state capitol in the United States.

Every CMS meeting has a number of aspects to it. This year, in addition to the numerous topical oral and poster sessions, we held a workshop, two field trips, a number of events for accompanying persons, as well as a number of administrative events.

The scientific sessions kicked off on Monday morning with words of welcome from the mayor of Santa Fe, from the President of the Society, Richard Brown, and from Randall Cygan (who did a vox pop on knowledge of Santa Fe—it is very important that you know whether you prefer red or green chiles in your food when ordering at any of the many eateries in Santa Fe), but it was clear to all present that the most rousing welcome to the meeting was given by a local group of Native American dancers. Ranging in age from 6 to 18, they provided the perfect backdrop to the opening talk by Paul Schroeder, recipient of the “Marion L. and Chrystie M. Jackson Mid-career Clay Scientist Award”, introduced by Ray Ferrell (“Life at the Edge: Clay mineralogy, microbiology and the International Kamchatka Microbial Observatory”). Paul gave a most enjoyable talk, beginning with a discourse on the challenges involved in working in Kamchatka, with an international, interdisciplinary group of scientists.

The “Pioneer in Clay Science” lecture was given by Spencer G. Lucas. Among many fine talks delivered during the conference, another highlight was “A two-decade review of polymer-clay nanocomposites” by A. Okada and A. Usuki.

Sessions

Sessions on the topics below, followed over three days:

Clays as Nanomaterials

Carbon Sequestration and Stabilization by Clays

Clays and Environmental Processes

Clays in Oil Shale and Kerogen-bearing Sediments

Clays in Soils and Sediments

Clays and Archeology

Clays in Extreme Environments

Characterizing Clay Minerals
Zeolites
Molecular Simulations of Clays

Workshop

As is customary, there was a Workshop on Sunday. This had the title ‘Carbon Stabilization by Clays in the Environment: Process and Characterization Methods”, and was organised by David Laird and Javiera Cervini-Silva. The convenors will edit a special volume arising out of the workshop, and David Laird has agreed to act as editor of the series while this one volume passes through the system.

Field trips

There were field trips to the Cerrillos Hills and Espanola Basin (held on both the Saturday and the Thursday). These were lead by Dewey Moore (George Austin, Steve Chipera, Shelley Roberts and David Vaniman helped to organize them), who was ably assisted by Paul Nadeau, who had done his doctoral thesis research in the area.

There was also a visit to the Harding pegmatite (once the primary source of beryllium for the United States). There was also a demonstration in the art of making adobe bricks, a skill first imparted by the Moors to the Spanish, and subsequently by the Spanish to the Pueblo people.

There were guided tours to the Los Alamos and Bandelier National Monument and to the Taos and northern New Mexico.

CMS administration

Several administrative groups meet during the annual conference. These include the Executive Committee, the Council, and the Editorial Board for the journal. Much of the nuts-and-bolts policy decisions for the next year are hammered out at these meetings which are an essential part of the Society. Michelle Johnson, from the CMS office, attended her first annual meeting. She manned the CMS booth and so had the opportunity to meet many of the members and others attending the meeting. There is a list of new appointments to important positions within the Society, including a new Editor-in-Chief for the journal, Joe Stucki, and a new Treasurer, Reed Glassman.

Sustaining members

The Society’s Sustaining Members were sustained with a luncheon event during the meeting. As always, this was a very pleasant event with both red and green chile present on the lunch plates. Another special luncheon was held for the past presidents of the society later in the week.

Students

There was a special reception for students held on Monday. CMS recognizes the importance of today’s students in its future, and seeks to encourage their development in the subject. This was also achieved by the award of travel grants to several of those attending the meeting.

Attendance

How many people were at meeting: Total = 181 (excludes guests)

Members	98 (excludes students)
Non-members	53 (excludes students)
Students	30 (25 CMS members; 5 non-members)
Significant others	29
Government	57
Academics	95 (includes students)
Industry	29

Meeting Web Page

<http://www.sandia.gov/clay/>

Enchanted Clays

**44th Annual Meeting of The Clay Minerals Society
Santa Fe, New Mexico, USA
June 2-7, 2007**

Organizing Committee

Randall T. Cygan, Chair, Sandia National Laboratories
Jeffery A. Greathouse, Sandia National Laboratories
George D. Guthrie, Los Alamos National Laboratory
Duane M. Moore, University of New Mexico

Field Trips

Duane M. Moore, Chair, University of New Mexico
George S. Austin, New Mexico Institute of Mining and Technology
Steve J. Chipera, Los Alamos National Laboratory
Shelley Roberts, University New Mexico
David T. Vaniman, Los Alamos National Laboratory

Workshop

Javiera Cervini-Silva, Universidad Nacional Autónoma de México
David A. Laird, National Soil Tilth Laboratory, Iowa State University

Abstracts

Louise J. Criscenti, Sandia National Laboratories
Carolyn L. Kirby, Sandia National Laboratories

Registration

Taunja Blair Osborn, Sandia National Laboratories

Web Site and Publications Design

Mona L. Aragon, Sandia National Laboratories

Computer Programming Support
Frances L. Kanipe, Sandia National Laboratories

Society Administration
Michelle Johnson, The Clay Minerals Society
J. Alexander Speer, Mineralogical Society of America

Session Chairs

Gary W. Beall, Texas State University
David L. Bish, Indiana University
Eric Blinman, Museum of New Mexico
John D. Bloch, University of New Mexico
J. William Carey, Los Alamos National Laboratory
Javiera Cervini-Silva, Universidad Nacional Autónoma de México
Steve J. Chipera, Los Alamos National Laboratory
Louise J. Criscenti, Sandia National Laboratories
Randall T. Cygan, Sandia National Laboratories
Heather M. Dion, Los Alamos National Laboratory
W. Crawford Elliot, Georgia State University
Jeffery A. Greathouse, Sandia National Laboratories
Hendrik Heinz, University of Akron
Martin J. Kennedy, University of California at Riverside
David A. Laird, National Soil Tilth Laboratory
Douglas K. McCarty, Chevron Energy Technology Company
Duane M. Moore, University of New Mexico
Philip S. Neuhoff, University of Florida
Roberto T. Pabalan, Southwest Research Institute
Peter C. Ryan, Middlebury College
Paul A. Schroeder, University of Georgia
Brian J. Teppen, Michigan State University
David T. Vaniman, Los Alamos National Laboratory

Sponsors

Chevron Energy Technology Company	Thiele Kaolin Company
H. H. Murray and Associates	University of New Mexico
Sandia National Laboratories	U.S. Department of Energy, Office of Science
Los Alamos National Laboratory	Wyo-Ben, Incorporated
St. Cloud Mining Company	

The Clay Minerals Society



President: Richard K. Brown, Wyo-Ben, Incorporated

Vice President: Ray E. Ferrell, Jr., Louisiana State University

Secretary: Warren D. Huff, University of Cincinnati

Treasurer: Andrew R. Thomas, Chevron Energy Technology Company

Editor-in-Chief, *Clays and Clay Minerals*:

Derek C. Bain, Macaulay Institute

Council:

James E. Amonette, Pacific Northwest National Laboratory

Christopher Breen, Sheffield Hallam University

Heather M. Dion, Los Alamos National Laboratory

Stephen J. Hillier, Macaulay Institute

Victoria C. Hover, University of Louisiana at Lafayette

Richard W. Lahann, Indiana University

Sridhar Komarneni, Pennsylvania State University

James D. Kubicki, Pennsylvania State University

Douglas K. McCarty, Chevron Energy Technology Company

Patricia A. Maurice, University of Notre Dame

Michael A. Velbel, Michigan State University

Lynda B. Williams, Arizona State University

Society Manager:

Michelle Johnson

The Clay Minerals Society

3635 Concorde Parkway, Suite 500

Chantilly, Virginia 20151-1125, USA

Phone: 703-652-9960

Fax: 703-652-9951

E-mail: cms@clays.org

The Clay Minerals Society

The Clay Minerals Society began as the Clay Mineral Committee of the National Academy of Sciences-National Research Council in 1952, in response to the need for a formal way to hold national clay conferences. By 1962, the Clay Minerals Committee had become strong enough to stand on its own, and The Clay Minerals Society was incorporated. From 1952 to 1964, proceedings of the annual conference were published. The journal *Clays and Clay Minerals* was first published in 1964.

The primary purpose of The Clay Minerals Society is to stimulate research and to disseminate information relating to all aspects of clay science and technology. Through its conferences and publications, the Society offers individuals a means of following the many-sided growth of the clay sciences and of meeting fellow scientists with widely different backgrounds and interests.

The primary activities of The Clay Minerals Society consist of publication of the bimonthly journal *Clays and Clay Minerals*, organization of the annual meeting, workshop, and field trips, awarding student research and travel grants, publication of a workshop lecture series, slide sets, and special publications, the providing of clays for research purposes through the Source Clays Repository, and publication of the society newsletter in the bimonthly *Elements*. Various committees within the Society deal also with such matters as regulatory issues, Eastern European liaison, and nomenclature. The Society also maintains a list server dedicated to increasing world-wide communications pertaining to clay minerals.

The membership of The Clay Minerals Society is a diverse group because the study of clay touches upon so many fields. Members include clay mineralogists, crystallographers, physicists, chemists, geochemists, soil scientists, agronomists, ceramic scientists, civil engineers, petroleum geologists and engineers, and industrial scientists in fields involving products ranging from catalysts to cat litter. The Society has about one thousand members, a third of whom represent countries outside the United States.

Awards given by the Society include the Marilyn and Sturges W. Bailey Award, the George W. Brindley Lecture, the Pioneer in Clay Science Lecture, and the Marion L. and Chrystie M. Jackson Mid-Career Clay Scientist Award. Awards are also presented for student papers and posters at the annual conference. Student research grants totaling \$10,000 per year are awarded.

The CMS Workshop Lectures Series includes *Quantitative Mineral Analysis of Clays*, *Electron-Optical Methods in Clay Science*, *Thermal Analysis in Clay Science*, *Clay-Water Interface and its Rheological Implications*, *Computer Applications to X-Ray Powder Diffraction Analysis of Clay Minerals*, *Layer Charge Characteristics of 2:1 Silicate Clay Minerals*, *Scanning Probe Microscopy of Clay Minerals*, *Organic Pollutants in the Environment*, *Synchrotron X-Ray Methods in Clay Science*, *Teaching Clay Science*, *Electrochemical Properties of Clays*, *Molecular Modeling of Clays and Mineral Surfaces*, *The Application of Vibrational Spectroscopy to Clay Minerals and Layered Double Hydroxides*, and *Methods for Study of Microbe-Mineral Interactions*. The Society also publishes various conference proceedings, annual abstract volumes, and other research and educational publications

Sustaining Contributors

Sustaining Benefactors

ExxonMobil Upstream Research Company
Southern Clay Products, Incorporated

Sustaining Patrons

American Colloid Company
Chevron Energy Technology Company
IMERYS
Nestlé Purina Golden Products Division
Thiele Kaolin Company

Sustaining Members

Burgess Pigment Company
Halliburton Energy Services
H. H. Murray and Associates
Oil-Dri Corporation of America
Wyo-Ben, Incorporated

Individual Sustaining Members

David L. Bish	Phoebe Hauff
Richard K. Brown	Wayne H. Hudnall
Randall T. Cygan	William D. Johns
Eric J. Daniels	Blair F. Jones
Joe B. Dixon	George H. Kacandes
Steven B. Feldman	Jessica Elzea Kogel
Will P. Gates	Duane M. Moore
J. Reed Glasmann	Kenneth M. Towe
Stephen Guggenheim	Don M. Triplehorn
Necip Güven	Charles E. Weaver

Funders of the Marilyn and Sturges W. Bailey Distinguished Member Award

Linda Bailey and David Bailey

Funders of the Marion L. and Chrystie M. Jackson Mid-Career Clay Scientist Award

Marion L. and Chrystie M. Jackson

Awards

Marilyn and Sturges W. Bailey Distinguished Member Award

The Marilyn and Sturges W. Bailey Distinguished Member is the highest honor of the Clay Minerals Society for scientific eminence as represented primarily by publication of outstanding original scientific research and by the impact of this research on the clay sciences. Technical contribution to clay science is the sole criterion for the award. Service to the Society, teaching, and administrative accomplishments are not to be considered.

Distinguished Members

1968 – Ralph E. Grim
1969 – Clarence S. Ross
1970 – Paul F. Kerr
1971 – Walter D. Keller
1972 – George W. Brindley
1975 – William F. Bradley
1975 – Sturges W. Bailey
1975 – José J. Fripiat
1977 – Marion L. Jackson
1979 – Toshio Sudo
1980 – Haydn H. Murray
1984 – C. Edmund Marshall
1985 – Charles E. Weaver
1988 – Max M. Mortland
1989 – Robert C. Reynolds, Jr.
1990 – Joe L. White

1990 – John Hower
1991 – Joe B. Dixon
1992 – Philip F. Low
1993 – Thomas J. Pinnavaia
1995 – William D. Johns
1996 – Victor Drits
1997 – Udo Schwertmann
1998 – Brij L. Sawhney

Bailey Distinguished Members

2000 – Boris B. Zvyagin
2001 – Keith Norrish
2002 – Gehard Lagaly
2004 – Benny K.G. Theng
2005 – M. Jeff Wilson
2006 – Frederick J. Wicks

Marion L. and Chrystie M. Jackson Mid-Career Clay Scientist Award

The Marion L. and Chrystie M. Jackson Mid-Career Clay Scientist Award recognizes mid-career scientists for excellence in the contribution of new knowledge to clay minerals science through original and scholarly research. The awardee must be between the ages of 39 and 60 years.

Jackson Awardees

1992 – Joseph W. Stucki
1993 – Jan Środoń
1994 – Stephen Guggenheim
1995 – David L. Bish
1996 – Darrell G. Schulze
1997 – Jerry M. Bigham
1998 – Murray B. McBride
1999 – Stephen A. Boyd

2000 – Jillian F. Banfield
2001 – Cliff T. Johnston
2002 – Sridhar Komarneni
2003 – Peter Komadel
2004 – Fred J. Longstaffe
2005 – Samuel J. Traina
2006 – J. Theo Kloprogge
2007 – Paul A. Schroeder

George W. Brindley Lecture

The George W. Brindley Lecture recognizes a clay scientist who will infuse the society with new ideas, someone who is both a dynamic speaker and involved in innovative research. Dr. Brindley himself approved the concept of the lecture, and the speaker should deliver a lecture that Brindley himself would applaud. The Brindley Lecturer is asked to submit a manuscript for publication in *Clays and Clay Minerals* that will serve as a convenient and permanent record of his/her contribution.

Brindley Lecturers

1984 – Walter D. Keller	1995 – Gerhard Lagaly
1985 – José J. Fripiat	1996 – Samuel M. Savin
1986 – Ralph E. Grim	1997 – Paul H. Nadeau
1987 – Sturges W. Bailey	1998 – Bruce Velde
1988 – Marion L. Jackson	1999 – Richard A. Eggleton
1989 – William D. Johns	2000 – Duane M. Moore
1990 – Alain Baronnet	2001 – Robert A. Schoonheydt
1991 – Thomas J. Pinnavaia	2002 – David L. Bish
1992 – Philip F. Low	2003 – Alain Manceau
1993 – Dennis D. Eberl	2005 – Maria Franca Brigatti
1994 – Robert C. Reynolds, Jr.	

Pioneer in Clay Science Lecture

The Pioneer in Clay Science Lecture recognizes research contributions that have led to important new directions in clay minerals science and technology. The awarded is selected by the local organizing committee of the Society Annual Meeting at which the award will be presented.

Pioneer Lecturers

1987 – Marion L. Jackson	1998 – Robert C. Reynolds, Jr.
1988 – Richard M. Barrer	1999 – Victor Colin Farmer
1989 – H. van Olphen	2000 – William F. Moll
1990 – John W. Jordan	2001 – Don Scafe
1991 – Charles E. Weaver	2002 – Victor Drits
1992 – Udo Schwertmann	2003 – Vernon J. Hurst
1993 – Linus Pauling	2004 – Hideomi Kodama
1994 – Joe L. White	2005 – Jillian F. Banfield
1995 – Rustom Roy	2006 – Jean-Maurice Cases
1996 – Max M. Mortland	2007 – Spencer G. Lucas
1997 – Koji Wada	

Citation of Special Recognition

1984 – Richards A. Rowland

1984 – Ada Swineford

1991 – Frederick A. Mumpton

1994 – Kenneth M. Towe

1996 – Don Scafe

2003 – William D. Johns

Editors of *Clays and Clay Minerals*

1952	J. A. Pash and M. D. Turner
1953	Ada Swineford and Norman Plummer
1954	W. O. Milligan
1955-1961	Ada Swineford
1962-1964	William F. Bradley
1964-1969	Sturges W. Bailey
1970-1972	Max M. Mortland
1973-1974	William T. Granquist
1975-1978	Richards A. Rowland
1979-1990	Frederick A. Mumpton
1990-1991	Kenneth M. Towe
1991-1995	Ray E. Ferrell, Jr.
1995-1998	Wayne H. Hudnall
1999-2000	Stephen Guggenheim
2000-present	Derek C. Bain

Field Trips for Professionals

Cerrillos Hills and Española Basin

Saturday June 2 and repeated on Thursday June 7, full-day trip

Meet at 7:30 AM in front of La Fonda on San Francisco Street just west of hotel parking garage

In the morning, we will travel about 15 miles southeast of Santa Fe to examine the relation between the intrusions forming the Cerrillos Hills and their contacts with the smectite-rich Mancos Shale. We will also consider the economic and social aspects of these intrusions that have produced turquoise from at least 600 BCE as well as lead, zinc, and silver. In the afternoon, we will travel north to the Española Basin to examine ash beds that are units of the Santa Fe Group, ashes from explosive volcanism in the Jemez Mountains immediately to the west. Here we will puzzle our way through alteration of the volcanic ashes to clay minerals and zeolites, which seems to be releasing uranium into the local groundwaters as uranyl carbonates with values ranging from less than 1 $\mu\text{g/L}$ to as high as 1820 $\mu\text{g/L}$. As for the general geology of this area, the Cerrillos Hills are part of a string of intrusions that make a boundary between the Española Basin and the Albuquerque Basin. Both basins are members of a series of basins from the Upper Arkansas graben in central Colorado to the New Mexico-Texas border. These basins, which collectively form the Rio Grande rift, are filled mostly with Miocene sediments. They were initially isolated and drained internally until the basins relatively recently (~1 Ma) cut through the divides and established a through-going drainage. If you would like to learn more: Chapin and Cather (1994) Tectonic Setting of the Axial Basins of the Northern and Central Rio Grande Rift; in Keller and Cather, editors, *Basins of the Rio Grande Rift*, Geological Society of America Special Paper 291, pp. 5-25.

Harding Pegmatite and Adobe Demonstration

Tuesday June 5, half-day trip

Meet at 7:30 AM in front of La Fonda on San Francisco Street just west of hotel parking garage

The morning field trip will focus on the famous Harding pegmatite mine on the west slope of the Sangre de Cristo Mountains, just south of Taos. At one time this pegmatite was the primary source of beryllium for the United States. The Earth and Planetary Sciences Department of the University of New Mexico, to whom the mine belongs, welcomes you to take a modest amount of sample. The host rock for the pegmatite is a micaceous schist that weathers to a micaceous clay, and is often used by some of the Pueblo potters. Depending on conditions, samples of this clay may be available. We have arranged a demonstration of the production of adobe bricks, a building material introduced to the Spanish by the Moors from northern Africa and then introduced to the Pueblo people by the Spanish. We will travel one way through small northern New Mexican villages settled in the 17th century as part of the Spanish empire: Chimayó, Truchas (where Robert Redford's film *The Milagro Beanfield War* was made), Chamisal, Peñasco, Dixon, Embudo, and return along the Rio Grande. If time allows, we will stop at one of New Mexico's wineries.

Guided Tours for Guests

Los Alamos and Bandelier National Monument

Monday June 4

Meet at 9:00 AM in front of La Fonda on San Francisco Street just west of hotel parking garage

You will explore Bandelier National Monument with optional hiking along a one-mile trail to see ancient Native American ruins and climb up to cliff dwellings. A picnic lunch at a Los Alamos park is included. You will also visit two museums in Los Alamos: the Los Alamos Historical Museum and the Bradbury Science Museum, focusing on the Manhattan Project and current science initiatives in the Los Alamos National Laboratory. We will leave at 9:00 AM from La Fonda and return to the hotel by 5:00 PM. This trip will be lead by Shelley Roberts, who was born and raised in Los Alamos.

Taos and Northern New Mexico

Wednesday June 6

Meet at 9:00 AM in front of La Fonda on San Francisco Street just west of hotel parking garage

This trip will take you to Taos by one scenic route and return by another. We will leave from La Fonda at 9:00 AM and return to the hotel by about 5:00 PM. In between, we hope to visit the Taos Pueblo which has no regular schedule, so we will take our chances. There are many art galleries and shops, and the Kit Carson Museum, to be seen in Taos proper. We will visit the Santuario de Chimayo, the Ortega Weavers in Chimayo, pass through Truchas (which provided the background for Robert Redford's movie *The Milagro Beanfield War*), and perhaps visit one of New Mexico's wineries. Individual camera permits for visiting the scenic Taos Pueblo are \$5 (not included in trip costs). Lunch in Taos will be on your own.

A Brief History of Santa Fe

In 1598, Santa Fe was the northernmost settlement along the Camino Real, the “Royal Road” from Mexico City. The city itself was founded as a city of New Spain in 1610 and its official name is “La Villa Real de la Santa Fe de San Francisco de Assisi” or “The Royal City of the Holy Faith of Saint Francis of Assisi.” This historic city was designed in the tradition of Spanish style around a central plaza which, by 1829, was the end of the Santa Fe Trail. Santa Fe is the oldest state capital in the United States, founded in 1610, and at one time all lands west of the Mississippi River were governed from the Palace of the Governors on the Santa Fe Plaza. Since the 1800s, Santa Fe has been the home of three distinct cultures: Native American, Hispanic, and Anglo. The city’s architecture reflects these tri-cultural influences as does the music, food, and art. Adobe homes, red and green chiles, mariachis, pueblo pottery, and cutting-edge art all coexist in a remarkable display.

Facts and Fables about Santa Fe—Altitude Makes a Difference

Fable: Santa Fe is a desert resort like Palm Springs, California. Wear sandals and skimpy clothes all year round.

Fact: We live in the high desert. We have seasons. That means it gets cold—very cold. That also means it gets hot—very hot . . . but we have low humidity so it is very comfortable here even when it is hot. Dress comfortably and casually. Bring layers and be prepared for wide fluctuations in temperatures, especially when the sun sets.

Fable: Don’t drink the water. You’ll get sick.

Fact: You are in New Mexico, not Old Mexico. The humidity is low and it gets very dry. Dehydration is a common problem. Drink water until you can’t stand it anymore, go to the bathroom, and then drink some more water. Bottled water is the best purchase you will make while here; keep the bottle and keep adding water.

Fable: You are away from home and it’s time to party. Drink as though you are at sea level.

Fact: You are in the foothills of the Rocky Mountains at 7,000 plus feet. Alcohol has a much larger impact at higher elevations so don’t say you weren’t warned. Most drinks will feel like a double. So as your conscience says, “don’t drink too much, don’t eat too much, and don’t forget your sunscreen.” But you also get an excuse not to exercise strenuously until you adjust. That’s not a bad tradeoff.

Fable: The old ruts in the roads and the uneven sidewalks date back to when wagons came west on the Old Santa Fe Trail.

Fact: This is the “City Different” and some things are just the way they are because they are. The sidewalks are awful (but they lead to great places) so pack comfortable shoes that can take abuse. The ruts are probably in the roads to slow people down. It doesn’t work.

A Brief History of La Fonda

From our Spanish to English dictionary: Fonda, s.f., inn, tavern (hostelereia). The venue for our meeting has had no name at times, as in “the inn at the end of the trail.” Its exact origins are obscure, but there’s reason to believe that there was some sort of inn on the present site of our modern La Fonda at approximately the time Santa Fe was founded in 1610, when the region that is now New Mexico was still a province of Spain. The Camino Real (King’s Road), now San Francisco Street, ran past what is now the front door and stretched southward to El Paso and on to Chihuahua. And it was just an inn without a name in 1822 when William Becknell arrived in the plaza as the first person to make the trek along what would become the Santa Fe Trail. He was pleased to find comfortable lodging and hospitality at this unnamed inn. The first identifiable operators were William and Mary Donoho (? to 1837) when it was known simply as “La Fonda Americana,” implying “the hotel where the Americans stayed.” Ownership between the Donohos and shortly after 1846 is unclear. Then Frank Green and Thomas Bowler took charge and called it the Exchange Hotel. For most of its early history (1822 to ~1900), an important part of its attraction was drinking, billiards, cards, and other forms of gambling. General Stephen Kearny, upon arrival with his conquering army in 1846, threw a large ball in the inn’s main hall. The Exchange went into decline in the early part of the 20th century and was closed for a few years. During the 1921-22, it was completely rebuilt in the Pueblo-Spanish style and at this time assumed its current name, La Fonda. It was acquired by the Atchison, Topeka, and Santa Fe Railroad, which leased it to Fred Harvey. Until 1969, it was one of the famous Harvey Houses associated with the Santa Fe Railroad. Since 1968, La Fonda has been locally owned and operated. Literally the inn at the end of the Santa Fe Trail, La Fonda still occupies the southeast corner of the Plaza where travelers of all descriptions have been welcomed for almost 400 years, and now you’re one of them. (M. Simmons, 1996, *The Old Trail to Santa Fe*, University of New Mexico Press)

Attractions in the Santa Fe Area

Brief descriptions and maps for self-guided tours are available at the CMS meeting office located in the Stiha Room on the upper level of La Fonda, or visit the La Fonda's concierge for additional information and brochures. You may want to consider the following self-guided tours prepared especially for CMS attendees:

- Walking Tour of Santa Fe I
- Walking Tour of Santa Fe II
- Santa Fe's Museum Hill
- A Visit to the Valles Caldera
- The Hot Springs of Ojo Caliente
- O'Keeffe Country: Chama River Valley and Ghost Ranch
- The Kasha-Katuwe Tent Rocks National Monument
- The Story of Turquoise: Cerrillos, Madrid, and Albuquerque
- Albuquerque, Tram Ride, Old Town, and the Balloon Museum
- A Visit to Acoma, the Sky City

You can also make arrangements to participate in numerous adventure activities, including:

Biking

Biking in Santa Fe can be rugged and wild or a calm ride on a quiet, paved road. Taking to the trails on two wheels is a wonderful way to see the state's numerous national and state parks and forests. New Mexico State Parks Division at 505-827-7465; USDA Forest Service at 505-842-3294; National Park Service at 505-988-6430.

Bird Watching

In addition to great bird-watching in the nearby wilderness areas, the Randall Davey Audubon Center offers 135 acres that provide safe habitat for birds, plants, and animals. Ranging from common to rare, approximately 130 species of birds can be found in or over the various ecosystems of this sanctuary.

Cross-Country and Downhill Skiing (when you return in winter)

New Mexico has more than nine million acres of national forest, and cross-country skiers are taking more and more to the back country where the snow is deep, the views spectacular and the solitude revitalizing. Visit Ski New Mexico on the web for more information. Downhill skiing is just a 25-minute drive from La Fonda at the Santa Fe Ski Area. Visit Ski Santa Fe on the web or call 505-982-4429.

Fishing

North of Santa Fe in the upper mountains near Taos and Chama are great places for fly fishing, and mountain trout are plentiful. Local lakes are stocked with trout and freshwater salmon. In the Pecos River, about 45 miles from Santa Fe, trout are plentiful and fly fishing is consistently

good. Fishing requires a license, available at hunting and fishing stores in the state. Visit New Mexico Department of Tourism Activities & Outdoor Recreation on the web, or call New Mexico Game and Fish at 505-827-7911.

Golf

Santa Fe has great golfing in naturally beautiful surroundings; at least five public courses are an easy drive from La Fonda. Golfers who are unaccustomed to higher altitudes will be thrilled with their driving where the air is so thin that golf balls sail into the air and down the fairway at great distance.

Hiking

Hiking trails are numerous for all levels of hikers, from easy trails to more rigorous climbs. For more information visit New Mexico Department of Tourism Activities & Outdoor Recreation on the web, or contact the National Forest Service at 505-842-3292, or the Bureau of Land Management at 505-438-7400.

Horseback Riding

Within New Mexico are more than 4,000 miles of designated horse trails on public land such as national forests and state parks. For more information visit New Mexico Department of Tourism Activities & Outdoor Recreation on the web or call the National Park Service at 505-988-6430. In and around Santa Fe several facilities offer guided trail tours on horseback and others offer longer wilderness excursions. Check with La Fonda's concierge for brochures.

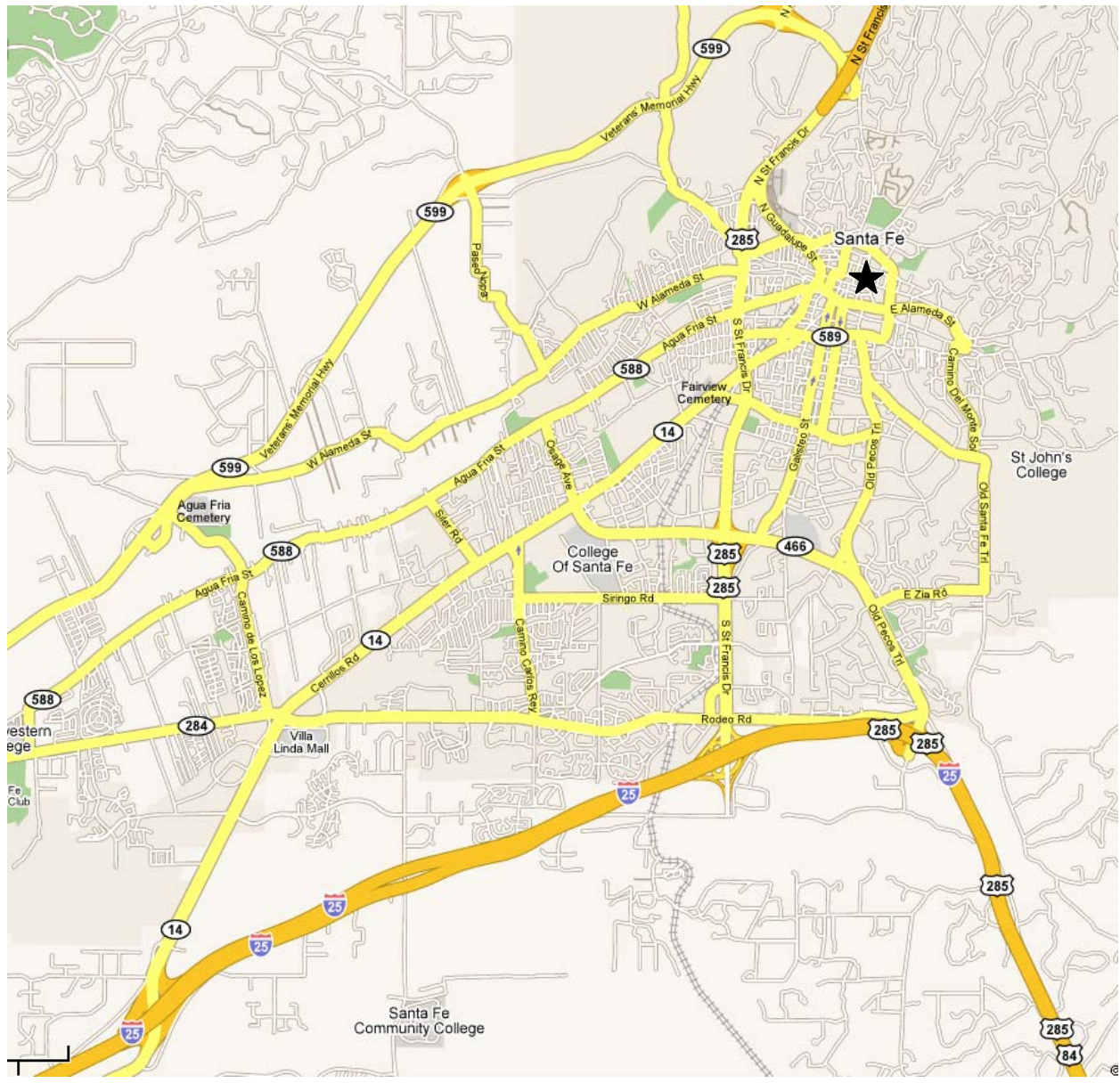
Rafting, Canoeing, Kayaking

Snow melting off the mountains make spring and summer rafting, canoeing and kayaking popular, with trips available from Santa Fe, Taos and Chama. Rafting opportunities range from calm and placid to class-four whitewater thrills on the Rio Grande and the Rio Chama. Visit New Mexico Department of Tourism Activities & Outdoor Recreation on the web.

Other activities available include: sailplane soaring among the clouds, early morning hot-air ballooning, boating in no-wake lakes, and rock climbing, running, swimming and tennis.

Map of Santa Fe Area

To Taos (~90 minute drive)

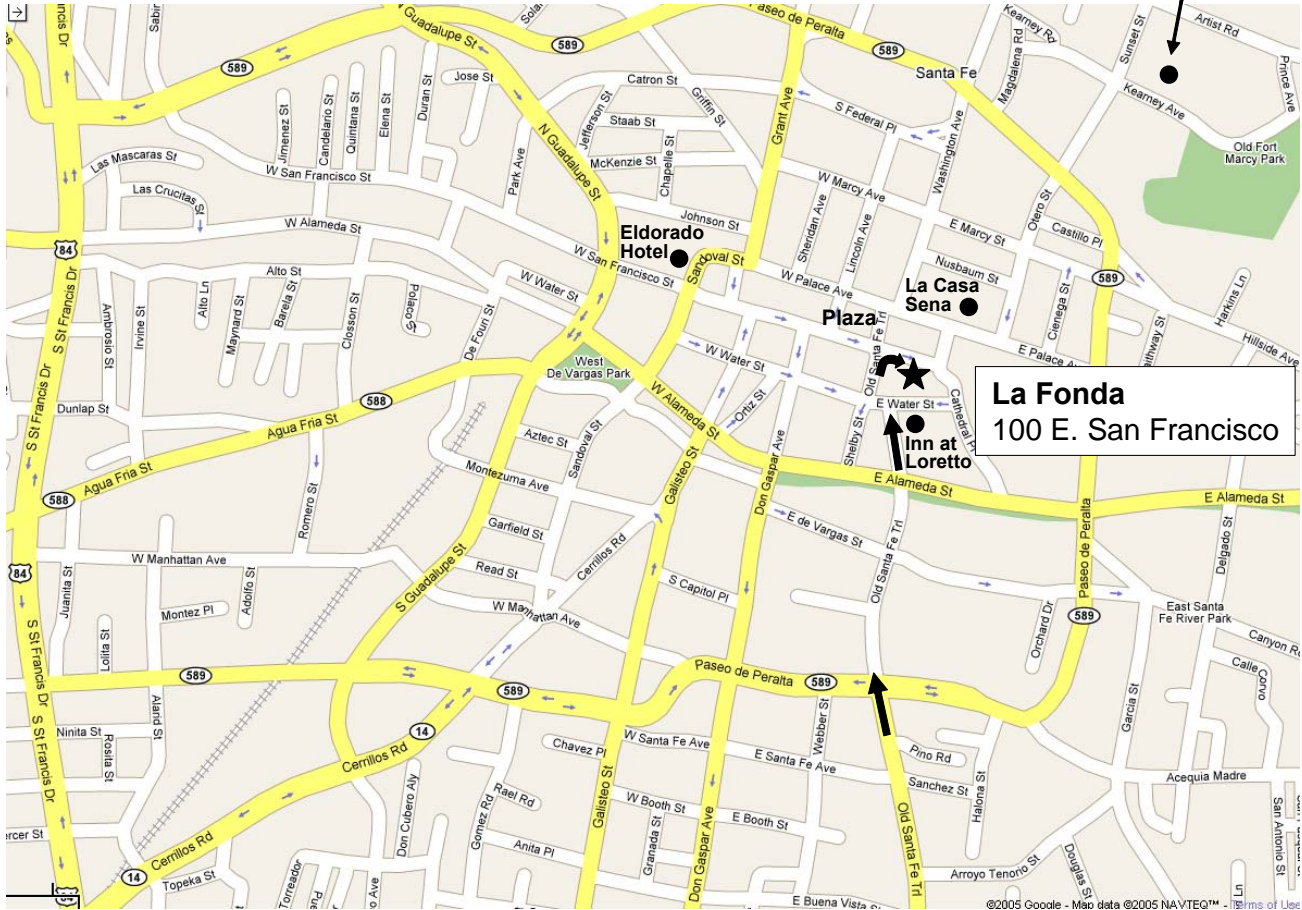


To Albuquerque (~50 minute drive)

To Denver (~6 hours)

Map of Downtown Santa Fe

Fort Marcy Hotel Suites
320 Artist Road

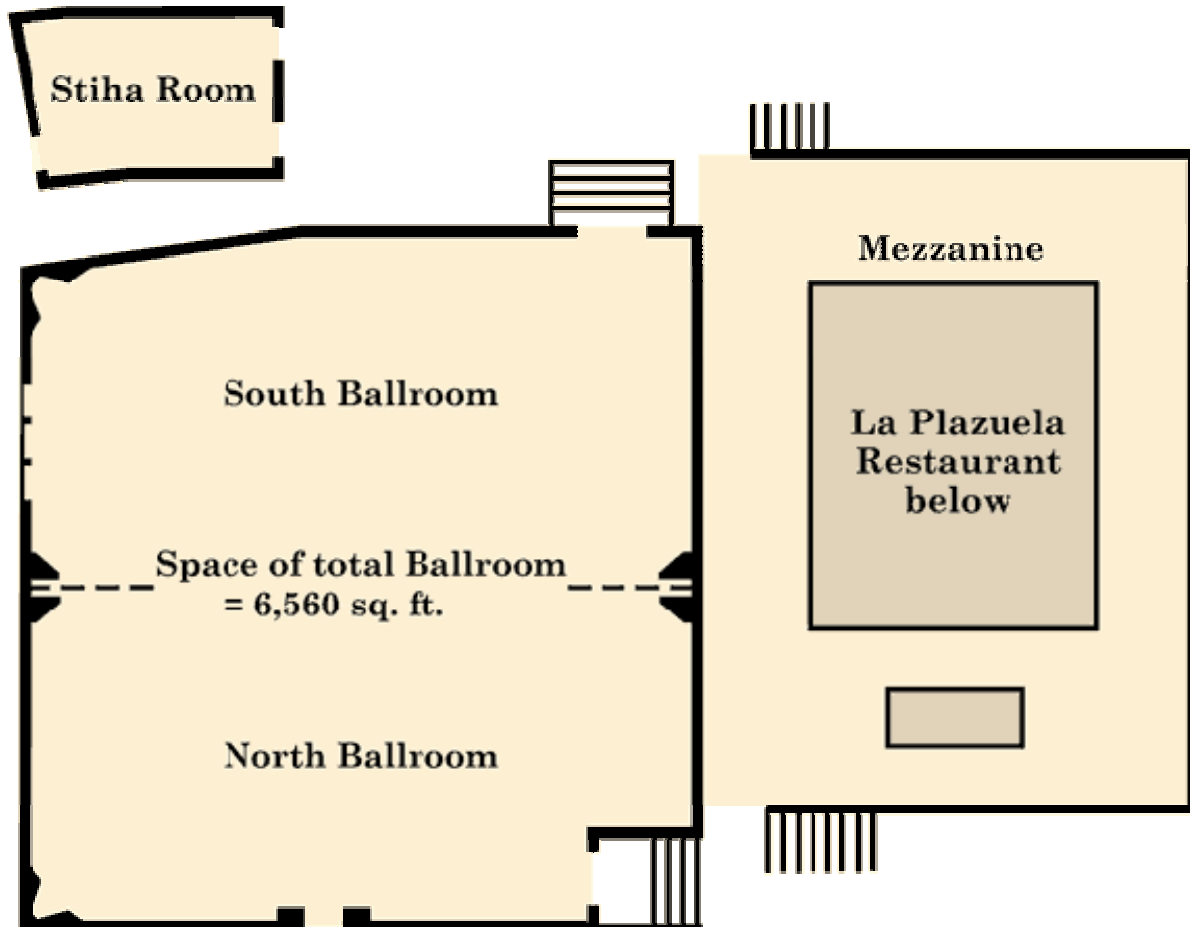


Driving Directions to La Fonda from Albuquerque Airport

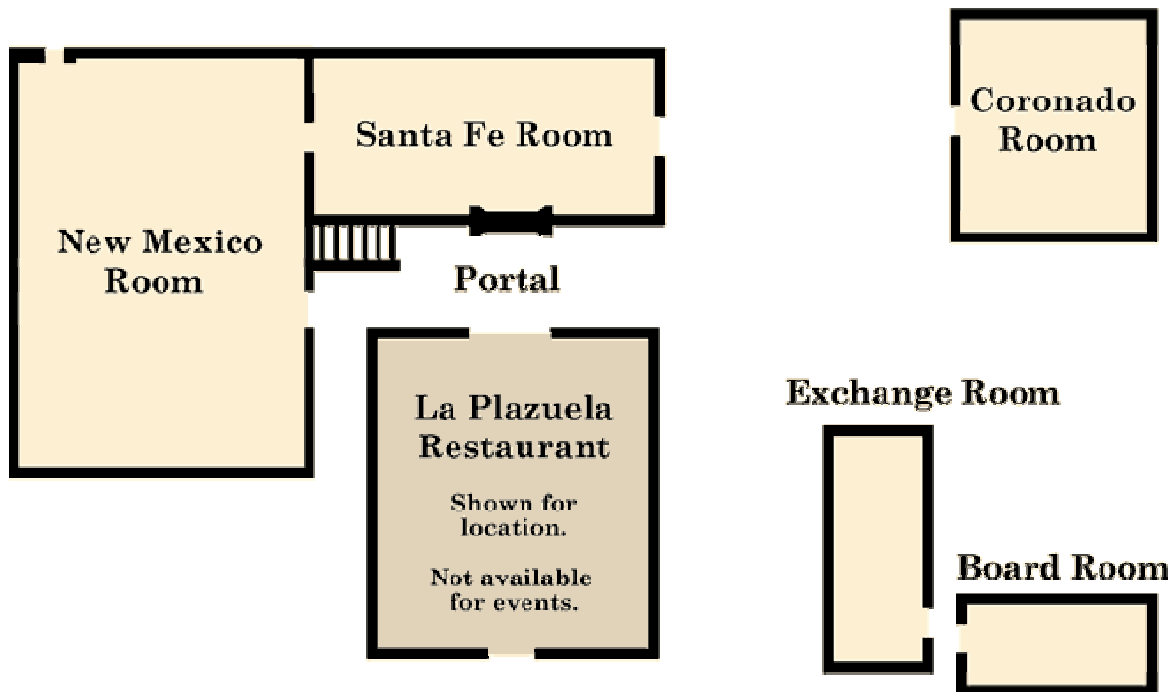
Follow Sunport Blvd. to I-25 north towards Santa Fe. Travel on I-25 north approximately 50 minutes to exit 284, Old Pecos Trail. At the stop sign at the top of the hill, turn left. Proceed north to the third traffic light and bear right to stay on Old Pecos Trail into town. Old Pecos Trail becomes Old Santa Fe Trail which dead ends into La Fonda at Water Street. Go around the hotel by turning left on Water, then making an immediate right. At the traffic light at San Francisco Street, turn right again—away from the Plaza and toward St. Francis Cathedral. Proceed to the hotel parking garage at the end of the block, on the right side of the street.

La Fonda Floor Plans

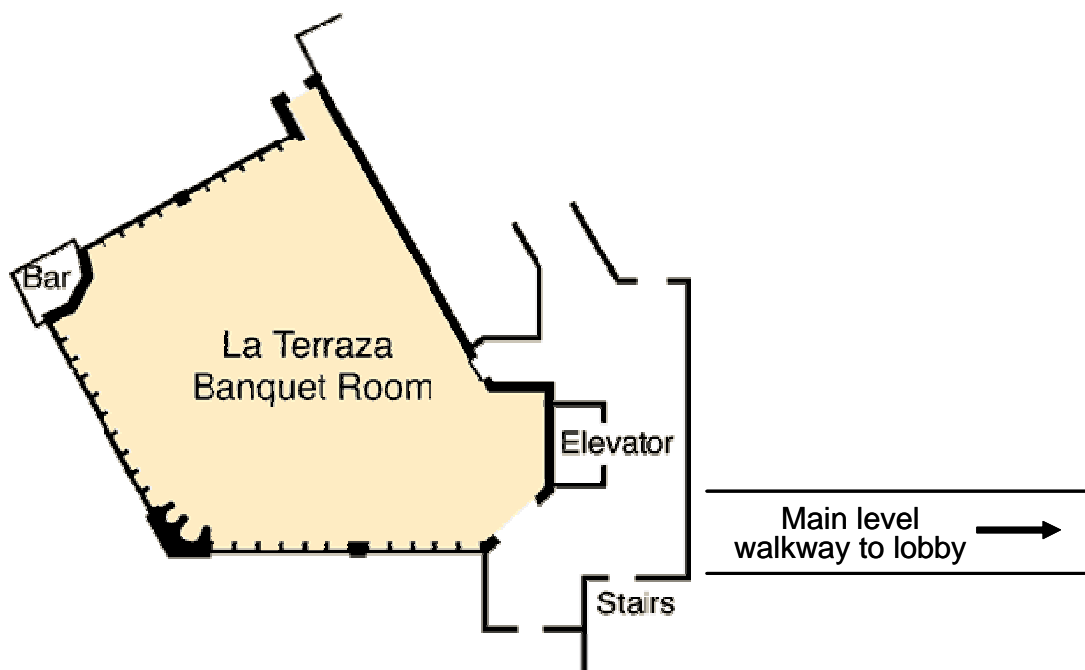
Upper Level Meeting Rooms



Main Level Meeting Rooms



La Terraza Room for Sunday Evening Reception and Tuesday Poster Session
Access from lobby by walking past lounge heading toward hotel garage, then use stairs or elevator to upper level



Saturday June 2	<p>7:00 AM Registration (Lobby)</p> <p>7:30 AM 8:00 AM CMS Council and Executive Committee Meeting (New Mexico Room)</p> <p>Field Trip #1 Cambios Hills and Espuelas Basin</p>	<p>7:30 AM Registration (Lobby)</p> <p>8:30 AM 9:00 AM Workshop Carbon Stabilization by Clays in the Environment and Characterization Methods (Santa Fe Room)</p> <p>9:30 AM 10:00 AM Break (Mezzanine)</p> <p>10:20 AM 10:50 AM Clays as Nanomaterials (Ballroom North)</p> <p>11:00 AM 11:30 AM Break (Mezzanine)</p> <p>11:40 AM 12:00 PM Registration and Reception (La Terraza Room)</p> <p>12:00 PM 12:30 PM Lunch Break</p> <p>12:30 PM 1:00 PM Sustaining Members Luncheon La Caja Seis (invitation only)</p> <p>1:20 PM 1:30 PM Clays as Nanomaterials (Ballroom North)</p> <p>1:40 PM 1:50 PM Break (Mezzanine)</p> <p>1:50 PM 2:00 PM Clays as Nanomaterials (Ballroom North)</p> <p>2:10 PM 2:20 PM Break (Mezzanine)</p> <p>2:20 PM 2:30 PM Clays as Nanomaterials (Ballroom North)</p> <p>2:40 PM 2:50 PM Break (Mezzanine)</p> <p>2:50 PM 3:00 PM Clays and Environmental Processes (Ballroom South)</p> <p>3:10 PM 3:30 PM Clays and Environmental Processes (Ballroom South)</p> <p>3:40 PM 3:50 PM Clays and Environmental Processes (Ballroom South)</p> <p>3:50 PM 4:00 PM Student Reception (invitation only) (New Mexico Room)</p>
Sunday June 3		<p>7:30 AM 8:00 AM Registration (Lobby)</p> <p>8:30 AM 9:00 AM Workshop Carbon Stabilization by Clays in the Environment and Characterization Methods (Santa Fe Room)</p> <p>9:30 AM 10:00 AM Break (Mezzanine)</p> <p>10:20 AM 10:50 AM Clays as Nanomaterials (Ballroom North)</p> <p>11:00 AM 11:30 AM Break (Mezzanine)</p> <p>11:40 AM 12:00 PM Registration and Reception (La Terraza Room)</p> <p>12:00 PM 12:30 PM Lunch Break</p> <p>12:30 PM 1:00 PM Sustaining Members Luncheon La Caja Seis (invitation only)</p> <p>1:20 PM 1:30 PM Clays as Nanomaterials (Ballroom North)</p> <p>1:40 PM 1:50 PM Break (Mezzanine)</p> <p>1:50 PM 2:00 PM Clays as Nanomaterials (Ballroom North)</p> <p>2:10 PM 2:20 PM Break (Mezzanine)</p> <p>2:20 PM 2:30 PM Clays as Nanomaterials (Ballroom North)</p> <p>2:40 PM 2:50 PM Break (Mezzanine)</p> <p>2:50 PM 3:00 PM Clays and Environmental Processes (Ballroom South)</p> <p>3:10 PM 3:30 PM Clays and Environmental Processes (Ballroom South)</p> <p>3:40 PM 3:50 PM Clays and Environmental Processes (Ballroom South)</p> <p>3:50 PM 4:00 PM Student Reception (invitation only) (New Mexico Room)</p>
Monday June 4		<p>7:30 AM 8:00 AM Registration (Mezzanine)</p> <p>8:30 AM 9:00 AM Plenary Session (Ballroom) Welcome and Open House Ceremony</p> <p>9:30 AM 10:00 AM Jackson Lecture Paul Schenck</p> <p>10:20 AM 10:50 AM Break (Mezzanine)</p> <p>11:00 AM 11:30 AM Clays as Nanomaterials (Ballroom North)</p> <p>11:40 AM 12:00 PM Break (Mezzanine)</p> <p>12:00 PM 12:30 PM Lunch Break</p> <p>12:30 PM 1:00 PM Registration (Mezzanine)</p> <p>1:20 PM 1:30 PM Carbon Sequestration and Stabilization by Clays and Clay Minerals (Ballroom South)</p> <p>1:40 PM 1:50 PM Break (Mezzanine)</p> <p>1:50 PM 2:00 PM Clays as Nanomaterials (Ballroom North)</p> <p>2:10 PM 2:20 PM Break (Mezzanine)</p> <p>2:20 PM 2:30 PM Clays as Nanomaterials (Ballroom North)</p> <p>2:40 PM 2:50 PM Break (Mezzanine)</p> <p>2:50 PM 3:00 PM Clays and Environmental Processes (Ballroom South)</p> <p>3:10 PM 3:30 PM Clays and Environmental Processes (Ballroom South)</p> <p>3:40 PM 3:50 PM Clays and Environmental Processes (Ballroom South)</p> <p>3:50 PM 4:00 PM Poster Session (La Terraza Room)</p>
Tuesday June 5		<p>7:30 AM 8:00 AM Registration (Mezzanine)</p> <p>8:30 AM 9:00 AM Field Trip #2 Hardin Escarpment and Adobe Demonstration</p> <p>9:30 AM 10:00 AM Pioneer Lecture Spencer Lucas</p> <p>10:20 AM 10:50 AM Break (Mezzanine)</p> <p>11:00 AM 11:30 AM Clays in Soils and Sediments (Ballroom North)</p> <p>11:40 AM 12:00 PM Break (Mezzanine)</p> <p>12:00 PM 12:30 PM Lunch Break</p> <p>12:30 PM 1:00 PM Registration (Mezzanine)</p> <p>1:20 PM 1:30 PM Characterizing Clay Minerals (Ballroom North)</p> <p>1:40 PM 1:50 PM Break (Mezzanine)</p> <p>1:50 PM 2:00 PM Clays in Archaeology (Santa Fe Room)</p> <p>2:10 PM 2:20 PM Break (Mezzanine)</p> <p>2:20 PM 2:30 PM Clays and Environmental Processes (Ballroom South)</p> <p>2:40 PM 2:50 PM Break (Mezzanine)</p> <p>2:50 PM 3:00 PM Characterizing Clay Minerals (Ballroom North)</p> <p>3:10 PM 3:30 PM Characterizing Clay Minerals (Ballroom North)</p> <p>3:40 PM 3:50 PM Molecular Simulations of Clays (Santa Fe Room)</p> <p>3:50 PM 4:00 PM CMS Business Meeting (Ballroom South)</p>
Wednesday June 6		<p>7:30 AM 8:00 AM Registration (Mezzanine)</p> <p>8:30 AM 9:00 AM Plenary Session (Ballroom) Field Trip #3 Cambios Hills and Espuelas Basin</p> <p>9:30 AM 10:00 AM Pioneer Lecture Spencer Lucas</p> <p>10:20 AM 10:50 AM Break (Mezzanine)</p> <p>11:00 AM 11:30 AM Clays in Extreme Environments (Santa Fe Room)</p> <p>11:40 AM 12:00 PM Break (Mezzanine)</p> <p>12:00 PM 12:30 PM Lunch Break</p> <p>12:30 PM 1:00 PM Registration (La Caja Seis (invitation only))</p> <p>1:20 PM 1:30 PM Zeolites (Ballroom South)</p> <p>1:40 PM 1:50 PM Break (Mezzanine)</p> <p>1:50 PM 2:00 PM Molecular Simulations of Clays (Santa Fe Room)</p> <p>2:10 PM 2:20 PM Break (Mezzanine)</p> <p>2:20 PM 2:30 PM Long Range Planning Dinner (Edificio Hotel, Wine Room - Old Rose Restaurant) (invitation only)</p> <p>2:40 PM 2:50 PM Break</p> <p>2:50 PM 3:00 PM Banquet (Ballroom)</p>
Thursday June 7		<p>7:30 AM 8:00 AM Registration (Mezzanine)</p> <p>8:30 AM 9:00 AM Plenary Session (Ballroom) Field Trip #3 Cambios Hills and Espuelas Basin</p> <p>9:30 AM 10:00 AM Pioneer Lecture Spencer Lucas</p> <p>10:20 AM 10:50 AM Break (Mezzanine)</p> <p>11:00 AM 11:30 AM Clays in Extreme Environments (Santa Fe Room)</p> <p>11:40 AM 12:00 PM Break (Mezzanine)</p> <p>12:00 PM 12:30 PM Lunch Break</p> <p>12:30 PM 1:00 PM Registration (La Caja Seis (invitation only))</p> <p>1:20 PM 1:30 PM Zeolites (Ballroom South)</p> <p>1:40 PM 1:50 PM Break (Mezzanine)</p> <p>1:50 PM 2:00 PM Molecular Simulations of Clays (Santa Fe Room)</p> <p>2:10 PM 2:20 PM Break (Mezzanine)</p> <p>2:20 PM 2:30 PM Long Range Planning Dinner (Edificio Hotel, Wine Room - Old Rose Restaurant) (invitation only)</p> <p>2:40 PM 2:50 PM Break</p> <p>2:50 PM 3:00 PM Banquet (Ballroom)</p>

Technical Program

Friday, June 1

6:00 PM Executive Committee Dinner, Inn at Loretto (Hopi Room at Baleen Restaurant)

Saturday, June 2

7:00 AM – Registration, La Fonda Lobby

8:00 AM

7:30 AM Field Trip #1: Cerrillos Hills and Española Basin (Meet in front of La Fonda on San Francisco Street just west of hotel parking garage)

8:00 AM CMS Council and Executive Committee Meeting, New Mexico Room

Sunday, June 3

7:30 AM – Registration, La Fonda Lobby

8:00 AM

8:00 AM Workshop: Carbon Stabilization by Clays in the Environment: Process and Characterization Methods, Santa Fe Room

6:00 PM Registration and Reception, La Terraza Room

Monday Morning, June 4

7:30 Registration, La Fonda Mezzanine

Plenary Session

Ballroom

8:15 Welcome and Introductory Remarks, Randall Cygan

8:20 Mayoral Welcome, David Coss, Mayor of the City of Santa Fe

8:30 Opening Ceremony, Native American Dancers

8:45 CMS Presidential Welcome, Richard Brown

8:55 Introduction of the Jackson Mid-Career Clay Scientist Lecturer by Ray Ferrell

9:00 Jackson Mid-Career Clay Scientist Lecture
Life at the Edge: Clay Mineralogy, Microbiology, and the International
Kamchatka Microbial Observatory
Paul A. Schroeder

9:50 **Break**, La Fonda Mezzanine

Clays as Nanomaterials

Ballroom North

Gary Beall and Hendrik Heinz, Chairs

10:20 A Two-Decade Review of Polymer-Clay Nanocomposites
Akane Okada and Arimitsu Usuki

10:50 Nanocomposites and Nanofluids
Emmanuel P. Giannelis

11:20 Identification and Characterization of Montmorillonite Binding Peptides
Lawrence F. Drummy, Sharon E. Jones, Richard A. Vaia, and Rajesh R. Naik

11:35 Fast Assembly of Nanocomposite Films and their Geometrical and Mechanical
Characterization
*Michael Plötze, Viatcheslav Vertlib, Marianne Dietiker, Alexander Puzrin, and
Ralph Spolenak*

Carbon Sequestration and Stabilization by Clays

Ballroom South

William Carey, Martin Kennedy, Javiera Cervini-Silva, and David Laird, Chairs

10:20 Radiogenic Carbon in Goethite from the Upper Ordovician Neda Formation
Jason C. Austin, Paul A. Schroeder, and Julia Cox

10:35 Reactivity of Serpentine with CO₂
J. William Carey, Hans-Joachim Ziock, and George D. Guthrie, Jr.

10:50 Carbon Sequestration in Clay-rich Mine Tailings
Gregory M. Dipple, S.A. Wilson, I. M. Power, J. M. Thom, G. Southam, and M. Raudsepp

11:20 Clay Mineral Control of Organic Carbon Deposition and the Implications of Clay Mineral Production of Soils in the Late Precambrian
Martin J. Kennedy, Mary Droser, David Pevear, and Lawrence Mayer

11:35 Potential for Chemical Sequestration of CO₂ in Oil sand Tailings
Oladipo Omotoso and Randy J. Mikula

General Session

Santa Fe Room

Duane Moore, Chair

10:20 PDF, a Powerfully Diverse Format for Instruction in Clay Mineralogy
Ray E. Ferrell

10:35 Novel Structure of 2:1 Layers Formed by Dehydroxylation of Fe³⁺, Mg-rich Mica
Toshihiro Kogure and Victor A. Drits

10:50 Dissolution Kinetics of Arsenopyrite in the Presence of Iron(III) - Sequestering Biogenic Ligands at pH 5
Hilda Cornejo Garrido, Pilar Fernández, José Guzmán, Sergey Sedov, and Javiera Cervini-Silva

11:05 Smectite Clay Sequestration of Aflatoxin B1: Mineral Dispersivity and Morphology
Ines Kannevischer, Maria G. Tenorio Arvide, G. Norman White, and Joe B. Dixon

11:20 Clay Surface Modification for Enhanced Aflatoxin Adsorption
William F. Jaynes, Richard E Zartman, and Wayne H. Hudnall

12:00 **Sustaining Members Luncheon**, La Casa Sena restaurant (Palace Avenue)
(invitation only)

Monday Afternoon, June 4

Clays as Nanomaterials

Ballroom North

Gary Beall and Hendrik Heinz, Chairs

1:20 Ethylbenzene Dehydrogenation Using Pt, Mo, and Pt-Mo Catalysts Supported on Clay Nanocomposites
Alexander Moronta, César Morán, Gabriela Carruyo, Eduardo González, Roger Solano, and Jorge Sánchez

1:35 Chemistry of Mechanical Performance: Memory, Self-healing Behavior, and High Impact Resistance in Nanocomposites
Clois E. Powell and Gary W. Beall

1:50 Protein-clay Bionanocomposites
Cliff T. Johnston, Robert A. Schoonheydt, Gnanasiri S. Premachandra, and Joyce Lok

2:05 Functionalized Nanohybrid Materials from Kaolinite
Sadok Letaief, Thomas Diaco, and Christian Detellier

2:20 Allophane from Ecuador
Stephan Kaufhold, A. Zeisig, R. Jahn, R. Dohrmann, and S. Brito

2:35 Direct Observation of the Constrained Polymer Region in Polyamide/Clay Nanocomposites
Daniel Adame and Gary W. Beall

2:50 **Break**, La Fonda Mezzanine

3:20 The Use of Small-Particle Size TiO₂ Supported on Clays as Photocatalytic Materials: A Low-Cost Alternative Technology for the Degradation of Air Pollutants
Javiera Cervini-Silva, Daria Kibanova, Martin Trejo, and Hugo Destaillats

3:35 Oriented Smectite Deposits as Model Shales
Mokhtar Zabat and Henri Van Damme

3:50 Electrokinetic Phenomena in Clays
Pierre M. Adler

4:05 Elastic Properties of Clays
Arpita P. Bathija, Haiyi Liang, Moneesh Upamanyu, Ning Lu, and Manika Prasad

Clays and Environmental Processes

Ballroom South

Roberto Pabalan and Peter Ryan, Chairs

1:20 Clay-Metal-Microbial Interactions in Aerobic Environments
Patricia A. Maurice

1:50 Iron Reduction by Biostimulation of Contaminated Soils: A Mössbauer Spectroscopic Study
Alexandre S. Anastácio, Denise M. Akob, Joel E. Kostka, and Joseph W. Stucki

2:05 Transmission Electron Microscopic Characterization of Microbially Induced Smectite-To-Illite Transformation
Jinwook Kim, Gengxin Zhang, Hailiang Dong, and Dennis D. Eberl

2:20 Monitoring Smectite Hydration in the Presence of Bacteria
Julia N. Berger, Laurence N. Warr, Marie-Claire Lett, and Nicolas Perdrial

2:35 Long Term-Immobilization of Technetium by Nontronite Aggregates
Deb P Jaisi, Hailiang Dong, Steve Heald

2:50 **Break**, La Fonda Mezzanine

3:20 High Level Radioactive Waste Disposal in a Deeply Buried Clay Formation: The French Case
Patrick Landais

3:35 Results On Pu Diffusion Experiments in the Opalinus Clay
Andreas Bauer, B. Fiehn, Ch. Marquardt, J. Römer, A. Görtzen, and B. Kienzler

3:50 Dissolution Kinetics of Smectite: pH and Temperature Dependence
Maria L. Rozalen, F. Javier Huertas, and Patrick V. Brady

4:05 Caffeine Adsorption On Clay Minerals and Natural Sediments
Keith E. Miller and Jeffrey A. Caulfield

4:20 Determination of Binding Interactions Between Tetracycline and Soil Components
Pankaj Kulshrestha, Rossman F. Giese, and Troy D. Wood

4:35 Cation and Anion Uptake by Anionic Clays
Sridhar Komarneni, Jingwen Zhang, and Kanchan Grover

Carbon Sequestration and Stabilization by Clays

Santa Fe Room

William Carey, Martin Kennedy, Javiera Cervini-Silva, and David Laird, Chairs

1:20 Clayey Cap-Rock Behavior in H₂O-CO₂ Media at Low Pressure and Temperature Conditions: An Experimental Approach
Teddy Parra and Eric Kohler

1:35 Altering the Hydrophobicity of Iron(III) - Exchanged Clay Catalysts to Improve Substrate Specificity
Philip J. Wallis, Will P. Gates, Antonio F. Patti, and Janet L. Scott

1:50 Thermal and Biochemical Characterization of Soil Clays from a Cultivation Chronosequence
Alain F. Plante, Laurent Grasset, André Amblès, Claire Chenu, and Dominique Righi

Clays in Oil Shale and Kerogen-Bearing Sediments

Santa Fe Room

Steve Chipera and Douglas McCarty, Chairs

2:10 Natural Zeolite-based Catalysts for Heavy Oil Applications
Steven M. Kuznicki, William C. McCaffrey, Junjie Bian, Abu S.M. Junaid, Brian R. Greenhalgh, and Andree Koenig

2:40 Origin of the Alberta Oil Sands Bitumen Deposits: Isotopic Evidence from K-bentonites in Key Source Rock Horizons
Paul Nadeau, Edward E. Meyer, James L. Aronson, Cindy Riediger, Martin Fowler, Steve Hillier, and Michele Asgar-Deen

2:55 **Break**, La Fonda Mezzanine

3:20 Black Shales: Enchanted Clays, Mysterious Organics, and Amazing Nanocomposites
Arkadiusz Derkowski, Martin J. Kennedy, and Thomas F. Bristow

3:35 Unique Mineralogy of Oil Shale from the Piceance Basin, Colorado
Steve J. Chipera, Giday WoldeGabriel, Marcus Wigand, J. William Carey, and John P. Kaszuba

3:50 Diagenetic Minerals and Textures in Oil Shale, Samples from the Piceance Basin, Colorado
Giday WoldeGabriel, Steve J. Chipera, Marcus Wigand, Melissa Fittipaldo, J. William Carey, and John P. Kaszuba

4:05 Reactivity of Mahogany Zone Oil Shale, Green River Formation
John P. Kaszuba and Marcus Wigand

4:20 Dawsonite Crystal Chemistry and Occurrence in Oil Shale
J. William Carey, John P. Kaszuba, and Steve J. Chipera

Monday Evening, June 4

5:00 **Student Reception**, New Mexico Room
(invitation only)

6:30 ***Clays and Clay Minerals Editors Dinner***, Coronado Room
(invitation only)

Tuesday Morning, June 5

7:30 Field Trip #2 (half-day): Harding Pegmatite and Adobe Demonstration (Meet in front of La Fonda on San Francisco Street just west of hotel parking garage)

Tuesday Afternoon, June 5

1:00 Registration, La Fonda Mezzanine

Clays in Soils and Sediments

Ballroom North

Louise Criscenti and Crawford Elliot, Chairs

1:30 Probing Clay Mineral Transformations and Contaminant Uptake in Sediments Reacted with Caustic Waste
Peggy A. O'Day, Sunkyung Choi, Karl T. Mueller, and Jon Chorover

2:00 Modeling the Acid-Base Surface Chemistry of Montmorillonite
Ian C. Bourg, Garrison Sposito, and Alain C. M. Bourg

2:15 Evidence for the Presence of Natural Organo-clay Nanocomposites in one Podzol from the Tatra Mountains, Poland
Michał Skiba

2:30 TEM Investigations on the Nature, Distribution, and Factors Affecting Clays and Nanoparticles in Soil Systems
Nicolas Perdrial, Françoise Elsass, and Nicole Liewig

2:45 Micromorphological Investigation of Sepiolite-bearing Petrocalcic Horizons Formed from Lacustrine Sediments on the Southern High Plains of West Texas and Eastern New Mexico
Dusten Russell, Wayne H. Hudnall, and B. L. Allen

Clays and Environmental Processes

Ballroom South

Roberto Pabalan and Peter Ryan, Chairs

1:30 Sources of Colloidal Material Observed During Rehabilitation of Los Alamos National Laboratory Water-Monitoring Wells
Steve J. Chipera and David T. Vaniman

1:45 Using Clays and Nano-Phase Minerals to Reveal Late Tertiary Paleoclimate Changes in Central China
Huifang Xu, Tianhu Chen, Junfeng Ji, Jun Chen, Qiaoqin Xie, Huayu Lu, and Xiaoyong Wang

2:00 Microstructure and Chemical Degradation of Adobe and Clay Brick
Juliana Calabria A., Wander L. Vasconcelos, and Aldo R. Boccaccini

2:15 Mineralogical Changes During Electrodialytic Remediation of Soil Material Polluted by Chemicals Used for Wood Impregnation
Bodil Karlsmose Kliem and Christian Bender Koch

2:30 Weathering Effects and Landsliding in the Bamouto Caldera, Cameroon, West Africa
Edwin B. Ntasin, S. N. Ayonghe, E. C. Suh, and E. V. Ranst

2:45 Mineralogy and Environmental Geochemistry of Open-Pit Lakes Related to Sedimentary Kaolin Deposits from Portugal
Iuliu Bobos

Clays and Archeology
Santa Fe Room
Eric Blinman, Chair

1:30 Linking Compositional Analyses of Pottery with Society: A Model from Comparative Ethnography
Dean E. Arnold

2:00 Clay Mineralogical Studies for Aeginetan Ware, Aegina, Greece
Christine M. Shriner, George E. Christidis, James G. Brophy, Kenneth L. Finger, and Haydn H. Murray

2:15 Clay Mineralogy of Prehistoric Gallina Ceramics From Northwest Mexico
Connie I. Constan

2:30 Firing Behavior of Ancestral Puebloan Pottery Clays, Clay Mineralogy, and Explanations of the Variability of Pottery Traditions in Time and Space
Eric Blinman and George S. Austin

2:45 Additional Studies of Carbon Paint Retention in Southwestern Native American Pottery Traditions
Eric Blinman and Duane M. Moore

3:00 Clay Mineralogical Studies for Greek Bronze Age Roofing Technology
Christine M. Shriner, Erika R. Elswick, Hannah L. Timm, and Haydn H. Murray

Poster Session
Randall Cygan, Chair
La Terraza Room
3:30 PM – 5:30 PM

Carbon Sequestration and Stabilization by Clays

Clayey Cap-Rock Behavior in H₂O-CO₂ Media at Low Pressure and Temperature Conditions: A Numerical Approach
E. Kohler, T. Parra, and A. Michel

Characterizing Clay Minerals

Heat-induced Structural Transformations and Cation Re-ordering in a Synthetic Swelling Mica
Geoffrey M. Bowers, Michael C. Davis, Karl T. Mueller, Ramesh Ravella, and Sridhar Komarneni

Mössbauer Spectroscopy of Phyllosilicates: Dependence of Recoil-free Fractions and %Fe³⁺ on Lineshape Models
M. Darby Dyar, Elizabeth C. Sklute, Martha W. Schaefer, and Janice L. Bishop

The CEC of the Special Clay SCa-3: Science or Science Fiction?

Alyx S. Frantzen

Trace Mineral Components in the Cheto, Arizona, Bentonite

Hongji Yuan and David L. Bish

Clays in Soils and Sediments

Iron Expulsion from the Octahedral Sheet of I/S Material: A Transmission Electron Microscopy Study of Well Characterized Samples from the Podhale Basin, Poland

Ruarri J. Day-Stirrat, Andrew C. Aplin, Kuncho D. Kurtev, and Andrew P. Brown

Late Paleozoic Weathering of the Elk Creek Carbonatite, Southeastern Nebraska, USA

Brian L. Nicklen and R. Matthew Joeckel

Conventional and Low-voltage Cryo-Field Emission Scanning Electron Microscopy of Pyroxene Weathering to Smectite, Koua Bocca Ultramafic Complex, Ivory Coast

Michael A. Velbel and William W. Barker

Clays and Environmental Processes

³⁹K NMR Investigation of Potassium Binding and Dynamics on Hectorite

Geoffrey M. Bowers and R. James Kirkpatrick

Ionic Diffusion in 2:1 Phyllosilicates

Michael A. Velbel

Vibrational Spectroscopic Study of Dibenzo-P-Dioxin Sorption to Cs-Saponite

Kiran Rana, Cliff T. Johnston, Gnanasiri S. Premachandra, Stephen A. Boyd, Brian J. Teppen, and Hui Li

In-Situ Attenuated Total Reflectance FTIR Study of Nitroaromatic Sorption to Smectite

Alteration of Synthetic Impact Crater Glass

Gnanasiri S. Premachandra and Cliff T. Johnston

Alteration of Synthetic Impact Crater Glass

Julien Declercq, Henning Dypvik, Per Aagaard, and Jens Jøhren

Clays as Nanomaterials

Rheology of the sonication-induced sol-gel transition of steam-treated sodium smectite

Liming Zhu and David L. Bish

Preparation of amphiphilic oligomer/halloysite composite materials and their adsorption properties for hydrocarbons

Kang-Sup Chung, Hwan Lee, Kwang-Kyun Hwang, Dae-Sup Kil, and Yong-Jae Suh

Tubular halloysite loaded with magnetite nanoparticles

Yong Jae Suh, Kang Sup Chung, Dae Sup Kil, Young Nam Chang, and Sujeong Lee

Clay-catalyzed incorporation of arsenic to bioorganic moieties: A low cost mechanism for ameliorating arsenic toxicity in aquatic systems

Jessica Hernández-Pineda, Pilar Fernández-Lomelin, Norma Ruth López-Santiago, and Javiera Cervini-Silva

Clays in Oil Shale and Kerogen-Bearing Sediments

Characterization of Clay Mineral Assemblages in the Barnett Shale: Its Diversity Explored

Ruarri J. Day-Stirrat, Kitty L. Milliken, Robert G. Loucks, and Ben E. van der Pluijm

The CO₂ Sealing Efficiency of Shales

Helge Stanjek, Andreas Busch, Sascha Alles, and Bernhard M. Krooss

General Session

Enthalpic Studies of Hydration/Dehydration Processes in Clay Minerals

Kristen M. Baugh and Alyx S. Frantzen

Infrared Analysis of Silicon Wafer-supported Clay Minerals

Keith E. Miller, Jeffrey A. Caulfield, and Todd A. Wells

Standards-based Pre-K-12 Curriculum for Clay Science

Audrey C. Rule and Stephen Guggenheim

Zeolites

Sorption of Hexavalent and Trivalent Chromium onto New Activated Clinoptilolite-Based Material

Juan C. Torres, Ana I. Pérez, and María E. Díaz

Prediction of Ion-interaction Parameters of Binary 2:1 and 2:2 Ion-Exchange Systems by the Coupling of the Margules Model with a Linear Free Energy Correlation Approach

Juan C. Torres and José C. Gubulin

Effect of Application of Iranian Natural Zeolite in Manure on Yield and Component Yield of Sunflower Under Different Irrigation Regimes

Majid Gholamhoseini, A. Ghalavand, and E. Jamshidi

Barrerite Twins, Nequen Province, Patagonia, Argentina

María Elena Vattuone, Carlos Latorre, and Pablo R. Leal

Disordered Natrolite of Nequen, Patagonia, Argentina

María E. Vattuone, Sabrina Crosta, Janina Berbeglia, Carlos Latorre, Carmen I. Martínez Dopico, and Ernesto Gallegos

Paulingite from Junin de Los Andes, Patagonia, Argentina

Maria E. Vattuone, Sabrina Crosta, Carlos Latorre, Pablo R. Leal, and Janina Berbeglia

Behavior of H₂O Molecules in the Channels of Natrolite: A Thermal Analysis and Powder X-ray Diffraction Study

Hsiu-Wen Wang and David L. Bish

A Comparative Study Using Sea and Distilled Water to Synthesize Zeolite from Coal Fly Ash Hydrothermally at Low Temperatures

Claudia Belviso, Francesco Cavalcante, and Saverio Fiore

Preparation and Application of Surfactant-Modified Zeolitic Materials for Removal of Chromate Species from Water

Jolanta K. Warchol, Robert S. Bowman, and Panagiotis Misaelides

Characterization of Nonequilibrium Sorption of Gasoline Components by Surfactant-Modified Zeolite

Joshua A. Simpson and Robert S. Bowman

An Integrated Process using Wyoming Zeolite for Treating Saline-Sodic Waters Produced from Coalbed Natural Gas Operations

Hongting Zhao, George F. Vance, Mike A. Urynowicz, Girisha K. Ganjegunte, and Robert W. Gregory

Tuesday Evening, June 5

6:30 Reception (sponsored by St. Cloud Mining Company), Ballroom

7:15 CMS Banquet featuring music by *Soulstice*, Ballroom

Wednesday Morning, June 6

7:30 Registration, La Fonda Mezzanine

Plenary Session

Ballroom

8:45 Introduction of the Pioneer in Clay Science Lecturer by Duane Moore

8:50 Pioneer in Clay Science Lecture
Twenty-Five Years Plus of Research on Impacts and Mass Extinctions
Spencer G. Lucas

9:40 **Break**, La Fonda Mezzanine

Clays in Soils and Sediments

Ballroom North

Louise Criscenti and Crawford Elliot, Chairs

10:10 Mineral Occurrence, Translocation, and Weathering in Soils Developed on Four Types of Alluvial Fan Deposits in the Mojave Desert, Southeastern California
Youjun Deng and Eric McDonald

10:25 Relations Among Mineralogy, Chemistry and Annual Precipitation for Soils from Two Continental-Scale Transects of North America.
Dennis D. Eberl and David B. Smith

10:40 A Smoking Gun for Precambrian Non-Marine Depositional Environments
Thomas F. Bristow, Martin J. Kennedy, and Arkadiusz Derkowsk

10:55 The Lower Silurian (Llandovery) Osmundsberg K-Bentonite in Baltoscandia and the British Isles: Age and Correlation
Warren D. Huff, Funda Ö. Toprak, Stig M. Bergström, and Roland Mundil

11:10 Volatile Light Element Distributions in Baltic Basin Bentonites: A Potential Connection to Hydrocarbon Sources
Lynda B. Williams, Jan Środoń, Warren D. Huff, and Richard L. Hervig

11:25 Detecting Undetectable: A New Approach to the K-Ar Dating of Glauconite
Arkadiusz Derkowsk, Jan Środoń, Wojciech Franus, and Michał Banaś

Zeolites

Ballroom South

David Bish and Phil Neuhoff, Chairs

10:10 Ion Exchange in Natural Heulandite: Experiments Under Geologically-Relevant Conditions and Equilibrium with Icelandic Geothermal Solutions
Thráinn Fridriksson, Stefán Arnórsson, Philip S. Neuhoff, and Dennis K. Bird

10:40 Dynamics of Nanoconfined Water in Clinoptilolite and Heulandite Microporous Zeolites
Nathan W. Ockwig, Randall T. Cygan, Tina M. Nenoff, Luc L. Daemen, Monika A. Hartl, and Louise J. Criscenti

10:55 Thermodynamic Model of Analcime Dehydration
Jie Wang and Philip S. Neuhoff

11:10 Solvus Models for Hysteresis in Water Adsorption/Desorption by Zeolites and Other Mineral Hydrates: Evidence from Thermal Analysis and Thermodynamic Modeling
Philip S. Neuhoff, Jie Wang, and Gökçe S. Atalan

11:25 Temperature Dependence of Hysteretic Hydration/Dehydration of the W1 Site in Laumontite
Gökçe S. Atalan and Philip S. Neuhoff

11:40 South African Natural Clinoptilolite: Structure, Physico-Chemistry and Industrial Properties
Antoine F. Mulaba-Bafubiandi, Lorraine T. Soko, and Bhekie Mamba

Clays in Extreme Environments

Santa Fe Room

Paul Schroeder and David Vaniman, Chairs

10:10 Phyllosilicates Formed by Olivine Hydration in Carbonaceous Chondrites: Aqueous Alteration in the Early Solar System
Michael A. Velbel, Eric K. Tonui, and Michael E. Zolensky

10:40 Hydrous Minerals Under Mars Surface Conditions
David L. Bish, J. William Carey, Steve J. Chipera, David T. Vaniman, and Claire Fialips

11:10 Characterization of Phyllosilicates on Mars: A Comparison of Crism Hyperspectral Data of Mawrth Vallis with Phyllosilicates and Hydrated Materials
Janice L. Bishop, Jean-Pierre Bibring, Adrian J. Brown, Roger N. Clark, M. Darby Dyar, Bethany L. Ehlmann, Ralph E. Milliken, Scott L. Murchie, John F. Mustard, Shannon M. Pelkey, Gregg Swayze, and the CRISM Team

11:25 Methane + H₂O in Smectite
Stephen Guggenheim and A. F. Koster van Groos

11:40 Nitrogen and Smectites from Terrestrial Hot Springs in the Uzon Caldera, Kamchatka, Far-Eastern Russia
Paul A. Schroeder, Elizaveta Bonch-Osmolovskaya, Elizabeth Burgess, Albert Colman, Douglas Crowe, Julie Fiser, Maggie Hodges, Elizabeth Hollingsworth, Gennady Karpov, Ilya Kublanov, Jennifer Kyle, Gary Mills, Andrew Neal, Nikolai Pimenov, Frank Robb, Christopher Romanek, Tatiana Slepova, Tatyana Sokolova, Elisabeth Spencer, Stephen Techtmann, Isaac Wagner, Juergen Wiegel, Noah Wittman, Chuanlun Zhang, and Weidong Zhao

12:00 **Past Presidents Luncheon**, La Casa Sena restaurant (Palace Avenue)
(invitation only)

Wednesday Afternoon, June 6

Characterizing Clay Minerals *Ballroom North* *John Bloch and Heather Dion, Chairs*

1:20 Aspects of the Evolution of Green Pelletal Clay
Jenny Hugget

1:50 Origins of Clay Minerals in the Goathill North Rock Pile, Questa Mine, Questa, New Mexico
Kelly Donahue, Nelia Dunbar, and Virginia McLemore

2:05 Glass to Glaucony: Greensand Genesis in the Late Cretaceous Kanguk Formation, Devon Island, Nunavut
John D. Bloch, Mike Spilde, Lynn L. Heizler, and Nelia Dunbar

2:20 Combined Mossbauer and Infrared Spectroscopic Examination of Site Occupancy in Ferruginous Smectites
Will P. Gates and John D Cashion

2:35 Characterization of San Juan Illite RM30: A Re-evaluation
Philip E. Rosenberg and Robert L. Hooper

2:50 **Break**, La Fonda Mezzanine

3:20 Chemical and Structural Characterization of Pharmaceutical Grade Kaolinites
A. Umran Dogan and Meral Dogan

3:35 Surface Modification of Laponite for Biomolecule Adsorption
Angela M. F. Guimarães, Virgínia S.T. Ciminelli, and Wander L. Vasconcelos

3:50 The Use of Calorimetric Techniques in the Determination of Cation Exchange Capacity
Alyx S. Frantzen

4:05 Improved Method for Measuring Smectite Surface Area and Abundance by Polyvinylpyrrolidone (PVP) Adsorption in Solution
Alex Blum, Dennis D. Eberl, Ronald Hill, and Neil Fishman

4:20 The Effect of Pressure on Nanomorphology in Kaolinite Under Wet and Dry Conditions. Correlation with Other Kaolinite Properties
Patricia Aparicio, E. Galán, G. Valdrè, and D. Moro

Zeolites

Ballroom South

David Bish and Philip Neuhoff, Chairs

1:20 Investigation of Adsorption and Ion Exchange Properties Magnetic Modified Natural Zeolites
Zafer Dikmen and Onder Orhun

1:35 The Effect of Microwave on the Ag Exchange in Na-clinoptilolite and its Antibacterial Activity
Yelda Akdeniz and Semra Ülkü

1:50 The Usage of Natural Zeolites to Prevent for Deficiency of Zinc Through the Earth
Onder Orhun, Gulcan Kinaci, and Ozlem Kazan

2:05 Field Evaluation of a Surfactant-modified Zeolite System for Removal of Organics from Produced Water
Robert S. Bowman, Enid J. Sullivan, Lynn E. Katz, and Kerry A. Kinney

2:20 Removal of Nitrate and Sulfate Anions from Aqueous Solution by HDTMA-modified Clinoptilolite
Sedef Dikmen and Ertuğrul Yörükogulları

2:35 Competitive Adsorption of Trace Elements on Surfactant Modified and Unmodified Clinoptilolite
Rona J. Donahoe, Sidhartha Bhattacharyya, and Elizabeth Y. Graham

Molecular Simulations of Clays

Santa Fe Room

Jeffery Greathouse and Brian Teppen, Chairs

1:35 A Force Field for Layered Silicates and Simulation of Interfaces with Surfactants and Peptides
Hendrik Heinz, Richard A. Vaia, Rajesh R. Naik, Ruth Pachter, and Barry L. Farmer

2:05 Molecular Dynamics Modeling and Experimental Studies of Layered Double Hydroxides Intercalated with Carboxylic and Amino Acids
R. James Kirkpatrick, Padma Kumar., Andrey G. Kalinichev, Qiang Li, and Marc X. Reinholdt

2:20 Molecular Simulation of the Structural and Vibrational Properties of Talc and Pyrophyllite
James P. Larentzos, Jeffery A. Greathouse, and Randall T. Cygan

2:35 Water and Ionic Exchange Between Interlayer and Microporosity from Molecular Dynamics Simulations
Benjamin Rotenberg, Virginie Marry, Natalie Malikova, Rodolphe Vuilleumier, Eric Giffaut, and Pierre Turq

2:50 **Break**, La Fonda Mezzanine

3:20 Alkaline Earth Metal Complexation to Aqueous Chloride and to the Gibbsite Surface: A Molecular Dynamics Investigation
Louise J. Criscenti and James P. Larentzos

3:35 Dynamics of Aqueous Species at Interfaces with Hydroxylated Mineral Surfaces: MD Simulation and NMR Spectroscopy
Andrey G. Kalinichev, Geoffrey M. Bowers, and R. James Kirkpatrick

3:50 Probing Clay Surfaces with NMR: Computing ^{27}Al and ^{29}Si Chemical Shifts
Nancy A. Washton, Karl T. Mueller, and James D. Kubicki

4:40 **CMS Business Meeting**, Ballroom South

Wednesday Evening, June 6

6:30 **Long Range Planning Dinner**, Eldorado Hotel (Wine Room at Old House Restaurant)
(invitation only)

Thursday Morning, June 7

7:30 Field Trip #3 (repeat): Cerrillos Hills and Espanola Basin (Meet in front of La Fonda on San Francisco Street just west of hotel parking garage)

DIRECT OBSERVATION OF THE CONSTRAINED POLYMER REGION IN POLYAMIDE/CLAY NANOCOMPOSITE

Daniel Adame¹ and Gary W. Beall²

¹Department of Chemistry and Biochemistry, Texas State University, 601 University Dr., San Marcos, TX 78666, USA; danieladame@systemsandmaterials.com

²Center for Nanophase Research, Department of Chemistry and Biochemistry, Texas State University, 601 University Dr., San Marcos, TX 78666, USA

It has been well established by many researchers that the gas permeability of polymer clay nanocomposites is lowered relative to the pure polymer film. A theory utilized by most researchers in the field has been proposed by Nielsen where the clay plates are acting as barriers to gas diffusion and is normally referred to as the “Tortuous Path” model. This model has been successfully utilized to predict the relative permeability of a number of polymer nanocomposites. There are, however, a number of polymer/clay nanocomposites that deviate significantly from this simple theory. Amorphous polymers especially deviate from this theory. A model that invokes a region around the clay particles which is constrained by the presence of the particle and behaves differently than bulk polymer was suggested by Beall. This model unfortunately requires two assumptions regarding the constrained region. The first is the size of the region and the second is the relative diffusion coefficient in this region. Using this modified model, data deviating from the tortuous path model could be predicted easily with the proper choice of the two variable parameters. In order to eliminate one of these variables, the size of the constrained polymer region has been measured in a MXD6 clay nanocomposite using atomic force microscopy. The constrained regions were measured after preparing samples with a microtome by allowing clay layers to swell in water and measurement of the resulting topology. The size of these constrained regions will be highlighted as well as the implications for prediction of gas permeability in polymer/clay nanocomposite.

Nielsen, L.E. (1967) Models for the permeability of filled polymer systems. *Journal of Macromolecular Science*, Part A, **1**, 929-942.

Beall, G.W. (2000) New conceptual model for interpreting nanocomposite behavior. *Polymer-Clay Nanocomposites*, Edited by T. J. Pinnavaia and G. W. Beall, John Wiley & Sons, Chichester, UK.

ELECTROKINETIC PHENOMENA IN CLAYS

Pierre M. Adler

UPMC-Sisyphe, Paris, France; padler@ccr.jussieu.fr

Electroosmotic phenomena, and more generally coupled transports, are generated at the local scale by the flow of an electrolyte close to charged solid surfaces while far from the walls, the solution can be considered as neutral. These phenomena may become very important when the characteristic length scales of the media are submicronic. This paper reviews our contributions to this field.

The problem is most complex on the pore scale. The medium filled by an electrolyte is submitted to macroscopic gradients of pressure, of electrical potential and of concentration. They induce fluxes of mass, current and solute. Close to equilibrium, the macroscopic coefficients which relate the fluxes and the forces, can be obtained by solving three coupled partial differential equations. Numerical results can be rationalised by means of a uniquely defined length scale Λ which depends only on the formation factor F and of the permeability K of the medium. More precisely, when made dimensionless, the coupling coefficients only depend on the product $\kappa\Lambda$ where κ^{-1} is the Debye-Hückel length, whatever the porous medium.

Systematic experimental checks of these properties were performed on various sorts of finely divided materials, including clays by Rosanne et al (2005 and 2006). The data were in agreement with the previous numerical predictions.

These properties can be extended to high values of the zeta potential ζ . A universal curve is found for the electroosmotic coefficient which is valid for any porous medium and any zeta potential.

These results are practically very important since good estimations of the coupling coefficients can be derived from the knowledge of F , K , κ and ζ which are much easier to measure than the coupling coefficients themselves.

Coelho, D., Shapiro, M., Thovert, J.-F., and Adler, P.M. (1996) Electro-osmotic phenomena in porous media. *Journal of Colloid and Interfacial Science*, **181**, 169-190.

Gupta, A., Coelho, D., and Adler, P.M. (2006) Electroosmosis in porous solids for high zeta potentials *Journal of Colloid and Interfacial Science*, **303**, 593-603.

Rosanne, M., Paszkuta, M., and Adler, P.M. (2006) Electrokinetic phenomena in saturated compact clays, *Journal of Colloid and Interfacial Science*, **297**, 353-364.

Rosanne, M., Paszkuta, M. Thovert, J.-F., and Adler, P.M. (2005) Electro-osmotic coupling in compact clays, *Geophysical Research Letters*, **31**, L18614.

THE EFFECT OF MICROWAVE ON THE AG EXCHANGE IN NA-CLINOPTIOLITE AND ITS ANTIBACTERIAL ACTIVITY

Yelda Akdeniz¹ and Semra Ülkü¹

¹İzmir Institute of Technology, Chemical Eng. Dept., Gülbahçe Köyü, Urla, İzmir, TURKEY,
email:yeldaakdeniz@iyte.edu.tr

The effect of microwave irradiation on the structure of clinoptilolite mineral and its resulting antibacterial activity has been examined in comparison with the conventional heat treatment in a waterbath. Natural zeolitized rock from the source in Manisa Gördes, Turkey (Western Anatolia) was used in the experimental work. The rock contains clinoptilolite, quartz, analcime and mordenite. Near homoionic clinoptilolite-rich samples were formed by treating with 1 N NaCl solution at 80 °C for 10 days. The exchange of Ag⁺ was done using 0.01M AgNO₃ at different solid to liquid ratios, exchange times, and temperature. Exchange in a microwave was conducted in a Mars 5-CEM Digestion and Extraction Microwave. Exchange under traditional thermal conditions was conducted in a constant temperature waterbath. The Ag exchanged samples were analyzed by X-ray diffraction and scanning electron microscopy. The resulting antibacterial activity of the Ag-exchanged clinoptilolites against *E. coli* was determined by the disk diffusion (Kirby–Bauer) method.

Microwave treatment was found to be more rapid compared to conventional waterbath treatment. Silver-exchanged minerals did not show considerable structural changes with either method and samples prepared both ways were effective against *E. Coli*.

IRON REDUCTION BY BIOSTIMULATION OF CONTAMINATED SOILS: A MÖSSBAUER SPECTROSCOPIC STUDY

Alexandre S. Anastácio¹, Denise M. Akob², Joel E. Kostka², and Joseph W. Stucki¹.

¹Department of Natural Resources and Environmental Sciences, University of Illinois, Urbana, Illinois, USA; jstucki@uiuc.edu

²Department of Oceanography, Florida State University, Tallahassee, Florida, USA

Metal contaminants, many of which are radioactive and/or toxic, are present in various subsurface soils and aquifers associated with mining, milling, and nuclear fuels processing sites across North America, South America, and Europe. The potential mobility of such metals represents a global-scale threat to human health. The U.S. Department of Energy, Environmental Remediation Science Program, is addressing this problem in uranium-contaminated subsoils at its Oak Ridge Field Research Center (ORFRC) by seeking to immobilize U(VI) through its reduction to U(IV) by the *in situ* stimulation of indigenous metal-reducing bacteria. One indicator of the robustness and sustainability of the *in situ* reduction method is the change that occurs in the constituent Fe minerals. Dissimilatory Fe(III)-reducing prokaryotes (FeRP) and sulfate-reducing prokaryotes (SRP) comprise the two major groups of metal-reducing organisms which are capable of Fe(III) and U(VI) reduction. Both the FeRP and SRP utilize U(VI) and Fe(III) as electron acceptors, and a subset of these groups have been shown to conserve energy for growth via Fe(III) and U(VI) reduction. Sediments from borehole FB61, 2 to 6 m below the surface and within the saturated zone of ORFRC soils, were collected and biostimulated (30 g) with either ethanol or glucose (20 mM final concentration) in 60 mL of deionized water under strictly anoxic conditions in a Coy anaerobic chamber for 27 days. Variable-temperature Mössbauer spectroscopy was employed to assess iron forms and distribution in the untreated and biostimulated samples. Ferrous and total Fe were also measured by wet chemical methods. Mössbauer spectra of the unaltered sediment revealed that the iron was distributed between superparamagnetic goethite and octahedral Fe(II) and Fe(III) in the silicate minerals. Upon biostimulation, Fe(III) in the silicate structure was reduced to Fe(II), but no change was observed in the goethite. According to chemical analyses, ethanol was more effective than glucose in the reduction of iron, but the Mössbauer spectra gave similar spectra regardless of which biostimulant was used. Thus, in batch reactors, iron in silicate minerals is reduced before the iron in goethite, which is consistent with redox potential calculations. This may have important implications for the synergistic relationships among redox reactive metals, i.e., Fe and U, in biologically active soils and sediments.

THE EFFECT OF PRESSURE ON NANOMORPHOLOGY IN KAOLINITE UNDER WET AND DRY CONDITIONS. CORRELATION WITH OTHER KAOLINITE PROPERTIES

Patricia Aparicio¹, E. Galán¹, G. Valdré², and D. Moro²

¹Departamento de Cristalografía, Mineralogía y Química Agrícola. Universidad de Sevilla, Apdo. 553, 41071, Sevilla, Spain; paparicio@us.es

²Dipartimento di Scienze della Terra e Geologico-Ambientali, Università degli Studi di Bologna, Porta San Donato 1, Bologna, Italy

Kaolin morphology has particular importance in paper filling and coating. Besides particle size distribution and shape, aspect ratio and aggregate structure have a dominant importance on the rheological behaviour of kaolin slurries, and in other properties such as opacity, gloss, printability and brightness.

The objectives of this investigation were to evaluate the changes produced by isostatic pressure on nanomorphology of kaolins and to determine the effect of the presence or absence of water during these experiments. Nanomorphology was evaluated by scanning electron microscopy (SEM), transmission electron microscopy (TEM) and atomic force microscopy (AFM). These results were correlated with the variations on kaolinite structural order by X-ray diffraction (XRD), particle size distribution, surface area (BET method) and pore total volume determined from N₂-adsorption.

Nanomorphology changed by effect of confined pressure, but the behaviour is different if the compaction is performed in absence or in presence of water. During dry pressure kaolinite crystals gradually lost their pseudohexagonal morphology, edges were rounded and books and vermicular stacks were fractured and distorted. By the contrary kaolinite morphology did not show apparently any change in wet conditions by SEM and TEM. Crystals maintained their pseudohexagonal morphology and particle-size. AFM study of wet pressed kaolinites shows an increment of edges perfection on kaolinite crystals and a low presence of deformed crystals.

In general isostatic pressure in dry conditions produces an increment of roughness whereas in wet conditions roughness decreased (40 wt% of mean). The nanomorphology change of kaolinite is inversely correlated with the variation of the degree of structural order as determined by XRD. In fact under dry conditions the percentage of low-defect phase decreased, showing the Hinckley index (HI) and Aparicio-Galán-Ferrell (AGFI) index a variation from low-defect to medium-(high) defect kaolinite. On the contrary, under wet conditions the percentage of low-defect kaolinite was maintained or increased. Specific surface area decreased under pressure treatment especially in wet conditions

Two factors in the multivariate analysis accounted for the 92% of the overall variance. Factor 1 (51%) related roughness inversely with the variation of the degree of kaolinite structural order as determined by X-ray diffraction and with the percentage of less than 40, 20, 10 and 5 µm. The second (41%) related the specific surface area with the percentage of less than 2 and 1 µm and roughness and inversely with total pore volume.

LINKING COMPOSITIONAL ANALYSES OF POTTERY WITH SOCIETY: A MODEL FROM COMPARATIVE ETHNOGRAPHY

Dean E. Arnold

Dept. of Sociology and Anthropology, Wheaton College, 501 E. College Ave., Wheaton, IL 60187, USA; dean.e.arnold@wheaton.edu

Chemical analyses of archaeological pottery (utilizing such techniques such as INAA) are commonly believed to reveal the clay sources of the pottery used to make it, and thus the geographical origins of the pottery. The data from such analyses, however, are far removed from the behavior of potters and the societies in which they live. Researchers who use these analyses employ terms such as 'source', 'reference group' and 'fingerprint', but these terms are geological ('source') and statistical ('reference group') and have no inherent connection with the behavior of potters ('fingerprint' of what in social terms?). When factors that contribute to compositional variability of the pottery are considered, one wonders what such chemical analyses actually mean in terms of the behavior of the potters and the societies from which they come. This paper develops three concepts derived from comparative ethnography that link compositional results to the behavior of potters. These concepts have emerged from compositional studies (INAA) of ethnographic pottery and raw materials (such as clays) collected and analyzed over a period of 32 years from seven different pottery producing communities in two distinct geological areas of Latin America (N=845). This broad ethnographic perspective provides a middle range theory for the interpretation of the compositional analyses of archaeological pottery.

TEMPERATURE DEPENDENCE OF HYSTERETIC HYDRATION/DEHYDRATION OF THE W1 SITE IN LAUMONTITE

Gökçe S. Atalan and Philip S. Neuhoff

Department of Geological Sciences, University of Florida, 241 Williamson Hall, 32611-2120 Gainesville; Florida; USA; Email: gokce@ufl.edu

Laumontite, $\text{Ca}_4\text{Al}_8\text{Si}_{16}\text{O}_{48}\cdot n\text{H}_2\text{O}$, is a common rock-forming zeolite occurring world-wide as a secondary mineral in low-grade metavolcanic and volcanically-derived sedimentary rocks. Fully hydrated laumontite contains 18 water molecules per unit cell (puc). Water molecules are distributed among four distinct water sites W1 (4 puc), W2 (4 puc), W5 (2 puc), and W8 (8 puc). While water molecules on the W2 and W8 sites solvate the Ca^{2+} cation, those on the other two sites, W1 and W5, are hydrogen bonded to framework oxygens and/or water molecules on the W2 and W8 sites (Fridriksson et al., 2003). Hydration and dehydration of the W5 site is completely reversible without hysteresis, while dehydration of W1 (the least energetic/last water site to be occupied upon hydration of laumontite) exhibits distinctly hysteretic sorption behavior associated with the coexistence of two phases, one with W1 occupied and one with W1 largely empty (0.68 puc; Fridriksson et al., 2003). In this study we investigated the hysteretic behavior of W1 site in laumontite with increasing temperatures.

Phase equilibrium experiments were conducted in triplicate on 200-300 mg samples of powdered laumontite from Drain, Oregon (USA). Samples were loaded into pre-weighed Eppendorf tubes and equilibrated at room temperature over a saturated MgNO_3 solution (52.89 % relative humidity; RH) for 1 day. Subsequently, these samples were equilibrated (for 1 day) sequentially over a series of saturated salt solutions (LiBr , LiCl , MgCl_2 , MgNO_3 , CoCl_2 , KI , NaNO_3 , NaCl , KCl , K_2SO_4) that buffered the water vapor pressure to relative humidities ranging from 5.5 to 95.8 % RH (precision better than 0.12 % RH). After equilibration under the highest humidity conditions, the procedure was reversed to study the dehydration behavior of the sample. Observations were conducted at room temperature (298 K) and at 5 K increments from 313 to 338 K by submersion in a temperature-controlled water bath.

At 298 K, hydration and dehydration of the W1 site is characterized by a broad, prominent hysteresis loop between 32.78 and 84.34 % RH. With increasing temperature, the hydration and dehydration branches converge and occur at progressively higher vapor pressures. Concurrently, total water occupancy on W1 decreases with temperature. At 323 K, no hysteresis is present. The water content of laumontite at temperatures >323 K is a continuous function of water vapor pressure but is restricted to relatively low occupancies. Thermodynamic modeling of these results indicates that the solid solution between laumontite with W1 full and W1 empty is characterized by a solvus with a critical temperature near 323 K.

Fridriksson, T., Bish, D.L. and Bird D.K. (2003) Hydrogen-bonded water in laumontite I: X-ray powder diffraction study of water site occupancy and structural changes in laumontite during room-temperature isothermal hydration/dehydration. *American Mineralogist*, **88**, 277-287.

RADIOGENIC CARBON IN GOETHITE FROM THE UPPER ORDOVICIAN NEDA FORMATION: IMPLICATIONS FOR POST-BURIAL RE-CRYSTALLIZATION

Jason C. Austin, Paul A. Schroeder, and Julia Cox

Department of Geology, 210 Field St., University of Georgia, Athens, GA 30602-2501, USA;
austinj1@uga.edu

The $\text{Fe}(\text{CO}_3)\text{OH}$ component of natural goethite from the Upper Ordovician Neda Formation type locality was analyzed for the presence of radiogenic carbon isotopes to test the hypothesis that the goethite has been re-crystallized in the recent past (< 50 ky). Atmospheric P_{CO_2} of the Ordovician has been estimated using the mole fraction of CO_2 in goethite from this formation (Yapp, 1996) assuming that the goethite acts as a closed system with respect to CO_2 . Evidence of the re-crystallization of the hematite (Kean, 1981) in the formation implies that the goethite was similarly affected. The presence of radiogenic carbon indicates that the goethite in these rocks is not a closed system after burial and lithification and therefore, inferences made about the environment of their formation, including atmospheric P_{CO_2} must take this alteration into account. The absence of radiogenic carbon isotopes indicates that re-crystallization has not occurred in the recent past and supports the theory that the goethite is a closed system.

Carbon dioxide was cryogenically collected from goethite under vacuum using the dehydration-decarbonation method of Schroeder and Melear (1999). 400 mg samples yielded ca. 15 μmol of CO_2 similar to that collected by Yapp (1996). Radiogenic carbon isotope analysis requires ca. 80 μmol CO_2 , thus multiple samples were required. Standards were exposed to the extraction line and collected over the same time-temperature conditions. These included the use of blanks and materials of known radiogenic carbon content (coal, tree lignin, and oxalic acid).

Kean, W.F. (2002) Paleomagnetism of the Late Ordovician Neda iron-ore from Wisconsin, Iowa and Illinois. *Geophysical Research Letters*, **8**, 880-882.

Schroeder, P.A. and Melear, N.D. (1999) Stable carbon isotopic signatures preserved in authigenic gibbsite from a forested granitic regolith: Panola Mt., Georgia, USA. *Geoderma*, **91**, 261-279.

Yapp, C.J. (1996) The abundance of $\text{Fe}(\text{CO}_3)\text{OH}$ in goethite and a possible constraint on minimum atmospheric oxygen partial pressures in the Phanerozoic. *Geochimica et Cosmochimica Acta*, **60**, 4397-4402.

ELASTIC PROPERTIES OF CLAYS

Arpita P. Bathija, Haiyi Liang, Moneesh Upamanyu, Ning Lu, and Manika Prasad

Colorado School of Mines, Golden, CO 80401, USA; abathija@mines.edu

The presence of clay minerals has significant consequences for the exploration and production of gas and oil as they affect seismic wave propagation. Knowledge of the elastic properties of clay is therefore essential for the interpretation and modeling of the seismic response of clay bearing formations. The elastic properties of clays and clay platelets are being studied experimentally, theoretically, computationally (molecular simulations) and by hybrid techniques.

These different techniques contribute to the large discrepancy in values of elastic moduli of clay minerals. In the literature, the reported Young's modulus for clays varies between 5 GPa and 400 GPa. This large variation may be due to different kinds of clays, different external environments or anisotropy owing to the layered structure of clays. Since several clay mineral layers with interlayer spacing between layers, form a sub-stack of clay, the Reuss average can be used to calculate the elastic properties of this sub-stack. The interlayer spacing, comprised mostly of bound water and some cations (with lower elastic properties), dominates the Reuss average.

We modeled the interlayer properties using Monte-Carlo molecular simulation for different stress values and number of water molecules. The Young's modulus of clay platelets reported from theoretical studies varies within the range 178–265 GPa. For our study we used a value of 200 GPa. The equilibrium interlayer spacing and Young's modulus of the interlayer obtained from molecular simulation (stress changes were in the order of GPa) were then used to compute the sub-stack properties. Using the Reuss average we found that the Young's modulus varied from 6 GPa to 21 GPa for a 2 layer sub-stack as we varied the water content from 112 to 0 molecules. Similarly, for a 3 layer sub-stack, the Young's modulus we obtained varied from 3 GPa to 10.5 GPa and for a 8 clay mineral sub-stack, the modulus varied from 1 GPa to 3 GPa. The elastic softening with increasing layers in the sub-stack as well as increasing water content is apparent.

We are currently measuring the Young's modulus and hardness of the reference clays using atomic force microscopy (AFM) for different stack thicknesses. The number of clay mineral layers forming the sub-stack can then be interpreted by comparing with model values obtained as above. SEM studies and grain size distribution of the clay mineral samples are used in conjunction with AFM in this study.

Since, measuring the Young's modulus of an individual clay platelet is complicated, this method will help in understanding the variation in AFM measurements. This work will give us insights into the elastic properties of these minerals which are still used as a fudge factor in seismic studies.

RESULTS ON Pu DIFFUSION EXPERIMENTS IN THE OPALINUS CLAY

Andreas Bauer, B. Fiehn, Ch. Marquardt, J. Römer, A. Görtzen, and B. Kienzler

Forschungszentrum Karlsruhe, Institut für Nukleare Entsorgung, PO Box 3640, D-76021 Karlsruhe

The Opalinus Clay (OPA) is a potential host rock for a repository for spent fuel, vitrified high-level waste and long-lived intermediate-level waste in Switzerland. Owing to its small hydraulic conductivity (10^{-14} - 10^{-13} ms $^{-1}$), it is expected that transport of solutes will be dominated by diffusion. Diffusion coefficients are very sensitive parameters in performance assessment (PA). The diffusion process is well understood for non-retarded solutes with simple chemistry, but little is known for retarded solutes such as strongly sorbing actinides. Therefore, the objective of this work is to understand Pu & Am diffusion in clay mineral-rich geological samples in order to provide support for improved representation of these processes in PA and to enhance safety case credibility.

A sample cell - autoclave system (SCAS) was developed for carrying out actinide diffusion experiments in clay stones under their natural, confining pressure. To verify our SCAS we performed HTO diffusion experiments. The effective diffusion coefficients of the OPA perpendicular to bedding was found to be 1.6×10^{-11} m 2 /s, which is in good agreement with the value determined by Van Loon et al., 2003. According to the results of batch sorption data, a strong ^{238}Pu sorption under the experimental conditions of the diffusion experiment is expected. After termination of the diffusion experiments the clay core was cut for autoradiography in two pieces perpendicular to the bedding plane. Autoradiography revealed a very heterogeneous distribution of ^{238}Pu on the inlet surface of the clay sample and also along the cut cross section. In the OPA porewater Pu(V) dominates speciation. If the OPA, porewater is circulated over the clay inlet surface, Pu(IV) becomes dominant.

These ongoing investigations will provide the necessary basis for credible description of sorbing radionuclide mobility in clay for the nuclear waste disposal safety case.

Van Loon, L. R., Soler, J. M., and Bradbury, M. H. (2003) Diffusion of HTO, Cl-36(-) and I-125(-) in Opalinus Clay samples from Mont Terri - Effect of confining pressure. *Journal of Contaminant Hydrology*, **61**, 73-83.

ENTHALPIC STUDIES OF HYDRATION/DEHYDRATION PROCESSES IN CLAY MINERALS

Kristen M. Baugh and Alyx S. Frantzen

Stephen F. Austin State University, Department of Chemistry, Nacogdoches, TX 75962 (USA); baughkm@titan.sfasu.edu

When clay is suspended in water, it undergoes three basic enthalpic processes. In the first stage of hydration, the clay particles are separated from one another. The particles are completely surrounded by water which is endothermic. After separation, water molecules act as wedges to separate the clay layers, exposing the interlamellar region. This step is also endothermic. Once exposed, the cationic species present in the interlamellar region can be hydrated. Most cationic species are more stable with a sphere of hydration; as such, this process is exothermic. The amount of energy released during this step is cation specific. In general terms, the higher the charge of the cation, the stronger its attraction for water, assuming similar size. For ions of the same charge, the smaller the ion, the stronger its attraction for water. Experiments using solution calorimetry and different clay-cation combinations support this trend. These results also indicate that the ΔH_{hyd} is exothermic, implying that the final step, cation hydration, is the enthalpic driving force in the overall hydration process.

Similar trends are expected in the dehydration process. For ions of the same charge, a smaller ion requires more energy to dehydrate since it has a greater affinity for water. For cations of similar size but differing charges, the cation with the higher charge should be more difficult to dehydrate due to its stronger attraction for water. However, experimental results involving differential scanning calorimetry seem counterintuitive. Since dehydration is an extensive process, the amount of water present in the sample must be taken into account. Cations that coordinate water better have larger spheres of hydration and therefore more water if present. It stands to reason that these cations would require more energy to dehydrate due to the sheer amount of water present around them. Cations with higher charges have fewer spheres of hydration as they cannot coordinate water as well as a similarly sized cation with a smaller charge. Smaller cations can have multiple spheres of hydrations, while larger cations cannot bind their outer layers of water. Therefore, the hydrated radius of the larger cation is smaller than that of the smaller cation. Thus, it should be easier to dehydrate the larger cations than a smaller cation of the same charge. This is the trend seen with differential scanning calorimetry.

A COMPARATIVE STUDY USING SEA AND DISTILLED WATER TO SYNTHESIZE ZEOLITE FROM COAL FLY ASH HYDROTHERMALLY AT LOW TEMPERATURES

Claudia Belviso^{1,2}, Francesco Cavalcante², and Saverio Fiore²

¹Università degli Studi di Bari, Bari, Italy; belviso@imaa.cnr.it

²IMAA-CNR, Tito Scalo (PZ), Italy

Coal fly ash is the most abundant coal combustion by-product. Some of it is used in concrete and cement manufacturing but more than half of it finds no applications and is disposed of in landfills. An area where fly ash utilization has gained ground in the last few years is in the synthesis of zeolites. This application is possible because the main component of fly ash is amorphous aluminosilicate glass which is a very reactive component. Synthetic zeolites are known for their ability to act as catalysts, to absorb liquids and gases, and to exchange ions.

In the present study, a sample of coal fly ash from an Italian thermoelectric power plant was used to synthesize geopolymers and zeolites X, A, and P. The large amount of amorphous aluminosilicates and the highly alkaline medium both acted to promote the geopolymerization reaction. Geopolymers can be viewed as the amorphous equivalent of some synthetic zeolites. Hydrothermal experiments were performed, after a fusion pre-treatment with NaOH, for four days using both sea water and distilled water at 25, 30, 35, 40, 45, 60, 70, and 90 °C. Chemical characterization of the fly ash for major constituents and trace elements was performed, respectively, by X-ray fluorescence and ICP-MS analysis, after acid dissolution. Products were characterized by X-ray diffraction, scanning electron microscopy, and Fourier-transform infrared spectroscopy. Our results showed that the geopolymerization reaction occurred in the 25 °C sample with distilled water, whereas geopolymeric material and crystalline phases formed in the product reacted at 25 °C with sea water. Significant modification of the fly ash occurred at 30 and 35 °C in distilled water, and large amounts of zeolite X formed at 40°C. These data indicate that the synthesis of zeolite X takes place readily at 35 °C in sea water. Minimal differences were detected in experiments carried out at 60 and 90 °C in both distilled and sea water.

Zeolitization at low temperatures could represent a potential application for fly ash with relatively low power requirements, yielding useful industrial products from waste material in an economically advantageous way. Both geopolymers and zeolites may be potentially useful to reduce the amount and mobility of metals in a variety of environmental applications.

Chang, H.C. and Shih, W.H. (1998) A general method for the conversion of fly ash into zeolites as ion exchangers for cesium. *Industrial & Engineering Chemistry Research*, **37**, 71-78.

Van Jaarsveld, J.G.S., Van Deventer, J.S.J. and Lorenzen, L. (1997) The potential use of geopolymeric materials to immobilize toxic metals: Part I. Theory and applications. *Minerals Engineering*, **10**, 659-669.

MONITORING SMECTITE HYDRATION IN THE PRESENCE OF BACTERIA

Julia N. Berger¹, Laurence N. Warr¹, Marie-Claire Lett², and Nicolas Perdrial¹

¹Centre de Géochimie de la Surface, 1 rue Blessig, 67084 Strasbourg, France;
Julia.Berger@illite.u-strasbg.fr

²Laboratoire de Microbiologie et de Génétique, rue Goethe, 67083 Strasbourg, France

An in-situ wet cell reaction chamber adapted for X-ray diffraction monitoring was used to study the hydration behavior of two different smectites (NAu-1 nontronite and MX80 bentonite) with and without bacteria. This experimental set up is suggested as an analogue for large scale confined volume environments such as underground repositories (Warr & Berger, 2006).

Partitioning of water between interlayers (responsible for sealing) and non-interlayer sites (open pores and absorption on free surfaces) was quantified as a function of packing density and the activity of the bacteria *Shewanella putrefaciens*. The bentonite samples show an expected increase in the total uptake of water with lower packing densities whereas the presence of bacteria (initial density 4.0E05 cfu/ml) enhances total water uptake by up to 18%. The sealing capacity of this clay is, however, maintained as almost all water is absorbed in the interlayer space. In contrast, the interlayer absorption of water in nontronite appears more strongly dependent on the presence of bacteria. Compared to sterile samples, the bacteria-containing nontronite increases in total water uptake by only 9% but at the same time shows a decrease in interlayer expansion. TEM observations indicate partial dissolution of clay particles by bacterial digestion and incorporation of major cations (Si, Ca and Fe). The consumption of interlayer Ca could lead to the fixation of other cations such as K and is suggested as a possible mechanism of water layer collapse and reduced sealing. Excess water is suggested to be used for bacterial growth and the production of biofilms that are observed to be abundant by optical microscopy. Depending on the type of clay, bacteria are seen to significantly alter the sealing capacity (e.g. by dissolution) and water retention potential of clays. These experiments provide additional experimental constraints for modeling elemental transport and sorption processes in porous media under the influence of bacterial activity.

Warr, L.N. and Berger, J.N. (2006) Hydration of bentonite in natural waters: Application of "confined volume" wet-cell X-ray diffractometry. *Physics and Chemistry of the Earth*. In press.

HYDROUS MINERALS UNDER MARS SURFACE CONDITIONS

David L. Bish¹, J. William Carey², Steve J. Chipera², David T. Vaniman², and Claire Fialips³

¹Department of Geological Sciences, Indiana University, 1001 E. 10th St., Bloomington, IN 47405, USA; bish@indiana.edu

²Los Alamos National Laboratory, Mail Stop D469, Los Alamos, NM 87545, USA

³Civil Engineering and Geosciences, Univ. of Newcastle upon Tyne, NE1 7RU, UK

Both orbital and lander data strongly suggest that Mars was once a wet planet and that H₂O exists today in surficial deposits. For example, the Mars Odyssey orbiter (Feldman et al., 2002) documented the spatially variable presence of H, presumably OH and/or H₂O, in amounts up to ~10 wt.%-equivalent H₂O at martian mid-latitudes. However, the nature of this H is uncertain, and it could exist in a variety of forms, including as ice and in hydrous minerals. Both remote sensing and *in situ* spectral data have been interpreted to support the presence of a variety of potentially hydrated minerals, including clay minerals, zeolites, and a large variety of sulfate and chloride minerals including jarosite, gypsum, and hydrated Mg-sulfates. For example, OMEGA spectral data suggest the existence of Fe-rich smectite, montmorillonite, and Fe-rich chlorite in Noachian rocks (> 3.5 billion years old) (Poulet et al., 2005). These deposits contrast with deposits of sulfate and chloride salts that are inferred to be much younger and to have formed via distinct processes (Squyres et al., 2004). We take the existence of such hydrated minerals for granted on the surface of Earth, but the lower total atmospheric pressure on Mars and the much lower P(H₂O) may make these minerals unstable on Mars' surface, particularly over the very long time spans since their inferred formation. It is therefore necessary to evaluate the stability of potential martian hydrous minerals; we have done so using a combination of experimental measurements and theoretical extrapolations to current Mars surface conditions. Experiments included water vapor adsorption measurements and controlled-temperature and -humidity X-ray powder diffraction experiments. Using this approach, we have shown that smectites and the zeolites clinoptilolite and chabazite can exist in a hydrous state under martian surface conditions. This is a reflection of the high energies with which water molecules are held in these minerals and also of the relatively low temperatures on Mars. Interestingly, their energetics and kinetics are such that many hydrous minerals have the potential to dehydrate and hydrate on a diurnal scale, making them possible contributors to diurnal atmospheric P(H₂O) variations. Many other minerals hold their water molecules so strongly (e.g., some ferric sulfates, Mg-Na-K sulfates and chlorides) that they are not expected to dehydrate under martian conditions. Not only do orbital and lander data support the presence of hydrous minerals on Mars, our data show that such minerals can be reasonably expected to remain hydrated under typical surface conditions. Hydrated minerals might be expected to be stable on other planetary bodies, such as Jupiter's moon, Europa, where low temperatures might stabilize some salt hydrates.

Feldman, W.C., et al. (2002) Global distribution of neutrons from Mars: Results from Mars Odyssey. *Science*, **297**, 75-78.

Poulet, F., et al. (2005) Phyllosilicates on Mars and implications for early martian climate. *Nature*, **438**, 623-627.

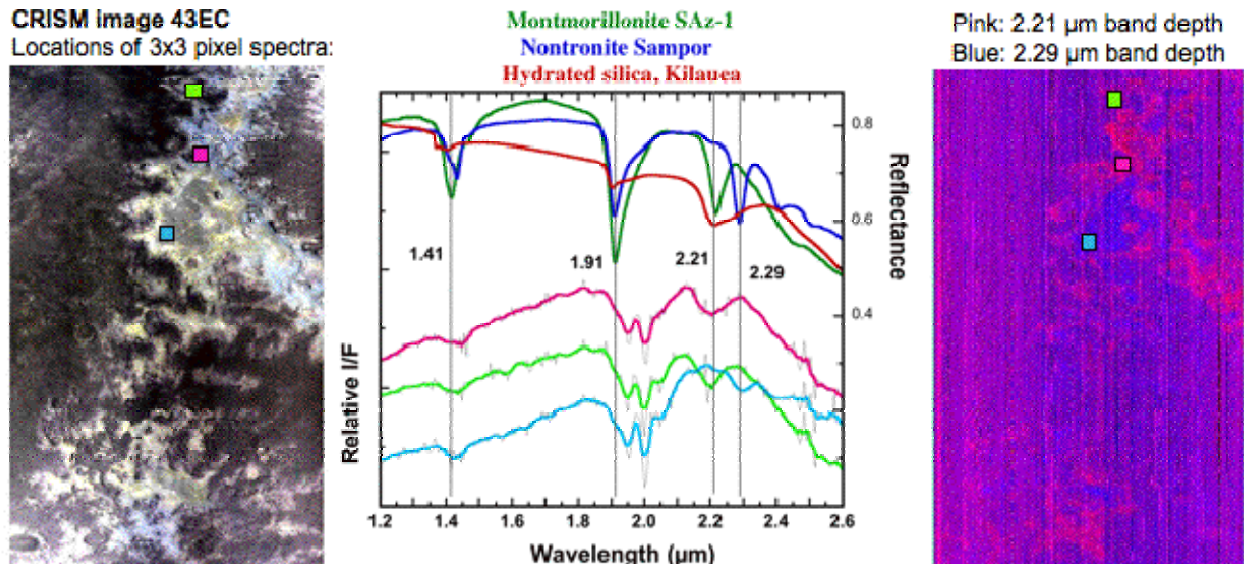
Squyres, S., et al. (2004) The Opportunity Rover's Athena science investigation at Meridiani Planum, Mars. *Science*, **306**, 1698-1703.

CHARACTERIZATION OF PHYLLOSILICATES ON MARS: A COMPARISON OF CRISM HYPERSPECTRAL DATA OF MAWRTH VALLIS WITH PHYLLOSILICATES AND HYDRATED MATERIALS

Janice L. Bishop¹, Jean-Pierre Bibring², Adrian J. Brown¹, Roger N. Clark³, M. Darby Dyar⁴, Bethany L. Ehlmann⁵, Ralph E. Milliken⁶, Scott L. Murchie⁷, John F. Mustard⁵, Shannon M. Pelkey⁵, Gregg Swayze³, and the CRISM Team

¹SETI Institute/NASA-ARC, Mountain View, CA 94043, USA; jbishop@arc.nasa.gov; ²IAS, Orsay, France; ³U.S.G.S., Denver, CO 80225, USA; ⁴Dept. of Astronomy, Mt Holyoke College, South Hadley, MA 01075, USA; ⁵Dept. of Geol. Sciences, Brown Univ., Providence, RI 02912, USA; ⁶JPL/Caltech, Pasadena, CA 91109, USA; ⁷JHU/APL, Laurel, MD 20723, USA.

Phyllosilicates were first observed in several ancient terrains using OMEGA hyperspectral images (Poulet et al. 2005). Ongoing studies of phyllosilicates in multiple CRISM images are confirming these observations and identifying new deposits. This image of Mawrth Vallis (HRL43EC: 24.7 Lat, 339 Lon) was collected at ~39 m/pixel with 544 channels from 0.36 to 3.9 μm and has been processed to remove most of the atmospheric features (strong bands near 2 μm). Spectroscopic bands due to surface minerals are observed near 1.41, 1.91 and 2.21 or 2.29 μm . Examples of three spectral types are shown in pink, green and blue. The pink region of the band map image (right) exhibits a band centered near 2.21 μm . Some of this material has a broad band characteristic of hydrated silica or glass. Other localities (e.g. green box and spectrum) have a narrower 2.21 μm band that is more similar to spectra of AlOH in phyllosilicates such as montmorillonite. Spectra of the blue regions exhibit a 2.29 μm band and are more consistent with Fe-rich phyllosilicates. Examples of lab spectra are shown for comparison. Continuing work involves comparing the CRISM spectra in this image to those in other phyllosilicate-rich regions and to additional lab spectra of phyllosilicates, hydrated materials and mixtures.



Poulet, F., Bibring, J.-., P., Mustard, J. F., Gendrin, A., Mangold, N., Langevin, Y., Arvidson, R. E., Gondet, B. & Gomez, C. (2005) Phyllosilicates on Mars and implications for the early Mars history. *Nature*, **438**, 632-627.

ADDITIONAL STUDIES OF CARBON PAINT RETENTION IN SOUTHWESTERN NATIVE AMERICAN POTTERY TRADITIONS

Eric Blinman¹ and Duane M. Moore²

¹ Museum of New Mexico, Office of Archaeological Studies, PO Box 2087, Santa Fe, NM 87504-2087, USA; eric.blinman@state.nm.us

² Dept. of Earth and Planetary Sciences, Univ. of New Mexico, Albuquerque, NM 87131, USA

Ancient and modern Southwestern pottery traditions are diverse, including many instances of reliance on carbon paints. Ancient carbon paint traditions are highly regionalized, with extremely consistent combinations of paste, slip, and paint characteristics within distinct cultures. Some of these traditions are associated with relatively high temperature firings (900° C or greater), with atmospheres that progress from reduction through neutral through light oxidizing conditions. Modern Rio Grande Valley carbon paint traditions are linked to a single slip clay source, a lower temperature firing, and relatively weaker reduction firing phases. Carbon paint retention has been associated with high-smectite clay minerals on theoretical and experimental grounds, but studies have been initiated by laboratory research rather than building from actual pottery traditions. This study examines the diversity of clay mineral compositions in ancient and modern carbon paint traditions, and it explores the interaction of clay characteristics and firing regime adaptations in the success of carbon paint retention.

FIRING BEHAVIOR OF ANCESTRAL PUEBLOAN POTTERY CLAYS, CLAY MINERALOGY, AND EXPLANATIONS OF THE VARIABILITY OF POTTERY TRADITIONS IN TIME AND SPACE

Eric Blinman¹ and George S. Austin²

¹Museum of New Mexico, Office of Archaeological Studies, PO Box 2087, Santa Fe, NM 87504-2087, USA; eric.blinman@state.nm.us

²New Mexico Bureau of Geology and Mineral Resources, New Mexico Tech, 801 Leroy Place, Socorro, NM 87801-4796, USA

As part of a larger study of clay pottery firing performance carried out by Lawrence Sitney, clay mineral characteristics were determined by X-ray diffraction studies of ten pottery clay samples and one fired test tile. Eight of the clays are from Colorado Plateau sedimentary formation sources that were accessible to Ancestral Puebloan potters, one sample is a residual clay from the Mogollon highlands, and the final clay sample is from an alluvial deposit within the Rio Grande Valley. The single fired test tile was from the least refractory of the Colorado Plateau clays. The clay mineral mixtures in the samples are compared with laboratory firing performance characteristics of the clays and expectations based on the clay mineral composition. The more refractory clays are correlated with “Anasazi” firing regimes that achieved reduction atmospheres at relatively high temperatures in formal trench or pit kilns. The less refractory clay mineral combinations are associated with less formal basin kiln features (Rio Grande Valley) or “Mogollon” firing regimes that were designed with less intensive reduction phases. The least refractory clay is from the Colorado Plateau and has dramatically different performance characteristics than the other Colorado Plateau clays. This clay is regionally associated with a distinctive Protohistoric Navajo pottery tradition that appears to combine strong reduction atmospheres and relatively low temperatures.

GLASS TO GLAUCONY: GREENSAND GENESIS IN THE LATE CRETACEOUS KANGUK FORMATION, DEVON ISLAND, NUNAVUT

John D. Bloch¹, Mike Spilde², Lynn L. Heizler³ and Nelia Dunbar³

¹Department of Earth & Planetary Sciences, University of New Mexico, Albuquerque, NM, USA; jdbloch@unm.edu

²Institute of Meteoritics, University of New Mexico, Albuquerque, NM, USA

³New Mexico Bureau of Geology and Mineral Resources, Socorro, New Mexico, USA

Marine to non-marine mudstones, glauconitic sandstones and interbedded, glass-bearing bentonites of the middle to late Campanian Kanguk Formation crop out in two north-south trending grabens on northern Devon Island (~76° N), Nunavut, Canada. In Eidsbotn Graben, glaucony facies are over 70 m thick and consist dominantly of moderately to intensely-bioturbated, pelletal, fine-grained sandstone. The mineralogy of these sandstones consists primarily of quartz and glaucony pellets with subordinate nontronite, feldspars, hematite and sporadic kaolinite. In contrast, the marine mudstones are composed of opaline silica, nontronite, illite, kaolinite and minor quartz, feldspars, and allochthonous glaucony pellets. The opaline silica is wholly opal-A diatomaceous remains.

The glaucony grains display two distinct morphologies: smooth pellets and cracked "brain" grains with irregular shape. Both morphologies occur as bright green, dominantly homogeneous grains and dark green to almost black grains with a more heterogeneous internal fabric.

Glaucony also occurs as a replacement phase of siliceous microfossils and detrital aluminosilicates. The bright green pellets have K₂O contents of between 6 and 8 wt% (hydrous basis) indicating an evolved to highly evolved character. The darker pellets and brains have K₂O contents of between 4 and 6 wt% suggesting a nascent to slightly evolved character. X-ray diffraction data indicate a mixed-layer component in the glaucony grains and the sandstone matrix material is largely nontronite.

Microprobe analysis of volcanic glass shards that are commonly preserved in the interbedded bentonites indicate a high-Fe rhyolite composition. Backscattered-electron microscopy reveals the alteration of this glass to nontronite. Al-normalized mass balance calculations suggest that one mole of rhyolite glass will yield ~1.9 moles of glauconite through a nontronite intermediary and provides silica and iron to fuel diatom growth. The mixture of nascent to evolved glaucony grains therefore is not potassium limited, but may result from either bioturbation and/or relatively rapid burial.

Moderate to intense bioturbation mixes low permeability mud with sand-sized material and may reduce K-diffusion necessary for "maturation" of glaucony. The significant thickness of glaucony facies in Eidsbotn Graben is most likely due to syndepositional faulting and associated subsidence. Thus, both depositional and tectonic factors result in the preservation of an unusual, high-latitude glaucony facies.

IMPROVED METHOD FOR MEASURING SMECTITE SURFACE AREA AND ABUNDANCE BY POLYVINYL PYRROLIDONE (PVP) ADSORPTION IN SOLUTION

Alex Blum¹, Dennis D. Eberl¹, Ronald Hill², and Neil Fishman²

¹USGS, 3215 Marine St., Boulder, CO 80303 USA aeblum@usgs.gov

²USGS, Box 25046, Mail Stop: 939 Denver, CO 80225-0046

We previously developed a method for quantitatively determining smectite abundance using polyvinylpyrrolidone (PVP) adsorption on smectite particles dispersed in solution. Adsorption density of PVP-55 on a wide range of smectites, illites and kaolinites is $\sim 0.95 \text{ mg/m}^2$. Smectites have high surface areas ($\sim 760 \text{ m}^2/\text{g}$) that usually dominate the surface areas of smectite containing samples, and the PVP uptake is then directly related to the smectite abundance. When illite and/or kaolinite are present in much greater abundance than smectite, quantitative XRD (Srodon et al. 2001) can be used correct the PVP determined surface area for these minerals, and to uniquely determine the smectite abundance. In the previous method for PVP surface area measurements (Blum & Eberl 2004) $\sim 50 \text{ mg}$ of Na-saturated smectite was dispersed in 5 ml of water and one ml of 10% by wt. PVP-55 (mean MW 55,000). The sample then was centrifuged, a portion of the solution decanted, and the PVP concentration in solution determined by mass after drying. The mass of PVP adsorbed on the sample was then computed by difference. This method while accurate, had several limitations for its practical application, which have now been overcome.

In the original technique, high charge smectites were found not to disperse completely if the solid/solution ratio of Na-sat smectite was greater than $\sim 10 \text{ mg}$ of smectite per ml (Blum & Eberl 2004), which limited the working range of the method. Using Li-sat clays permits much greater solid:solution ratios of high charge smectites, eliminating this complication. Determination of PVP concentrations in solution by evaporation and weighing also presented several practical difficulties. PVP is very hydroscopic, and variations in moisture content could lead to errors in the measured PVP mass. Additionally, any other solid or solute in solution would lead to an error in the mass measurement, so that complete removal of excess salt, suspended clay particles and dissolved organic matter was essential. Finally, the determination of PVP by mass required precise laboratory technique that was difficult to sustain on a routine basis.

We now determine the PVP concentration in solution by attenuated-reflectance FTIR. FTIR is insensitive to LiCl in solution up to 1 M and to natural DOC and suspended solids. This reduces the need to wash and centrifuge the samples, greatly simplifying the method, and reducing the need for meticulous laboratory technique required by the mass determination. Removing organics by low temperature ashing of mature shales from the North Sea increases PVP uptake by $\sim 25\%$, presumably by releasing smectite particles bound in aggregates by organic matter exposing new surface area. The kerogen itself does not appear to adsorb, or otherwise interfere with the PVP measurement.

Blum, A. E. and Eberl, D. D. (2004) Measurement of clay surface areas by polyvinylpyrrolidone (PVP) sorption and its use for quantifying illite and smectite abundance. *Clays and Clay Minerals*, **52**, 589-602.

Srodon J., Drits, V. A., McCarty, D. K., Hsieh, J. C. C., and D. D. Eberl. (2001) Quantitative X-ray diffraction analysis of clay-bearing rocks from random preparations. *Clays and Clay Minerals*, **49**, 514-528.

MINERALOGY AND ENVIRONMENTAL GEOCHEMISTRY OF OPEN-PIT LAKES RELATED TO SEDIMENTARY KAOLIN DEPOSITS FROM PORTUGAL

Iuliu Bobos

Departamento de Geologia, Universidade do Porto, Rua do Campo Alegre 687, Porto 4168-007, Portugal; ibobos@fc.up.pt

To evaluate mass transfer chemistry from kaolin rocks to open-pit lake, the mineralogy and geochemistry of a sedimentary kaolin deposit from the Estremadura region (Portugal) was investigated. The kaolin deposit occurs in a very extensive drainage basin that was active during Mesozoic and Tertiary time and accumulated eroded metamorphic rocks that were deposited close to the Atlantic Ocean. Water samples collected from open-pit lakes were filtrated and the residue was analysed for mineralogical and chemical content. Electrical conductivity and pH were measured at several sites of each open-pit lake and measurements were also made on leaching kaolin suspensions. Samples were analysed for mineralogical composition by X-ray diffraction, Fourier-Transform Infrared spectroscopy and scanning electron microscopy (SEM). Major, trace and rare earth elements were determined by inductively-coupled spectroscopy analyses.

The mineralogy of the kaolin-rich rocks is constituted mainly by kaolinite \pm halloysite-7Å \pm iron oxides. Non-crystalline Si-Al material was identified in aqueous solutions. Clusters of isolated grains that are a few micrometers in diameter are rich in SiO_2 and poor in Al_2O_3 or rich in Al_2O_3 and poor in SiO_2 , as observed in SEM analyses. The water chemistry of open-pit lakes is characterized by a relatively high concentration of total Si, Al and Na. The pH of waters from open-pit lakes becomes weakly acid (3.8 –4.5) and enriched in REE's. The interaction of kaolin rocks with plankton and microbiological communities are characterised. The concentration of Al_{tot} in equilibrium with gibbsite was calculated. Also, REEs were physically mobilized in aqueous systems. Chondrite-normalized REE patterns of kaolin samples were correlated to REE normalizations obtained from waters. Both patterns exhibit a positive Eu-anomaly, where the first displays higher REE contents than former. Using mineralogical sources for released major elements and REEs, the weathering balance and mass transfer from kaolin deposits to open-pit lakes and tailings were estimated. The mobility of silica, aluminum and REEs becomes more pronounced during a period of high-charge discharge.

Both processes of hydration and hydrolysis of kaolinite occur in the catchment area, where the removal of Si and Al was accelerated during humid periods by the waters that drained the kaolin deposits.

MODELING THE ACID-BASE SURFACE CHEMISTRY OF MONTMORILLONITE

Ian C. Bourg^{1,2,3,4}, Garrison Sposito^{1,3}, and Alain C.M. Bourg²

¹Department of Civil and Environmental Engineering, University of California, Berkeley, CA, USA; ibourg@nature.berkeley.edu

²Environmental HydroGeochemistry (LHGE-JE2397), Université de Pau et des Pays de l'Adour, Pau, France

³Geochemistry Department, Earth Sciences Division, Lawrence Berkeley National Laboratory, Berkeley, CA, USA

⁴Agence Nationale pour la Gestion des Déchets Radioactifs (ANDRA), Châtenay-Malabry, France

Proton uptake on montmorillonite edge surfaces can control pore water pH, solute adsorption, dissolution kinetics and clay colloid behavior in engineered barriers and natural weathering environments. Knowledge of proton uptake reactions, however, is currently limited by strong discrepancies between reported montmorillonite titration data sets and by conflicting estimates of edge structure, reactivity and electrostatics. In the present study, we show that the apparent discrepancy between titration data sets results in large part from the widespread use of an erroneous assumption of zero specific net proton surface charge at the onset of titration. Using a novel simulation scheme involving a surface chemistry model to simulate both pretreatment and titration, we find that montmorillonite edge surface chemistry models, that account for both the “spillover” of electrostatic potential from basal onto edge surfaces and for the stabilization of deprotonated Al-Si bridging sites through bond-length relaxation at the edge surface, can reproduce key features of the best available experimental titration data (the influence of pretreatment conditions on experimental results, the absence of a point of zero salt effect, buffer capacity in the acidic pH range). However, no combination of current models of edge surface structure, reactivity and electrostatics can quantitatively predict, without fitted parameters, the experimental titration data over the entire pH range (4.5 to 9) and ionic strength (0.001 to 0.5 mol dm⁻³) covered by available data.

Bourg, I.C., Sposito, G. and Bourg, A.C.M. (2007) Modeling the acid-base surface chemistry of montmorillonite. *Journal of Colloid and Interface Science*, submitted.

HEAT-INDUCED STRUCTURAL TRANSFORMATIONS AND CATION RE-ORDERING IN A SYNTHETIC SWELLING MICA

Geoffrey M. Bowers¹, Michael C. Davis², Karl T. Mueller², Ramesh Ravella³, and Sridhar Komarneni³

¹Department of Geology, University of Illinois, 245 Natural History Building, 1301 W. Green Street, Urbana, IL, USA, 61801; gbowers@uiuc.edu

²Department of Chemistry, Penn State University, University Park, PA, USA.

³Department of Crop and Soil Sciences, Penn State University, University Park, PA, USA.

One swelling sodium mica of Paulus and colleagues (Na-4 mica, nominally $\text{Na}_4\text{Mg}_6\text{Al}_4\text{Si}_4\text{O}_{20}\text{F}_4$) is known to selectively bind strontium from aqueous solutions of moderate pH up to a loading of ~ 50% of the cation exchange capacity and sequester it after heat treatment at 500°C. However, the cation binding mechanisms before and after heating along with any alterations of the mica structure induced by the treatment have yet to be explored on the molecular-level. In this work, we combine ²⁷Al, ²⁹Si, ¹⁹F, and ²³Na magic angle spinning (MAS) nuclear magnetic resonance (NMR) to characterize the structure and interlayer cation environments in strontium-saturated Na-4 mica before and after a heat-induced collapse of the interlayer space. The ²⁷Al and ²⁹Si MAS NMR demonstrate that the sample consists mainly of swelling mica, though the composition does not match the ideal structural formula. Aluminum NMR also shows that a small fraction of the aluminum shifts from a tetrahedral to an octahedral coordination environment upon heating. The ²⁹Si NMR displays a nearly uniform +2.5 ppm shift for the swelling mica resonances after heating, indicative of an increased average T-O-T (T = Si or Al) bond angle in the tetrahedral sheet. Two ¹⁹F resonances are observed, one of which increases in breadth and shifts in frequency by roughly +5 ppm following heat treatment. The latter two changes in structure and local fluorine environment are consistent with a re-arrangement of the tetrahedral sheet to permit the binding of larger cations in the di-trigonal cavity. The ²³Na MAS NMR results indicate the presence of three unique sodium environments before and after heating. The heat-invariant resonance is consistent with the presence of sodium carbonate nucleated at the surface of the mica or a contaminant phase. The other two resonances are associated with interlayer sodium and reflect a migration of sodium from two unique partially hydrated binding environments to a dominantly anhydrous di-trigonal binding structure with heating. Considering the larger ionic radius of strontium and site populations from ¹⁹F NMR, it is most likely that interlayer strontium is also bound deep within the ditrigonal cavity of the collapsed micas, consistent with previously reported ⁸⁷Sr NMR (Bowers, 2006).

Bowers, G.M., Ravella, R., Komarneni, S., and Mueller, K.T. (2006) NMR Study of Strontium Binding by a Micaceous Mineral. *Journal of Physical Chemistry B*, **110**, 7159-7164.

Paulus, W.J., Komarneni, S. and Roy, R. (1992) Bulk Synthesis and Selective Exchange of Strontium Ions in $\text{Na}_4\text{Mg}_6\text{Al}_4\text{Si}_4\text{O}_{20}\text{F}_4$ Mica. *Nature*, **357**, 571-573.

³⁹K NMR INVESTIGATION OF POTASSIUM BINDING AND DYNAMICS ON HECTORITE

Geoffrey M. Bowers¹ and R. James Kirkpatrick¹

¹Department of Geology, University of Illinois, 245 Natural History Building, 1301 W. Green Street, Urbana, IL, USA 61801, gbowers@uiuc.edu

The structure and dynamics of cations in disordered interlayers and on mineral surfaces can be difficult to characterize and have been the focus of intense experimental and computational effort. K⁺ is an important cation in many minerals, including clays and micas, and we show here that ³⁹K NMR spectroscopy has significant potential to advance understanding of its behavior in disordered environments. Few applications of ³⁹K NMR appear in the literature because of its relatively low resonance frequency and potentially large quadrupolar couplings. We present here the results of a study of K-exchanged hectorite designed to (i) characterize K⁺ binding and dynamics in this swelling clay, (ii) observe any displacement of K⁺ from the surface of hectorite immersed in aqueous solution, and (iii) determine if pH (H₃O⁺ concentration) affects K⁺ binding and/or dynamics. Hectorite is a trioctahedral clay that develops negative structural charge by octahedral Li⁺ for Mg⁺² substitution. We used the Hector, CA, sample (CMS SHCa-1), which has a total layer charge of -0.36/4-Si formula unit. The ³⁹K NMR data here were collected at 14.4 T using a Varian Infinity Plus spectrometer.

The K-exchanged and dried hectorite yields a broad resonance that is skewed to more negative chemical shifts and is generally similar that of muscovite (Stebbins *et al.*, 2002). Such tailing resonances without sharp singularities reflect a distribution of local quadrupole couplings caused by structural disorder. Here these characteristics are consistent with turbostratic disorder of the exchanged sample, as observed by XRD. Spectra and T₁ relaxation rates for K-exchanged paste samples with solid/solution ratios of 1/1.5 by mass prepared from HCl solutions with pH 3, 5, and 7 provide important insight into the behavior of hydrated clays. In all three pastes, only a single resonance is visible and no pH-dependent changes in the spectra or relaxation behavior are observed. At temperatures below -10°C, the resonances are broad and featureless, indicative of rigidly held K⁺. However, above this temperature the peaks undergo dynamical narrowing, demonstrating the effects of atomic motion at frequencies in the kHz to MHz regime. However, the relaxation rate data, solid-like nutation (pulse length) behavior, and quadrupolar product calculations show that the K⁺ does not undergo solution-like motion and suggests that it maintains a strong association with the hectorite layers at all temperatures. We hypothesize that the narrowing is due to motion of interlayer water rather than to displacement and subsequent motion of K⁺ itself. Variable temperature ²H NMR experiments are underway to test this hypothesis.

Stebbins, J.F., Lin-shu Du, Kroeker, S., Neuhoff, P., Rice, D., Frye, J., and Jakobsen, H.J. (2002) New Opportunities for High-Resolution Solid-State NMR Spectroscopy of Oxide Materials at 21.1- and 18.8-T Fields. *Solid State Nuclear Magnetic Resonance*, **21**, 105-115.

FIELD EVALUATION OF A SURFACTANT-MODIFIED ZEOLITE SYSTEM FOR REMOVAL OF ORGANICS FROM PRODUCED WATER

Robert S. Bowman¹, Enid J. Sullivan², Lynn E. Katz³, and Kerry A. Kinney³

¹Department of Earth and Environmental Science, New Mexico Tech, Socorro, NM USA; bowman@nmt.edu

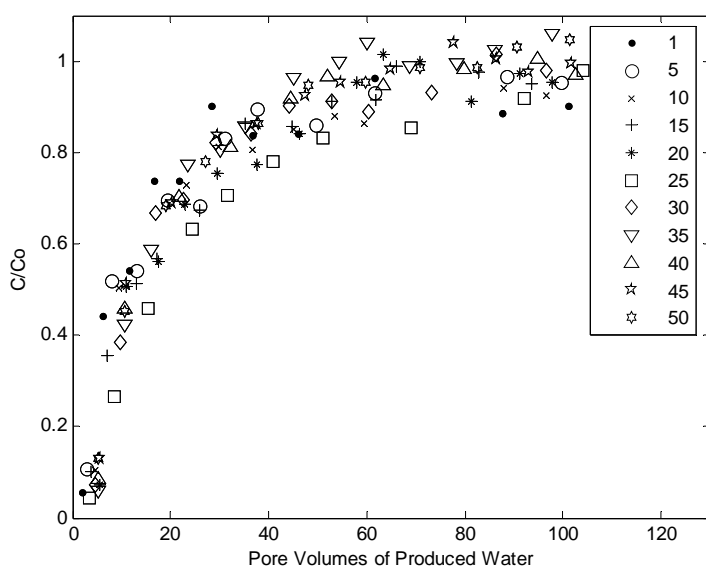
²C-ACDI Group, Los Alamos National Laboratory, Los Alamos, NM, USA

³Department of Civil Engineering, University of Texas, Austin, TX USA

Approximately 2.3 billion cubic meters (600 billion gallons) of wastewater (produced water) is generated each year as a byproduct of oil and gas operations in the continental USA. Disposal of this water represents about 10% of the cost of hydrocarbon production. Inexpensive treatment technologies can lower the cost of disposal and also generate higher quality water for other uses. Surfactant-modified zeolite (SMZ) has been shown to effectively sorb a variety of nonpolar organic compounds from water. In this study, SMZ was tested as a medium to remove benzene, toluene, ethylbenzene, and xylenes (BTEX) from produced water generated during extraction of coal bed methane. BTEX removal is necessary prior to surface discharge of produced waters or as a pretreatment for reverse osmosis.

We demonstrated in laboratory column experiments that BTEX-saturated SMZ is readily regenerated by air sparging. There was no loss in BTEX sorption capacity, and a minor decrease in hydraulic conductivity, after 50 sorption/regeneration cycles (Fig. 1). Based upon the laboratory results a pilot-scale produced-water treatment system was designed and tested at a reinjection facility in the San Juan Basin, New Mexico. The SMZ-based system was designed to treat up to 110 liters (30 gallons) of produced water per hour on a continuous basis by running two SMZ columns in series. The system performed as predicted based on laboratory results over repeated feed and regeneration cycles during the month-long operation. The BTEX-laden sparge gases were treated with a vapor-phase bioreactor system resulting in an emissions-free process.

Figure 1. Breakthrough curves for benzene transport through packed columns of SMZ. Sorption curves for every 5th sorption/regeneration cycle are shown.



A SMOKING GUN FOR PRECAMBRIAN NON-MARINE DEPOSITIONAL ENVIRONMENTS

Thomas F. Bristow, Martin J. Kennedy, and Arkadiusz Derkowsk

Department of Earth Sciences, University of California, Riverside, CA 92521. USA;
tbris001@student.ucr.edu

The Doushantuo Formation (635 to 551 Ma) spans most of Ediacaran Period, hosts the oldest animal fossils (Yin et al., *in press*) and is assumed to have a marine origin. Based on this environmental interpretation the Doushantuo fossil record has been used to support hypotheses that animal evolution was triggered by global climatic change or worldwide oxidation of the oceans. In our study, we demonstrate how the unique diagenesis of authigenic clays indicates that parts of the Doushantuo, which host the oldest animal fossils, should be reinterpreted as lacustrine.

The lower part of Doushantuo Formation, in the Yangtze Gorges area, consists of interbedded mudstones and dolomite. The shales are dominantly composed of trioctahedral smectite (saponite) and its low-temperature diagenetic product – corrensite – R1 chlorite/smectite. In contrast, two thin ash beds, one from the top of the Doushantuo Formation, the other interbedded with saponitic mudstone from the lower part of the section, are highly illitized. Stratigraphically equivalent horizons from marine sections >200 Km to the south and shales from the upper Doushantuo also contain illitized dioctahedral smectite (probably also authigenic), indicating the same diagenetic pathway as in ash beds. The advanced illitization of dioctahedral smectites proves, together with high degree of organic matter maturation, that the section has been exposed to advanced diagenetic temperatures. We suggest that the chloritization of saponite was restricted by chemical conditions during burial, while the illitization of dioctahedral smectite could progress a typical way.

The occurrence of saponite is horizontally and vertically limited. Considering other geochemical results, we interpret saponitic shales as reflecting primary depositional assemblage of an alkaline lacustrine environment. This interpretation is independently confirmed by trace element chemistry, covariation between authigenic clay content and C and O stable isotopes, typical for modern lacustrine series, and differences in C/N ratios of organic matter from marine and lacustrine facies. Our findings support hypothesis that animals developed in non-marine habitats that were more hospitable for life than the ocean, up until the Late Precambrian (Knauth, 2005). Closer attention to the clay mineral record in Precambrian sediments may provide a new tool for recognizing non-marine environments that may be a better place to look for early animal fossils.

Knauth, L.P. (2005) Temperature and salinity history of the Precambrian ocean: implications for the course of microbial evolution. *Palaeogeography, Palaeoclimatology, Palaeoecology*, **219**, 53-69.

Yin, L., Zhu, M., Knoll, A.H., Yuan, X., Zhang, J., and Hu, J., *in press*, Doushantuo embryos preserved within diapause egg cysts. *Nature*.

MICROSTRUCTURE AND CHEMICAL DEGRADATION OF ADOBE AND CLAY BRICK

Juliana Calabria A.¹, Wander L. Vasconcelos¹, and Aldo R. Boccaccini²

¹Federal University of Minas Gerais – Dept of Metallurgical and Materials Eng. Rua Espírito Santo, 35/206 Cep 30160-030, Belo Horizonte, M.G. - Brasil; j.azevedo@imperial.ac.uk, jucalabria@terra.com.br

²Imperial College London – Department of Materials, London SW7 2 BP, UK

The environmental degradation of adobe and fired clay brick was studied. Leaching media based on a $\text{Na}_2\text{S}_2\text{O}_5$ solution and deionized water were used. The microstructures, compositions and mineralogical properties of the samples were evaluated by a range of techniques including: X-ray diffraction, nitrogen sorption-desorption (BET method), Fourier transform infrared spectroscopy and scanning electron microscopy. The phases detected were kaolinite, quartz, gibbsite and goethite for the adobe and the fired brick. The high surface reactivity associated with a large amount of OH groups contributes to the significant degradation of adobe. The fired clay brick showed a significant decrease in the average pore diameter after the first day of the leaching process; its specific surface area exhibited a reduction of about three orders of magnitude. The results of the present investigation contribute to a better understanding of the correlation between structure and leaching behaviour in adobe and clay brick, and contribute to renewed interest in these materials as sustainable building blocks.

DAWSONITE CRYSTAL CHEMISTRY AND OCCURRENCE IN OIL SHALE

J. William Carey, John P. Kaszuba, and Steve J. Chipera

Earth and Environmental Sciences Division, Los Alamos National Laboratory, Los Alamos, NM 87545; bcarey@lanl.gov

Dawsonite, $\text{NaAl}(\text{OH})_2\text{CO}_3$, is a rare mineral with only a few 10's of known localities. Although it was first described in a hydrothermal environment, it occurs more frequently as an authigenic mineral including cement in siliciclastic rocks, in coal-bed fractures (cleats), and in lacustrine basins. The latter includes one of the great oil shale deposits of the western US, the Piceance Basin, in which dawsonite is a major rock-forming mineral.

Geochemical calculations suggest that dawsonite should be much more common than is observed. In this investigation, we review the literature and describe the results of synthesis and dissolution/precipitation experiments we have conducted to shed light on the genesis and petrologic implications of dawsonite occurrences. The questions we examined concerned the possibility of solid solution-induced stabilization between Na and K-dawsonite; whether dawsonite precipitation kinetics from various Al-precursors was rate-limiting; and if published thermodynamic data could accurately predict dawsonite solubility relations.

Na- and K-dawsonite were found to crystallize in distinct crystal structures and do not show evidence for solid solution between the endmembers. Thus Na-dawsonite is not stabilized by the presence of K in aqueous solution and thermodynamic calculations should apply directly to natural occurrences.

Na-dawsonite is readily synthesized from gibbsite in concentrated NaHCO_3 solutions in hours (150°C) to months ($\leq 75^\circ\text{C}$). However, syntheses from mixtures of gibbsite and opal-CT showed inhibited development of dawsonite. Syntheses with kaolinite yielded small amounts of dawsonite but other aluminosilicates (notably albite and K-feldspar) did not produce dawsonite. Synthesis studies with gibbsite at $\text{PCO}_2 = 14 \text{ MPa}$ also produced dawsonite, but a minimum bicarbonate concentration of 0.5 M NaHCO_3 was required at 150°C . These results indicate that dawsonite forms readily from Al-minerals but that silica in aluminosilicates may be an inhibitor.

Dissolution studies indicate that the thermodynamic data for Na-dawsonite accurately predicts solubility and thus geochemical calculations should provide reasonable indications of dawsonite stability. These studies also provided a solubility product for K-dawsonite ($\log K_{\text{sp}} \approx 3.2$).

The literature review is broadly consistent with these results. Dawsonite is more common in silica-depleted environments. In the Piceance Basin, Smith and Milton (1966) suggest formation of dawsonite by reaction of volcanic glass and nepheline with NaHCO_3 to produce dawsonite+analcime. In other authigenic occurrences, Al-hydroxides and/or kaolinite are present, also indicating low silica availability.

Smith, J. W. and Milton, C. (1966) Dawsonite in the Green River Formation of Colorado. *Economic Geology*, **61**, 1029-1042.

REACTIVITY OF SERPENTINE WITH CO₂: APPLICATION TO CO₂ SEQUESTRATION

J. William Carey, Hans-Joachim Ziock, and George D. Guthrie, Jr.

¹Earth and Environmental Sciences Division, Los Alamos National Laboratory, Los Alamos, NM 87545; bcarey@lanl.gov

The reactivity of CO₂ with clay minerals is relevant to both geologic storage of CO₂ (where reactions may lead to precipitation of carbonates) and to proposed industrial mineralization processes in which mined rock is reacted with CO₂ to form stable carbonates. In this study, we focused on the reactivity of serpentine [Mg₃Si₂O₅(OH)₄] because very large, relatively pure deposits exist and the resulting carbonate, magnesite, represents a potentially permanent storage form of CO₂.

We conducted experiments in a stirred autoclave at 150 °C and 140 bar CO₂ pressure in H₂O and various brines as a function of pH and the addition of potential catalyzing agents (weak acids). Reaction products were studied by X-ray diffraction; fluids were extracted with an in situ sampling device and were collected at the end of the experiments for chemical analysis; and geochemical modeling was conducted to provide insight into geochemical processes.

Magnesite formation from serpentine was kinetically limited in all solutions examined. Heat treatment (dehydroxylation) or intense grinding of serpentine did result in favorable kinetics but are probably economically unfeasible. The kinetic factors limiting the reactivity of serpentine remain obscure. Our observations indicate that the rate of dissolution of serpentine cannot explain the limited reactivity. We have also shown that nucleation and growth of magnesite occurs in other Mg-oxides and in thermally or mechanically treated serpentine and so magnesite precipitation kinetics alone cannot explain the lack of carbonation of serpentine.

Our data suggest two possible explanations. We note that Mg-oxides, Mg-silicates with a lower degree of silica polymerization, and thermally and mechanically treated serpentine yield magnesite. On dissolution in water, all of these compounds produce (or are likely to produce) more Mg²⁺ than serpentine does and, upon exposure to CO₂, will be more supersaturated with respect to magnesite than serpentine. This greater degree of supersaturation may be necessary to overcome some kinetic barrier, such as the release of Mg²⁺ from the structure or the growth of the Mg-carbonate. Our second suggestion is that the greater degree of silica polymerization in serpentine compared to Mg oxides interferes with reactivity. In this model, only the near-surface Mg is accessible for dissolution and precipitation of magnesite. Further growth of magnesite relies on extracting Mg from greater depths in the serpentine crystal where it is effectively shielded by a silica-rich carapace on the serpentine crystal. Thermal and mechanical treatment of serpentine disrupts the crystal structure thus yielding defects in the silica-enriched carapace that permit the carbonation process to proceed.

THE USE OF SMALL-PARTICLE SIZE TiO₂ SUPPORTED ON CLAYS AS PHOTOCATALYTIC MATERIALS: A LOW-COST ALTERNATIVE TECHNOLOGY FOR THE DEGRADATION OF AIR POLLUTANTS

Javiera Cervini-Silva¹, Daria Kibanova^{1,2}, Martin Trejo³, and Hugo Destaillats^{4,5}

¹Instituto de Geografía, UNAM, Ciudad Universitaria, Circuito Exterior, Coyoacán, México, C.P. 04510, México; jcervini@igg.unam.mx

²Facultad de Química, UNAM, Ciudad Universitaria, Circuito Exterior, Coyoacán, México, C.P. 04510, México

³Instituto de Física, UNAM, Ciudad Universitaria, Circuito Exterior, Coyoacán, México, C.P. 04510, México

⁴Lawrence Berkeley National Laboratory, Environmental Energy Technologies Division, Berkeley, California, USA

⁵Arizona State University, Department of Civil and Environmental Engineering, Tempe, Arizona, USA

Assisted photocatalysis by TiO₂ is an advanced oxidation process that has been employed for air and water remediation. Clays are natural porous materials bearing high surface areas and interlayer spacing that allows entrapment of small-sized particles. Pillared clays exchanged with small-sized TiO₂ can constitute materials with interesting photocatalytic properties because high surface area values and large contents of mesospores, which enables analyte trapping. Furthermore, intercalation at the clay interlayer enables TiO₂ to become more resistant to aggregation when in solution. Just recently it has been reported that clays can lead to increases in the photocatalytic activity of TiO₂ when the mesospore size is adequate to host organic solutes and ensures their effective interaction with the TiO₂ particles.

In this paper we study the photocatalytic properties of small-sized TiO₂ supported on the following clay samples: Montmorillonite [SWy-2, Na_{0.2}Ca_{0.1}Al₂Si₄O₁₀(OH)₂(H₂O)₁₀] from Crook County, Wyoming, USA; Hectorite [SHCa-1, Na_{0.4}Mg_{2.7}Li_{0.3}Si₄O₁₀(OH)₂] from San Bernardino County, California, USA; Kaolinite [KGa-1b, Al₂Si₂O₅(OH)₄] from Washington County, Georgia, USA. Deposition of TiO₂ on the clay surface was conducted using a sol-gel synthetic method. Anatase TiO₂ particles transformation at the clay interlayer was achieved by thermic treatment at 180°C. Material characterization was conducted using FTIR micro spectroscopy, Scanning Electron Microscopy (SEM), and XRD analysis. The organic compound used as probe was ethanol.

SOURCES OF COLLOIDAL MATERIAL OBSERVED DURING REHABILITATION OF LOS ALAMOS NATIONAL LABORATORY WATER-MONITORING WELLS

Steve J. Chipera and David T. Vaniman

Earth & Environmental Science, Los Alamos National Laboratory, Mail Stop D469, Los Alamos, NM, USA; chipera@lanl.gov

During the 2006 field season, Los Alamos National Laboratory conducted well rehabilitation activities on several of their water-monitoring wells, including aggressive pumping to clean well screens of sediment and blockage. In the course of pumping, turbid water samples with suspended colloids were obtained at different time intervals for further examination to determine (i) whether the colloidal suspensions were derived from the host-rock or from well construction materials and (ii) any effect these materials might have on well performance during contaminant monitoring. The three wells considered in this study were drilled to depths of 869 to 1365 ft; each well has three screens to sample the transmissive intervals in either perched or regional groundwater aquifers. The wells considered all had some screens that have continued to produce turbid water even after well development. Bentonite-based and/or polymer additives were used during drilling of the wells, and bentonite chips or coated bentonite pellets were emplaced as annular fill between the screens to seal off crossflow between screened intervals along the well casing.

Samples were obtained in 5-gallon Nalgene bottles that were allowed to sit undisturbed for periods ranging from several weeks up to several months. The water was then carefully decanted and the sediment was extracted for further analysis. Sample yields ranged from less than 10 mg to over one gram. The samples were analyzed by X-ray diffraction using a Siemens D500 diffractometer with Cu radiation. Samples were mounted either in cavity mounts or as suspensions deposited on off-axis-cut (zero background) quartz plates. Quantitative mineral abundances were obtained using the FULLPAT full pattern fitting method (Chipera and Bish, 2002). Mineralogical results suggest that the sediments extracted during the well rehabilitation were neither pure host-rock particulates nor purely well construction materials, but are a combination of the two sources. Unique minor and trace minerals from both the formation and the well construction materials are apparent in most samples. One of the materials used during well construction was called Pel-Plug, which is a coated bentonite product. The coating is diagnostic as it contains talc along with carbonates and gypsum; talc and gypsum do not occur in any of the well host rocks. Host rock particulates from the sampled intervals often have a large unaltered glass component and a complex silica polymorph assemblage (tridymite, cristobalite, and quartz). Tridymite and glass are not components in the well construction materials and are thus diagnostic of the host-rock. Trying to determine precise ratios of the colloidal material sources is not straightforward as the clays (mainly smectite) are structurally indistinguishable; both local and well-construction clays are products of alteration of rhyolitic volcanic ash. Chemical analysis may aid in distinguishing local from introduced smectites, but has not yet been conducted due to budget limitations.

Chipera, S.J., and Bish, D.L. (2002) FULLPAT: A full-pattern quantitative analysis program for X-ray powder diffraction using measured and calculated patterns. *Journal of Applied Crystallography*, **35**, 744-749.

UNIQUE MINERALOGY OF OIL SHALE FROM THE PICEANCE BASIN, COLORADO

Steve J. Chipera¹, Giday WoldeGabriel¹, Marcus Wigand², J. William Carey¹, and John P. Kaszuba¹

¹Earth & Environmental Science, Los Alamos National Laboratory, Mail Stop D469, Los Alamos, NM, USA; chipera@lanl.gov

²Chemistry Division, Los Alamos National Laboratory, Los Alamos, NM, USA;

Recent events have once again made oil shale an attractive potential resource to help fuel the world's energy requirements. One of the largest deposits, estimated at well over 700 billion barrels, is situated in the western United States in the Piceance Basin of western Colorado. The rather distinct mineralogy of these rocks represents unique conditions for deposition and subsequent diagenetic alteration.

Several outcrop samples of Piceance Basin oil shale were examined for mineralogic content and associations using X-ray powder diffraction analyses (XRD), scanning electron microscope analyses (SEM), and thin section analyses using petrographic, cathodoluminescence, and fluorescence microscopy. The samples analyzed consist of kerogen-rich materials that are representative of the Mahogany zone of the Green River Formation.

The bulk mineralogy of the samples varies from that of regular shale containing significant quantities of clay minerals (such as smectite and illite) to carbonate marl (composed of calcite and dolomite/ankerite). The oil shale samples are finely laminated with prominent mineral segregation between the various layers of inorganic and organic materials. When the layers are composed of clay minerals, the clays are found to be oriented with the microbedding and readily expand and contract with changes in water activity. Organic content (kerogen and bitumen) in the samples examined varied from absent to as high as ~40 wt% and is present as either distinct bedded layers, or as minute fragments of organic material distributed within the inorganic matrix. Sulfides are quite prevalent and associated with the organics, presumably due to the naturally reducing conditions. Outside of the organics, sulfides are present at very low abundance, either having not been present initially, or having been altered to sulfates and then extracted from the rock via water migration. Significant surficial deposits of Ca, Na, and Mg sulfates are present in western Colorado attesting to the migration and removal of sulfates from the local rock.

Other interesting minerals observed in these oil shale samples include significant quantities of the mineral dawsonite $[\text{NaAl}(\text{CO}_3)(\text{OH})_2]$, which is rather unique as it is extremely rare in nature but very abundant in the Piceance Basin. Analcime is also observed in significant quantities in these samples, (especially as nodules and clasts that appear to spread apart bedding). The sodic-rich character of this rock sequence is exemplified by the occurrence of the dawsonite and analcime as well as by nahcolite (NaHCO_3), which forms economic deposits deeper in the basin. Buddingtonite, (analogous to an ammonium version of K-feldspar) is also present and indicates an authigenic origin forming simultaneously with the maturation of the organic materials.

PREPARATION OF AMPHIPHILIC OLIGOMER/HALLOYSITE COMPOSITE MATERIALS AND THEIR ADSORPTION PROPERTIES FOR HYDROCARBONS

Kang-Sup Chung, Hwan Lee, Kwang-Kyun Hwang, Dae-Sup Kil, and Yong-Jae Suh

Korea Institute of Geoscience and Mineral Resources (KIGAM), 30 Gajeong-dong, Yuseong-gu, Daejeon, Korea 305-350; ksc@kigam.re.kr

Amphiphilic oligomer/halloysite composite materials were prepared and their adsorption properties for hydrocarbons examined. As hydrocarbon materials, various kinds of agricultural chemicals and essence oils were trapped in microtubules of halloysite and the amounts of adsorption were measured by UV-detected HPLC. Most of agricultural chemicals, including thiamethoxam [$C_8H_{10}ClN_5O_3S$] and Pyroquilon [$C_{11}H_{11}NO$] showed about 70% adsorption while thenylcholor [$C_6H_{18}ClNO_2S$] showed 90% of adsorption, which is the highest value in this work. In the case of essence oil trapped in oligomer/halloysite composite, the persistence lasted more than 10 times longer relative to non-trapped oil. This study should aid in understanding of the use of the material in additional areas such as the agrichemical, cosmetic and detergent industries, and is certain to lead to many interesting applications in these and other fields for commercial exploitation.

Levis, S.R., Deasy, P.B. (2002) Characterisation of halloysite for use as a microtubular drug delivery system. *International Journal of Pharmaceutics*, **243**, 125-134.

Joussein, E., Petit, S., Delvaux, B. (2007) Behavior of halloysite clay under formamide treatment. *Applied Clay Science*, **35**, 17-24.

CLAY MINERALOGY OF PREHISTORIC GALLINA CERAMICS FROM NORTHWEST NEW MEXICO

Connie I. Constan

Dept. of Anthropology, MSC01-1040, Univ. of New Mexico, Albuquerque, NM 87131, USA;
cconstan@unm.edu

In archaeology, the issue of resource selection is most commonly applied to rock and precious minerals, such as obsidian, chert, steatite or soapstone, metals, and ornamental stone. The goal of this project is to expand these earlier investigations to the study of ceramic technology. Compositional analyses assist in assessing an artifact's archaeological provenance, which aids archaeological interpretation. They provide a tangible link between material culture and behavior. X-ray diffraction has been applied to various American Southwest ceramics, such as Cibola, White Mountain, Salado, and Little Colorado wares.

X-ray diffraction is used here to examine the clay mineralogy of ceramic matrices from prehistoric Gallina pottery. The area of the Gallina culture is located in northwest New Mexico and dates between A.D. 850 and 1275. The Gallina ceramic assemblages include both decorated and utility wares with only extremely rare evidence of exchange of finished ceramics. I focused on two small villages: the Davis Ranch Site and Nogales Cliff House. The Davis Ranch Site has been tree-ring dated between A.D. 1049 and 1256 with a clustering of dates in the A.D. 1240s. Nogales Cliff House has tree-ring dates from only A.D. 1239 to 1267 with dates clustering in the A.D. 1250s and 1260s.

It appears that Gallina potters were using quartz, feldspar, and mica sand-size temper in their ceramics. The ceramic matrix seems to be a poorly crystallized illite-smectite mixed-layered clay mineral with perhaps a small amount of discrete illite. Kaolin mineral may also be present. The potters themselves may have mixed natural clays from more than one geologic unit, which could lead to this composition. In addition, the firing process for these ceramics reached temperatures between 750° and 850°C. This temperature range is typical for open fired ceramics in the American Southwest. At these temperatures, smectites and kaolins begin to lose their characteristic crystalline structure. The x-ray diffraction patterns show evidence of an amorphous material, indicating vitrification in the ceramic.

DISSOLUTION KINETICS OF ARSENOPYRITE IN THE PRESENCE OF IRON(III)-SEQUESTERING BIOGENIC LIGANDS AT pH 5.

Hilda Cornejo Garrido^{1,2}, Pilar Fernández², José Guzmán³, Sergey Sedov⁴, and Javiera Cervini-Silva²

¹Facultad de Química, UNAM, Ciudad Universitaria, Circuito Exterior, Coyoacán, México, C.P. 04510, México

²Instituto de Geografía, UNAM, Ciudad Universitaria, Circuito Exterior, Coyoacán, México, C.P. 04510, México

³ Instituto de Investigación en Materiales, UNAM, Ciudad Universitaria, Circuito Exterior, Coyoacán, México, C.P. 04510, México

⁴ Instituto de Geología, UNAM, Ciudad Universitaria, Circuito Exterior, Coyoacán, México, C.P. 04510, México

Arsenopyrite is one of the most important natural sources of Arsenic on Earth. Arsenopyrite is relatively insoluble in pure water. That is not the case if it is exposed to environmental conditions. Notably, arsenopyrite surfaces exposed to biological activity undergo changes in lattice energy, surface morphology, particle size, and other properties, typical of mineral dissolution. Iron biogeochemical cycling is pivotal to electron transferring in nature. Therein, the need to further scrutinize on the mechanism of arsenopyrite dissolution induced by biological activity.

In oxic environments, such as highly weathered soils or surficial seawater, microorganisms and higher plants produce biogenic ligands such as siderophores to mobilize Fe that otherwise would be unavailable. Siderophores ligands facilitate the dissolution of natural particles that represent a primary reservoir of iron. In this paper we study the stability of arsenopyrite in the presence of desferrioxamine (DFO-B), a common siderophore ligand, at pH 5. Arsenopyrite specimens from mines from Panasqueira, Portugal, were used for this study. Batch dissolution experiments of arsenopyrite (1 g L^{-1}) in the presence of DFO-B ($[\text{DFO-B}]_0 < 200 \mu\text{M}$) were conducted for 7 days. The initial pH was adjusted to 5. Samples were stirred at 150 rpm. Sieving was conducted to homogenized the particle size 0.149-0.1 mm before conducting the dissolution experiments. Corresponding experiments in the absence of DFO-B for the purpose of comparison were also conducted. Analyses for soluble metals were conducted by AA. Surface characterization was conducted by XRD and SEM-EDX. Incrustations of Pb(0) were detected in the arsenopyrite samples used for this study. In the presence of DFO-B, releases of Fe, As, and Pb showed positive trends with time. A shallower dependency was observed for release of Fe, As, and Pb in the presence of water only under similar experimental conditions. Detected concentrations of Fe, As, and Pb, after 100 h of reaction time in the presence of DFO-B were 0.3, 0.26, and 0.13 μM , respectively. Concentrations of Fe, As, and Pb, in the presence of water only were *ca.* 0.06, 0.13, and 0.01 μM , correspondingly. Hence, the effectiveness of DFO-B for releasing Pb was almost three times higher than that for releasing Fe. These results cannot be accounted for by size-to-charge considerations prevailing in metal complexation by DFO-B only.

Elemental sample enrichment as evidenced by SEM-EDX support the idea the Fe-S subunit bond energy is limiting for Fe release, while likely, the mechanism(s) of dissolution for Pb is independent and occurs concurrently to than for Fe or As.

ALKALINE EARTH METAL COMPLEXATION TO AQUEOUS CLORIDE AND TO THE GIBBSITE SURFACE: A MOLECULAR DYNAMICS INVESTIGATION

Louise J. Criscenti and James P. Larentzos

Geochemistry Department, Sandia National Laboratories, P.O. Box 5800 MS 0754, Albuquerque, NM, USA; ljcrisc@sandia.gov

The adsorption of contaminant metals onto oxide and clay minerals is a critical process that affects the extent of contaminant migration in ground water. Surface complexation models suggest that metal-anion pairs such as SrOH^+ and PbCl^+ form on mineral surfaces. Because these surface complexes are very difficult to identify using spectroscopic techniques, molecular dynamics (MD) simulations are used to assess the potential for different metal species to be present at mineral surfaces. We started our investigation by examining the relative stability of alkaline earth metals ($\text{M}^{2+} = \text{Mg}^{2+}, \text{Ca}^{2+}, \text{Sr}^{2+}, \text{and Ba}^{2+}$) and their chloride complexes in both aqueous solution and at the gibbsite (001) surface using the CLAYFF force field with a flexible SPC water model.

For each metal in aqueous solution, the free energy profile between a metal cation and a chloride anion was calculated via potential of mean force simulations. Three types of ion pairs can be identified: a contact ion pair with no water molecules between M^{2+} and Cl^- , a solvent-shared ion pair with one shared water molecule between M^{2+} and Cl^- , and a solvent-separated ion pair in which each ion retains one full hydration shell. The calculated association constants for MCl^+ suggest that the ion pair stability decreases with ionic radius, consistent with bulk thermodynamic experiments. In addition, the simulations provide more detailed information regarding the relative stability of the different types of metal-chloride pairs. The preference for contact ion pair formation increases with increasing ionic radii and is directly related to the metal hydration energies.

Surface potential of mean force curves suggest that the alkaline earth metals prefer to adsorb as outer-sphere complexes, where one water molecule is located between the metal and the gibbsite surface. Large activation barriers associated with removing water from the first solvation shell make it difficult for ions to adsorb as inner sphere complexes. However, inner sphere complexes are more likely to occur for larger ions such as Ba^{2+} , due to weaker metal-water interactions. For both the aqueous metal-chloride system and metal adsorption onto the gibbsite surface, the most dramatic variance in the free energy profiles is associated with the release of water from the solvation shell between the metal and the ligand involved - either the chloride ion or the gibbsite surface.

Sandia is a multiprogram laboratory operated by Sandia Corporation, a Lockheed Martin Company, for the United States Department of Energy's National Nuclear Security Administrator under contract DE-AC04-94AL85000.

CHARACTERIZATION OF CLAY MINERAL ASSEMBLAGES IN THE BARNETT SHALE; ITS DIVERSITY EXPLORED

Ruarri J. Day-Stirrat¹, Kitty L. Milliken², Robert G. Loucks¹, and Ben E. van der Pluijm³

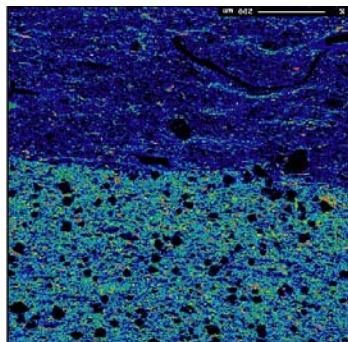
¹Bureau of Economic Geology, John A. and Katherine G. Jackson School of Geosciences, The University of Texas at Austin, University Station, Box X, Austin, TX 78713, USA. Ruarri.Day-Stirrat@beg.utexas.edu

²John A. and Katherine G. Jackson School of Geosciences, The University of Texas at Austin, University Station, Box X, Austin, TX 78713, USA.

³Department of Geological Sciences, University of Michigan, C.C. Little Building, 425 E. University Ave., Ann Arbor, MI 48109-1063, USA.

The Barnett Shale is a large onshore natural gas field located in the Fort Worth Basin, Texas. It is proven to contain 59 km³ of natural gas held in what is described as a tight gas reservoir. The unit acts as both source and seal for its high kerogen content. Currently, there are more than 100 operators working in the play applying fracture techniques to extract the natural gas reserves. Despite its economic importance, the complex petrologic character of the Barnett has received remarkably little attention.

Core material from four wells has been subjected to analysis via optical petrography, backscattered-electron imaging (BSE-I), X-ray mapping, X-ray diffraction (XRD), and high-resolution X-ray diffraction (HRXTG). These techniques reveal a variety of depositional fabrics as well as mineralogical assemblages. Clay minerals only comprise an average of around 30% of the rock and are predominantly high illite I/S. Minor quantities of chlorite have also been recorded. HRXTG reveals random orientations of phyllosilicates in carbonate-rich concretions. Carbonate-poor lithologies adjacent to the concretions reveal more strongly aligned clay fabrics indicative of burial and effective stress increases, with amount of clay material and the presence of non-platy phases dictating the degree of alignment. BSE-I and X-ray Mapping help to clarify the distinct textures and compositional variations that characterize different lithologies in the Barnett. Potassium X-ray maps provide visual confirmation of the HRXTG data. In addition, distinct depositional segregation of micaeous material within horizons of high clay content are visible within some of the carbonate-rich lithologies. In these latter zones, the thin clay drapes revealed by this technique may prove to be important zones of mechanical weakness for fracture propagation.



Scanning X-ray Map of Potassium. Bottom of image is a mica-dolomite-rich zone erosional overlain by a carbonate-rich zone with mica drapes.

IRON EXPULSION FROM THE OCTAHEDRAL SHEET OF I/S MATERIAL: A TRANSMISSION ELECTRON MICROSCOPY STUDY ON WELL CHARACTERIZED SAMPLES FROM THE PODHALE BASIN, POLAND

Ruarri J. Day-Stirrat^{1,*}, Andrew C. Aplin¹, Kuncho D. Kurtev¹ and Andrew P. Brown²

¹School of Civil Engineering and Geosciences, Devonshire Building, Newcastle University, Newcastle upon Tyne, NE1 7RU, U.K.; Ruarri.Day-Stirrat@beg.utexas.edu

²Institute for Materials Research, University of Leeds, Leeds, LS2 9JT, UK.

* now at: Bureau of Economic Geology, John A. and Katherine G. Jackson School of Geosciences, The University of Texas at Austin, University Station, Box X, Austin, TX, 78713, USA.

Transmission Electron Microscopy (TEM) has been used on separated clay dispersions to assess the change in composition of the less than 2 micrometer illite/smectite (I/S) material in a series of mudstones buried to temperatures between 75 and 175°C. Core chips from two wells in the Podhale Basin, Chochołów PIG-1 and Bukowina Tatrzanska PIG-1, straddle the bulk of the I/S transition as documented by (Srodon et al., 2006) and show smooth diagenetic trends with increasing depth/temperature: 40% illite in I/S at ~2500m increases to 75% illite in I/S at 5000m, with a further 2000m containing zero apparent I/S change. The preferred orientation of phyllosilicate minerals (I/S, chlorite+kaolinite) increases strongly through the zone of illitization (Day-Stirrat et al., submitted) and is consistent with a mineral growth mechanism involving dissolution and precipitation. Over the two kilometers below the illitization zone, there is minor reorientation.

TEM data presented here point to a systematic change in the octahedral cation ratio with increasing depth/temperature within the main zone of illitization. Results show Fe is lost and replaced by Al, with Mg and Ti remaining constant. Si in the tetrahedral sheet also remains constant. More interestingly, the same changes are noted at greater depth beyond illitization in the zone of zero apparent I/S change. The mineralogical data was collected from thin, well dispersed grains showing well developed Selected Area Diffraction Patterns (SAED) with d-spacings characteristic of illitic material. The differences in octahedral and tetrahedral cation composition between samples were tested statistically using the Kolmogorov-Smirnov test. Systematic changes with increasing burial diagenesis were noted both within the zone of maximum illitization and beyond I/S termination (slow down). This could represent inherited differences, but given the smooth diagenetic trends described by Srodon et al. (2006) this is interpreted as continued diagenetic recrystallisation beyond illitization.

Day-Stirrat, R. J., Aplin, A. C., Srodon, J. and van der Pluijm, B. A. (2007) Diagenetic reorientation of phyllosilicate minerals in Palaeogene mudstones of the Podhale Basin, southern Poland, submitted.

Srodon, J., Kotarba, M., Biron, A., Such, P., Clauer, N. and Wojtowicz, A. (2006) Diagenetic history of the Podhale-Orava Basin and the underlying Tatra sedimentary structural units (Western Carpathians): evidence from XRD and K-Ar of illite-smectite: *Clay Minerals*, **41**, 751-774.

ALTERATION OF SYNTHETIC IMPACT CRATER GLASS

Julien Declercq, Henning Dypvik, Per Aagaard, and Jens Jahren

Department of Geoscience, University of Oslo, P.B. 1047 Blindern, NO-0316 Oslo;
julien.declercq@geo.uio.no

During meteorite impacts, impact glass and melt are commonly produced in various amounts. The melt can be part of meltsheets and breccias, such as the suevite, which contain clasts of melt in a clastic matrix.

The alteration of impact melt is common, but this process has not been studied much, and consequently it is rather poorly understood. The transformation of melt to clay minerals has been recognized in several impacts and the formation of smectitic clay minerals is often registered. In this project we will study the alteration of both artificially produced glass and melt particules from the suevites of the Eyreville Core of the Chesapeake Bay impact structure. In this particular presentation the first results of the artificial melt transformations will be presented.

The glasses were specifically designed to mimic their *alter ego* from an impact into a wet target impact in the Chesapeake Bay region. Prior to any alteration the melt samples were crushed in an opal mortar, then processed in a 450ml ParrTM mixed flow reactor without using the stirring equipment. The reactor was half filled with artificial seawater and the samples were altered for one week. In order to speed up the reactions we have used temperatures at both 200°C and 300°C.

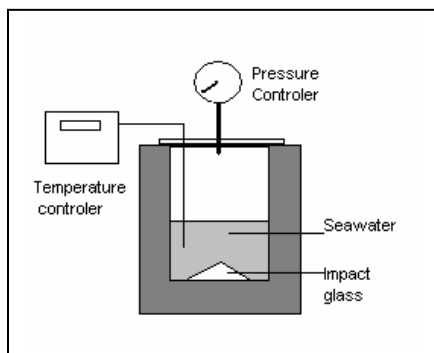


Fig. 1: Sketch of the experimental setup.

The alteration experiments of the melt have shown occurrence of possible clay minerals, on the surface of the glass shards, as well as in the fine fraction in suspension material in the solution. This study is a part of the Chesapeake Bay Impact project and the first alteration results of glass of the Eyreville Core will be published in the fall of 2007.

Horton, J.W., Jr., Ormö, J., Powars, D.S. and Gohn, G.S. (2006) Chesapeake Bay impact structure: Morphology, crater fill, and relevance for impact structure on Mars. *Meteoritics and Planetary Science*, **41**, 1613-1624.

Powars, D.S. and Bruce, T.S. (1999) The effects of the Chesapeake Bay impact crater on the geological framework and correlation of hydrogeologic units of the lower York-James Peninsula, Virginia. *USGS Professional Paper*, **1612**, 82.

MINERAL OCCURRENCE, TRANSLOCATION, AND WEATHERING IN SOILS DEVELOPED ON FOUR TYPES OF ALLUVIAL FAN DEPOSITS IN MOJAVE DESERT, SOUTHEASTERN CALIFORNIA

Youjun Deng and Eric McDonald

Division of Earth and Ecosystem Sciences, Desert Research Institute, 2215 Raggio Parkway, Reno, NV 89512; yjd@dri.edu.

Soil geomorphology and mineral composition can reveal important clues about Quaternary climate change in desert environment and offer guidance about the use and management of desert soils. The objectives of this study are to investigate (1) the mineral transformation pathways (pedogenic), if any, in desert soils weathered under the same conditions of climate and landscape; and (2) the effects of age, parent materials, and eolian processes on the transformation and translocation of the minerals. Mineralogy analysis was conducted on soils developed from the following four types of alluvial-fan deposits along the Providence Mountains piedmont, Mojave Desert, southeastern California, USA: (1) fine- to coarse-grained mixed plutonic (PM) rocks, (2) coarse-grained quartz monzonite (QM), (3) carbonate rocks, primarily limestone and marble (LS), and (4) fine-grained rhyodacite and rhyolitic tuff mixed with plutonic and carbonate rocks (VX). These juxtaposed fan deposits are physically correlated in a small area (about 20 km by 15 km) and experienced the same climatic changes in the late Pleistocene and Holocene. The surface soils, parent materials, and if present, the argillic horizons were fractionated by sieving, sedimentation, and centrifugation. Preliminary mineralogy analysis indicates that the soils show characteristic mineral compositions of arid/semiarid soils: calcite is present in nearly all of the samples, and some old soils contain gypsum and soluble salts. Parent material has profound influence on clay mineral composition of the soils: (1) talc/pyrophyllite were observed only in soils developed on the volcanic mixture fan deposits, and they occur in the entire profiles; (2) palygorskite was observed in lower horizons (B and C) of soils developed on the LS fan deposit and much less palygorskite was observed in the surface soils, which could be the result of weathering; (3) chlorite was observed mainly in soils developed on VX fan deposits and on some LS deposits, but it is absent in soils developed on PM fan deposits; and (4) vermiculite was common in soils developed on plutonic rock fan deposits. These mineralogical differences suggest that minerals in the soils are primarily inherited from their parent materials and that mineral weathering in this area was weak. Soils developed on alluvial fans with different ages (~4000 to ~200,000 yrs old) did not show distinct mineralogy difference as a function of age and soil development, which also supports the weak weathering of soils. Results indicate that the clays in the argillic horizons are primarily derived from the accumulation of desert dust, and with time, are translocated into subsoil horizons. The pedogenic accumulation of dust is a soil-geomorphic process common to the Mojave Desert, as well as other deserts in the world. More detailed electron microscopic analysis and geochemical analysis will be performed to complement the mineralogical results.

BLACK SHALES: ENCHANTED CLAYS, MYSTERIOUS ORGANICS, AND AMAZING NANOCOMPOSITES.

Arkadiusz Derkowsk, Martin J. Kennedy, and Thomas F. Bristow

Department of Earth Sciences, University of California, Riverside, 900 University Ave, Riverside, 92521, CA, USA; e-mail: arkadd@ucr.edu

Black shales can exhibit extremely high contents of organic matter, reaching 25% of total organic carbon (TOC). Such exceptional values require very unique association of conditions allowing for organic matter (OM) preservation. Beside conventional environmental factors controlling the rate of supply and decay of organic material in marine sediments such as primary productivity, oxidant concentration, rate of OM particle sinking and burial and productivity (Tyson, 2005), additional mechanisms of OM preservation such as vulcanization of organic compounds and mineral surface effects (Kennedy et al., 2002) may be important. Clay surfaces have strong physicochemical interactions between organic matter (OM) and interlayer sites within expandable clays may provide nanosites for preservation as well as spatial relationships, between clay flocs. The intercalation of OM into interlayer has not been conclusively demonstrated in ancient sediments.

We investigate the applicability of clay-OM concepts determined in nanocomposite technology (Alexandre and Dubois, 2000) to understand the resistance to temperature and oxidation many clay and organic rich sediments show. To determine the role of OM inclusion in interlayer spaces we performed several tests using samples from the Monterey Formation (California, USA) as an example of an important source rock. The behavior of natural samples, samples after OM removal, clay fractions separated directly from natural samples, and separated after the complete Jackson procedure, has been compared with artificial intercalates of standard clays and organic molecules. Tetramethylammonium and polyvinylpyrrolidone have been used as model systems representing charged and non-charged molecules, intercalated into clays through cation-exchange or surface adsorption, respectively. The tests involved: detecting structural changes and collapse temperatures of clays using XRD. The variability of surface properties before and after heating was also determined. TGA analyses showed differences in stability of OM. The results indicate that a significant portion of OM exists as intercalated (charged and adsorbed, polymerized) into interlayer space, changing the typical behavior of clay.

Organic matter exhibits markedly improved resistance to oxidation after being intercalated into clay interlayers, enhancing the OM against natural degradation. OM in sediment can beunderstood using the nanocomposite paradigm and maybe widely applicable to global-scale patterns of OM preservation

Tyson, R.V. (2005) The “productivity versus preservation” controversy: cause, flaws, and resolution. In: *Harris, N.B. (ed.)*. The deposition of organic-carbon-rich sediments: models, mechanisms, and consequences. SEPM, Special Publ. **82**, Tulsa, Oklahoma, USA.

Kennedy, M.J., Pevear, D.R. and Hill, R.H. (2002) Mineral surface control of organic carbon in black shale. *Science*, **295**, 657-660.

Alexandre, M., and Dubois, P. H. (2000) Polymer-layered silicate nanocomposites: preparation, properties and uses of a new class of materials. *Materials Science and Engineering*, **28**, 1-63.

DETECTING UNDETECTABLE: A NEW APPROACH TO THE K-Ar DATING OF GLAUCONITE

Arkadiusz Derkowski^{1*}, Jan Środoń¹, Wojciech Franus², and Michał Banaś¹

¹Institute of Geological Sciences, PAS, Senacka 1, 31-002 Kraków, Poland, * present address:

UC Riverside; 900 University Ave, 92521, CA, USA; e-mail: ndderkow@cyf-kr.edu.pl

²Lublin University of Technology, Nadbystrzycka 40, 20-618 Lublin, Poland

Immature glauconites are unsuitable for dating because of detrital contamination (Odin, 1982). An apparently mature and datable purified glauconite (*sensu* Odin, 1982) may contain conventionally undetectable traces of detrital micas and K-feldspars, which raise the absolute K-Ar age significantly. In this study we propose a method to extract the true K-Ar age even for immature glauconite and we demonstrate that a pure mature glauconite can give an incorrect age.

Our method takes advantage of the differences in dissolution rates of glauconite and its contaminants. The dissolution rates in extremely low pH of most common K-bearing detrital minerals are lower (feldspars, Al-rich dioctahedral micas) or higher (trioctahedral micas) compared to glauconite (Fe-rich dioctahedral mica), as predicted from studies of smectite behavior (Novák and Čícel, 1978). Therefore, the treatment with acid may cause full or partial dissolution of detrital and authigenic minerals, leading to changes in apparent age of the assemblage.

We used purified glauconites collected in two localities in Poland, from the Lower Cretaceous (Wąwał section, 6.25% K₂O) and the Upper Paleogene (Lublin area, 7.28% K₂O). Progressive acid dissolution (up to 7 hrs, in 3M HCl solution, at 99°C±2) was performed to determine the variability of K-Ar dates at subsequent reaction steps. Differential dates of the dissolved fractions were calculated. In the course of dissolution, K and octahedral cations were leached continuously, while the tetrahedral layer persisted as amorphous silica of microporous character, evidenced by a significant increase of BET-N₂ surface area (Temuujin et al., 2003). Generally, the apparent ages of both glauconites increased remarkably at subsequent steps of the dissolution: from 125.7 Ma to 394.7 Ma, and from 44.6 Ma to 107 Ma, respectively. This clearly suggests a decrease of glauconite content in relation to a more resistant detrital material (Al-mica and K-feldspar). The latter minerals can be observed in SEM-BSE images as single crystals strongly bound within the glauconite grains. The estimation of differential ages, based on mass balance and elements removed during the dissolution steps, revealed a pathway of K and Ar leaching. Selected differential ages can be interpreted as true ages of glauconite, free of the “excess argon”.

Removal of silica from a sample after 7 hrs of dissolution, decreases its K-Ar age from 107.0 Ma to 96.1 Ma, demonstrating Ar entrapment in residual microporous silica. Silica content and Ar retention by silica can be estimated to correct the differential ages.

Odin G.S. (1982) How to measure glaucony ages. In: *Numerical dating in stratigraphy*. Odin G.S. (ed.) John Wiley & Sons.

Temuujin J., Okada K., and MacKenzie K.J.D. (2003) Preparation of porous silica from vermiculite by selective leaching. *Applied Clay Science*, **22**, 187-195.

Novák I. and Čícel B. (1978) Dissolution of smectites in hydrochloric acid: II. Dissolution rate as a function of crystallochemical composition. *Clays and Clay Minerals*, **25**, 5, 341-344.

REMOVAL OF NITRATE AND SULPHATE ANIONS FROM AQUEOUS SOLUTION BY HDTMA-MODIFIED CLINOPTIOLITE

Sedef Dikmen and Ertuğrul Yörükogulları

Anadolu University, Science Faculty, Department of Physics, Eskişehir, Turkey;
sdikmen@anadolu.edu.tr

In the present study, we modified the surface of a natural clinoptilolite-rich tuffs with quaternary ammonium, hexadecyl trimethyl ammonium bromide (HDTMA-Br) and the adsorption of nitrate and sulphate onto HDTMA – modified clinoptilolite was investigated in aqueous solution in a batch system with respect to contact time and pH. The surface modification of HDTMA-modified clinoptilolite was monitored using the FTIR technique. BET surface areas of natural clinoptilolite and HDTMA-clinoptilolite were determined. The initial nitrate and sulphate concentrations studied were in the range of 5- 250 mg/liter. The results showed that the adsorption reached equilibrium in 15 minute for each anion. It was found that the amount of adsorbed nitrate did not change with pH while the amount adsorbed of sulphate increased with increasing pH.

INVESTIGATION OF ADSORPTION AND ION EXCHANGE PROPERTIES MAGNETIC MODIFIED NATURAL ZEOLITES.

Zafer Dikmen and Onder Orhun

Anadolu University, Science Faculty, Physics Department, Eskisehir-Turkey;
zdikmen@anadolu.edu.tr

Magnetic modification processes were first reported for synthetic zeolites and remain an active area of research (Petridis et al, 2003, Čapek et al, 2005). Although magnetic modification has shown considerable promise for applications of synthetic zeolites, similar studies on natural zeolites are rare.

In this study, magnetic modified forms of natural clinoptilolite obtained from the Bigadic and Gordes regions, Turkey, have been prepared and then characterized by XRD, XRF, DTA, and DSC. The ion exchange, adsorption and magnetic properties of these samples have been investigated. Magnetic modified forms of natural clinoptilolite samples were prepared from sived separated with particle sizes less than 63 μ m. The samples were mixed with magnetite in a mortar and intensively ground into powder. The resulting powder mixture was slowly heated up to 550°C at 1°C/min and maintained at this temperature for 6 hours. The solid sample was cooled and washed with de-ionized water until no Cl⁻ ions were detected in the eluted water. The mixture solid sample was then dried at 80°C during 16 hours (Čapek et al., 2005).

Ion exchange isotherms, ion selectivity-sequences and ion exchange capacities of the prepared samples were determined. Also, the adsorption isotherms of various gases on modified clinoptilolites were determined along with their magnetic properties.

Čapek, L., Kreibich, V., Dědeček, J., Grygar, T., Wichterlová, B., Sobalík, Z., Martens, J.A., Brosius, R. and Tokarová, V. (2005) Analysis of Fe species in zeolites by UV–VIS–NIR, IR spectra and voltammetry. Effect of preparation, Fe loading and zeolite type. *Microporous and Mesoporous Materials*, **80**, (1-3), 279-289.

Petridis, D., Bourlinos, B.A. and Zboril, R. (2003) A simple route towards magnetically modified zeolites. *Microporous and Mesoporous Materials*, **58**, 2, 155-162.

CARBON SEQUESTRATION IN CLAY-RICH MINE TAILINGS

Gregory M. Dipple¹, S.A. Wilson¹, I.M. Power², J.M. Thom¹, G. Southam², and M. Raudsepp¹

¹Mineral Deposit Research Unit, Department of Earth and Ocean Sciences, The University of British Columbia, Vancouver, British Columbia, V6T 1Z4 Canada; gdipple@eos.ubc.ca

²Department of Earth Sciences, The University of Western Ontario, London, Ontario, N6A 5B7 Canada.

We document at four sites globally, the sequestration of carbon dioxide (CO₂) in serpentine-rich mine tailings by carbonate mineral precipitation. Sequestration occurs by natural weathering of mine tailings at inactive mines and by mineral processing and weathering at active mines. The annual sequestration capacity of active mines that produce serpentine-rich tailings is typically about 10 times greater than total mine greenhouse gas (GHG) production (measured as CO₂ equivalent). Acceleration of weathering may therefore produce GHG-neutral mines. In favourable climatic conditions, abandoned mines may sequester sufficient atmospheric CO₂ by natural weathering to offset total historical mine GHG production within a few decades. Continued weathering could turn abandoned mines into net GHG sinks.

Mineral precipitates that fix CO₂ are predominantly the Mg-carbonate minerals nesquehonite, dypingite and hydromagnesite. Other Mg, Ca and Na carbonate minerals are present, but generally in limited abundance. Mineralogically and isotopically distinct abiotic and microbially mediated precipitation pathways have been identified during natural weathering. Isotopic fingerprinting is also employed in active mines to identify carbon sources and to differentiate between the tapping of industrial, atmospheric and bedrock carbon reservoirs. Quantitative phase analysis with X-ray powder-diffraction data is used to determine the modal abundance of mineral hosts for trapped CO₂ and to provide an estimate of the amount of CO₂ stored in tailings. By combining tracer studies with quantitative phase analysis, we are able to accurately assess the role that mineral processing and accelerated weathering play in reducing the greenhouse gas content of the atmosphere.

Our inorganic and microbially-mediated mineral dissolution experiments indicate that large mining operations could be engineered to capture and store carbon dioxide at a rate of 10⁴ to 10⁶ tonnes per year. Our laboratory experiments also suggest that cyanobacteria could be employed to catalyze precipitation of magnesium-carbonate minerals. Magnesium-silicate tailings are abundant and distributed globally. The annual global storage capacity of tailings produced by the mining of nickel, diamond, platinum-group elements, talc and serpentine is approximately 200 megatonnes of carbon dioxide. A parallel but less efficient pathway for carbon capture and storage in other silicate tailings increases this capacity about five-fold. Global implementation of carbon sequestration in mine tailings could therefore contribute significantly toward the stabilization of atmospheric carbon dioxide levels.

CHEMICAL AND STRUCTURAL CHARACTERIZATION OF PHARMACEUTICAL GRADE KAOLINITES

A. Umran Dogan¹ and Meral Dogan²

¹Department of Geological Engineering, Ankara University, Ankara, Turkey
dogan@eng.ankara.edu.tr

²Department of Geological Engineering, Hacettepe University, Ankara, Turkey

Seven pharmaceutical grade kaolinites (kaolins) were used in this study, which include: K1004 kaolin from Spectrum Chemical, KA105 kaolin from Spectrum Chemical, 2242-01 kaolin from J. T. Baker, K2-500 kaolin from Fisher, Acros-mono kaolin from Acros, Acros kaolin from Acros, and KX0007-1 kaolin powder from EM Science. These kaolins were compared with two kaolinites from the Clay Minerals Society source clays (KGa-1b and KGa-2). The kaolin samples are examined in detail using a high resolution Hitachi S-4000 Field Emission Scanning Electron Microscope. The powder X-ray diffraction patterns of the kaolins were recorded from the random mounts using a Rikagu D-max 2200 Powder Diffractometer with a Ni filter and Cu K α X-ray source having 0.15418 nm wavelengths. The kaolin samples were analyzed by inductively coupled plasma spectroscopy (ICP) for major oxides at ACME Laboratory, Canada. The major oxide results from ICP data of the kaolins were used as a base to calculate cation distributions in their crystal structures. Structural formulae of these kaolins were calculated on the basis of 18 oxygens.

Among the pharmaceutical grade kaolins, the KA105 and Acros-mono contained minor amounts of illite demonstrated both compositionally and structurally by using ICP and powder XRD. The KX0007-1 kaolin powder was found to be heavily contaminated with silica group minerals including quartz, opal-A, opal-CT, and cristobalite. Crystal structure computations also showed excess Si in its tetrahedral site and it does not have typical kaolinite crystal structure. These widely used industrial standards might be consumed by humans and thus should be better characterized.

COMPETITIVE ADSORPTION OF TRACE ELEMENTS ON SURFACTANT MODIFIED AND UNMODIFIED CLINOPTIOLITE

Rona J. Donahoe, Sidhartha Bhattacharyya, and Elizabeth Y. Graham

Department of Geological Sciences, The University of Alabama, Tuscaloosa, AL 35487-0338, USA; rdonahoe@geo.ua.edu

Less than a third of the fly ash produced in the U.S. by coal-fired power plants is reused, due to concerns about the trace element content of the ash. The majority of the fly ash therefore is disposed of either in dry landfills or in ash pond disposal facilities. Many of these ash disposal facilities are unlined and the potential for trace element leaching by infiltrating rain water is an environmental concern. Effective, yet low-cost, treatment methods are needed to immobilize trace elements associated with coal fly ash. The purpose of this study is to investigate the ability of surfactant-modified zeolite (SMZ) to bind trace elements associated with coal fly ash.

The trace elements associated with coal fly ash present a challenge for development of effective treatment methods because both cationic and anionic elements must be immobilized simultaneously. The zeolite mineral clinoptilolite has a high adsorption capacity for the cationic metal elements and has been used in a variety of industrial and waste treatment applications. Bowman has developed a method by which the outer surfaces of clinoptilolite and other zeolites can be modified by the addition of a bilayer of hexadecyltrimethylammonium (HDTMA) in either the chloride or bromide form. This modification allows anionic trace elements to be adsorbed on the outer surface of the zeolite, while cations can continue to be adsorbed in the zeolite's internal channelways.

Natural clinoptilolite obtained from the St. Cloud mine in New Mexico was modified with the surfactant HDTMA-Br after the method of Haggerty & Bowman (1994). A 100 ppm trace element stock solution was prepared from reagent grade soluble salts of As, B, Cr, Mo, Ni, Se, Sr and V to represent a synthetic coal fly ash leachate. Surfactant-modified zeolite and unmodified zeolite (UMZ) were reacted with the trace element solutions for 24 hours in 80 sets of batch experiments using the following variables: pH = 4, 5, 6 and 7, metal concentrations = 5, 10, 20, 50 and 100 ppm and solid:liquid (S:L) ratios = 1:15 and 1:30.

Compared to the UMZ, surfactant modification dramatically increases the ability of the zeolite to adsorb Cr and V, and significantly improves the extent of As, Mo and Se adsorption. As expected, surfactant treatment decreases the ability of the zeolite to adsorb cationic metals (Ni, Sr, K, Na). Boron adsorption by clinoptilolite is low, but is improved slightly by surface modification. Adsorption of the oxyanion elements and cationic metals both decreased with decreasing S:L ratio. The SMZ oxyanion selectivity sequence at S:L=1:15 and pH=5 is V > Cr > Mo > As \sim Se \gg B. SMZ cation selectivity sequence at S:L = 1:15 and pH=5 is Sr > Ni. These results indicate that SMZ shows promise as an additive to coal fly ash prior to its disposal to reduce trace element mobility.

Haggerty and Bowman (1994) Adsorption of chromate and other inorganic anions by organo-zeolite. *Environmental Science and Technology*, **28**, 452-258.

ORIGINS OF CLAY MINERALS IN THE GOATHILL NORTH ROCK PILE, QUESTA MINE, QUESTA, NEW MEXICO

Kelly Donahue, Nelia Dunbar, and Virginia McLemore

New Mexico Bureau of Geology and Mineral Resources, New Mexico Institute of Mining and Technology, Socorro, NM 87801, kdonahue@gis.nmt.edu

Three principle lines of evidence indicate that the clay minerals found in the Goathill North (GHN) rock pile at Molycorp's Questa mine are predominantly a product of hydrothermal alteration, not weathering: (1) Similar types and abundances of clay mineral groups, based on XRD analysis, occur both in samples of unweathered hydrothermally altered drill core and in fine-grained matrix material of the rock pile. (2) Electron microprobe chemical analyses of hydrothermally formed clay minerals in drill core samples are similar to the clay minerals both in rock fragments and in fine-grained matrix material of the rock pile. (3) Petrographic and microprobe examination of GHN's fine-grained matrix material suggests the clay minerals did not form in-situ. The mechanical grain size reduction from mining activities would have released the clay minerals contained within the hydrothermally altered silicate minerals, resulting in abundant hydrothermal clay minerals within the fine-grained matrix of the rock pile. However, clay minerals forming as a result of silicate mineral weathering could be occurring in the GHN rock pile in amounts that are too low to determine using the techniques of this study. Further investigation into analog sites with similar mineralogies but longer weathering regimes might lead to more information on the processes related to the formation of clay minerals as a result of weathering.

IDENTIFICATION AND CHARACTERIZATION OF MONTMORILLONITE BINDING PEPTIDES

Lawrence F. Drummy, Sharon E. Jones, Richard A. Vaia, and Rajesh R. Naik

Air Force Research Laboratory, Materials and Manufacturing Directorate, WPAFB, Ohio 45433, USA; Lawrence.Drummy@WPAFB.AF.MIL

We have used phage display to determine a number of specific peptide sequences that bind to montmorillonite (MMT) clay. Phage display is a combinatorial technique which uses a library of genetically engineered bacteriophage viruses presenting 5 identical copies of a single peptide sequence for binding to surfaces or particles. A series of washes are applied leaving only the most specific peptide sequences adhered to the surface. Each library of phage contains two billion 12 amino acid peptide sequences. Three different samples were examined, including a Na^+ MMT, and two surfactant exchanged MMTs, one primary ammonium and one quaternary ammonium. Verification of phage binding was performed using immunofluorescence as well as low voltage transmission electron microscopy. Characterization of the peptide intercalation/binding to the MMT in solution, by determination of the interlayer spacing using X-ray diffraction on the dried powder, showed reproducible values depending on the particular peptide used. Competition assays were used to quantify binding constants. MMT provides a well characterized materials system for the study of peptide-inorganic interactions.

MÖSSBAUER SPECTROSCOPY OF PHYLLOSILICATES: DEPENDENCE OF RECOIL-FREE FRACTIONS AND % Fe^{3+} ON LINESHAPE MODELS

M. Darby Dyar¹, Elizabeth C. Sklute¹, Martha W. Schaefer², and Janice L. Bishop³

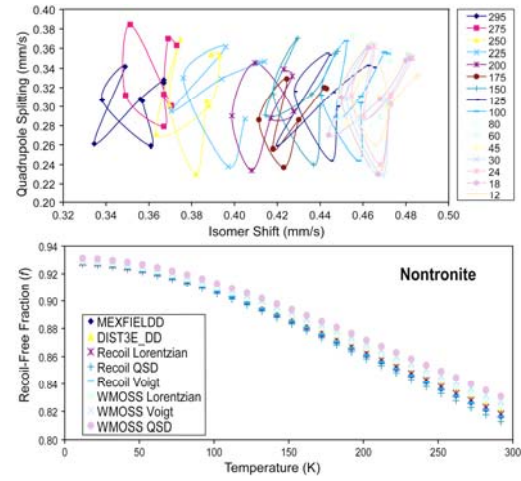
¹Dept. of Astronomy, Mount Holyoke College, South Hadley, MA 01075, USA;
mdyar@mtholyoke.edu

²Dept. of Geology & Geophysics, Louisiana State University, Baton Rouge, LA 70803, USA.

³SETI Institute/NASA-Ames Research Center, Mountain View, CA, 94043, USA.

Phyllosilicates are ubiquitous constituents in soils on Earth, are infrequently found in meteorites, and also occur on planetary surfaces in the presence of water. However, little is known about the fundamental Mössbauer parameters (including the recoil-free fraction, f) that are characteristic of clay minerals, and are critical to correctly interpreting $\text{Fe}^{3+}/\Sigma\text{Fe}$ ratios as well as mineral modes. Multi-temperature spectra of well-characterized single mineral samples at multiple temperatures are required for the determinations of f . Thus, we present here measurements of six phyllosilicates with a range of layer types, including glauconite, zinnwaldite, clinochlore, biotite, nontronite, and smectite. Spectra were fit using 1) WMOSS from WEB Research Co. in Minnesota (Lorentzian, Voigt, and quadrupole splitting distributions, or QSD); 2) RECOIL from the University of Ottawa in Canada (Lorentzian, Voigt, and QSD); and 3) an implementation of the Wivel-Mørup program as used at the University of Ghent in Belgium ((Lorentzian and QSD). This resulted in eight possible lineshape/software combinations to use for each spectrum. Values of f were determined using the method of DeGrave and VanAlboom (1998).

Spectra of nontronite and smectite, which contained only Fe^{3+} , were modeled with two doublets each using the models and programs described above. Variation in isomer shift is generally ± 0.02 mm/s but the quadrupole splitting values vary over a range of ± 0.06 -0.08 mm/s when different models are employed (e.g., figure at right). In the mixed valence minerals where $\text{Fe}^{2+} \gg \text{Fe}^{3+}$, Mössbauer parameters for Fe^{3+} were even more poorly constrained (though the percentage of the total Fe present as Fe^{3+} does not appear to be model-dependent). Fe^{2+} parameters for well-resolved peaks were ± 0.05 mm/s for variable models. Values for f were calculated at each temperature and for each different lineshape available to us through the three different software packages (a total of 8 possible models for 6 samples, 17 spectra each). Errors on f values are estimated from these curves to be no more than ± 0.02 , though there are a few outliers. No single lineshape model yielded the best χ^2 values for all minerals studied here, even though all were phyllosilicates. We conclude that optimal interpretation of these Mössbauer spectra requires critical use of multiple lineshape models and restraint in interpreting the results for site occupancies and Fe^{3+} contents.



DeGrave, E., and Van Alboom, A. (1991) Evaluation of ferrous and ferric Mössbauer fractions, *Physics and Chemistry of Minerals*, **18**, 337-342.

RELATIONS AMONG MINERALOGY, CHEMISTRY AND ANNUAL PRECIPITATION FOR SOILS FROM TWO CONTINENTAL-SCALE TRANSECTS OF NORTH AMERICA

Dennis D. Eberl¹ and David B. Smith²

¹U. S. Geological Survey, 3215 Marine St., Suite E-127, Boulder, CO 80303 U.S.A;
ddeberl@usgs.gov

²U. S. Geological Survey, MS 973, Denver Federal Center, Denver, CO 80225 U.S.A.

Quantitative mineralogy, determined by X-ray diffraction and RockJock, a computer program that calculates quantitative mineralogy from X-ray diffraction data, correlates with major, minor, and trace element chemistries for 387 specimens of A- and C-horizon soils sampled from east-west and north-south transects across the USA and Canada. Concentrations of the major elements were found to correlate with specific mineral phases. For example, changes in the concentration of Si in the soils are related primarily to the presence of quartz. Al is related to feldspar + clays, Ca to carbonate minerals, or to plagioclase when carbonates are not present, Fe to ferromagnesian minerals and clays, K to potassium feldspar and illite, Mg to ferromagnesian minerals, dolomite and chlorite, Na to plagioclase, and C to carbonate minerals in the C-horizon and to organic carbon in the A-horizon. Minor and trace element concentrations correlate with the same phases as the major elements with which they share similar geochemical behavior. For example, Rb follows K into feldspar and illite. Concentrations of quartz and feldspar correlate with rainfall trends east of the Rocky Mountains, suggesting that soils in this region may have reached a steady-state mineralogy. The average mineralogy of transect A-horizon soils is the same, by chi-square test, as that found for Mississippi River bottom sediments. The combination of quantitative mineralogy and chemical analysis yields a much richer portrait of soils than can be gained from chemistry alone, because the origins of chemical trends and the chemical availability of specific elements often are related to mineralogy.

PDF, A POWERFULLY DIVERSE FORMAT FOR INSTRUCTION IN CLAY MINERALOGY

Ray E. Ferrell

Department of Geology & Geophysics, Louisiana State University, Baton Rouge, LA 70803;
rferrell@lsu.edu

Knowledge of clay mineralogy is acquired in a variety of ways depending on the “learning style” of the student. The student may be a multimodal learner or rely heavily on single approaches emphasizing visual, auditory, reading/writing or kinesthetic methods for the assimilation of information. The Adobe Acrobat application can be used to prepare pdf-lessons in clay mineralogy that emphasize one or more of these styles in an easy to use cross-platform format. The “pdf” is versatile, diverse, and easy to use. Examples from the CD by Ferrell (2006) illustrate this approach for teaching basic clay mineralogy.

The course content is presented: in text modules written by the author; as reproduced journal articles; with animated and individual, multi-colored illustrations; as EXCEL spread sheets and downloadable computer applications; with Internet links; and via narrated movies. Navigation buttons provide easy access to all instructional materials from the Table of Contents and from points within the modules.

Materials related to the “structural formula” concept are typical of the various ways in which learning objectives are facilitated for different types of learners. There are a text summary and detailed literature references to support the reading/writing learner. Numerous triangular and histogram plots of chemical variability based on structural formulas appeal to the visual learner. The kinesthetic learner may download an EXCEL spreadsheet for the hands-on conversion of a chemical analysis to a 44-charge, 2:1 clay structural formula. Basic XRD clay identification procedures are presented in a similar fashion, supplemented by narrated movies to support the visual and auditory learner. The major themes in clay mineralogy are illustrated by sequential exposure to details contained in the included articles while challenging the student to globalize their understanding.

The integrated presentation of course material appealing to the different learning styles of students in a “stand alone” format is one major advantage of this approach. Members of The Clay Minerals Society are encouraged to adapt this pdf-style for the preparation of other CDs on general or specific topics of interest to students of clay mineralogy.

Ferrell, R. E. (2006) *Clay Mineralogy: An Introductory Course*. E-Series #1, The Clay Minerals Society, Chantilly, VA.

THE CEC OF THE SPECIAL CLAY SCA-3: SCIENCE OR SCIENCE FICTION?

Alyx S. Frantzen

Stephen F. Austin State University, Department of Chemistry, Nacogdoches, TX 75962, USA;
afrantzen@sfasu.edu

The cation exchange capacity (CEC) of the special montmorillonite clay SCa-3 has been reported in the literature as 153 meq/100 g. Results of experimentation in this laboratory do not coincide with this published value. The CEC was examined using several different methods including x-ray diffraction (XRD), ammonium exchange/ammonia electrode (Busenberg/Clemency method), solution calorimetry, and combustion analysis. The results of XRD of porphyrin exchanged SCa-3 were inconclusive and indicated either a significantly smaller CEC (~100 meq/100 g) or an unexpected arrangement of porphyrin molecules. A standard method of CEC determination using ammonium exchanged clay and an ammonia electrode also indicated a smaller CEC of 102 meq/100 g. The determination of the enthalpy of hydration of cationic SCa-3 species (sodium, potassium, magnesium, and calcium) also resulted in a CEC of approximately 105 meq/ 100 g. A final combustion analysis of tetraalkylammonium exchanged SCa-3 resulted in a CEC of 105 meq/100g. The reported value of 153 meq/100 g is questionable as the results of four completely different independent analyses all indicate a CEC of approximately 105 meq/ 100 g.

THE USE OF CALORIMETRIC TECHNIQUES IN THE DETERMINATION OF CATION EXCHANGE CAPACITY

Alyx S. Frantzen

Stephen F. Austin State University, Department of Chemistry, Nacogdoches, TX 75962 (USA); afrantzen@sfasu.edu

Some techniques employed in the determination of the cation exchange capacity of clay minerals are cumbersome to perform and provide the user with erroneous results. The use of ion selective electrode is one such method. Once the clay is prepared, the ISE must be standardized, and then the ammonium-clays samples run. This is a very time intensive procedure. Additionally, ISE's have particularly slow response times, especially in systems with low concentrations of analyte. Techniques using absorption spectroscopy are easy to perform, but accuracy and precision are lost due to Tyndall scattering.

Calorimetric techniques have been employed in the determination of the cation exchange capacity of clay minerals. This includes the use of Bomb Calorimetry and Solution Calorimetry. Bomb calorimetry is used to determine the energy involved with the combustion of material. Clays are exchanged with tetraalkylammonium salts and combusted in a pure oxygen environment. The temperature change detected is directly related to the energy of combustion. Since the cation exchange capacity is the number of charge sites available in the clay structure, and the combustion is due to the tetraalkylammonium ions, the energy determined should also be directly related to the temperature change. Results indicate just such a relationship. A similar trend is seen using solution calorimetry. In this technique, clays are exchanged with simple cations; sodium, potassium, magnesium, and calcium, and exposed to water. The temperature change detected upon immersion is directly related to the energy of complete hydration. Both of these techniques are substantially easier to employ than those previously mentioned and have high precision and accuracy. The time involved in both techniques is minimal compared to other procedures, especially in solution calorimetry, as the clays do not have to be exchanged with a 'special' guest cation before analysis.

ION EXCHANGE IN NATURAL HEULANDITE: EXPERIMENTS UNDER GEOLOGICALLY-RELEVANT CONDITIONS AND EQUILIBRIUM WITH ICELANDIC GEOTHERMAL SOLUTIONS

Thráinn Fridriksson¹, Stefán Arnórsson², Philip S. Neuhoff³, and Dennis K. Bird⁴

¹Iceland GeoSurvey, Grensásvegur 9, 108 Reykjavík, Iceland; thf@isor.is

²University of Iceland, Sturlugata 7, 101 Reykjavík, Iceland

³University of Florida, 241 Williamson Hall, Gainesville, Florida 32611-2120, USA

⁴450 Serra Mall, Building 320, Stanford University, Stanford, CA 94305-2115, USA

Heulandite is a common rock-forming zeolite that exhibits wide solid solution of extraframework cations, presumably due to its ready ion exchange with aqueous solutions. In order to provide a quantitative basis for interpreting and predicting the distribution of aqueous species between heulandite and aqueous solutions, ion exchange experiments were conducted. Binary ion exchange isotherms were determined at 55 and 85 °C for the following cation pairs: $\text{Ca}^{2+} - \text{K}^+$, $\text{Ca}^{2+} - \text{Na}^+$, $\text{K}^+ - \text{Na}^+$, $\text{K}^+ - \text{Sr}^{2+}$, and $\text{Na}^+ - \text{Sr}^{2+}$. In general, the experiments equilibrated within 11-15 weeks at 55 °C and 3-4 weeks at 85 °C. The binary exchange between Ca^{2+} and Sr^{2+} did not equilibrate even after 3 months at 55 °C and 4 weeks at 85 °C. Experimentally determined isotherms were used to derive equilibrium constants for the ion exchange reactions and asymmetric Margules models describing the extent of non-ideality in extraframework solid solutions in heulandite.

The applicability of the experimental results and thermodynamic models was assessed by calculating the composition of heulandite in Icelandic geothermal systems from known compositions using the regressed thermodynamic properties of $\text{Ca}^{2+} - \text{Na}^+$ exchange at 85 °C and reported compositions of Icelandic geothermal solutions in the temperature range between 75 and 93 °C. Calculations predict an average Ca mole fraction [defined as $\text{Ca}/(\text{Ca}+\text{Na})$] in heulandite of 0.74, in excellent agreement with observed compositions of heulandite from geothermal and metamorphic systems in Iceland (0.75).

The results were also used to evaluate the ion exchange equilibria between heulandite and thermal groundwater solutions in basaltic, zeolite bearing aquifers in Skagafjördur, N-Iceland. The ground waters in this region are characterized by very high Ca/Sr molar ratios (~5000) relative to bedrock and surface waters (730 and 1350, respectively). The consistently low Sr concentrations and high Ca/Sr in the ground waters implicate control by ion exchange reactions with a mineral phase with strong preference for Sr relative to Ca. Thermodynamic data for $\text{Ca}^{2+} - \text{Sr}^{2+}$ binary ion exchange between heulandite and aqueous solution, derived from the abovementioned experimental results were used along with the observed $\text{Ca}^{2+}/\text{Sr}^{2+}$ activity ratios in the ground water solutions to compute the composition of heulandite in equilibrium with the ground water. The predicted compositions of heulandite ranged between a Sr mole fraction of 0.01 and 0.03 [defined as $\text{Sr}/(\text{Sr}+\text{Ca})$], in excellent agreement with analyses of natural heulandite from Iceland.

COMBINED MOSSBAUER AND INFRARED SPECTROSCOPIC EXAMINATION OF SITE OCCUPANCY IN FERRUGINOUS SMECTITES

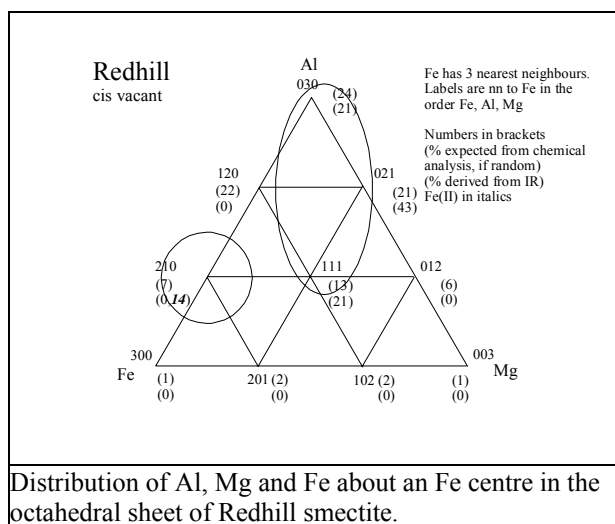
Will P. Gates^{1,2} and John D. Cashion³

¹Geomechanics, Department of Civil Engineering, Monash University, Clayton, Victoria 3800 Australia

²SmecTech Research Consulting, Bentleigh East 3165 Victoria Australia;
gateswp@smectech.com.au

³School of Physics, Monash University, Clayton, Victoria 3800 Australia

The distribution of cations within the octahedral sheet of ferruginous smectites having similar octahedral compositions was examined using infrared and Mössbauer spectroscopies. IR spectral decompositions agreed well with smectite chemistry, and the distribution of the OH-sharing octahedral cation pairs were used to model an octahedral layer for each smectite. Voigtian distributions were applied to decompose RT Mössbauer spectra of both Ca^{2+} - and Na^+ -saturated samples. The resulting distributions of quadrupole splitting (QS) and isomer shift (IS) were examined statistically. Typically, decomposition in this way resulted in two distinct distributions for QS and IS: a wide distribution (WD) and a narrow distribution (ND). Our analysis indicates that the Mössbauer derived ND is representative of Fe^{3+} centers having as nearest neighbors Fe^{3+} and Al^{3+} , and the WD represents doping of Mg^{2+} as a nearest neighbor. The distribution of the three octahedral neighbors about an Fe^{3+} center can be estimated and compared with the number expected from chemical analysis and simple Poisson statistics. For the smectites examined here, Mössbauer analysis increases the population in the 120 and 021 region of the plot, corresponding to a central Fe having $1\text{Fe}^{3+}, 1\text{Al}^{3+}, 1\text{Mg}^{2+}$ as neighboring cations, whereas IR analysis increases preferentially the 021 portion. The observed differences in octahedral populations are probably due to differences in the way IR and Mössbauer probe neighboring octahedral cation environments. Some evidence exists of Mg – Mg clustering in ferruginous smectites, which may also explain in part the differences observed.



EFFECT OF APPLICATION IRANIAN NATURAL ZEOLITE IN MANURE ON YIELD AND COMPONENT YIELD OF SUNFLOWER UNDER DIFFERENT IRRIGATION REGIMES

Majid Gholamhoseini, A.Ghalavand, and E. Jamshidi

Tarbiat Modares University of Tehran, Iran; gholamhoseinitmu1541@yahoo.com

In order to study the effect of Iranian natural zeolite (clinoptilolite) in manure on the yield of sunflower under different irrigation regimes in order to decrease use of chemical fertilizers, experiments were conducted on the research farm of Tarbiat Modares University, College of Agriculture, Tehran, Iran in 2006-2007. The experimental design was a split plot with four replicates in the form of a complete randomized block. Different irrigation regimes were the main plot factor with two levels: irrigation after using 30% available water and irrigation after using 70% available water. Different treatments of manure were the sub plot factors: f1, supplying 100% nitrogen needed for plant by urea (chemical fertilizer); f2, supplying 60% nitrogen needed for plant by urea and supplying 40% nitrogen needed for plant by manure; f3, supplying 60% nitrogen needed for plant by urea and supplying 40% nitrogen needed for plant by manure in combination with 5% weight of manure, natural zeolite; f4, supplying 60% nitrogen needed for plant by urea and supplying 40% nitrogen needed for plant by manure in combination with 10% weight of manure, natural zeolite; and f5, supplying 60% nitrogen needed for plant by urea and supplying 40% nitrogen needed for plant by manure in combination with 15% weight of manure, natural zeolite. Different irrigation regimes, different treatment of manure, and interactions of two factors showed significant variation in grain yield, oil percent, oil yield, protein percent, weight of thousand seeds, cap diameter, height, dry matter and amount of nitrogen in plant. The greatest grain yield, oil yield and protein percent (important attributes) was obtained by treatments f5&f6 (application 10 and 15% weight of manure, natural zeolite) in first irrigation regime.

The results of this experiment indicate a significant effect of application of Iranian zeolite for decreasing of using chemical fertilizers and avoiding of unsuitable effects of these chemical materials on environment. Supplying 40% nitrogen required for plant by manure in combination with 10 and 15% weight of manure, natural zeolite under the first irrigation regime is the best treatment.

NANOCOMPOSITES AND NANOFLOIDS

Emmanuel P. Giannelis

Cornell University, Materials Science and Engineering, 326 Bard Hall, Ithaca, NY 14853, USA;
epg2@cornell.edu

In the first part of this talk, I will review our work in polymer nanocomposites including our latest efforts to organize nanoparticles in controlled assemblies. In the second part, I will present our newest work on “solvent-free” nanoparticle fluids. These new hybrid systems consist of inorganic nanoparticle cores functionalized with a charged corona. Because of their molecular architecture they flow like liquids but possess no volatility. In addition, because of their hybrid nature their optical, magnetic, electronic, and other properties can be fine-tuned to meet potential applications.

METHANE + H₂O IN SMECTITE

Stephen Guggenheim and A. F. Koster van Groos

Department of Earth and Environmental Sciences, University of Illinois at Chicago, 845 West Taylor Street, Chicago, IL 60607-7059, USA; xtal@uic.edu

Guggenheim and Koster van Groos (2003) have shown by X-ray diffraction methods combined with a specially developed environmental chamber (Koster van Groos et al., 2003) that smectite can intercalate methane-hydrate (CH₄ - H₂O) complexes between the 2:1 layer of this clay. Molecular modeling (Cygan et al., 2004) supported the results of the experimental work. We are reporting here on our recent results on the ability of smectite to incorporate methane-hydrate intercalates as a function of the nature of the interlayer cation and smectite composition.

Methane-hydrate intercalates with a natural, Na-rich montmorillonite (SWy-1), with Na-exchanged montmorillonite (SWy-2), and with Na-exchanged nontronite (NAu-2). In earlier experiments (Guggenheim and Koster van Groos, 2003), synthesis of the CH₄ - hydrate smectite intercalate was slow and proceeded with difficulty. More recent experiments, using thin-film samples, show that these intercalates form nearly instantaneously, and that this reaction is easily reversible, confirming that the intercalated methane-hydrate smectite compound is thermodynamically stable at the appropriate pressure-temperature (PT) conditions.

The methane-hydrate smectite intercalate forms phases with *d*-values of ~18 to ~22 Å at moderately elevated pressures and low temperatures (e.g., > 25 bars and > 0 °C). The upper temperature stability of these phases is very similar to that of methane hydrate. In many experiments at lower temperatures and using Na-exchanged SWy-2, intercalated phases formed with discrete reflections of ~18.5, ~17.5, and ~16 Å. The 18.5-Å and 17.5-Å phases behaved with ambiguity, as the reflections either persisted or were not observed when pressure was released, suggesting that there are two different phases with the same *d*-value, either containing complexes of CH₄ - H₂O or H₂O only. The phase with a *d*-value of 16 Å contains H₂O complexes only.

We gratefully acknowledge support by the Petroleum Research Fund of the American Chemical Society under grant PRF# 43871-AC2.

Cygan, R.T., Guggenheim, S., and Koster van Groos, A.F. (2004) Molecular models for the intercalation of methane hydrate complexes in montmorillonite clay. *Journal of Physical Chemistry B*, **108**, 15141-15149.

Koster van Groos, A.F., Guggenheim, S., and Cornell, C. (2003) Elevated-pressure, low-temperature environmental chamber for powder X-ray diffractometers. *Reviews of Scientific Instruments*, **74**, 273-275.

Guggenheim, S. and Koster van Groos, A.F. (2003) A new gas hydrate phase: Synthesis and stability of clay-methane hydrate intercalate. *Geology*, **31**, 653-656.

SURFACE MODIFICATION OF LAPONITE FOR BIOMOLECULE ADSORPTION

Angela M. F. Guimarães¹, Virgínia S.T. Ciminelli,² and Wander L. Vasconcelos²

¹Departament of Engineering – Minas Gerais Federal Center for Technological Education. Av. Amazonas, 7675, Nova Gameleira, Belo Horizonte - MG - CEP 30 510 000 – Brazil;
angelamello@des.cefetmg.br

²Departament of Metallurgical and Materials Engineering - Federal University of Minas Gerais. Rua Espírito Santo, 35, Centro, Belo Horizonte - MG - CEP 30160 030 - Brazil

This work describes the process for functionalization of laponite through the grafting of 3-mercaptopropyltrimethoxysilane (MPTS). Laponite is synthetic smectite clay with surface area of 350 m²/g. The samples, prior to and after functionalization, were characterized by chemical analyses, DRIFT, XRD, TGA and MEV/EDS. Infrared spectroscopy and elemental analyses confirmed the presence of organic chains and thiol groups in the modified clay. The immobilized and available thiol group, measured according to the Volhard method, totaled 1.4 meq/g of clay, with approximately 90% accessible for Ag⁺ trapping. These results represent an improvement as compared to other works concerning the functionalization of smectite-type clays in which the affect produced by functional group blockage limits the access of species to less than 10% of the complexing sites.

A FORCE FIELD FOR LAYERED SILICATES AND SIMULATION OF INTERFACES WITH SURFACTANTS AND PEPTIDES

Hendrik Heinz¹, Richard A. Vaia², Rajesh R. Naik², Ruth Pachter², and Barry L. Farmer²

¹Department of Polymer Engineering, University of Akron, Ohio 44325; hh29@uakron.edu

²Air Force Research Laboratory, Materials and Manufacturing Directorate, WPAFB, Ohio 45433

The derivation and validation of a force field for layered silicates (mica, montmorillonite, and pyrophyllite) will be discussed. Major challenges to obtain a semiempirical energy model that reproduces the crystal structure and the surface energy of clay minerals are the assignment of atomic charges and of van-der-Waals parameters. We rely on X-Ray measurements of the electron deformation density and an extended Born model (Heinz and Suter, 2004a) to determine atomic charges, and present guidelines how to assign van-der-Waals (Lenard-Jones parameters). The van-der-Waals parameters are ultimately fine-tuned to reproduce experimentally determined values of the surface energy. The validation of computed surface energies in force fields of minerals is important and has hitherto received marginal consideration (leading to deviations up to one order of magnitude). Our force field parameters are very accurate and integrated in/compatible with common energy expressions (PCFF, CVFF, CHARMM, GROMACS) (Heinz et al., 2005).

The force field has been applied to study the self-assembly of an extensive series of alkylammonium surfactants on montmorillonite and mica surfaces (Heinz and Suter, 2004b; Heinz et al. 2003, 2007), as well as the interaction energy between the silicate sheets and surface reconstruction upon separation (Heinz et al., 2006), as it occurs during exfoliation in clay/polymer nanocomposites. The simulation aids in the molecular-level interpretation of available XRD, NMR, DSC, IR, and NEXAFS data, and the agreement with directly comparable data (basal plane spacings, phase transition temperatures, trans/gauche ratio in chain backbones) has been quantitative. In particular, the conformational analysis of the surfactant molecules, effects of hydrogen bonding of primary ammonium head groups to the surface, and the process of separation of the clay sheets are explained.

Recent simulations of the montmorillonite-water interface and the adsorption of short peptides (~12 amino acids) will also be discussed. Such systems are currently explored for applications in sensors and formation of nanocomposites with silk fibers and other biological matrices.

Heinz, H. and Suter, U.W. (2004a) Atomic charges for classical simulations of polar systems.

Journal of Physical Chemistry B, **108**, 18341-18352.

Heinz, H. and Suter, U.W. (2004b) Surface structure of organoclays. *Angew. Chem. Int. Ed.*, **43**, 2239-2243.

Heinz, H., Castelijns, H.J. and Suter, U.W. (2003) Structure and phase transitions of alkyl chains on mica. *Journal of the American Chemical Society*, **125**, 9500-9510.

Heinz, H., Vaia, R.A., Krishnamoorti, R. and Farmer, B.L. (2007) Self-assembly of alkylammonium chains on montmorillonite: effect of chain length, headgroup structure, and cation exchange capacity. *Chemistry of Materials*, **19**, 59-68.

Heinz, H., Vaia, R.A. and Farmer, B.L. (2006) Interaction energy and surface reconstruction between sheets of layered silicates. *Journal of Chemical Physics*, **124**, 224713:1-9.

Heinz, H., Koerner, K.L. Anderson, R.A. Vaia, and B.L. Farmer (2005) Force field for phyllosilicates and dynamics of octadecylammonium chains grafted to montmorillonite. *Chemistry of Materials*, **17**, 5658-5669.

**CLAY-CATALYZED INCORPORATION OF ARSENIC TO BIOORGANIC MOITIES:
A LOW-COST MECHANISM FOR AMELIORATING ARSENIC TOXICITY IN
AQUATIC SYSTEMS**

Jessica Hernández-Pineda^{1,2}, Pilar Fernández-Lomelin², Norma Ruth López-Santiago²,
and Javiera Cervini-Silva²

¹Facultad de Química, UNAM, Ciudad Universitaria, Circuito Exterior, Coyoacán, México, C.P. 04510, México; elocho.jhp@gmail.com

²Instituto de Geografía, UNAM, Ciudad Universitaria, Circuito Exterior, Coyoacán, México, C.P. 04510, México

A method for ameliorating the toxicity of arsenic has been developed. Successive methylation of arsenic has been reported to represent an important detoxification pathway in aquatic systems. Clays are natural porous materials bearing high surface areas and interlayer spacing that allows entrapment of small-sized particles. Thus, clays are natural nanomaterials that can serve as efficient catalysts in natural or engineered systems. In this paper we study the kinetics of transformation of inorganic arsenic to arseno-organic complexes as affected by the following clay samples: Montmorillonite [SWy-2] from Crook Country, Wyoming, USA, and Hectorite [SHCa-1] from San Bernardino. Country, California, USA, and Nontronite [NG-1] from Australia. The effect of environmental factors, arsenic initial concentration and speciation are discussed.

THE LOWER SILURIAN (LLANDOVERY) OSMUNDSBERG K-BENTONITE IN BALTOSCANDIA AND THE BRITISH ISLES: AGE AND CORRELATION

Warren D. Huff¹, Funda Ö. Toprak¹, Stig M. Bergström², and Roland Mundil³

¹Department of Geology, University of Cincinnati, Cincinnati, OH 45221; warren.huff@uc.edu

²School of Earth Sciences, The Ohio State University, 155 S. Oval Mall, Columbus, OH 43210

³Berkeley Geochronology Center, 2455 Ridge Rd., Berkeley, CA 94709

The Lower Silurian (early Telychian) Osmundsberg K-bentonite is a widespread altered volcanic ash bed that occurs throughout Baltoscandia and other parts of northern Europe. K-bentonite samples from sections containing the Osmundsberg K-bentonite beds were investigated to determine whether the chemical composition of these beds can be used as a basis for high-resolution chemostratigraphic correlation on a regional scale. Bivariate plots of Eu-Th/Yb, Zr-Eu, Yb-Th, Eu-La/Lu, V-Hf, Zr/Tb-Th/Yb, Eu-Ta/Yb and Zr-Th/Yb show the separation of the groups when trace elements and elemental ratios are used as discriminators. The Osmundsberg samples plot away from the other three groups and show good clustering. Thirty-three samples were analyzed for 26 trace elements by Instrumental Neutron Activation Analysis (INAA) and the data subjected to multivariate statistical analysis. The results of the discriminant analysis of these models generally support the correlation of the Osmundsberg K-bentonite bed from Baltoscandia to the British Isles and northern Europe as suggested by Bergström et al. (1998) based on biostratigraphy, but with some minor corrections.

Radiometric analysis of zircons from the Osmundsberg K-bentonite gave a 207Pb/235U age of 437.6 ± 0.5 Ma. Analyzed samples came from the type locality of this volcanic ash bed at Osmundsberget in the Siljan area of central Sweden where it occurs in the lower part of the Spirograptus turriculatus Graptolite Zone and in the lower part of the Angochitina longicollis Chitinozoan Zone. The Llandovery time scale is still in a highly provisional state with most published isotopic dates of zones and stage boundaries based on extrapolation rather than on direct radiometric analysis. This new age will bring much-needed stability to this portion of the early Paleozoic time scale.

Bergström, S.M., Huff, W.D., and Kolata, D.R. (1998) The lower Silurian Osmundsberg K-bentonite; Part I, Stratigraphic position, distribution, and palaeogeographic significance: *Geological Magazine*, **135**, 1-13.

ASPECTS OF THE EVOLUTION OF GREEN PELLETAL CLAY

Jenny Hugget

Petroclays, Heathfield, E Sussex, TN21 8QP, UK, info@petroclays.com
and The Natural History Museum, Cromwell Rd., London, SW7 4BD, UK.

The transformation of detrital clay to iron-rich clay minerals is a complex process involving mixed layer clays and it is not yet well understood (McCarty et al. 2004; Huggett et al. 2006). Nor is the geographic and environmental distribution of glaucony and verdine as clear cut and simple as was once thought. If we are to use these clays as environmental or reservoir quality indicators we need to understand what controls their formation rather better than we do at present. Temperature, water depth, latitude, rate of deposition, Eh, organic matter abundance are all factors that have been invoked as controls on which iron-rich clays form and the intensity of the mineralisation. This talk will examine all of these potential controls, and attempt to make sense of them through analysis of both new and published data.

Huggett, J.M., McCarty, D., Calvert, C.C., Gale, A.S. and Kirk, C. (2006) Odinite-smectite-vermiculite mixed layer clay from the Weches Formation Claiborne Group, Middle Eocene, NE Texas. *Clays and Clay Minerals* **54**, 101-115.

McCarty, D.K., Drits, V.A., Sakharov, B., Zvyagina, B.B., Ruffell, A. and Wach, G. (2004) Heterogeneous mixed-layer clays from the Cretaceous Greensand, Isle of Wight, southern England. *Clays and Clay Minerals* **52**, 552-575.

LONG-TERM IMMOBILIZATION OF TECHNETIUM BY NONTRONITE AGGREGATES

Deb P Jaisi¹, Hailiang Dong¹, and Steve Heald²

¹Miami University, Department of Geology, Oxford, OH 45056

²Argonne National Laboratory, Advanced Photon Source, Argonne, IL 60439

Subsurface technetium (⁹⁹Tc) contamination is of particular concern at Hanford and other U.S. Department of Energy sites for several reasons. First, the long-lived ⁹⁹Tc isotope (half-life of 2.15×10^5 years) exhibits very fast migration (as a stable pertechnetate species, TcO_4^-) through soils due to its low partitioning coefficient. Second, it easily enters into the food chain as a sulfate (SO_4^-) analogue. Our experiments showed that the Fe(II) indifferent chemical environments in reduced nontronite (NAu-2), an iron-rich smectite clay mineral, was capable of reducing mobile Tc(VII) to immobile Tc(IV) with a relative rate of reduction as follows: Fe(II) at amphoteric sites > Fe(II) at exchange sites > Fe(II) at structural sites. More importantly, NAu-2 was unique for the long term immobilization of Tc(VII). The EXAFS results suggested that ~70% of the Tc(IV) formed chains similar to $\text{TcO}_2 \cdot n\text{H}_2\text{O}$ and the remaining 30% Tc(IV) formed a bidentate-complex with Fe sites in NAu-2. The presence of Tc(IV) promoted clay particle aggregation, possibly due to chemical bonding of Tc(IV) to high energy sites of NAu-2, thus decreasing the unbalanced structural negative charge of NAu-2 and promoting cation bridging. The Tc(IV) bound to NAu-2 aggregates by these mechanisms was very recalcitrant to reoxidation in the presence of thermodynamically more favorable electron acceptors such as oxygen, nitrate, Fe(III), and Mn(III/IV) oxides at concentrations even higher than those in published inventories of nuclear fuel cycle wastes. Since the clay aggregates are relatively stable and are less likely perturbed by any transient changes in the aquifer geo-, hydro- and biochemistry, these findings may provide an important step forward for long term immobilization of contaminants such as Tc(VII).

CLAY SURFACE MODIFICATION FOR ENHANCED AFLATOXIN ADSORPTION

William F. Jaynes, Richard E Zartman, and Wayne H. Hudnall

Texas Tech University, Lubbock, Texas 79409 USA; william.jaynes@ttu.edu

Aflatoxins are toxic fungal metabolites produced by *Aspergillus* fungi in infested grain crops. Human and animal ingestion of aflatoxins can lead to cancer and death. Worldwide, 4.5 billion people may suffer chronic aflatoxin exposure. Clay mineral feed additives are used to prevent caking, but have also been shown to effectively bind aflatoxins and reduce aflatoxicosis. Clay minerals modified by treatment with organic cations more effectively sorb weakly-soluble, aqueous organic contaminants than untreated clays. Aflatoxin B1 (AfB1) is the most abundant and most toxic of the aflatoxins. Clay minerals treated with organic cations or other compounds might more effectively bind aflatoxins in feed and reduce or prevent aflatoxicosis. In this study, the aflatoxin sorption capacities of CMS reference clay minerals and surface-modified clay minerals were compared. Novasil plus, a commercial montmorillonitic clay product demonstrated to reduce aflatoxicosis when added to animal feeds, was also examined. The toxic organic cations, hexadecyltrimethylammonium (HDTMA) and trimethylphenylammonium (TMPA) were used to prepare organoclays. Organoclays were also prepared using the nutritional supplement, choline, and other non-toxic organic compounds. The AfB1 sorption capacities followed the order SWy-Choline = SWy-TMPA = 0.35Li-250-SA_z-Choline >> SWy = Novasil plus = SA_z-Choline >> SWy-HDTMA. The low-charge SWy-Choline and 0.35Li-250-SA_z-Choline clays were far more effective AfB1 sorbents than high-charge SA_z-Choline. These sorption characteristics suggest that AfB1 is retained via clay surface adsorption, not by partitioning into the cation-derived organic phase. Modified clays prepared using non-toxic organic cations, such as choline, might be used in feeds to prevent aflatoxicosis.

Jaynes, W.F., Zartman, R.E and Hudnall, W.H. (2007) Clay surface modification for enhanced aflatoxin adsorption. *The 44th Annual Meeting of the Clay Minerals Society. Santa Fe, New Mexico.*

PROTEIN-CLAY BIONANOCOMPOSITES

Cliff T. Johnston¹, Robert A. Schoonheydt², Gnanasiri S. Premachandra¹, and Joyce Lok¹

¹Crop, Soil and Environmental Sciences, 915 W. State St. Purdue University, W. Lafayette, IN 47907, USA; cliffjohnston@purdue.edu

²Centre for Surface Science and Catalysis, K.U.Leuven, Kasteelpark Arenberg 23, B-3001 Leuven, Belgium

The interaction of biological molecules with clay minerals is a topic of growing interest. In this study, the interaction of three model proteins, lysozyme, bovine serum albumin (BSA), and Fibrinogen, on saponite was examined using sorption, structural and spectroscopic methods. These proteins were selected on the basis of their amino acid composition, molecular weight, and isoelectric point. Protein sorption isotherms revealed that all three proteins showed a high affinity for Na-exchange saponite. In the case of fibrinogen and lysozyme, the amount of protein sorbed by Na-saponite was $> 1000 \text{ mg}_{\text{protein}}/\text{g}_{\text{clay}}$. The sorption capacity of BSA on Na-saponite was $\sim 300 \text{ mg/g}$. Powder X-ray diffraction analysis showed that interlayer sorption occurred for lysozyme and BSA with d-spacings approaching 4.5 nm. Intermediate phases were also detected with lower d-spacings. There was no evidence of interlayer sorption of fibrinogen. FTIR spectroscopic analysis of the clay-protein complexes indicated that the overall conformation of the protein was slightly perturbed by clay surface based on the analysis of the amide bands. Protein sorption and overall stability of the resulting bionanocomposites will be discussed on the basis of clay surface chemistry as well as the nature of the protein.

DYNAMICS OF AQUEOUS SPECIES AT INTERFACES WITH HYDROXYLATED MINERAL SURFACES: MD SIMULATION AND NMR SPECTROSCOPY

Andrey G. Kalinichev^{1,2}, Geoffrey M. Bowers¹, and R. James Kirkpatrick^{1,2}

¹Department of Geology, University of Illinois, Urbana, IL 61801, USA; kalinich@uiuc.edu

²NSF WaterCAMPWS, University of Illinois, Urbana, IL 61801, USA

At hydroxylated mineral-solution interfaces, individual water molecules and hydrated ions simultaneously participate in several dynamic processes, all of which can be characterized by different, but equally important time- and length- scales. Most of these processes can be effectively studied by classical molecular dynamics simulations in a single MD run. On a relatively long time scale (~10-100 ps), we are able to quantify the diffusional processes related to reformation of the entire interfacial H-bonding network, surface adsorption of H₂O molecules, and ions. The interfacial dynamics on the intermediate time scale (~1-10 ps) is dominated by the molecular librational and re-orientational motions. The librations (hindered rotations) of surface hydroxyls also occur at this time scale. These motions are responsible for the reformation and breaking of individual hydrogen bonds, while the strength of these bonds can be directly correlated with the frequencies of intra-molecular O–H vibrations on the shortest, sub-ps time scale. Here we compare the dynamic behavior of interfacial aqueous species at several model hydroxylated mineral surfaces investigated by MD computer simulations and NMR spectroscopy. At the (001) surface of tobermorite in contact with 0.25 M KCl aqueous solution, we are able to effectively distinguish H₂O molecules that spend most of their time within channels between the tetrahedral chains on the tobermorite surface from the adsorbed molecules residing slightly above the interface. Within the channels, H₂O molecules donate H-bonds to both the bridging and non-bridging oxygens of the bridging Si-tetrahedra as well as to other H₂O. Some of the molecules form strong H-bonds persisting over 100 ps and longer, but many others undergo librations and occasional diffusional jumps from one surface site to another. The average diffusion coefficients of the surface-associated H₂O molecules that spend most of their time in the channels and those that lie above the nominal interface differ by about an order of magnitude ($D_{H2O}=5.0\times10^{-11}\text{ m}^2/\text{s}$ and $D_{H2O}=6.0\times10^{-10}\text{ m}^2/\text{s}$, respectively). The average diffusion coefficient for all surface-associated H₂O molecules is about $1.0\times10^{-10}\text{ m}^2/\text{s}$. All of these values are significantly less than the value of $2.3\times10^{-9}\text{ m}^2/\text{s}$, characteristic of H₂O molecules in the bulk liquid, but in good quantitative agreement with ¹H NMR results for surface-associated water in tobermorite (Korb et al, 2007). The interfacial dynamics of a simple neutral hydroxylated (001) surface of quartz is noticeably faster for both H₂O molecules and dissolved ions. Na⁺ and Cl⁻ are able to adsorb and desorb from the surface on the time scale of ~100 ps and are present at the interface predominantly as outer-sphere complexes. These results are in good agreement with our ²³Na and ³⁵Cl NMR relaxation measurements. Furthermore, the uniformity of the relaxation behavior observed in the NMR experiments suggests that the degree of the quartz surface hydroxylation does not vary significantly in the entire pH range examined here (3 < pH < 10.5).

Korb, J.-P., McDonald, P.J., Monteilhet, L., Kalinichev, A.G. and Kirkpatrick, R.J. (2007)
Comparison of proton field-cycling relaxometry and molecular dynamics simulations for
proton–water surface dynamics in cement-based materials. *Cement and Concrete Research*,
37, 348-350.

SMECTITE CLAY SEQUESTRATION OF AFLATOXIN B₁: MINERAL DISPERSIVITY AND MORPHOLOGY

Ines Kannewischer, Maria G. Tenorio Arvide, G. Norman White, and Joe B. Dixon

J.B. Dixon, Soil and Crop Sciences Department, Texas A&M University, College Station, TX 77843-2474, USA; j-dixon@tamu.edu

The extent and conditions of aflatoxin (AfB₁) sorption have previously been modelled and correlations evaluated with exchange cations and relationships with AfB₁ sorption have been poor. In our earlier research we found that the sorption of AfB₁ was between smectite layers.

Recently, Fourier transform infrared analysis (FTIR) data have shown that the octahedral composition of the smectites is an indicator of smectite quality as an AfB₁ sorbent. In this study we further explore properties that might influence the sequestration of AfB₁. Laser diffraction particle size analysis (LDPSA) indicated that smectite clay size influences amount of AfB₁ sorbed and helps identify good smectite AfB₁ adsorbents. Good adsorbent smectites disperse well in sodium hexametaphosphate solution yet some exceptions were observed. Dispersivity explained 65% of the variability for most of the samples investigated as received.

Transmission electron microscope (TEM) images show typical smectites and reveal the very diverse morphological nature of smectites in bentonites. Cloudy smectite, i.e. thin particles in TEM images related positively to AfB₁-sorption capacity. Particles that are thin, often fold, and usually about 0.5 μ m across seem to be optimal. Extremely thin particles that are prone to have disorderly stacking or the relatively opaque ones in the electron beam tend to be poor sorbents of this mycotoxin. A combination of FTIR evidence of octahedral composition and dispersivity in a hexametaphosphate solution provide the most reliable indication of AfB₁ sequestration thus far.

REACTIVITY OF MAHOGANY ZONE OIL SHALE, GREEN RIVER FORMATION

John P. Kaszuba¹ and Marcus Wigand²

¹Los Alamos National Laboratory, Earth and Environmental Sciences (EES-6), Los Alamos, New Mexico 87545, USA; kaszuba@lanl.gov

²Los Alamos National Laboratory, Chemical Science and Engineering (C-CSE), Los Alamos, New Mexico 87545, USA

New approaches to *in-situ* development of oil shale resources in the Piceance Basin are being evaluated by several operators. We are conducting a suite of hydrothermal experiments to understand potential fluid-rock reaction processes that may occur with *in-situ* development. Experiments are being conducted in flexible cell hydrothermal apparatus (Dickson cells) to permit manipulation of pressure and temperature without liquid-vapor phase restrictions and to promote *in-situ* fluid/gas sampling to gauge reaction progress. Kerogen-rich outcrop samples representative of the Mahogany zone of the Green River Formation are being investigated, including a carbonate marl (composed of calcite and dolomite/ankerite) containing 10% illite. Aqueous fluids reacted with the shale include synthetic brines representative of the lower aquifer of the Piceance Basin. Experiments probe a range of temperatures, from formation temperatures (40°C) to 300°C, at reservoir (100 bars) pressure. Reaction progress is monitored by periodic sampling of evolved fluids. Aqueous sample analysis includes analysis of pH by microcombination electrode, inorganic and organic aqueous geochemistry, and total carbonate by coulometric titration. Gas sample analysis includes carbon dioxide and hydrogen sulfide. The former evolves due to dissolution of carbonates, particularly dawsonite. Quench solids are evaluated by x-ray diffraction and scanning electron microscopy to evaluate impacts to clay and carbonate mineralogy. In addition to evaluating pertinent fluid-rock reaction processes, we will present an analysis of how these properties affect predictions for *in-situ* methods of resource development and geochemical signatures of success, including indicators for environmental integrity.

ALLOPHANE FROM ECUADOR

Stephan Kaufhold¹, A. Zeisig², R. Jahn², R. Dohrmann^{1,3}, and S. Brito⁴

¹BGR, Federal Institute for Geoscience and Natural Resources, Stilleweg 2, D-30655 Hannover, Germany; s.kaufhold@bgr.de

²Martin-Luther Universität Halle-Wittenberg, Institute for agricultural and nutritional science, Ludwig-Wucherer-Straße 2Weidenplan 14, D-06108 Halle, Germany

³LBEG, State Authority for Mining, Energy, and Geology, Stilleweg 2, D-30655 Hannover, Germany

⁴DINAGE, Dirección Nacional de Geología, Juan León Mera y Orellana (esquina), Quito, Ecuador

Allophane is known as a short range order clay mineral with a high reactive surface area. Primary particles are hollow spherules with a diameter ranging from 3 – 5 nm and hence can be considered as nano-particles. Allophane occurs in different soils, particularly in andosols. The high surface reactivity is important for a lot of soil properties and additionally has been recognized by industry. Accordingly, several patents exist – predominately from Japan, New Zealand and Korea –, dealing with allophane production (synthesis, purification of soils) and application (mainly as adsorber material). Nevertheless, allophane is not available on the global market. This is supposed to be due to the lack of high class allophane deposits: Relevant allophane concentrations are only reported in andosols having low thickness and high content of organic carbon blocking the highly reactive sites.

In the 90s, the Ecuadorian and German geological survey discovered an unusual allophane occurrence which is located W' of Santo Domingo de los Colorados, Ecuador. Within a 10 – 15 m layer consisting of weathered volcanic ash a 4 m thick layer has been found containing 80 wt.% allophane and only 0.5 wt.% organic carbon. The BET surface (N₂ adsorption) of dried and crushed material varies from 300 – 340 m²/g.

By using hydrocyclones this material can be used to produce a 95 wt.% allophane quality on industrial scale in a significantly cheaper way than proposed in the various patents. Furthermore, a variety of application tests proved the applicability of this material as an adsorber in many fields (from exhaust gas cleaning to PO₄ and/or AsO₄ adsorption e.g. from contaminated drinking water).

CLAY MINERAL CONTROL OF ORGANIC CARBON DEPOSITION AND THE IMPLICATIONS OF THE ONSET OF CLAY MINERAL PRODUCTION OF SOILS IN THE LATE PRECAMBRIAN

Martin J. Kennedy¹, Mary Droser¹, David Pevear¹, and Lawrence Mayer²

¹Department of Earth Science, University of California, Riverside CA, 92521-0423
martink@ucr.edu, 951-827-2025

²Darling Marine Center, University of Maine, Walpole ME 04573

Previous work has shown a strong positive correlation between mineral surface area and adsorption of organic carbon in modern marine sediments. Our studies of black shales of varying thermal maturity and stages of diagenesis show a strong positive correlation between mineral surface area and total organic carbon in representative black shale deposits. This relation suggests that adsorption of dissolved carbon compounds or other mechanisms of preservation by clay mineral surfaces played a fundamental role in the burial and preservation of organic carbon. Additionally we have focused on the interlayer space of 2:1 smectitic clays. Our results imply that both polar and non-polar organic compounds are capable of gaining entry to the interlayer sites of smectite clay minerals. The MSA-TOC (mineral surface area) association implies organic carbon sequestration in an important class of black shales and petroleum source rocks may be more closely related to patterns of continental weathering and secular clay mineral trends than to the traditional models that consider only ocean water chemistry or marine productivity. Because most clay minerals owe their genesis to biotic soils, and the first soils are relatively late in Earth's history, secular trends in clay deposition may have played an important role in controlling organic carbon deposition and a related rise in atmospheric oxygen.

TRANSMISSION ELECTRON MICROSCOPIC CHARACTERIZATION OF MICROBIALLY INDUCED SMECTITE-TO-ILLITE TRANSFORMATION

Jinwook Kim¹, Gengxin Zhang², Hailiang Dong² and Dennis D. Eberl³

¹Naval Research Laboratory, Seafloor Sciences Branch, Stennis Space Center, MS 39529, U.S.A.; jkim@nrlssc.navy.mil

²Department of Geology, Miami University, Oxford, OH 45056, U.S.A.

³US Geological Survey, Boulder, CO 80303

The characterization of mineral transformation associated with bacterial Fe(III) reduction was made on the TEM lattice fringe images, Electron Energy Loss Spectroscopy (EELS), and selected area diffraction patterns. The microbial Fe(III) reduction in cysteine-intercalated nontronite (NAu-2) by *Shewanella oneidensis* CN32 at room temperature and bioreduction of Fe(III) in nontronite (NAu-2) at 65 °C by *Thermoanaerobacter ethanolicus* CCSD_DF_M168 isolate were studied. Previously, Kim et al. (2004) hypothesized that the microbial Fe(III) can promote the smectite-to-illite reaction at room temperature. This presentation was focused to verify the evidence for the structural mineral transformation associated with microbial Fe(III) reduction at various conditions. The statistical data on the measurements of d-(001) spacings of bioreduced nontronite inoculated with *Thermoanaerobacter ethanolicus* CCSD_DF_M168 at 65 °C show that about 55% of 132 bioreduced smectite packets transformed to the illite phase, while around 30% of 55 bioreduced organo-smectite inoculated with *Shewanella oneidensis* CN32 at room temperature showed the illite spacing. The clay-bacteria interaction at high temperature has an important implication because this condition is more relevant to diagenetic environments.

Kim, J.W., Dong, H., Seabaugh, J., Newell, S.W., and Eberl, D.D. (2004) Role of microbes in the smectite-to-illite reaction. *Science*, **303**, 830-832.

MOLECULAR DYNAMICS MODELING AND EXPERIMENTAL STUDIES OF LAYERED DOUBLE HYDROXIDES INTERCALATED WITH CARBOXYLIC AND AMINO ACIDS

R. James Kirkpatrick¹, Padma Kumar¹, Andrey G. Kalinichev¹, Qiang Li^{1,2}, and Marc X. Reinholdt^{1,3}

¹Department of Geology, University of Illinois at Urbana-Champaign, 245 Natural History Bldg., 1301 W. Green Street, Urbana, IL 61801, USA

²CTLGroup, 5400 Old Orchard Road, Skokie, Illinois 60077, USA

³Département de Génie Chimique, Université Laval Cité Universitaire, QC G1K 7P4, Canada

Computational molecular dynamics (MD) simulation provides otherwise unobtainable molecular scale insight into the structure, dynamics, and energetics of mineral interlayers and surfaces that complement and expand upon experimental observations. We describe here MD results for the Mg,Al layered double hydroxide (LDH) hydrotalcite (HT) containing interlayer carboxylic acids (citrate, formate, acetate, and propanoate) and an amino acid (glutamate) and compare these results to experimental data for citrate and glutamate HT. LDH compounds, also known as anionic clays, are of rapidly growing interest in catalysis, electrochemistry, medicine, environmental remediation, and as molecular sieves. Hydrogen bonding plays a key role in the behavior of organo-LDHs and is effectively modeled using the combination of the CLAYFF force field for the metal hydroxide layers and the CVFF force field for the organic molecules. CLAYFF uses the SPC model for water, and we used the flexible version of SPC here. A similar approach should also be effective for silicate clays with interlayer organic species. The computations show that the hydration energies of these LDHs approach the energy of bulk liquid water with increasing water content. In contrast to the behavior of LDHs containing small inorganic interlayer species, however, the hydration energies show no distinct minima as functions of water content, indicating the absence of energetically well defined structural states with specific water contents. This result is consistent with experimentally observed large basal spacings and even delamination of such HTs. The interlayer structural behavior is directly related to the energetic relationships, with electrostatic interactions and the development of an integrated H-bond network among the anions, the M-OH sites of the metal hydroxide sheets, and the interlayer H₂O molecules playing a central role. The hydrogen bonds donated to the anions from water molecules are energetically preferable to those from M-OH sites, resulting in decreasing occurrence of the anions in inner sphere coordination environments to the hydroxide sheets with increasing water content. The total number of H-bonds received by the anions becomes similar to the number they receive in bulk solution at relatively low water contents, but those from water molecules progressively replace those from M-OH sites at higher water contents. At high water contents the anions occur principally as outer sphere complexes to the metal hydroxide surfaces.

MINERALOGICAL CHANGES DURING ELECTRODIALYTIC REMEDIATION OF SOIL MATERIAL POLLUTED BY CHEMICALS USED FOR WOOD IMPREGNATION

Bodil Karlsmose Kliem and Christian Bender Koch

Department of Natural Sciences, Faculty of Life Sciences, Copenhagen University, DK-1871 Frederiksberg, Denmark; cbk@life.ku.dk

During electrodialytic remediation (EDR), an electric DC current is passed through the soil with the purpose of removing a specific pollutant. The remediation process inherently has the potential to induce oxygen and protons to the soil solution, resulting in accelerated weathering. Here we report on effects of EDR on the mineralogy of a clay sample subjected to copper pollution.

Results from Mössbauer spectroscopy showed that essentially all Fe(II) in layer silicates was oxidised in the part of the clay where the content of oxygen was high and pH low during the EDR process. A Fe(II) gradient was established along the clay volume. Total chemical analyses showed that particular plagioclase feldspars and magnesium- and aluminium-containing layer silicates are susceptible to dissolution during EDR. Copper was found by STEM and SEM to be associated with either 1) iron and minor amounts of silicon, aluminium, and arsenic, or with 2) iron-containing smectite. After EDR, copper was mainly found associated with iron and smectite, containing less copper than before remediation.

If soil pH in an EDR situation of polluted soil is not controlled, it may drop to values around 2.5-3. Besides the release of adsorbed metals from the exchange sites of the clay particles, the consequence of this low pH was dissolution of both feldspars and silicate minerals. Thus, the presence of oxygen and low pH result in accelerated weathering and consequently structural transformations affect the medium during this remediation method. Because of the considerable changes in the composition of the soil, preventing such drops in pH is generally preferable.

NOVEL STRUCTURE OF 2:1 LAYER FORMED BY DEHYDROXYLATION OF Fe^{3+} , Mg-RICH MICA

Toshihiro Kogure¹ and Victor A. Drits²

¹Department of Earth and Planetary Science, Graduate School of Science, The University of Tokyo, 7-3-1 Hongo, Bunkyo-ku, Tokyo, 113-0033, Japan; kogure@eps.s.u-tokyo.ac.jp

²Geological Institute of the Russian Academy of Sciences, Pyzhevsky per 7, Moscow, Russia

After the structure analysis by Pauling¹⁾ in 1930, 2:1 layer is the most fundamental and universal structure unit in phyllosilicates and clay minerals. Except for a variety of the site occupancies for octahedral cations (di- or tri-octahedral and *trans*- or *cis*- vacant), the structure of 2:1 layer is basically identical for phyllosilicate minerals. However, we have found and report here the first substantial structural modification of 2:1 layer in phyllosilicates.

The new structure was found in celadonite, a *trans*-vacant dioctahedral mica with Fe^{3+} and Mg as major octahedral cations, annealed in a furnace at 800C for 1 hour. By this annealing, dehydroxylation and subsequent migration of octahedral cations are expected²⁾. Plan-view TEM observation indicated a super cell with $A = 3a$ and $B = b$. By observing cross-sectional TEM specimens along the $\langle 010 \rangle$ direction, it was found that reciprocal lattice rows with $h \neq 3n$ are completely streaked. Surprisingly, $h0l$ ($h = 3n$) reflections form completely orthogonal lattice, which is not expected for micas with one-layer periodicity (Fig. 1). The HRTEM image along $\langle 100 \rangle$ is similar to that expected from normal mica but the image along $\langle 010 \rangle$ is completely different (Fig. 2). From these images, it is concluded that the two tetrahedral sheets in a 2:1 layer are facing with no lateral $a/3$ stagger. A structural model that can explain these HRTEM contrasts is shown in Fig. 3. In this model, two third of the spaces surrounded by two facing tetrahedral rings accommodate three Fe^{3+} , Mg cations each and one third is empty. Fe^{3+} , Mg cations are coordinated by six or five oxygen atoms, forming trigonal prisms or square-base pyramids, respectively. 1) Pauling, L. (1930) *Proc. Natl. Acad. Sci.*, **16**, 123-129. 2) Muller et al. (2000) *Clay Miner.*, **35**, 491-504.

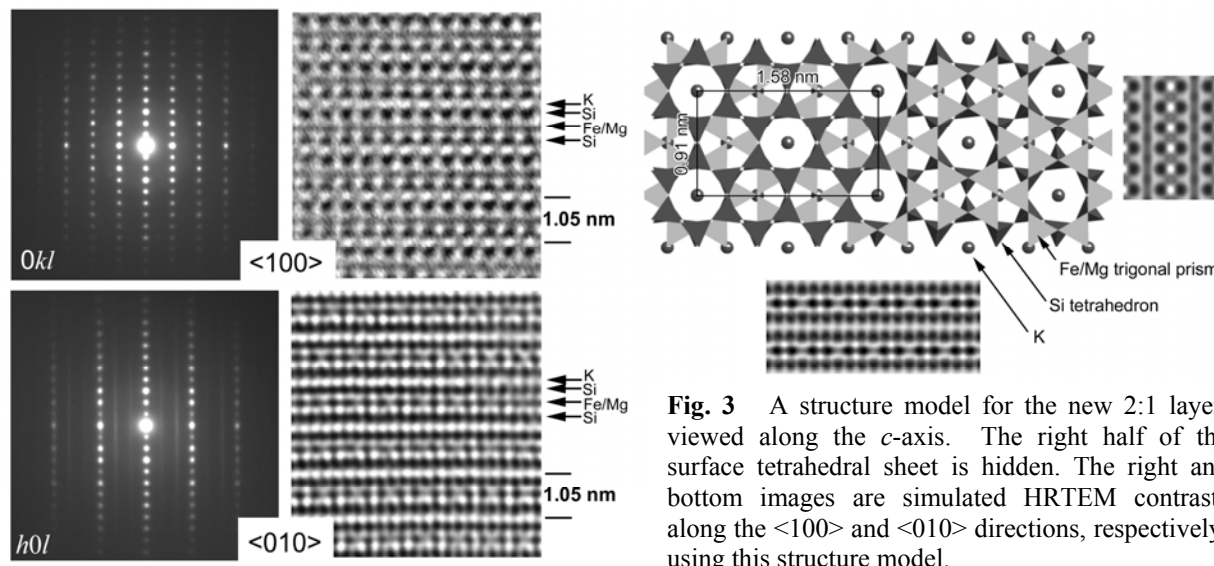


Fig. 1

Fig. 2

Fig. 3 A structure model for the new 2:1 layer, viewed along the *c*-axis. The right half of the surface tetrahedral sheet is hidden. The right and bottom images are simulated HRTEM contrasts along the $\langle 100 \rangle$ and $\langle 010 \rangle$ directions, respectively, using this structure model.

CLAYEY CAP-ROCK BEHAVIOR IN H₂O-CO₂ MEDIA AT LOW PRESSURE AND TEMPERATURE CONDITIONS: A NUMERICAL APPROACH

Eric Kohler¹, T. Parra¹ and A. Michel²

¹Institut Français du Pétrole, Direction Géologie-Géochimie-Géophysique, 1-4 Avenue de Bois Préau, 92025 Rueil-Malmaison, France; eric.kohler@ifp.fr

²Institut Français du Pétrole, Direction Technologie, Informatique et Mathématiques Appliquées, 1-4 Avenue de Bois Préau, 92025 Rueil-Malmaison, France

The CO₂ storage in depleted hydrocarbon reservoirs requires the understanding of the CO₂ impact on clay-rich sealing cap-rocks and demonstrating the safety of the site over thousands of years. In particular, the knowledge of the critical parameters that modify physical properties such as permeability and fracturing are key factors. The PICOREF project (Brosse *et al.* 2006) has identified a potential experimental site for CO₂ geological storage at SMB (Saint Martin de Bossenay, Paris Basin, France).

The purpose of this work is to model the experimental results that have been detailed in a companion oral presentation (Parra and Kohler). This experimental work studied the physico-chemical reactivity of SMB clayey materials, as a function of the H₂O-CO₂ ratio in the fluids. Two kinds of experiments were designed to determine reaction paths and diffusion processes around 150°C and 150 bars. The first set of experiments involves ground materials with various amounts of CO₂ in water. The second set of experiments concerns cm-scale samples enclosed in H₂O or CO₂ pure media. These experiments served as key indicators to determine the mineralogical sequences.

In this study, the mineralogical sequences experimentally obtained are then subjected to reactive transport models (Coores: CO₂ Reservoir Environmental Simulator. Institut Français du Pétrole). A first of set of models were done using literature data on diffusion, kinetics and thermodynamics for minerals, aqueous species and gas. These data do not fit experimental results so that a second set of parameters have been chosen *following a trial and error procedure*. These input data (diffusion, kinetics and thermodynamics) have been progressively adapted to fit the reactive fronts. Results show that *several* couple of diffusion and kinetics driven reactions could satisfy the experimental constraints. However, even if diffusion and kinetics are strongly correlated, one of the possible couple has been used to model the behavior of a cap-rock over a CO₂ reservoir. *It shows that diffusion does occur through caprocks and shouldn't be neglected however how much the model can have realistic value remains to be seen.*

This underlines the porosity-permeability changes due to mineral reactivity and shows the importance of taking into account such precise reactive path to understand and predict long-term storage.

Brosse, E., de Smedt, G., Bonijoly, D., Garcia, D., Sayssset, S., Manai, T., Thoraval, A. and Crepin, S. (2006) PICOREF: Towards an experimental site for CO₂ geological storage in the Paris basin? Proceedings of the 8th International Conference on Greenhouse Gas Control Technologies, 19-22 June, Trondheim, Norway.

CATION AND ANION UPTAKE BY ANIONIC CLAYS

Sridhar Komarneni, Jingwen Zhang, and Kanchan Grover

Department of Crop and Soil Sciences, The Pennsylvania State University, University Park, PA 16802, USA. Komarneni@psu.edu

Layered double hydroxides (LDH) or anionic clays are versatile materials with many functions. Although their anion exchange properties are well known, their cation uptake is little known. This presentation will show that the anionic clays are capable of removing cations from solution by a process known as “diadochy”. Anionic clays of variable layers (Mg-Al and Ca-Al) and interlayers (nitrate, carbonate and chloride) were synthesized by precipitation and/or hydrothermal methods at different temperatures to vary their crystallinity. Phase formation was confirmed by powder X-ray diffraction (XRD), and shape and size were determined by scanning electron microscopy (SEM). The uptakes of cations (Co^{2+} , Zn^{2+} , and Ni^{2+}) and anions (PO_4^{3-} and SeO_3^{2-}) were conducted with batch experiments. The metal cation uptake by various LDHs will be reported. For an example, almost all the Mg-Al LDHs synthesized by the different methods had the highest Zn^{2+} uptake capacities followed by Ni^{2+} and then Co^{2+} with one or two exceptions. Poorly crystallized LDHs synthesized by precipitation at room temperature showed higher metal uptake capacities than the well crystallized samples prepared by hydrothermal method. The above inverse correlation of metal cation uptake with XRD crystallinity of the various LDHs could be explained by the fact that it is more difficult to break the bonds in well crystallized LDHs compared to those in poorly crystallized samples. Results from the anion uptake studies revealed that the Ca-Al nitrate containing LDHs exhibited the highest PO_4^{3-} uptake while the Mg-Al chloride containing LDHs showed the highest uptake of SeO_3^{2-} . The results obtained indicate that the PO_4^{3-} and SeO_3^{2-} reactions occurred by anion exchange and/or dissolution-reprecipitation.

DETERMINATION OF BINDING INTERACTIONS BETWEEN TETRACYCLINE AND SOIL COMPONENTS

Pankaj Kulshrestha¹, Rossman F. Giese², and Troy D. Wood¹

¹Department of Chemistry and ²Department of Geology, University at Buffalo, The State University of New York, Buffalo, NY, USA, 14260; pk9@buffalo.edu

The interactions of tetracycline with model clay adsorbents and humic materials were investigated as a function of suspension pH, which could influence their fate and transport in the environment. The clay adsorbents used were native montmorillonite (SWy-2), Na-montmorillonite (Na-SWy-2), and hexadecyl trimethyl ammonium-montmorillonite (HDTMA-SWy-2). Humic-montmorillonite (humic-SWy-2) was used as an example of organic matter coated clay adsorbent. The tetracycline molecule interacts with the interlamellar exchangeable cations in the montmorillonite by displacing water from the clay mineral interlamellar spaces. This was confirmed by X-ray diffraction (XRD) observation of a primary lattice distance expansion of about 4.7 Å. Attenuated Total Reflectance Fourier Transform Infrared Spectroscopy (ATR-FTIR) showed that adsorption of tetracycline in the SWy-2 and Na-SWy-2 is highest at acidic pH of 1.5 and 5.0 whereas no adsorption was seen at alkaline pH of 8.7 and 11.0. This trend is consistent with cationic exchange interactions that are dominant at lower pH values when tetracycline has a net positive charge. On the other hand, complexation of negatively charged tetracycline with the cations present in HDTMA-SWy-2 and Humic-SWy-2 contributes to the sorption at higher pH values as evident from the ATR-FTIR spectrum of the HDTMA-SWy-2 and humic-SWy-2 adsorbed with tetracycline. ¹H NMR transverse relaxation times (T_2) were measured at multiple molecular sites of tetracycline to determine its preferential interaction sites with clay. Chemical shifts and increase in signal line broadening were observed in 1D [¹H] NMR spectra and natural abundance ¹³C NMR spectra of tetracycline intercalated with clay and humic acid, which are clearly indicative of non-covalent interactions. ¹H and ¹³C spin-lattice relaxation times (T_1) for aromatic protons and carbons of tetracycline were found to decrease with increasing additions of humic acid. Tetracycline is transformed by covalently bonding to oligomers of natural organic matter constituent through oxidative cross coupling reactions mediated by extracellular soil oxidoreductases. Appearance of new peaks in 1D [¹H] nuclear magnetic resonance spectroscopy (NMR) and new cross-peaks in 2D [¹³C, ¹H] HSQC NMR was followed by confirmation of reaction products in solution using ion trap mass spectrometry with positive electrospray ionization, which provide evidence of horseradish peroxidase (HRP) mediated cross coupling of tetracycline with syringic oligomers. Incubation of tetracycline with humic and fulvic acid in presence of HRP for a period of 10 days showed appearance of new cross peaks in 2D [¹³C, ¹H] HSQC and high molecular weight ion peaks in fast atom bombardment mass spectrometry (FAB-MS). Our results indicate that initially the adsorption of tetracycline into soil occurs via non-covalent interactions. Longer term sequestration of adsorbed tetracycline residues in soil could result in their slow irreversible chemical incorporation into humus via covalent bonding. This may result in their diminished mobility, bioavailability, and biological activity.

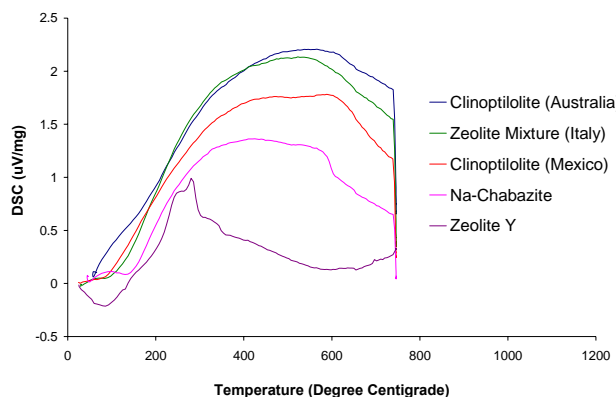
NATURAL ZEOLITE-BASED CATALYSTS FOR HEAVY OIL APPLICATIONS

Steven M. Kuznicki, William C. McCaffrey, Junjie Bian, Abu S.M. Junaid, Brian R. Greenhalgh, and Andree Koenig

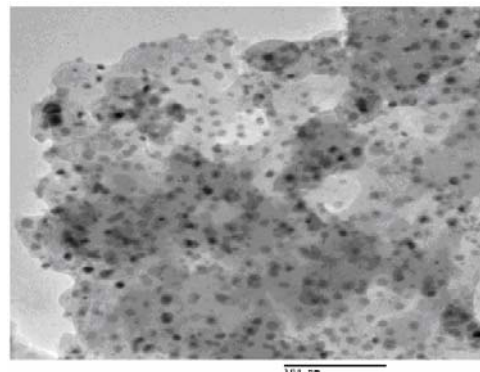
Department of Chemical and Materials Engineering, University of Alberta, Edmonton, AB, Canada T6G 2G6; steve.kuznicki@ualberta.ca

The unique surface chemistry and low cost of mineral molecular sieve zeolites may open new opportunities in the processing of highly contaminated heavy oils such as bitumen (Kuznicki et al. 2007a). Natural zeolites such as chabazite and clinoptilolite can be made distinctly more acidic than commercial synthetic cracking catalysts. With crystalline morphology that promotes high exterior surface area and disposability associated with low cost, such materials lend themselves to single pass precracking and upgrading by the removal of nitrogen bases, associated heavy metals and sulfur in ways that synthetic zeolites cannot.

The strong surface sites in chabazite introduce an additional phenomenon of potential value in the processing of heavy, highly contaminated oils. Metals reduced after exchange form stable nanoparticulates (Kuznicki et al. 2007b) on the order of 1-10 nanometers in size depending upon the conditions of reduction. For metals such as nickel, this may form a new route to cost effective, high performance hydrogenation catalysts.



Acid Strength of NH₄-Zeolites by TPD



Nickel Nanospheres on Chabazite Surfaces

Kuznicki, S.M., McCaffrey, W.C., Bian, J., Wangen, E., Koenig, A. and Lin, C.C.H. (2007a) Natural zeolite bitumen cracking and upgrading. *Microporous and Mesoporous Materials*, in press.

Kuznicki, S.M., Kelly, D., Bian, J., Lin, C.C.H., Liu, Y., Chen, D., Mitlin, D. and Xu, Z. (2007b) Metal nanodots formed and supported on chabazite and chabazite-like surfaces. *Microporous and Mesoporous Materials*, in press.

HIGH-LEVEL RADIOACTIVE WASTE DISPOSAL IN A DEEPLY BURIED CLAY FORMATION: THE FRENCH CASE

Patrick Landais

National Radioactive Waste Management Agency. 1/7 rue jean Monnet – 92298 Châtenay-Malabry cedex. France. patrick.landais@andra.fr

Since 1991, Andra has launched a major research programme to study waste disposal in a clay formation. In eastern France (the Meuse/Haute-Marne site), a stiff clay rock (argillite: percentage of clay mineral ranging between 25 and 55%; mainly illite and illite-smectite) approximately 155 million years old (Callovo-Oxfordian) occurs at a depth of 400 to 600 m. The work on the site and in the Meuse Haute-Marne laboratory sector has allowed collection of much scientific information and an in-depth understanding of this site's geological environment to ensure that the clay layer of the Callovo-Oxfordian provides the expected favourable properties and to assess its long-term behaviour, notably by taking into account the waste repository impact. Therefore, 27 deep bore-holes have been drilled since 1994 and 2,300 m of argillite core samples have been extracted (from 4,200 m of cored samples). Andra has taken over 30,000 samples and analysed 5,300 rock samples. Furthermore, scientific activity has been going on in 40 m of drifts at a depth of 445 m and over 550 m of drifts have been excavated at a depth of 490 m. In all, over 1,400 sensors have been installed for measurement in the rock and in situ observation of its behaviour.

The porosity of the argillites is low (between 10 and 18 %) and the pore radius is lower than $1/10^{\text{th}}$. The resulting permeability ranges between 10^{-12} and 10^{-14} m/s. Those characteristics indicate that the chemical elements move mainly by diffusion. *In situ* diffusion experiments designed to measure the diffusion velocity of the water (molecules containing tritium) and of specific radioactive elements present in the waste (iodine-125, chlorine-36, sodium-22, caesium-134). Monitoring these *in situ* diffusion tests over 6 months showed that the rock appears to display a diffusive behaviour in line with the diffusion parameters established in the laboratory. This retention capability of argillites is also confirmed by in situ diffusion tests on cationic species (caesium) and has been tested in different experimental configurations (water chemistry, element concentration in solution).

Experiments have also confirmed the mechanical parameters of the rock (resistance to single-axis compression ranging between 20 MPa and 25 MPa on average) and demonstrated the absence of any fractured zone around the structure. It has also revealed that rock density evolution around the excavation is very slight (reduction of less than 2% in seismic wave propagation velocities). This modification is perceptible up to 1-1.5 m from the shaft wall (microfissured zone). Beyond that distance, the properties of the massif do not show any change.

Additional experiments concern the influence of alteration processes originating from the interactions of clay with repository components such as cement or metallic materials. It is shown that the extent of the mineralogical and geochemical transformations does not exceed 1 to 1.5 m. Finally, the influence of temperature on the hydro-mechanical behaviour of argillites was also studied in the laboratory by varying the temperature and the level of saturation of the samples. Up to around 70°C, there is practically no visible effect on the mechanical parameters (elasticity, plasticity threshold, creep velocity); above that temperature, the most noticeable effect is an increase in the creep velocity.

MOLECULAR SIMULATION OF THE STRUCTURAL AND VIBRATIONAL PROPERTIES OF TALC AND PYROPHYLLITE

James P. Larentzos, Jeffery A. Greathouse, and Randall T. Cygan

Geochemistry Department, Sandia National Laboratories, Albuquerque, NM 87185, USA;
jlarent@sandia.gov

The structural and vibrational properties of talc and pyrophyllite are investigated with *ab initio* and classical molecular dynamics simulations. The quantum mechanical simulations are based on density functional theory (DFT), which is sufficiently accurate to predict the structural and vibrational properties of these two clay minerals. However, to understand the nature of adsorption, diffusion, and other complex processes in clay minerals, simulation of these systems in a full quantum mechanical manner becomes infeasible due to the computational burden. The classical molecular dynamics (MD) simulation using an accurate force field (CLAYFF) is a viable alternative, where it has been shown to faithfully reproduce the crystal structures with relatively simple analytical functions that include primarily non-bonded interactions. Comparison of the *ab initio* and classical MD structures provides a detailed understanding of the important physics that must be included in future refinements of the empirical force field.

In particular, the disposition of the hydroxyl group in the octahedral sheet is critical in understanding adsorption properties in charged and uncharged clays. Signature spectroscopic peaks that are characteristic of the hydroxyl group vibrations and bends are easily identified experimentally. With the assistance of molecular simulation, the relationship between hydroxyl group vibrational modes and the molecular-scale structure is explored. The orientation of the hydroxyl group is closely monitored to understand the effects of the dioctahedral vacancy on the uncharged clay behavior. While the talc hydroxyl orientation is essentially perpendicular to the *ab* plane and has a relatively narrow angle distribution, the presence of octahedral vacancies in pyrophyllite significantly alters the hydroxyl behavior to produce a very broad angle distribution, as shown in Figure 1. The results for the two simulation methods are in agreement for talc. However, the hydroxyl orientation in pyrophyllite differs between the *ab initio* and classical MD simulations.

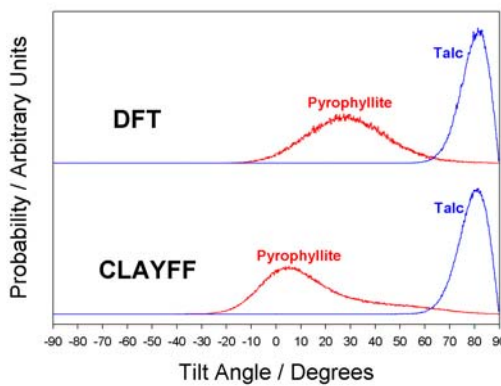


Figure 1: The DFT and CLAYFF hydroxyl angles relative to the *ab* plane

Sandia is a multiprogram laboratory operated by Sandia Corporation, a Lockheed Martin Company, for the United States Department of Energy's National Nuclear Security Administration under contract DE-AC04-94AL85000.

FUNCTIONALIZED NANOHYBRID MATERIALS FROM KAOLINITE

Sadok Letaief, Thomas Diaco, and Christian Detellier

Centre for Catalysis Research and Innovation and Department of Chemistry, University of Ottawa, 10 Marie Curie, Ottawa, Ontario K1N 6N5, Canada; lsado816@science.uottawa.ca

Novel organic–inorganic nanohybrid materials were obtained from the clay mineral kaolinite by (i) the intercalation in the interlamellar spaces of ionic liquids based on pyridinium, imidazolium and pyrrolidinium derivatives and by (ii) grafting functionalized organic units on the interlayer aluminol surfaces. The intercalation and/or grafting procedures were successfully accomplished *via* a melt reaction strategy using the dimethylsulfoxide–kaolinite intercalate (DMSO-K) as well as urea-Kaolinite as a precursor. ^{13}C MAS NMR as well as XRD, TGA/DTA and FTIR studies confirmed the complete displacement of DMSO or urea molecules by the salts during the intercalation processes. The intercalation of ionic liquids and the grafting of organic units increase strongly the thermal stability of the resulting material. This observed high thermal stability is promising for the use of these nanohybrid materials as precursor for the synthesis of new nanocomposites by incorporation of polymer in kaolinite at high temperature. The conductivity of the materials based on ionic liquids is reported.

TWENTY-FIVE YEARS PLUS OF RESEARCH ON IMPACTS AND MASS EXTINCTIONS

Spencer G. Lucas

New Mexico Museum of Natural History, 1801 Mountain Road NW, Albuquerque, NM 87104;
spencer.lucas@state.nm.us

Paleontologists identify several diversity crashes (mass extinctions) during the Phanerozoic; five stand out as much larger than the rest: end-Ordovician (~ 450 Ma), Late Devonian (~ 374 Ma), end-Permian (~ 251 Ma), end-Triassic (~ 200 Ma) and end-Cretaceous (~ 65 Ma). Of these “big five,” the end-Permian extinction was the most severe mass extinction in the history of life. However, despite the identification and dating of numerous impact structures, the evidence for extraterrestrial involvement in most earthly mass extinction remains circumstantial and suspect at best. Indeed, the underlying cause(s) of each of the “big five” extinctions stands out as a unique set of circumstances.

For the end-Ordovician extinction, current estimates suggest that in the oceans about 26% of families and 49% of genera became extinct in two pulses. No evidence of an extraterrestrial impact contemporaneous with either of the extinctions at the end of the Ordovician exists, and the most likely cause involves a short, but severe high latitude ice age. Near the end of the Devonian, the main extinctions are the ~ 374 million year old Frasnian-Fammenian boundary, and the ~ 360 million year old Devonian-Carboniferous boundary extinction. But, whether there are one, two or 40 extinctions has been debated, so the Late Devonian looks more like a prolonged biotic crisis, and not simply a single (or even double) mass extinction. The end-Permian mass extinction has long been recognized as the most severe and sudden mass extinction in Earth history. However, the end-Permian extinction was selective, and the story is not simple. No convincing evidence for an impact coincident with the Permo-Triassic boundary exists, so the climatic effects of Siberian Trap volcanism—from acid rain to global warming—are considered likely factors. The end-Triassic has long been portrayed as a land- and sea-based extinction of comparable magnitude to the end-Cretaceous extinction. No widely accepted evidence for impact has been demonstrated at the end of the Triassic. The extensive CAMP volcanic field, comparable in size to the Siberian traps, may have played a role in the extinctions, although the precise mechanism has not been elucidated. The Late Triassic was an interval of elevated extinction rates (a prolonged biotic crisis), encompassing several distinct extinction events during the last 15 million years of the Triassic. The end-Cretaceous extinction, about 65 million years ago, stands as the most intensively studied extinction and the only one that coincides with a major impact event.

Thus, after 25 years of feverish study of the biggest extinctions in the history of life, only one mass extinction coincides with a documented impact—the end Cretaceous extinction. Extraterrestrial impacts as a general cause of mass extinction (or, if you like, a general theory of mass extinction based on extraterrestrial impacts) can be laid to rest.

CLAY-METAL-MICROBIAL INTERACTIONS IN AEROBIC ENVIRONMENTS

Patricia A. Maurice

Center for Environmental Science and Technology, University of Notre Dame, Notre Dame, IN 46556 USA; pmaurice@nd.edu

At the micron scale, i.e., the scale of clays and clay minerals, life and geochemistry interplay as organisms seek energy and substrates on which to exist and grow, along with mechanisms that decrease the bioavailability of toxic substances. We now know that microorganisms can affect fundamental parameters, such as pH and redox potential, as well as particle aggregation, mineral growth and dissolution, fate and transport of metals and radionuclides, and both creation and biodegradation of different types of organic compounds.

Clay scientists and biologists have both relied on ‘rose-colored glasses’ to ignore interactions that simply could not be studied. However, during the last few decades, advancements in both clay science and biology have been accomplished by interdisciplinary investigators who have developed the new discipline of geomicrobiology. Through this revolution at the micron scale, geologists and biologists have recognized the critical role of clay science in understanding the interactions of the geosphere and the biosphere.

This talk will discuss several example studies of clay-metal-microbial interactions with an emphasis on aerobic environments. The talk will focus on new frontiers arising from the integration of techniques from microbiology, geochemistry, hydrology, surface science, environmental physics, and computer science with clay science and the importance of such research not only to the environmental field but also to medical science.

CAFFEINE ADSORPTION ON CLAY MINERALS AND NATURAL SEDIMENTS

Keith E. Miller and Jeffrey A. Caulfield

University of Denver, Department of Chemistry and Biochemistry, Denver, CO 80208, USA;
kmiller3@du.edu

Caffeine has been proposed for use as an anthropogenic marker in aquatic systems. Despite its high water solubility, however, caffeine adsorbs significantly to some sediments and clay mineral surfaces. Adsorption isotherms were performed with caffeine on natural sediments collected from the South Platte River and reference sediments obtained from the U.S. Geological Survey. In addition, caffeine absorption was measured on a series of homoionic montmorillonites. The experimental K_d values for caffeine ranged from < 0.7 to $> 2.5 \times 10^3$ L/kg for all substrates tested, with the homoionic clays exhibiting the highest values. Adsorption measurements were made under varying ionic strength conditions to simulate both fresh water and estuarine systems. Further investigation into the binding mechanism(s) of caffeine on the clay mineral surfaces was conducted using FTIR methods and molecular modeling. Based on these experiments, three different potential adsorption mechanisms for the binding of caffeine to the montmorillonites have been identified and will be discussed. The mechanisms and magnitude of the K_d value are a function of the cation exchanged on the mineral surface. This work demonstrates that mineral composition of soils and sediments should not be neglected when caffeine is used as an anthropogenic marker.

INFRARED ANALYSIS OF SILICON WAFER-SUPPORTED CLAY MINERALS

Keith E. Miller, Jeffrey A. Caulfield and Todd A. Wells

University of Denver, Department of Chemistry and Biochemistry, Denver, CO 80208, USA;
kmiller3@du.edu

A facile technique for the analysis of clay minerals using Fourier Transform Infrared (FTIR) spectroscopy has been developed. In this technique, suspensions of the clay minerals are applied and dried on a silicon wafer. The transmission IR spectra of natural clays SWy-2, SAz-1, SHCa-1 and KGa-1b, as well as a Laponite-RD (a synthetic hectorite) are presented to demonstrate the technique. These IR spectra compared to those spectra generated from KBr pellet and ATR methods. In addition, the spectra of pharmaceuticals and nitro-aromatic compounds adsorbed to the mineral surfaces are reported to show the versatility of the technique. The method reported here provides two major advantages over traditional sample preparation methods. First, the technique allows for the characterization of nanometer sized clay particles (for example, Laponite-RD) where the preparation of a self-supporting film is difficult, if not impossible. Second, the silicon wafer mounts allow the sequential analysis of additional non-destructive techniques on the same samples, such as XRD analysis.

ETHYLBENZENE DEHYDROGENATION USING PT, MO AND PT-MO CATALYSTS SUPPORTED ON CLAY NANOCOMPOSITES

Alexander Moronta¹, César Morán², Gabriela Carruyo¹, Eduardo González¹, Roger Solano¹, and Jorge Sánchez¹

¹Instituto de Superficies y Catálisis, Facultad de Ingeniería, Universidad del Zulia, Maracaibo 4003A, Venezuela; amoronta@cantv.net

²Universidad Rafael Urdaneta, Facultad de Ingeniería, Escuela de Ingeniería Química, Maracaibo, Venezuela

A synthetic clay (TS-1) was modified with a non-ionic surfactant (IGEPAL CO-720) and magnesium oxide. The resulting solid was used as a support of Pt, Mo and Pt-Mo catalysts. The catalysts were prepared by wet impregnation with aqueous solutions of $H_2PtCl_6 \cdot 6H_2O$ and $(NH_4)_6Mo_7O_{24} \cdot 4H_2O$. In both monometallic and bimetallic catalysts, the molybdenum content was 3%.wt and the platinum content was 0.5 and 1%.wt. The surface area of the starting clay was $454\text{ m}^2/\text{g}$ and after the modification treatment it increased to $649\text{ m}^2/\text{g}$, while platinum and molybdenum catalysts showed surface areas between 495 and $550\text{ m}^2/\text{g}$. The reduction profiles showed different Pt and Mo species and the existence of support-metal interactions. The reduced catalysts were more active than those in the unreduced form. The most active catalysts towards the ethylbenzene dehydrogenation were those of monometallic Pt (0.5 and 1%) with a maximum styrene conversion around 60%. Reduction treatment resulted in a higher selectivity and activity towards styrene for all catalysts.

SOUTH AFRICAN NATURAL CLINOPTIOLITE: STRUCTURE, PHYSICO-CHEMISTRY AND INDUSTRIAL PROPERTIES

Antoine F. Mulaba-Bafubiandi¹, Lorraine T. Soko², and Bhekie Mamba²

¹Minerals Processing and Technology Research Group, Department of Extraction Metallurgy, Faculty of Engineering and the Built Environment, University of Johannesburg, P.O. Box 526, Wits 2050, South Africa; amulaba@uj.ac.za

²Department of Chemical Technology, Faculty of Science, University of Johannesburg, P.O. Box 17011, Johannesburg 2028, South Africa.

Natural clinoptilolite found in the Vulture Creek, Kwazulu Natal, South African geological formation is the focus of this paper. A typical composition of 70% SiO₂, 12% Al₂O₃, 2% Na₂O, 5% K₂O, 2% CaO, 2.5% Fe₂O₃ with traces of other elements was observed.

The mineralogy and physico-chemical properties were studied using X-ray diffraction, TPD, BET surface area analysis, FTIR, and Mössbauer spectroscopy. XRD analysis revealed that in addition to clinoptilolite, cristobalite, opal, α -quartz and mordenite were present as impurities.

The BET analysis showed an increase in the surface area from 16 to 36.7 m²/g as a result of acid treatment. This effect had a strong influence on the selectivity of methylamines by allowing a larger surface area to be in contact with feed reagents.

The catalytic properties of this natural clinoptilolite depend on the type of the treatment received. Room temperature Mössbauer features of structural Fe²⁺ and Fe³⁺ as well as an attempt to extract cobalt and copper ions from hydrometallurgical sulphate solutions using treated and untreated natural clinoptilolite will be discussed.

Acknowledgements

Lance Levin conducted the physico-chemical tests. His partial involvement in the results presented and discussed in this paper is appreciated. The Faculty of Engineering and the Built Environment (FEBE) and the University (of Johannesburg) Research Committee (URC) funded the project on the beneficiation of industrial minerals with the grant number 05150689202533000.0

ORIGIN OF THE ALBERTA OIL SANDS BITUMEN DEPOSITS: ISOTOPIC EVIDENCE FROM K-BENTONITES IN KEY SOURCE ROCK HORIZONS

Paul Nadeau¹, Edward E. Meyer², James L. Aronson², Cindy Riediger³, Martin Fowler⁴, Steve Hillier⁵, and Michele Asgar-Deen⁴

¹Statoil ASA, Stavanger, Norway; PHN@statoil.com

²Dartmouth College, Hanover, NH, USA

³University of Calgary, Calgary, AB, Canada

⁴Geol. Survey of Canada, Calgary, AB, Canada

⁵Macaulay Institute, Aberdeen, UK

Petroleum systems in foreland basins remain enigmatic. These prolific basins contain the world's largest petroleum reserves, including the Central Arabian / Rub Al Khali, East Venezuela, and Western Canada sedimentary basins (WCSB). The Lower Cretaceous sandstones in Western Canada contain enormous reserves of conventional crude oil, heavy oil and bitumen, with estimates exceeding a trillion barrels of oil in place. Numerous studies have characterized these extensively biodegraded oils and bitumens, resulting in conflicting views as to which source rock interval is dominantly responsible for their formation. Geological evidence as well as recent Re-Os dating of the bitumens supports the hypothesis that oil arrived in eastern Alberta shortly after deposition of the host sandstones, about 115 to 110 Ma.

This presentation examines new results from measurements of the age of illitization in K-bentonites from the main candidate source rocks, the Devonian-Mississippian Exshaw Formation and the Jurassic Fernie Group, from several outcrop localities in the Rocky Mountain Fold and Thrust Belt in southern Alberta. These results suggest that Exshaw source beds currently exposed at the surface in the Fold and Thrust Belt were unfaulted and laterally continuous within an undeformed portion of the WCSB at the time of hydrocarbon generation, and could thus have contributed to the giant accumulations of hydrocarbons along the eastern edge of the basin. These data assist reconstruction of the basin near the critical moment of maturation, and suggest a much larger extent of the presumed Exshaw Formation "oil kitchen" at the time of oil generation and migration than has previously been considered. The new data, therefore, have important implications for basin analysis studies, which must consider the tectonic evolution of foreland basin sedimentary accumulations, and their controls on ultra-rich petroleum systems.

SOLVUS MODELS FOR HYSTERESIS IN WATER ADSORPTION/DESORPTION BY ZEOLITES AND OTHER MINERAL HYDRATES: EVIDENCE FROM THERMAL ANALYSIS AND THERMODYNAMIC MODELING

Philip S. Neuhoff, Jie Wang, and Gökçe S. Atalan

Department of Geological Sciences, University of Florida, 241 Williamson Hall, Gainesville, Florida 32611-2120, USA; neuhoff@ufl.edu

Nano-scale water occluded in mineral hydrates like zeolites, clays, and salt minerals and in nm-scale pores between minerals is a volumetrically-important component of Earth's hydrologic cycle. The partitioning of water between bulk phases (ice, liquid water, and vapor) and mineral hydrates plays a critical role in controlling mineral stability and driving fluid fluxes in Earth's crust. In many cases, dehydration of mineral hydrates is fully reversible, and considerable progress has been made in developing thermodynamic models capable of predicting their hydration state as a function of temperature (T), pressure (P) and the chemical potential of H_2O (μ_{H_2O}). However, a number of important mineral hydrates, including some zeolites and smectites as well as water adsorbed into nm-scale pores, exhibits hysteretic sorption and desorption behavior in which the water contents at constant T, P, and μ_{H_2O} are different depending on whether the sample is undergoing dehydration or hydration. Although several qualitative explanations for this behavior have been suggested in the literature, thermodynamic description of this phenomenon remains elusive.

Our recent experimental studies of the zeolites natrolite, laumontite, and gonnardite (paranatrolite and tetranatrolite) have (re)confirmed the presence of hysteresis during hydration and dehydration. In natrolite, this phenomenon is manifested by differing hydration states obtained during de- and rehydration during dynamic (scanning-heating) thermogravimetric analysis (TGA). In laumontite and gonnardite, this phenomenon is only exhibited during formation of the hyperhydrate forms of laumontite and paranatrolite and is clearly manifest in adsorption isotherms. Thermodynamic modeling of these systems suggests that solvi are present in the solutions between the relatively hydrated and dehydrated phases. The presence of solvi accounts for both the hysteretic behavior and previously reported observations that two distinct phases of differing hydration state are present under the conditions of hysteresis. The oft-reported decreasing degree of hysteresis with temperature is also consistent with this model.

During the course of thermal analytical (TGA and calorimetric) investigations of these systems, several characteristic behaviors were noted that are indicative of solvus behavior. In scanning-heating TGA experiments, mass loss often ends abruptly, rather than asymptotically as is generally observed and predicted from thermodynamic models of reversible dehydration. This is interpreted to reflect supercritical dehydration. Similar behavior is observed in nanopore systems. Isothermal heat of adsorption measurements on natrolite also point to two distinct manifestations of solvus behavior and thermodynamics. First, the temperature dependence of the heat of hydration is significantly larger than predicted from the heat capacity of reaction, suggesting that these solutions are characterized by excess heat capacities of solution (a characteristic of many, but not all, solvus systems). Second, the rates of isothermal hydration during immersion do not decrease with reaction progress, as predicted by rate laws and observed in hydrates exhibiting reversible dehydration, but rather are generally independent of reaction progress. This is a direct consequence of phase immiscibility.

LATE PALEOZOIC WEATHERING OF THE ELK CREEK CARBONATITE, SOUTHEASTERN NEBRASKA, USA

Brian L. Nicklen¹ and R. Matthew Joeckel²

¹Department of Geology, University of Cincinnati, Cincinnati, OH 45221-0013, USA;
nicklebl@email.uc.edu

²Conservation and Survey Division, School of Natural Resources, University of Nebraska-Lincoln, Lincoln, NE 68583-0996, USA

Analysis of several deep well cores from Pawnee and Johnson counties Nebraska, reveal a mantle of pre-Late Pennsylvanian (pre-mid-Missourian/Kasimovian) regolith overlying the 0.5 Ga Elk Creek Carbonatite (ECC). The regolith is predominantly *in-situ* and typically ranges from 0 to >15 m in thickness. A distinct pattern of red heavily slickensided claystone (paleo-Vertisol) above intensely weathered red carbonatite saprolite appears in multiple cores, although marine transgression completely eroded the weathering profile in some areas. The ECC intrudes Precambrian basement granite and gneissic granite as beforsite (dolomite-carbonatite) in the northern end of the Nehama Uplift, which was a positive relief feature prior to its burial by Missourian/Kasimovian cyclothsems. Elucidating the complex history of Paleozoic sea-level change and uplift for this region by examining the regolith is a primary objective of this ongoing investigation.

Samples of the red carbonatite saprolite are characterized by the presence of hematite and chlorite in whole-rock X-ray diffraction analysis. Initial examination of the <2 μ m fraction of the saprolite shows a dominance of chlorite and illite-smectite, while the slickensided claystone is dominated by illite-smectite. Both portions of the regolith appear to exhibit a noteworthy absence of kaolinite and aluminum hydroxides.

WEATHERING EFFECTS AND LANDSLIDING IN THE BAMBOUTO CALDERA, CAMEROON, WEST AFRICA

Edwin B. Ntasin¹, S.N Ayonghe¹, E.C. Suh¹, and E.V. Ranst²

¹Department of Geology and Environmental Sciences, Faculty of Science, University of Buea, P.O. Box 63. Buea, Cameroon.

²Soil Science Laboratory, Ghent University, Gent, Belgium.

The extent of weathering within various joint systems and the presence of friable pyroclastics contributed immensely to the destabilization of slopes within the Bambouto caldera, resulting in landslides that killed 23 people. The common occurrence of spheroidal and tortoise skin features found on fresh road cuttings are indicative of the effect of intensive weathering of the volcanic rocks. This resulted in an increase in Al_2O_3 , Fe_2O_3 , total water (H_2O+LOI) and SiO_2 with associated decrease in K_2O , Na_2O and MgO (soluviation). It was revealed that the soils produced are richer in Al_2O_3 and total water than the rock samples. The materials along the sliding surfaces were exceptionally richer in Al_2O_3 and total water than the other soil samples. The common minerals identified are gibbsite, sanidine, kaolinite, montmorillonite, orthoclase, quartz and muscovite. This study documents for the first time that the distribution of these minerals with respect to the location of the landslides is related to the progressive change from sliding zones with greater than 95% gibbsite (sliding surfaces), to units richer in kaolinite and then to the sanidine and quartz rich units. The gibbsitic zones with their good sealing properties form aquiclude capable of retaining moisture that facilitates weathering at these interfaces. The change in strength of the material during rain storms, together with steep slopes, results in slope failure within the caldera.

DYNAMICS OF NANOCONFINED WATER IN CLINOPTIOLITE AND HEULANDITE MICROPOROUS ZEOLITES

Nathan W. Ockwig¹, Randall T. Cygan¹, Tina M. Nenoff², Luc L. Daemen³, Monika A. Hartl³, and Louise J. Criscenti¹

¹Geochemistry Department and ²Surface and Interface Sciences Department, Sandia National Laboratories, Albuquerque, New Mexico 87185, USA; nockwig@sandia.gov

³Manuel Lujan Jr. Neutron Scattering Center LANSCE-LC, Los Alamos National Laboratory, Los Alamos, New Mexico 87545, USA

Understanding the behavior of confined molecular species in microporous materials is a challenging research effort that spans a wide variety of both experimental and theoretical approaches. Water is arguably one of the most important nanoconfined species in these materials because of its ubiquitous nature and impact across many geologically and industrially significant processes. The structural and dynamical properties of bulk water are well understood in a wide range of temperatures and pressures. It is also well known that the bulk properties of water are significantly modified when placed under confined conditions and, despite its relatively simple molecular structure involving only three atoms, the complex collective behavior of confined water remains a major challenge for current scientific research. Quantifying the behavior of molecular water in such confined systems such as zeolites is the first step towards understanding its role in macroscopic phenomena.

Our current research efforts are focused on the HEU-CLI zeolite system using classical molecular dynamics (MD) and experimental spectroscopy to correlate water behavior as a function of Si/Al framework substitution and cation identity. The most abundant naturally-occurring zeolites are heulandite (HEU) and clinoptilolite (CLI), which have a generalized formula of $[\text{Ca,Na,K}]_{4-6}[\text{Al}_6(\text{Al,Si})_4\text{Si}_{26}\text{O}_{72}] \cdot 24\text{H}_2\text{O}$. These two isostructural minerals have the HEU topology and can be synthesized over a range of Si/Al values (from 2.5 to 6) with a variety of alkali and alkaline earth charge-compensating cations. The distinction between these two materials is based on both their Si/Al values and thermal stabilities. Abundant deposits of clinoptilolite have fueled interests in commercial applications in gas separations, ion exchange, agriculture, and waste water remediation. Large-scale MD simulations are used to derive equilibrium structures, enthalpies, and the dynamical behavior of these phases. Power spectra derived from the atomic trajectories provide a theoretical basis for interpretation of inelastic neutron data obtained from the neutron facility. The combined theoretical and experimental approaches allows a determination of the role that hydrogen bonding, charge density, and steric effects have on water confined in the zeolite phases, and evaluate which factors are the most influential.

Sandia is a multiprogram laboratory operated by Sandia Corporation, a Lockheed Martin Company, for the United States Department of Energy's National Nuclear Security Administration under contract DE-AC04-94AL85000.

PROBING CLAY MINERAL TRANSFORMATIONS AND CONTAMINANT UPTAKE IN SEDIMENTS REACTED WITH CAUSTIC WASTE

Peggy A. O'Day¹, Sunkyung Choi¹, Karl T. Mueller², and Jon Chorover³

¹School of Natural Sciences, University of California, Merced, CA 95344 USA;
poday@ucmerced.edu

²Department of Chemistry, Penn State University, University Park, PA 16802 USA

³Department of Soil, Water and Environmental Science, University of Arizona, Tucson, AZ 85721 USA

Soils and sediments are complex mixtures of inorganic, organic, and biological components. Clay minerals and clay-sized particles disproportionately influence the overall reactivity of soils and sediments because of their ability to sorb, dissolve, and re-precipitate on fast time scales. Mechanistic and scaleable descriptions of chemical reactivity in soils and sediments, integrated with material and fluid transport models, are needed to describe and perhaps even predict complex phenomena such as migration of contaminants, nutrient fluxes, redox changes, and changes in solid and solution composition over a range spatial and temporal scales. However, significant challenges remain in identifying and quantifying the multiple and often parallel reactive processes associated with the clay fraction of a soil or sediment mixture.

From a kinetic standpoint, chemical reactivity associated with clays can be divided into relatively fast processes, such as adsorption and ion exchange, versus slower processes, such as mineral dissolution and precipitation of new phases, which may be metastable. In recent studies, we have used a variety of spectroscopic and microscopic characterizations to determine molecular modes of Sr and Cs sequestration in Hanford sediments reacted with caustic synthetic tank waste leachate, and compared their behavior to identical batch experiments with reference clays (illite (Il), vermiculite (Vm), montmorillonite (Mt) and kaolinite (Kt)). For both sediments and model clays, uptake of Sr exceeded that of Cs in co-contaminant experiments aged for up to one year. In general, Sr and Cs became progressively recalcitrant to desorption with time, with the fraction of recalcitrant Sr highest in Kt, Mt, and Hanford sediments and recalcitrant Cs higher in Il and Vm after one year of reaction. Evidence from Sr EXAFS, bulk and microfocused XRD, NMR, SEM/TEM, and FTIR shows that neoformed aluminosilicate phases, primarily the feldspathoid phases sodalite and cancrinite, are responsible for irreversible sequestration of Sr and some Cs. A smaller fraction of Sr is associated with easily extractable $\text{SrCO}_3(\text{s})$ that can form at both early and late time steps. The rate of clay mineral alteration and Si release correlate directly with formation and increasing crystallinity of aluminosilicates that sequester Sr and Cs. In the case of slow primary mineral dissolution (e.g., Il), Si release is limited and the rate of aluminosilicate formation is slower, resulting in precipitation of $\text{SrCO}_3(\text{s})$ when its solubility is exceeded and easy removal of Sr in desorption experiments. Collectively, these results highlight the co-temporal adsorption, dissolution, and precipitation processes that lead to different modes of contaminant uptake from solution. Reassuringly, microscopic and macroscopic observations indicate that similar mechanistic processes occurring in model clay systems can be recognized in the sediment systems, and that weathering and neo-phase formation rates appear to correlate with the type and amount of clay fractions in the sediments.

A TWO-DECADE REVIEW OF POLYMER-CLAY NANOCOMPOSITES

Akane Okada and Arimitsu Usuki

Toyota Inc., Central R&D Labs., Nagakute, Aichi, 480-1192, Japan; aokada@mosk.tylabs.co.jp

Two decades have passed since we invented polymer-clay nanocomposites (PCN), in which only a few wt.-% of each clay layer is randomly and homogeneously dispersed in the polymer matrix. When molded, these nanocomposites show superior properties compared to pristine polymers such as tensile strength, tensile modulus, heat distortion temperature, gas barrier property, and so on. The number of papers on PCN has increased rapidly in recent years, reaching 600 only in 2006. As the pioneers of the new technology, we will review its history highlighting our works. Epoch-making events of PCN are as follows:

- In 1985 we invented the first PCN, nylon 6-clay hybrid (NCH).
- In 1987 we first presented NCH at the ACS Fall Meetings.
- In 1989 Toyota launched cars equipped with a NCH part.
- In 1996 we found that clay causes a memory effect in liquid crystals.
- In 1997 Gilman of NIST found revolutionary fire retardency in NCH.
- In 1997 we prepared PP-clay nanocomposites.
- In 1998 we established a compounding method for producing NCH.
- In 2002 Haraguchi of Kawamura Institute of Chemistry invented a nanocomposite hydrogel.

So far only nylon-clay nanocomposites are used in practice, but other PCN will become increasingly useful in the future.

Okada, A. and Usuki, A. (2006) Twenty years of polymer-clay nanocomposites.
Macromolecular Materials and Engineering, **291**, 1449-1476.

POTENTIAL FOR CHEMICAL SEQUESTRATION OF CO₂ IN OIL SAND TAILINGS

Oladipo Omotoso and Randy J. Mikula

CANMET Energy Technology Centre, Natural Resources Canada. #1 Oil Patch Drive, Devon, Alberta CANADA; oomotoso@nrcan.gc.ca.

The production of synthetic crude oil from oil sands has generated close to 900M m³ of a slow settling silt and clay slurry known as mature fine tailings (MFT) that are currently contained in tailings ponds behind several square kilometers of sand dykes. To reclaim the tailings ponds to a natural landscape, a great deal of laboratory and pilot studies have been conducted in search of economically viable reclamation technologies. The consolidated tailings (CT) process is the most successful to date. The CT process involves chemical amendments to the silt and clays, then combination with the coarser sand components to create a non-segregating tailings (NST) mixture that will rapidly consolidate. Gypsum has been the chemical of choice for strengthening MFT to support a sand surcharge in CT mainly because it is readily available as a by-product of the use of coke for power generation via the associated flue-gas desulfurization process. In the years following the commercialization of the gypsum CT process, carbon dioxide was also investigated as a CT process aid in order to mitigate the green house gas impact of oil sands extraction and upgrading. This study evaluates the extent to which carbon dioxide will be sequestered in the CT process, therefore reducing the environmental impact of oil sands extraction. The mechanism by which carbon dioxide affects the strength of the MFT component is investigated, and the potential for carbon dioxide sequestration is quantified.

THE USAGE OF NATURAL ZEOLITES TO PREVENT FOR DEFICIENCY OF ZINC THROUGH THE EARTH

Onder Orhun¹, Gulcan Kinaci², Ozlem Kazan¹

¹Anadolu University, Science Faculty, Physics Department, Eskisehir, Turkey;
oorhun@anadolu.edu.tr

²Eskisehir Osmangazi University, Faculty of Agriculture, Eskisehir, Turkey

Recently, zeolites have been widely used to increase the effectiveness of fertilizers and to produce higher quality crops per unit field in the agricultural sector. The fact that natural zeolites can be easily and cheaply obtained in Turkey (with a reserve potential of 45 billion tons) and used as soil regulator without complex processing has gradually increased the interest in natural zeolites. Studies show that 30 % of the world's agricultural lands and around 14 million hectares of land in Turkey suffer from the lack of zinc (Cavdar et al., 1983).

In this study, raw clinoptilolite obtained from Manisa-Gordes region and a zinc form prepared by contacting it with 1 N ZnCl₂ solution for 72 hours were used. The zinc form contained 0.24 ppm zinc at the beginning. They were applied at densities of 0 kg/da, 1.0 kg/da, and 1.5 kg/da to the soil. Total area of the four plots (located on the research fields at Eskisehir Osmangazi University, the Faculty of Agriculture) was 7 m². Chickpea sample Akcin 91 was used as the test crop.

Total productivity was assessed by measuring the number of peas, their weights, height above ground of the lowest peas, and the number of peas attached to one root. Productivity generally increased with dosage. Chickpeas grown on plots with zinc form clinoptilolite contained an average of 28 ppm zinc. For human nourishment, leguminosae should include 20 ppm zinc at most (Khan et al, 1998). Therefore, it has been observed that the product includes more zinc than is optimal. This study is successful in demonstrating that zeolites are useful for introduction of micro elements into crops. In order to decrease the amount of zinc in the produce, studies in future should be conducted on the zeolites produced with lower zinc contents.

Cavdar, A.O., Arcasoy, A., Cin, S., Babacan, S., Gozdasoglu, S. (1983) Geophagia in Turkey,: Iron and zinc deficiency, Iron and zinc absorption studies and response to treatment with zinc in geophagia cases. *Progress in Clinical Biologic Research*, **129**, 71-97.

Khan, H.R., Mc Donald, G.K., Rengel, Z.(1998) Assessment of the zinc status of chickpea by plant analysis. *Plant and Soil*, **198**, 1-9.

CLAYEY CAP-ROCK BEHAVIOR IN H₂O-CO₂ MEDIA AT LOW PRESSURE AND TEMPERATURE CONDITIONS: AN EXPERIMENTAL APPROACH

Teddy Parra and Eric Kohler

Institut Français du Pétrole, Direction Géologie-Géochimie-Géophysique, 1-4 Avenue de Bois Préau, 92025 Rueil-Malmaison, France; teddy.parra@ifp.fr

The CO₂ storage in depleted hydrocarbon reservoirs requires the understanding of the CO₂ impact on clay-rich sealing cap-rocks and demonstrating the safety of the site over thousands of years. In particular, the knowledge of the critical parameters that modify physical properties such as permeability and fracturing are key factors. The PICOREF project (Brosse *et al.* 2006) has identified a potential experimental site for CO₂ geological storage at SMB (Saint Martin de Bossenay, Paris basin, France).

The purpose of this work is to study the physico-chemical reactivity of SMB clayey materials, as a function of the H₂O-CO₂ ratio in the fluids. Two kinds of experiments were designed to determine reaction paths and diffusion processes around 150°C and 150 bars. The first set of experiments involves ground materials with various CO₂ amounts in water. These experiments aim at increasing the minerals reactivity and at generating mineral sequences ideally up to thermodynamic equilibrium. The second set of experiments concerns cm-scale samples enclosed in H₂O or CO₂ pure media. The reaction fronts that can be observed on sample borders gives a direct observation of the mineralogical changes through time.

All samples were analyzed before and after alteration using XRD and FTIR to quantify mineralogical evolutions and using electron microprobe and AEM/TEM to estimate chemical variations according to the observed reactions and migration fronts in clay minerals.

Our results evidence a strong impact of the H₂O-CO₂ media on clayey materials and carbonates in these thermobarometric conditions above the maximum burial temperature and pressure conditions (63 °C, 145 bars). The different experiments serve as key indicators to determine the mineralogical sequences. Water-pure experiments show a muscovite enrichment of clays, whereas CO₂-pure experiments show a splitting of clay compositions toward an interfolial-poor phyllosilicate and a trioctahedral end-member. As observed in powder experiments, salinity does not seem to have a strong impact on mineralogical sequence, but can change the mineral compositions. These mineralogical sequences are used to constrain the numerical modeling of the experiments presented as a poster in the present session.

Brosse, E., de Smedt, G., Bonijoly, D., Garcia, D., Saysset, S., Manai, T., Thoraval, A. and Crepin, S. (2006) PICOREF: Towards an experimental site for CO₂ geological storage in the Paris basin? Proceedings of the 8th International Conference on Greenhouse Gas Control Technologies, 19-22 June, Trondheim, Norway.

TEM INVESTIGATIONS ON NATURE, DISTRIBUTION AND FACTORS AFFECTING CLAYS AND NANOPARTICLES IN SOIL SYSTEM

Nicolas Perdrial¹, Françoise Elsass^{1,2}, and Nicole Liewig³

¹Centre de Géochimie de la Surface, CNRS-ULP, F-Strasbourg; perdrial@illite.u-strasbg.fr

²PESSAC, INRA, RD 10, F-Versailles

³IPHC, Ecologie Physiologie Ethologie, CNRS-ULP, F-Strasbourg

Suspended particulate matter (SM) in rainfall and soil solution had been sampled for nine months in order to study the factors affecting the nature and the distribution of nanoparticles in natural environments. Investigation of individual particles by coupling transmission electron microscopy (TEM) for the morphology and energy dispersive spectroscopy (EDX) for the chemical composition allows a quantitative typological classification taking into account mineral and organic types of constituents present in the soil system. Eight different types of particles were determined: (1) clays, (2) weathered clays and (3) oxi-hydroxides for the minerals, (4) biofilms and (5) bacteria for the organic types, (6) organic-mineral associations as aggregates, (7) salts precipitated from the soil water and (8) an undetermined type. By using a new *in situ* microlysimeter specially designed for this study, we performed a field experiment where SM was collected directly on TEM grids.

The nature and abundance of particles in rainfall and percolating soil water were monitored during nine months. TEM-EDX data highlighted the importance of microorganisms and clays in terms of chemical reactivity. Moreover it appeared that these two types of particles were often aggregated as highly reactive pollution vectors. As a parallel result it appeared that bacteria were the main vector of lead transport in studied natural environments (atmospheric and soil). TEM-EDX investigations and image analysis on the sampled material allowed characterizing the nature, the reactivity and the interactions between particles according to time and/or depth.

Over a nine months period, results showed that the hydrodynamic properties of the soil were the main factors controlling the distribution of particles. Along the soil profile clays were increasingly aggregating with bacteria generating highly reactive compounds. The proposed process controlling this behavior is the dynamic of the water saturation of the soil. At a monthly scale, the investigation of a one-off arsenic input showed that the soil water was quickly eliminating the pollution by rapid runoff.

Finally it appeared that: (i) atmospheric fallout and soil solution are transporting the same types of particles, (ii) aggregation of clays and bacteria form highly reactive compounds, (iii) one-off events are rapidly smoothed by the hydrodynamic properties of the soil.

THERMAL AND BIOCHEMICAL CHARACTERIZATION OF SOIL CLAYS FROM A CULTIVATION CHRONOSEQUENCE

Alain F. Plante¹, Laurent Grasset², André Amblès², Claire Chenu³, and Dominique Righi⁴

¹ Dept. Earth & Environmental Science, University of Pennsylvania, 254-B Hayden Hall, 240 South 33rd Street, Philadelphia, PA, 19104-6316, USA; aplante@sas.upenn.edu

² SRSN, UMR CNRS 6514, 40, Av. du Recteur-Pineau, 86022 Poitiers, France

³ Bioemco, UMR CNRS- UPMC- INRA- INAPG-ENS-ENSCP, Bâtiment EGER, 78850 Thiverval-Grignon, France

⁴ HydrASA, UMR CNRS 6532, 40, Av. du Recteur-Pineau, 86022 Poitiers, France

Clay-associated organic matter (OM) resistant to hydrogen peroxide (H_2O_2) treatment is presumed to have higher proportions of recalcitrant OM (Plante et al., 2004), some of which has been shown to be enriched in aliphatic compounds. The objectives of this study were to characterize clay-associated OM using thermal analysis techniques before and after hydrogen peroxide treatment and secondly, to characterize the molecular structure of the hydrophobic part (e.g. lipids) of this resistant OM pool to determine the impact of land use. Clay-sized fractions were isolated from a cultivation sequence located in southwest France consisting of continuous forest, and 7 and 35 years of corn cultivation after forest clearing. Fractions were analyzed by thermogravimetry and differential scanning calorimetry using a Netzsch STA 409 thermal analyzer. The lipidic parts of the fractions were also analyzed using preparative thermochemolysis with TMAH (Gobé et al., 2000; Grasset et al., 2002).

Differential scanning calorimetry analyses showed significant differences in the quality of OM with changing land-use, marked by a large decrease in thermally labile OM and a relative increase in more thermally recalcitrant OM. Lipid analyses showed a relative enrichment of whole lipidic and simple lipids parts in samples after H_2O_2 treatment and a relative impoverishment after corn cultivation. Identified simple lipids before H_2O_2 treatment are mainly fatty acids, aliphatic hydrocarbons and alkanols. The H_2O_2 -resistant pools of simple lipids are preferentially comprised of compounds which have a strong microbial signature.

While proportions of H_2O_2 -resistant OM in the clay-sized fractions across the chronosequence were not consistent with current expectations, these analyses confirm the presence of highly recalcitrant OM that may be physically protected within clay-sized microaggregates.

Gobé, V., Lemée, L. and Amblès, A. (2000) Structure elucidation of soil macromolecular lipids by preparative pyrolysis and thermochemolysis. *Organic Geochemistry*, **31**, 409-419.

Grasset, L., Guignard, C. and Amblès, A. (2002) Free and esterified aliphatic carboxylic acids in humin and humic acids from a peat sample as revealed by pyrolysis with tetramethylammonium hydroxide or tetraethylammonium acetate. *Organic Geochemistry*, **33**, 181-188.

Plante, A.F., Chenu, C., Balabane, M., Mariotti, A. and Righi, D. (2004) Peroxide oxidation of clay-associated organic matter in a cultivation chronosequence. *European Journal of Soil Science*, **55**, 471-478.

FAST ASSEMBLY OF NANOCOMPOSITE FILMS AND THEIR GEOMETRICAL AND MECHANICAL CHARACTERISATION

Michael Plotze¹, Viatcheslav Vertlib¹, Marianne Dietiker², Alexander Puzrin¹ and Ralph Spolenak²

¹ETH Zurich, Institute for Geotechnical Engineering, ClayLab, CH-8093 Zurich, Switzerland;
michael.plotze@igt.baug.ethz.ch

²ETH Zurich, Laboratory for Nanometallurgy, Department of Materials, CH-8093 Zurich, Switzerland

Multi-layered polymer-clay nanocomposites attract considerable attention due to their mechanical properties, which resemble those of naturally occurring composite materials with layered structure such as nacre, bone, and tooth enamel. Currently, the most commonly used method to prepare multi-layered polyelectrolyte-clay nanocomposites is based on a dip self assembly process, in which a flat substrate (typically an oxidized silicon wafer) is sequentially dipped in polyelectrolyte and clay solutions. This method allows the layered morphology to be controlled at the nanoscale, however it also possesses the serious disadvantage of being extremely time consuming. We have recently developed a spin coating layer-by-layer assembly process, which allows for the rapid production of films with controlled layered structure.

Thin nanocomposite films (up to 0.5 μm) have been prepared with poly(diallyldimethylammonium) chloride, (PDDA) and a variety of smectite clays, such as Laponite (a synthetic) and a natural sodium montmorillonite (CMS source clay SWy-2). The single clay-polyelectrolyte layer thickness as well as linear growth of the nanocomposite on silicon substrates has been carefully characterized by ellipsometry. The surface roughness and total thickness of the nanocomposite films on silicon substrates have been measured by AFM. We have also optimized the conditions that yield films appropriate for mechanical testing by nanoindentation (hardness and modulus).

The experimental results are interpreted in the context of mechanical data for similar nanocomposites prepared by the dip coating method. It was found that the spin coated nanocomposite film exhibits clearly improved mechanical properties compared to the 'pure' polymer film and that the improved production route leads to equal hardness and modulus values compared to conventional dipping procedure.

CHEMISTRY OF MECHANICAL PERFORMANCE: EMORY, SELF-HEALING BEHAVIOR, AND HIGH IMPACT RESISTANCE IN NANOCOMPOSITES

Clois E. Powell and Gary W. Beall

Texas State University-San Marcos, 601 University Drive, San Marcos, Texas 78666-4616,
USA; Cp21@txstate.edu

The relation between chain conformation and relaxation dynamics in polymers to the development of shape memory, self healing in polymers is of fundamental and application significance. Preliminary data on the introduction of nanoparticles into the polymer indicated a larger elongation at break and enhanced shape memory. This is unprecedented in commercial polymer composites. The incorporation of nanoscale ceramic platelets, rather than microscale additives, break the traditional paradigm of decreased elongation with the incorporation of reinforcing additives into polymers. In the last 15 years, major advancements have been made in the development of polymer nanocomposites, polymers with memory, and polymers that exhibit self-healing properties. The scientific and technological importance of these polymers can be measured by the enormous increase in international scientific publications and patents focused on these polymer types. Texas State University (TxState) has developed a new family of polymers that exhibit all of these characteristics in addition to unprecedented impact resistance and nanocomposites of this polymer family. The objective of the presentation is an investigation of the short and long term time dependent effects in a new high impact polymer and polymer nanocomposites and to provide a fundamental investigation to identify the structure-property relationships that define the chemistry of polymer mechanical performance in the areas of memory, self-healing behavior and high impact resistance.

IN SITU ATTENUATED TOTAL REFLECTANC FTIR STUDY OF NITROAROMATIC SORPTION TO SMECTITE

Gnanasiri S. Premachandra and Cliff T. Johnston

Crop, Soil and Environmental Sciences, 915 W. State St. Purdue University, W. Lafayette, IN 47907; prema@purdue.edu

Nitroaromatic compounds (NACs) are widely used as pesticides, explosives, solvents and intermediates in chemical syntheses. NACs and their degradation products pose a potential threat to ecological and human health because they are toxic contaminants that can be found in soils at elevated concentrations. Over the past five years, we have systematically investigated the sorption of a wide range of nitroaromatics and related compounds to soil minerals (e.g., (Boyd, et al. 2001; Johnston, et al. 2004; Johnston, et al. 2001; Li, et al. 2004; Sheng, et al. 2001). Our prior spectroscopic work analyzed mainly 'dry' clay-nitroaromatic complexes. In this study, however, we examined the ability of ATR-FTIR spectroscopy to study nitroaromatic sorption to smectite in aqueous suspension. TNB (1,3,5-trinitrobenzene) on SWy2 smectite was selected as a model system. The presence of TNB sorbed to the SWy-2 smectite was confirmed by the three TNB bands at 3108, 1548 and 1353 cm^{-1} . The 1353 ν_{sym} (NO_2) stretching band of TNB was used for qualitative and quantitative measurements. The influence of exchangeable cations on the TNB band position was observed using SWy-2 exchanged with different cations (Cs, K, Na, Li, Ba, Ca and Mg). The ATR-FTIR method provided a means of constructing spectroscopic sorption isotherms that were then compared to traditional HPLC-based sorption isotherms. Finally, polarized ATR-FTIR methods were used to study the orientation of the sorbed species.

Boyd, S.A., Sheng, G., Teppen, B.J., and Johnston, C.T. (2001) Mechanisms for the adsorption of substituted nitrobenzenes by smectite clays. *Environmental Science and Technology*, **35**, 4227-4234.

Johnston, C.T., Boyd, S.A., Teppen, B.J., and Sheng, G. (2004) Sorption of nitroaromatic compounds on clay surfaces. p. 155-189 *In* S.M.Auerbach, K.A.Carrado, and P.K.Dutta(ed.) *Handbook of layered materials*, Marcell Dekker Inc., New York, NY.

Johnston, C.T., Oliveira, M.F.D., Sheng, G., and Boyd, S.A. (2001) Spectroscopic Study of Nitroaromatic-Smectite Sorption Mechanisms. *Environmental Science and Technology*, **35**, 4767-4772.

Li, H., Teppen, B.J., Laird, D.A., Johnston, C.T., and Boyd, S.A. (2004) Geochemical modulation of pesticide sorption on smectite clay. *Environmental Science and Technology* **38**, 5393-5399.

Sheng, G.Y., Johnston, C.T., Teppen, B.J., and Boyd, S.A. (2001) Potential contributions of smectite clays and organic matter to pesticide retention in soils. *Journal of Agriculture and Food Chemistry*, **49**, 2899-2907.

VIBRATIONAL SPECTROSCOPIC STUDY OF DIBENZO-P-DIOXIN SORPTION TO Cs-SAPONITE

Kiran Rana¹, Cliff T. Johnston¹, Gnanasiri S. Premachandra¹, Stephen A. Boyd², Brian J. Teppen², and Hui Li²

¹Crop, Soil and Environmental Sciences, 915 W. State St. Purdue University, W. Lafayette, IN 47907; krana@purdue.edu

²Department of Crop and Soil Sciences, Michigan State University, East Lansing, MI 48824-1325

The sorption of polycyclic aromatic hydrocarbons (PAHs), polychlorinated biphenyl (PCBs), and dioxins in soils and sediments is critical to understanding their environmental fate and transport. Recently, expandable clay minerals have been shown to have a higher-than-expected affinity for these intrinsically nonpolar compounds. To gain additional perspective on the mechanisms that govern dioxin-PAH-PCB sorption to soil minerals, this study focused on the interaction of dibenzo-p-dioxin with Cs-saponite as a model system by integrating macroscopic batch sorption experiments with spectroscopic analysis. Sorption of dibenzo-p-dioxin (DPD) from aqueous suspension to Cs-saponite was investigated by high-performance liquid chromatography (HPLC). In addition, parallel experiments using Fourier transform infrared spectroscopy (FTIR), attenuated total reflectance FTIR, and Raman spectroscopy of clay-DPD complexes were conducted. In order to assign the IR- and Raman-active vibrations of DPD, polarized single crystal Raman spectra of oriented DPD crystals were obtained and compared to ATR-FTIR and FTIR spectra of DPD. Excellent agreement was found between the HPLC batch sorption study and an *in situ* ATR FTIR study of DPD sorption to Cs-saponite. IR- and Raman-active bands of DPD sorbed to Cs-saponite in the 1280 to 1500 cm⁻¹ region were perturbed compared to the 'reference' IR and Raman spectra of DPD. Sorption mechanisms of DPD to Cs-saponite will be related to clay surface chemistry and to the molecular properties of DPD.

CHARACTERIZATION OF SAN JUAN ILLITE RM30: A REEVALUATION

Philip E. Rosenberg¹ and Robert L. Hooper²

¹School of Earth and Environmental Sciences, Washington State University, Pullman, WA 99164-2812, USA; e-mail: rosenberg@wsu.edu

²Department of Geology, University of Wisconsin-Eau Claire, Eau Claire, WI 54701, USA

A reinvestigation of San Juan illite RM30 (Eberl et al., 1987) was undertaken to clarify its chemical composition and polytypism. Single crystal AEM analyses (Rosenberg and Hooper, 1996) on an aliquot of the original material generally agreed with XRF analyses but recent AEM analyses by Peacor et al. (2002) found a bimodal chemistry correlated with the presence of both a Mg-rich ($0.31\text{ Mg}^{2+}\text{ pfu}$) 1M polytype and a Mg-poor (0.10 pfu) 1Md polytype in equal proportions. Significant differences were also observed in the K-content: $0.80\text{--}0.79\text{ K}^+\text{ pfu}$ Eberl et al. (1987); Rosenberg and Hooper, (1996)] and $0.73\text{--}0.74\text{ K}^+\text{ pfu}$ (Peacor et al., 2002).

XRD studies in the current study suggest that the 1M polytype is predominant. The “illite hump” which is characteristic of the 1Md polytype (Grathoff and Moore, 1996) was not observed. To minimize the possibility that the current AEM analyses are biased as a result of electron beam sensitivity, eleven successive AEM analyses of a single grain were collected. AEM analyses of thirty-two (32) individual grains provide no hint of bi-modal grain chemistry. The average illite composition determined by AEM, $\text{K}_{0.80}\text{Na}_{0.01}\text{Ca}_{0.01}(\text{Al}_{1.87}\text{Mg}_{0.12}\text{Fe}_{0.01})[\text{Si}_{3.24}\text{Al}_{0.76}\text{O}_{10}](\text{OH})_2$ is in excellent agreement with the original XRF compositions reported by Eberl et al. (1987). The new AEM analyses represent significantly improved quantification with considerably smaller standard deviations.

The apparent differences in polytypism and chemical composition of RM30 can not be explained by systematic analytical uncertainties or the fortuitous analysis of impurity phases during bulk XRF analysis and therefore, may indicate real variability between samples. Furthermore, 1M stacking may not necessarily be caused by “compositional anomalies” as suggested by Peacor et al. (2002).

Eberl, D.D., Srodon, J., Lee, M., Nadeau, P.H., and Northrup, H. R. (1987) Sericite from the Silverton caldera Colorado: Correlation among structure, composition, origin and particle thickness. *American Mineralogist*, **72**, 914-934.

Grathoff, G.H. and Moore, D.M. (1996) Illite polytype quantification using WILDFIRE calculated X-ray diffraction patterns. *Clays and Clay Minerals*, **44**, 835-842.

Peacor, D.R. Bauluz, B., Dong, H., Tillick, D. and Yan, Y. (2002), Transmission and electron microscopy evidence for high Mg contents of 1M illite: Absence of 1M polytypism in normal prograde diagenetic sequences of pelitic rocks. *Clays and Clay Minerals*, **50**, 757-765.

Rosenberg, P.E. and Hooper, R.L. (1996) Determination of the chemical composition of natural illites by analytical electron microscopy. *Clays and Clay Minerals*, **44**, 569-572.

WATER AND IONIC EXCHANGE BETWEEN INTERLAYER AND MICROPOROSITY FROM MOLECULAR DYNAMICS SIMULATIONS

Benjamin Rotenberg^{1,2}, Virginie Marry¹, Natalie Malikova^{3,4}, Rodolphe Vuilleumier⁵, Eric Giffaut¹, and Pierre Turq¹

¹Université Pierre et Marie Curie, Laboratoire LI2C, UMR CNRS 7612, CC51, 4 pl. Jussieu, Paris F-75005, France; rotenber@ccr.jussieu.fr

²ANDRA, Parc de la Croix Blanche, 1/7 rue Jean Monnet, 92298 Châtenay-Malabry Cedex, France

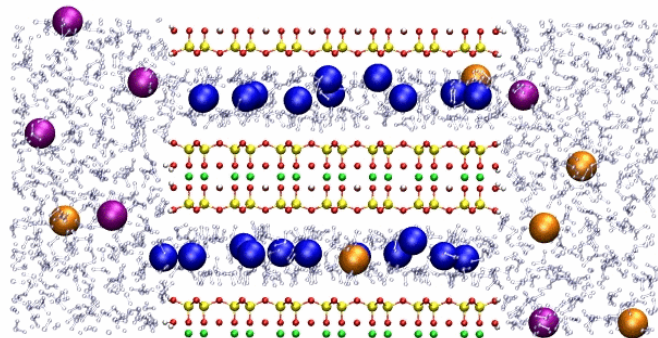
³Argonne National Laboratory, IPNS Division 9700 S Cass Avenue, Argonne, IL 60611, USA

⁴Laboratoire Léon Brillouin, CEA Saclay, 91191 Gif-sur-Yvette Cedex, France

⁵Université Pierre et Marie Curie, Laboratoire LPTMC, UMR CNRS 7600, 4 pl. Jussieu, Paris F-75005, France

Mobility of ions in clays is greatly affected by their interactions with the mineral surfaces. Depending on their charge, they explore a different fraction of the porosity : Cations can enter into the clay interlayers by exchanging with the natural counterions, whereas it is believed that anions remain in larger porosities ($> \text{nm}$). Understanding cationic exchange and anionic exclusion is necessary to provide a consistent picture of ionic transport through clay minerals. This is particularly important in the context of geological storage of toxic or radioactive waste, where the geological medium acts as a barrier preventing the release of waste into the biosphere.

We present a molecular dynamics study of water and ionic exchange, with simulation of a system including both clay particles (with interlayer porosity and counterions) and a bulk salt solution (micropore). A force field based on ab-initio simulations was developed for the description of the clay edges.



Equilibrium simulations show that a Cs^+ ion near the lateral surface can enter into the interlayer within a few nanoseconds, and that water can exchange between interlayer and microporosity on this time scale. On the contrary, no anion was found to enter into the interlayer during the 10 ns simulation. The free energy cost of forcing an anion into the interlayer was estimated using a set of biased simulations combined with an unbiased scheme (Weighted Histogram Analysis Method). The relatively high value of this penalty (about 12 times the thermal energy) confirms that anions are excluded from the interlayer.

DISSOLUTION KINETICS OF SMECTITE: PH AND TEMPERATURE DEPENDENCE

Maria L. Rozalen¹, F. Javier Huertas², and Patrick V. Brady¹

¹Sandia National Laboratories, Albuquerque, NM 87185, USA; mlrozal@sandia.gov

²Estacion Experimental del Zaidin, CSIC, Granada, 18008, Spain

Smectite clays are both abundant and ubiquitous at the Earth's surface. They are also being considered as engineered barriers for nuclear waste repositories in Europe. Smectite stability in natural and engineered settings depends upon mineral surface-controlled dissolution/precipitation reactions. Often these reactions occur at temperatures above 25 °C and/or at extreme pHs (e.g., at the hyperalkaline conditions imposed by interaction of groundwater with concrete in an engineered repository), where the mineral-fluid interface is not well understood. Here we examine the combined effect of pH and temperature on smectite dissolution.

Dissolution experiments at 25, 50, and 70 °C were performed in flow-through cells using input solutions buffered at pH 1 to 13.5 until steady state conditions were achieved. The output solutions were analyzed for Si, Al and pH. Smectite dissolution rates were calculated from steady-state Si and Al concentrations. We have obtained equations that describe the pH-dependent dissolution rate at each temperature. The results show a clear dependence of dissolution rates on both pH and temperature. Dissolution is minimal around neutral pH (6-7), but increases in more acidic and alkaline solutions. The dissolution profiles become concave at higher temperature.

The fact that the kinetic parameters, reaction order and constant, vary with temperature point to an apparent activation energy that varies with pH. This differs from two previous studies. Köhler et al. (2003) measured temperature-dependent illite dissolution at 5, 25 and 50 °C and found a pH-independent activation energy, as was originally proposed by Bauer and Berger (1998). We believe that the larger number of data points measured in the present study provide a stronger basis for pH-dependent activation energies (see also Carroll and Walther, 1990; Sato et al., 2003) and point to the importance of understanding pH and temperature-dependent smectite surface chemistry.

Bauer, A., Berger, G. (1998) Kaolinite and smectite dissolution rate in high molar KOH solutions at 35 and 80 °C. *Applied Geochemistry*, **13**, 905-916.

Carroll S.A., Walther J.V. (1990) Kaolinite dissolution at 25, 60 and 80°C. *American Journal of Science*, **290**, 797-810.

Köhler, S.J., Dufaud, F., Oelkers, E.H. (2003) An experimental study of illite dissolution as a function of pH from 1.4 to 12.4 and temperature from 5 to 50 °C. *Geochimica et Cosmochimica Acta*, **67**, 3583-3594.

Sato, T., Kuroda, M., Yokoyama, S., Fukushi, K., Tanaka, T., and Nakayama, S. (2003) Mechanism and kinetics of smectite dissolution under alkaline conditions. *Geochimica et Cosmochimica Acta*, **67**, S1, A415.

STANDARDS-BASED PRE-K-12 CURRICULUM FOR CLAY SCIENCE

Audrey C. Rule¹ and Stephen Guggenheim²

¹Department of Curriculum and Instruction, 250-G Wilber Hall, State University of New York at Oswego, Oswego, NY 13126, USA; arule@oswego.edu

²Earth and Environmental Sciences, 845 West Taylor Street, University of Illinois at Chicago, Chicago, IL 60607-7059, USA

Two National science education documents, the *Benchmarks for Science Literacy* and the *National Science Education Standards*, are used to design a prekindergarten to 12th grade curriculum with clay concepts that support learning in chemistry, physical science, and Earth science (Rule & Guggenheim, in press). The curriculum is divided into concepts and activities for early childhood, elementary, middle school, and high school students. Activities are shown in the table below.

Level	Activities				
Early Childhood	Identify local places when clay can be seen. Examine and describe mud samples.	Experiment with rolling, pressing, molding, impressing clay. Compare sand to clay. Compare wet to dry clay.	Assemble a classroom collection of objects that are made with clay. Organize the collection.	Pour water on cat litter. Make observations.	Make a simple pinch pot. List the steps. Use a wheel or other tools to make a clay pot.
Elementary	Examine SEM photographs of clays and other substances or life forms. View photomicrographs of hexagonal kaolinite crystals.	Compare natural clay or greenware with a variety of ceramic items. Compare heat conduction of a ceramic mug, a plastic mug, and a paper cup filled with a hot liquid.	Shake a jar with sand, silt, clay and water. Watch the particles settle. Smear clay into a pan and sand. Run a fan and then pour water over both and observe.	Experiment with making statues from plain clay and clay with lint. Describe how fibers reinforce it. Investigate the history of ceramics and impact on society.	Investigate soil samples from different local places. Identify some of the life forms present. Create a poster display of findings.
Middle School	Examine mudstone, siltstone, claystone, shale, and localities. Compare to schist and slate.	View drawings and models of clay structures. View photomicrographs of clay crystals. Match products to clays with specific properties.	Create a poster or electronic presentation of the steps in making a specific product containing clay.	Investigate a soil profile. Chart the different layers and their compositions/ characteristics.	Visit the web sites of different societies for clay scientists. Investigate the skills needed to work as a clay scientist.
High School	Investigate how clays are used in landfills and water treatment.		Investigate dispersion, absorption, and cation exchange of swelling clay.		

American Association for the Advancement of Science. (1993) *Benchmarks for science literacy*.

Washington, DC, Author, 454 p.

National Research Council. (1996) *National science education standards: Observe, interact, change, learn*. National Academy Press, Washington, DC, 262 p.

Rule, A. C., & Guggenheim, S. (in press). A standards based curriculum for clay science. *Journal of Geoscience Education*.

**MICROMORPHOLOGICAL INVESTIGATION OF SEPIOLITE-BEARING
PETROCALCIC HORIZONS FORMED FROM LACUSTRINE SEDIMENTS ON THE
SOUTHERN HIGH PLAINS OF WEST TEXAS AND EASTERN NEW MEXICO**

Dusten Russell, W. H. Hudnall, and B.L. Allen

Texas Tech University, Plant and Soil Science Department, USA, Lubbock TX, 79409;
dusten.russell@ttu.edu

Petrographic and Scanning Electron Microscopy (SEM) were used in the investigation of depositional and pedogenic processes of petrocalcic horizons formed in lacustrine sediments on the Southern High Plains (SHP) of Texas and New Mexico. This investigation was carried out within the ancestral Brazos River drainage system. Sepiolite formation on the SHP of Texas and New Mexico has been found to be commonly associated with lacustrine environments in conjunction with dolomite and calcite. The presence of sepiolite in soils has long been thought to have been inherited from parent materials via secondary (eolian, alluvial) depositional processes due to the apparent instability of sepiolite in pedogenic environments. The petrocalcic horizons that formed in the lacustrine sediments are multicyclic with varying degrees of laminae formation and pisolithic features. Macromorphology and micromorphology of the petrocalcic horizons show extensive influence of pedogenic processes. Typical sepiolite morphology displays lath-like or fibrous needle-shaped particles, often interbedded with calcite and dolomite. Petrographic analysis and SEM's show unique spheroids comprised of sepiolite. The spheroids occur within multiple laminae throughout the petrocalcic horizons. Micritic calcite has precipitated on the surface of the sepiolite spheroids. The sepiolite spheroids may have formed as Mg-rich waters reacted with the silica-rich volcanic ash.

LIFE AT THE EDGE: CLAY MINERALOGY, MICROBIOLOGY, AND THE INTERNATIONAL KAMCHATKA MICROBIAL OBSERVATORY

Paul A. Schroeder, Douglas Crowe, and Christopher Romanek

Department of Geology, University of Georgia, Athens, GA, USA schroe@uga.edu

New challenges abound in the area of integrated clay mineral and microbiological studies. Both fields are dedicated to finding ways to better characterize micron to molecular scale structures and to more fully understand the biogeochemical pathways used in response to environmental change. One approach to fostering progress in these two fields is to establish large collaborative groups, such as the Kamchatka Microbial Observatory (KMO). The KMO is situated in the Uzon Caldera, which is a large geothermal area located in Far Eastern Russia. This collaborative effort includes U.S. and Russian scientists with a wide variety of skills and skill levels (undergraduate students, graduate students, post-docs, and senior researchers). If successful outcomes are to be expected with this approach the effort must be based on holistic guiding principles that take full advantage of the differing cultural backgrounds, skill levels, areas of expertise, and environmental settings. The following perspectives from U.S. mid-career earth scientists studying terrestrial hot springs are offered to advance integration efforts. Whether you are a senior level scientist or a beginning graduate student, the following are likely to be true:

1. It takes time to learn the jargon and methodology of both clay mineralogists and microbiologists. Allow several years to be conversant with each other.
2. It takes time to learn cultural nuances and the bureaucracies of different countries. Allow several years to be conversant with each other.
3. Expertise and sampling must be holistic (or ecological). In addition to studying clay minerals, the fluids, gases, other minerals, and biological components must be considered and analyzed at all scales. Different disciplines have different scales of observation that need to be accommodated into field plans.
4. Sampling protocols and instruments do not necessarily translate between disciplines and environments. For instance artifacts are common when analyzing waters from hot springs compared to simpler meteoric waters (arsenate interferes with phosphate measurements; sulfide interferes with ammonium, electronics such a pH meters fail within minutes of use; and clay mineral – microbe relations can be destroyed). Be prepared to develop new protocols.
5. Development of outreach components (workshops, web sites, lectures, and documentaries) takes resources, time, and expertise beyond clay mineralogy or microbiology. Museums and educators need to be included in the research.
6. Perhaps the most important key to success is the ability to compromise and say, “I don’t understand. Please explain it again (and again)”. Two-way communication is essential for integrating clay mineralogy and microbiology. Admitting you do not understand something makes you a better scientist and what you learn benefits the group.

In 4 years the KMO has hosted 13 principal investigators, 6 senior researchers and post-docs, 17 graduates students, 9 undergraduates, 3 guest scientists, and 4 members of the press. The discovery of novel species of thermophilic bacteria and archea in the KMO is rapidly progressing. It appears that clays and clay minerals are integral to microbial metabolic pathways and perhaps serve as refugia for nitrogen species (e.g., interlayer NH_4^+) and V^{I} Fe-clays facilitate redox reactions.

NITROGEN AND SMECTITES FROM TERRESTRIAL HOT SPRINGS IN THE UZON CALDERA, KAMCHATKA, FAR-EASTERN RUSSIA

Paul A. Schroeder¹ Elizaveta Bonch-Osmolovskaya², Elizabeth Burgess⁵, Albert Colman³, Douglas Crowe¹, Julie Fiser⁷, Maggie Hodges¹, Elizabeth Hollingsworth¹, Gennady Karpov⁶, Ilya Kublanov², Jennifer Kyle¹, Gary Mills⁴, Andrew Neal^{4,5}, Nikolai Pimenov², Frank Robb³, Christopher Romanek^{1,7}, Tatiana Slepova², Tatyana Sokolova², Elisabeth Spencer⁷, Stephen Techtmann³, Isaac Wagner⁵, Juergen Wiegel⁵, Noah Wittman⁷, Chuanlun Zhang⁴, and Weidong Zhao⁴

¹Dept. of Geology, Univ. Georgia, Athens, GA, USA schroe@uga.edu; ²Winogradsky Inst., Russian Academy of Sciences, Moscow, Russia; ³Center of Marine Biotechnology, Univ. Maryland Biotech. Inst., Baltimore, MD, USA; ⁴Savannah River Ecology Lab, Aiken, SC, USA; ⁵Dept. of Microbiology, Univ. Georgia, Athens, GA, USA; ⁶Inst. Volcanology and Seismology, Russian Academy of Sciences, Petropavlovsk-Kamchatsky, Russia; ⁷The Exploratorium, San Francisco, CA, USA.

The Uzon Caldera constitutes a large geothermal region that includes varied high-temperature, acidic, and strong redox environments hosting novel life forms. Springs and associated microbial mats and sediments were sampled within this context, to characterize the thermophilic and hyperthermophilic microbial populations. Carboxydrotrophs, ferric iron reducers, sulfate reducers, and arsenate reducers among others were targeted through isolation of novel species, MPN field incubations, 16S rDNA clone libraries, metagenomic libraries, enrichment culturing, and radiotracer experiments. We have isolated new species/genera related to *Carboxydocella*, *Dictyoglomus*, *Thermoanaerobacter*, *Thermobaculum*, *Geobacillus*, *Bacillus*, and *Anoxybacillus*. PLFA profiles and lipid stable isotope measurements have provided an independent survey of the major clades present and dominant carbon fixation pathways. Archaeal lipid biomarkers (GDGTs) in Uzon are different from those in other hot springs such as those found in Nevada and California.

Minerals in sediments, sinters, and mats were studied using X-ray diffraction, TEM, SEM/EDS, stable isotope geochemistry, and microbiological methods. High-resolution electron microscopy has revealed intimate and potentially functional relationships between nano-crystalline mineral surfaces (smectite, opal, pyrite, and ferrihydrite) and thermophilic microbes. Hot spring chemistries indicate dissolved ammonium levels averaging about 30 ppm, with some ranging up to 530 ppm. Fe-bearing smectite-rich clay fractions show ammonium and organic-N exchangeability by X-ray diffraction d_{001} response, labeled ^{15}N measurements, and C/N ratios. Preliminary PCR-based detection strategies for anoxic ammonium oxidizing organisms (anammox) indicate their presence in the hot springs. Clone sequences confirm anammox priming sites are present. PCR product from reactions with environmental DNA further indicate there are crenarchaeota and bacteria in springs that have the *amoA* gene, which is a subunit of the protein ammonia monooxygenase used in the first step of the pathway from NH_4^+ to NO_2^- . Although not yet supported by culture work in the presence/absence of clay minerals, the close association of ammonium-bearing Fe-smectites, anammox genes, and archaeal biomarkers suggests that clay mineral octahedral Fe-redox and interlayer nitrogen storage may be part of an essential pathway for high temperature anoxic ammonium oxidation. If such a pathway can be demonstrated, then paradigms for early earth nitrogen cycling may need to be modified.

CLAY MINERALOGICAL STUDIES FOR AEGINETAN WARE, AEGINA, GREECE

Christine M. Shriner¹, G. E. Christidis², J. G. Brophy¹, K. L. Finger³, and H. H. Murray¹

¹Dept. of Geological Sciences, Indiana Univ., Bloomington, IN, USA; cshriner@indiana.edu

²Dept. of Mineral Resources Engineering, Technical Univ. of Crete, Chania, Greece

³Museum of Paleontology, Univ. of California, Berkeley, CA, USA

The volcanic island of Aegina was a major producer of both fine ware and structural ceramics in the ancient world from at least the Greek Middle Bronze Age through the Classical period (2000-400 B.C.). Based on a combination of petrography, amphibole chemistry and REE chemistry, we have shown that a *single*, extensive early Pliocene volcanic ash horizon, altered to clay, was utilized for ceramic production over that time. A new definition for Aeginetan Ware that is based on the physical properties of its raw material source allowed us to develop a model for the process of local cultural change in the Third Millennium B.C. Our model suggests that ceramic change from predominantly fine fabrics to a coarser fabric was the result of exploitation of large proto-industrial clay deposits and not the importation of technological processes. This shift in raw material usage reflects a time period in which rapidly emerging technologies in many industrial pursuits required more structurally reliable ceramics (Shriner et al., *A Method of Explanation for the Process of Cultural Change II, Hesperia*, submitted).

In order to further substantiate our model, we examined the geological, mineralogical and geochemical characteristics of this early Pliocene clay-rich horizon. Furthermore, we compared the results with the mineralogical and textural characteristics of a local Neogene marl. This marl is utilized today for ceramic production and also considered by many researchers (e.g. Hein et al., 2004) the main clay source for Bronze Age Aeginetan Ware. The archaeological question is whether or not the volcanic clay horizon would make a better proto-industrial mineral deposit than the marl.

The clay mineralogy, and the major and trace element chemistry of the Neogene marl is distinctively different from the early Pliocene volcanic clay. The clay fraction of the Neogene marl is dominated by R0 mixed-layer illite-smectite, with subordinate mica and chlorite. The volcanic clay contains abundant discrete chlorite and R0 mixed-layer chlorite-rich C/S, which contributes to a longer vitrification range. Minor smectite and traces of palygorskite are also present. The smaller abundance of smectite contributes to the workability of the ceramic body, without considerable drying and/or firing shrinkage. The different mineralogy and chemistry suggests different sources for the two clays. The Neogene marl has a fine macrofabric, whereas the early Pliocene clay has both fine-grained and coarse-grained microfabrics, reflecting the distance of deposition from the source area. Utilization of the Neogene marl for structural ceramics would necessitate the addition of a temper. Based on the differences in mineralogical composition and particle size distribution, the volcanic ash clay exhibits superior firing properties potential to the Neogene marl and would be a better proto-industrial deposit for various structural ceramics.

Hein, A., H. Mommsen, and G. Zender. 2004. "Pliocene Clays from Aegina (Greece): Reference Material for Chemical Provenance Studies on Bronze Age Pottery from the Island," *Geoarchaeology* 19.6, pp. 553-564.

CLAY MINERALOGICAL STUDIES FOR GREEK BRONZE AGE ROOFING TECHNOLOGY

Christine M. Shriner, Erika R. Elswick, Hannah L. Timm, and Haydn H. Murray

Dept. of Geological Sciences, Indiana Univ., Bloomington, IN, USA; cshriner@indiana.edu

The Early Helladic II period (2650-2150 B.C.) of the Greek Bronze Age terminates with the introduction of a monumental architectural phenomenon, termed the “corridor house”. This building structure is verified at Lerna, Akovitika, Kolonna on Aegina, Thebes, and Zygouries. All of these structures exhibit a basic design: rectangular, free-standing, a linear series of rectangular rooms, and corridors on the long sides which also serve as stairwells to a second story. There has been an archaeological emphasis on reconstruction and stylistic development of this building type (e.g. Shaw, 1987). The form is presumed to be part of an indigenous development. However, due to a lack of local raw material references, the construction technology of this architectural form is not well understood. The “House of Tiles” at Lerna is the best preserved corridor house, and the one from which we have obtained the most artifactual evidence. By employing an approach referred to by us as the *Integrated Petrologic Approach*, the local material references were analytically compared with fired terracotta roof tiles, clay sealings of boxes and baskets, and hearth material from the House of Tiles. It was concluded that these ceramic artifacts could be provenanced to local micaceous sediments, derived from the metamorphosed flysch of the lowest stratigraphic unit in the Lerna area, the Plattenkalk Series (Shriner, 1999). It was further hypothesized that the “schist” slabs used as eaves for the House of Tiles roofing system were derived from this same local stratigraphic package.

Petrographic analysis of twenty stone eaves reveals a fine-grained fabric in line with shale, rather than the expected chloritoid phyllite. In order to further characterize the bulk mineral assemblage, X-ray diffraction analysis was undertaken on the eaves, as well as samples from the local schist, phyllite and flysch deposits. The results indicate that patterns for the majority of eave samples are similar to the mineralogy of shale or siltstones obtained from specific flysch deposits, the Pindos and Tripolitza. The clay mineralogy is chlorite and illite, with accompanying quartz, calcite and muscovite. Bulk geochemical data was retrieved for all eave samples and source materials. Once again, the eaves appear to be quarried from a local geological sedimentary unit, rather than the presumed metamorphic unit. Bulk chemical composition indicates that the eaves analyzed were from one source, based on major oxide and key trace element cross plots. The artifactual data for the House of Tiles samples grouped together in a very homogenous cluster. These results indicate raw material extraction from a specific source location. A local source is suggested on the basis of the previous artifactual provenance evidence. The location of this quarry is predicted to be in the vicinity of the metamorphic window, 15 km northwest of Lerna, or located on the Arcadian border to the west.

Shaw, J. W. 1987. “The Early Helladic II Corridor House: Development and Form,” *American Journal of Archaeology* 91, pp. 59-79.

Shriner, C. M. 1999. “Ceramic Technology at Lerna, Greece in the Third Millennium B.C.: Economic and Social Implications” Ph.D. diss. Indiana University [University Microfilms 99.32706], 261 p.

CHARACTERIZATION OF NONEQUILIBRIUM SORPTION OF GASOLINE COMPONENTS BY SURFACTANT-MODIFIED ZEOLITE

Joshua A. Simpson and Robert S. Bowman

Department of Earth and Environmental Science, New Mexico Tech, Socorro, NM 87801, USA;
jasimpso@nmt.edu

Surfactant-modified zeolite (SMZ) has been shown to effectively remove benzene, toluene, ethylbenzene, and xylene (BTEX) from water generated during oil and gas production (produced water). The BTEX sorption isotherms are linear and noncompetitive, suggesting that the removal mechanism is partitioning into the surfactant's hydrophobic bilayer formed on SMZ. Even though BTEX sorption in batch systems is rapid, chemical equilibrium models do not accurately describe BTEX transport through packed beds of SMZ. Comparison with transport of a nonreactive tracer (tritium) suggests that two-site diffusive nonequilibrium sorption-desorption controls BTEX transport. We conducted batch experiments with SMZ to determine the nonequilibrium sorption kinetics of each BTEX constituent. The kinetic measurements were used to parameterize a nonequilibrium transport model to predict BTEX removal under varying flow conditions. The accuracy of predictions is being tested using laboratory column experiments with produced water from the San Juan Basin, New Mexico.

EVIDENCE FOR THE PRESENCE OF NATURAL ORGANO-CLAY NANOCOMPOSITES IN ONE PODZOL FROM THE TATRA MOUNTAINS, POLAND

Michał Skiba

Desert Research Institute, 2215 Raggio Parkway, Reno 89512-1095 Nevada, USA;
michal.skiba@dri.edu

Expanding clay minerals show great ability for interaction with different types of organic compounds, which may lead to the formation of organo-clay nanocomposites. Many experimental studies on the preparation and properties of this “new class of materials” have been conducted. The possibility of the natural nanocomposites formation has rarely been suggested, and there does not seem to be convincing evidence for their existence.

The aim of this paper is to present some evidence for the natural nanocomposite formation in the albic (E) horizon of one podzol profile from the Tatra Mts in Poland. The profile was selected because according to the available laboratory results from previous studies (Ohashi and Nakazawa 1996), its mineral composition (presence of significant amount of Al rich smectite and vermiculite in the E horizon), organic matter (humic and fulvic acids) and low pH (3.9 in H₂O) strongly favor the formation of nanocomposites.

Oriented mounts of three clay sub-fractions separated from the natural bulk soil were analyzed by X-ray diffraction (XRD), in natural state and after being subjected to organic matter removal, saturation with different cations and heating at 330°C and 550°C. All the fractions contain significant amounts of quartz, “~14Å clay”, and kaolinite. Mica and feldspars are also present. In natural state the “~14Å clay” shows high heat resistance, manifested by a partial shift to 10Å after heating at 550°C. This behavior strongly suggests the presence of interlayering. After saturation with K⁺, some shift of the 14Å reflection toward 10Å occurs at room temperature, and the heat resistance diminishes, but there is no complete shift to 10Å after heating at 550°C. This indicates that only parts of the interlayer fillings are highly reactive, and can be exchanged by standard procedures used for the saturation of clays with different cations. After continual treatment with oxidation agents, the “14Å clay” becomes more unstable during heat treatment, and eventually its (001) reflection shifts to ~10Å after heating at 330°C. This may be attributed to the organic interlayering rather than hydroxy-interlayering. After the oxidation step, the intensity of the (001) reflection increases and the peak becomes sharper. At the same time the intensity of (020) clay reflection decreases significantly. This is obviously caused by the better orientation obtained after removal of organic matter and is probably connected with destruction of organo-clay complexes during oxidation. The nature of the destroyed complexes is unclear, but it is possible that these are either exfoliated organo-clay nanocomposites or aggregates composed of clay minerals randomly dispersed in organic matter (microcomposites).

Ohashi, H., and Nakazawa, H. (1996) The microstructure of humic acid-montmorillonite composites. *Clay Minerals*, **31**, 347-354.

THE CO₂ SEALING EFFICIENCY OF SHALES

Helge Stanjek¹, Andreas Busch², Sascha Alles², and Bernhard M. Krooss²

¹RWTH Aachen University, Clay and Interface Mineralogy, Wüllnerstrasse 2, 52056 Aachen, Germany; Stanjek@iml.rwth-aachen.de

²RWTH Aachen University, Institute of Geology and Geochemistry of Petroleum and Coal, Lochnerstr. 4-20, 52056 Aachen, Germany

Shale lithotypes of various compositions occur abundantly in sedimentary basins and act as natural seals for petroleum and natural gas reservoirs over extended geologic periods. Based on their mechanical, petrophysical and chemical/mineralogical properties, shales become increasingly interesting in the context of long-term isolation of anthropogenic (e.g. radioactive) waste and subsurface storage of fluids. The efficiency and long-term integrity of seal formations (caprocks) is also one of the central issues for CO₂ storage in saline aquifers, depleted oil and gas reservoirs and coals. Due to its chemical reactivity and physico-chemical properties, CO₂ is expected to differ substantially from other natural gas components in terms of transport behaviour and interaction with the mineral/water system.

An experimental procedure has been developed to measure molecular diffusion of CO₂ in water saturated shales. This non-steady state method provides information on the effective diffusion coefficients and the CO₂ storage capacity of the shales. Effective diffusion coefficients for CO₂ were found to range between 10⁻⁹ and 10⁻¹¹ m²/s. Storage capacities were found to vary significantly but can be as high as 0.14 mmol CO₂/g sample. Single-phase (water) flow tests prior to the breakthrough experiments yielded absolute permeability coefficients in the range from 10⁻¹⁸ to 10⁻²² m².

Volumetric sorption experiments with CO₂ at pressures up to 20 MPa have been performed on dry and moist shale samples to verify the findings noted above. The results of these experiments revealed unexpectedly high storage potentials of the same order of magnitude as those from the diffusion measurements. The CO₂ storage capacities are not only related to organic carbon content. In further experimental studies it was shown that the sorptive CO₂ storage potential of clay minerals (montmorillonite, kaolinite, etc.) can be significantly high. Comparison of X-ray diffraction patterns of post-experiment samples and original samples did not reveal any detectable mineralogical differences.

These findings may provide a new view on the issue of caprock integrity. In addition to their sealing properties, natural shale sequences could represent a significant sink for carbon dioxide deposited in the subsurface by fixing and immobilising it and hence reduce the risk of leakage to the surface.

TUBULAR HALLOYSITE LOADED WITH MAGNETITE NANOPARTICLES

Yong Jae Suh, Kang Sup Chung, Dae Sup Kil, Young Nam Chang, and Sujeong Lee

Korea Institute of Geoscience and Mineral Resources, 30 Gajeong, Yuseong, Daejeon, Republic of Korea 305-350; aumsuh@kigam.re.kr

We produced magnetic microtubules by filling tubular halloysite with magnetite nanoparticles of 6–34 nm in average diameter. The magnetite nanoparticles synthesized by thermal decomposition of iron acetate were used to prepare magnetic fluids. In these fluids, the halloysite was dispersed and sonicated until the tubes were filled with the fluids by capillary action. The micrographs of the halloysite tubes by a transmission electron microscope showed a high density of the magnetite nanoparticles inside the tube. Due to these nanoparticles, the halloysite became magnetic and was attracted to a magnet. However, the saturated magnetization measured by a vibrating sample magnetometer was much smaller than that of the nanoparticles themselves because of a relatively lower mass loading.

These magnetic microtubules can be used in a light-weight composite to find applications to the shielding of radio-frequency and electromagnetic interference. Our results may overcome the difficulties in well dispersing the nanoparticles in a polymer matrix. Nanoparticles tend to be clustered together as their concentration goes up in a medium. This clustering limits their dispersing power and in turn leads to anisotropy of the composites.

Pant, R.P., Dhawan, S.K., Kataria, N.D. and Suri, D.K. (2002) Investigations on ferrofluid-conducting polymer composite and its application. *Journal of Magnetism and Magnetic Materials*, **252**, 16-19.

Srikanth, H., Poddar, P., Wilson, J.L., Mohomed, K. and Harmon, J.P. (2003) In-situ synthesis and magnetic properties of polystyrene/polypyrrole nanocomposite materials with uniformly dispersed iron nanoparticles. *Materials Research Society Symposium – Proceedings*, **788**, 243-248.

PREDICTION OF ION-INTERACTION PARAMETERS OF BINARY 2:1 AND 2:2 ION-EXCHANGE SYSTEMS BY THE COUPLING OF THE MARGULES MODEL WITH A LINEAR FREE ENERGY CORRELATION APPROACH

Juan C. Torres¹ and José C. Gubulin²

¹Bento Carlos 750, São Carlos 13566-000, São Paulo, Brazil; juan116br@yahoo.es

²Washington Luiz Km 235, São Carlos 13565-905, São Paulo, Brazil

In this work, the Margules empirical model was applied to derive the ion-lattice interaction parameters (A_{ij}) and the Gibbs energies of reaction ($\Delta G_{\text{MM}}^{\circ}$) of the set of binary 1:2 and 2:2 0.005 N ion-exchange systems $\text{Na}^+/\text{Cu}^{2+}$, $\text{Na}^+/\text{Zn}^{2+}$, $\text{Na}^+/\text{Pb}^{2+}$, $\text{Cu}^{2+}/\text{Zn}^{2+}$, $\text{Cu}^{2+}/\text{Pb}^{2+}$, $\text{Zn}^{2+}/\text{Pb}^{2+}$, on clinoptilolite at 30°C. The linear correlations between A_{ij} (which account for the framework stabilization when cation j^{z+} replaces cation i^{z+} from a homoionic i -zeolite) and $\Delta G_{\text{MM}}^{\circ}$, obtained for the former 1:2 and 2:2 exchange systems, allow the evaluation of the interaction parameters A_{ij} for other 1:2 and 2:2-exchange systems at $T=30^{\circ}\text{C}$ if $\Delta G_{\text{MM}}^{\circ}=\Delta G_{\text{LCA}}^{\circ}$, where $\Delta G_{\text{LCA}}^{\circ}$ is the Gibbs energy of reaction evaluate through a linear correlation approach (Wang and Xu, 2000) that correlates thermodynamic parameters with cation properties.

The values of $\Delta G_{\text{MM}}^{\circ}$ for the 1:2 exchange (i^{z+}/j^{z+}) systems $\text{Na}^+/\text{Cu}^{2+}$, $\text{Na}^+/\text{Zn}^{2+}$ and $\text{Na}^+/\text{Pb}^{2+}$ were 5.5, 6.6 and 1.5 kJ mol^{-1} , respectively, and for the 2:2 systems $\text{Zn}^{2+}/\text{Cu}^{2+}$, $\text{Cu}^{2+}/\text{Pb}^{2+}$ and $\text{Zn}^{2+}/\text{Pb}^{2+}$ were 1.4, -4.2 and -3.0 kJ mol^{-1} , respectively. The values for the interaction parameters A_{ij} and A_{ji} were $\text{Na}^+/\text{Cu}^{2+}$: -1.7783 and -4.4774; $\text{Na}^+/\text{Zn}^{2+}$: -1.4921 and -4.2959; $\text{Na}^+/\text{Pb}^{2+}$: -3.0376 and -1.8981; $\text{Zn}^{2+}/\text{Cu}^{2+}$: -2.3911 and -1.7781; $\text{Cu}^{2+}/\text{Pb}^{2+}$: -7.6791 and -1.1179; $\text{Zn}^{2+}/\text{Pb}^{2+}$: -6.7434 and -1.9352, respectively. Gibbs energies and ion-interaction parameters predicted from the $\Delta G_{\text{MM}}^{\circ}$ - $\Delta G_{\text{LCA}}^{\circ}$ couplings for different 1:2 and 2:2 ion-exchange systems appear listed in Table 1.

Table 1. Gibbs energies and ion-interaction parameters for different ion-exchange systems.

System (i^{z+}/j^{z+})	$\Delta G_{\text{LCA-MM}}^{\circ}$	A_{ij}	A_{ji}
$\text{Na}^+/\text{Sr}^{2+}$	-3.73	-4.6350	0.7136
$\text{Na}^+/\text{Cd}^{2+}$	5.01	-1.9458	-3.8218
$\text{Na}^+/\text{Hg}^{2+}$	-4.13	-4.7599	0.9243
$\text{Ca}^{2+}/\text{Cd}^{2+}$	-12.63	-15.9198	-0.7558
$\text{Ca}^{2+}/\text{Sr}^{2+}$	-26.79	-29.6133	0.3786
$\text{Mg}^{2+}/\text{Cd}^{2+}$	-1.63	-5.2780	-1.6375
$\text{Mg}^{2+}/\text{Pb}^{2+}$	-4.20	-7.7691	-1.4311

Linear correlations ($\Delta G_{\text{MM}}^{\circ}=\Delta G_{\text{LCA}}^{\circ}$ couplings) for (2-2)-exchange systems:

$\{ RTz_j A_{ij} = -18.65 + 4.87 \Delta G_{\text{LCA}}^{\circ} ; -RTz_i A_{ji} = 8.90 + 0.40 \Delta G_{\text{LCA}}^{\circ} \}$, (1-2)-systems:

$\{ RTz_j A_{ij} = -17.57 + 1.55 \Delta G_{\text{LCA}}^{\circ} ; -RTz_i A_{ji} = 3.08 + 1.31 \Delta G_{\text{LCA}}^{\circ} \}$.

Wang, Y. and Xu, H. (2000) Prediction of trace metal partitioning between minerals and aqueous solutions: A linear free energy correlation approach. *Geochimica et Cosmochimica Acta* **65**, 1529-1543.

SORPTION OF HEXAVALENT AND TRIVALENT CHROMIUM ONTO A NEW ACTIVATED CLINOPTIOLITE-BASED MATERIAL

Juan C. Torres¹, Ana I. Pérez², and María E. Díaz³

¹Bento Carlos 750, São Carlos 13566-000, São Paulo, Brazil; juan116br@yahoo.es

²San Lázaro s/n, Ciudad Habana 10400, Cuba

³Argüelles 39 2º 33003, Oviedo, Spain

In this study an activated clinoptilolite was tested for sorption of Cr(VI) and Cr(III) from aqueous solutions at 30°C. The Na-form of a chemical/thermal activated clinoptilolite, NaCC1, was employed in the sorption of Cr(III) whereas a surfactant (HDTMA)-modified clinoptilolite, prepared from the activated NaCC1, SMAC, was used in the sorption of Cr(VI). The sorption of both Cr(VI) and Cr(III) were well-described by the Langmuir isotherm. The greater values for the Langmuir parameters obtained using SMAC indicate a strong affinity (K_L) and adsorption capacity (S_m) between chromate and the surfactant bilayer on the SMAC when compared with the chromate affinity encountered using other surfactant-modified materials (see Table 1).

Diffuse-Reflectance IR spectra of SMAC, Cr(VI)/SMAC and HDTMA showed two intense absorption bands between 3000-2850 cm⁻¹ assignable to C-H stretching vibrations of saturated hydrocarbons, which gives a strong evidence of surfactant molecules sorbed onto the activated clinoptilolite surface. The UV-Vis spectra of Cr(VI)/SMAC exhibited absorption bands at 263 and 347 nm, assignable to electronic *d* transitions of chromium bonded to oxygen atoms interacting with strong electron receptors such like positively charged species. The relatively lower intensity encountered for these bands along with shifts to higher frequencies are indicative of more energetic (and less probable) electron *d* transitions of Cr when two oxygen atoms of chromate (CrO₄²⁻, HCrO₄⁻) sorbed onto SMAC interact with positively charged species, such as the cationic HDTMA head groups.

Table 1. Fitted Langmuir parameters for the sorption of chromium species.

Parameter	Adsorbent							
	SMAC ^a	SMAC ^b	NaCC ^c	KGa-1b ^d	IMt-2 ^e	SAz-1 ^f	SMZ ^g	SMZ ^h
K_L / 1 mmol ⁻¹	31	32	-	20	2	10	4	5
S_m / mmol Kg ⁻¹	43	31	70	13	8	54	21	17
r^2	0.999	0.990	0.999	0.996	0.991	0.960	0.985	0.981
SD	10^{-4}	3×10^{-4}	4×10^{-4}	-	-	-	-	-

^a0.25g; ^b0.50g; ^cSorption of Cr(III) onto NaCC-1, present work; ^dLow defected kaolinite; ^eillite;

^fCa-smectite (Li, 1999); ^gCBP-clinoptilolite (Li, 1999); ^hHDTMA-clinoptilolite (Guiachi, et al.).

Ghiaci, M., Kia, R., Abbaspur, A. and Seyedeyn-Azad, F. (2004) Adsorption of chromate by surfactant-modified zeolites and MCM-41 molecular sieve. *Separation and Purification Technology*, **40**, 285-295.

Li, Z. (1999) Oxyanion sorption and surface anion exchange by surfactant modified clay minerals. *Journal of Environmental Quality*, **28**, 1457-1463.

BARRERITE TWINS, NEUQUEN PROVINCE, PATAGONIA, ARGENTINA

María Elena Vattuone^{1,2}, Carlos Latorre^{1,2}, and Pablo R. Leal^{1,2}

¹Depto de Geología, FCEyN, Universidad de Buenos Aires, Argentina; elena@gl.fcen.uba.ar

²CONICET, Buenos Aires, Argentina.

Twinning barrerite belongs to a mineral assemblage formed during very low grade metamorphism of Paleogene metabasalts from the Andesitic Formation ($40^{\circ}46' / 40^{\circ}54' S$ and $71^{\circ}03' / 71^{\circ}07' W$). It was found in veins and amygdales with Ca-heulandite, tetratnatrolite/Na-gonnardite, Ca-stilbite, stellerite and analcime which replace barrerite in the central parts of the veins. The twins of barrerite have not been described before. This sodic zeolite has grown by replacement of albite. Some colorless and transparent crystals of twin barrerite were found together with Ca-heulandite.

In these rocks, barrerite shows crystals of above 0.5 cm long with $\{010\}$, $\{001\}$, $\{111\}$, $\{011\}$ and $\{h0l\}$ forms; cell parameters are $a = 13.62 \text{ \AA}$; $b = 18.14 \text{ \AA}$; $c = 17.85 \text{ \AA}$; $2V\alpha = 80^\circ$ and chemical analyses by EDAX show Si/Al ratio that ranges between 3.50 and 2.82. Thermal analysis indicate a water loss of 18% (Vattuone et al. 2001a, b).

Figure 1 shows the twins of barrerite in a polarizing microscope on a $\{010\}$ section. These are composed of six sectors interpenetrated, two of them with fine multiple twins parallel to $\{001\}$. Deer et al. (2004) show a sketch of stilbite twins, which is similar to the twins described in this abstract.

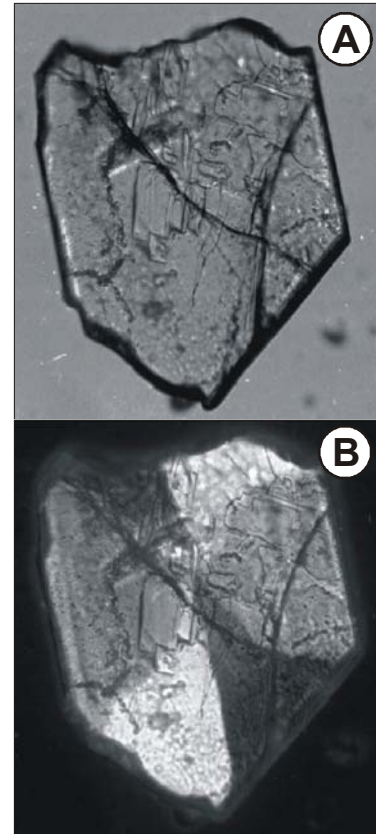


Figure 1: Barrerite twins on polarizing microscope. A) plane-polarized light; B) crossed polars.

Deer, W., Howie, R., Zussman, J. and Wise, W. (2004) Rock Forming Minerals - Framework Silicates: London, England, *The Geological Society*, 982p.

Vattuone, M., Latorre, C. and Leal, P. (2001a) Barrerita en metavolcanitas de Confluencia, Neuquén, Patagonia Argentina. *Boletín de la Soc. Española de Mineralogía*, **24**, 23-32.

Vattuone, M., Latorre, C. and Leal, P. (2001b) Procesos de formación de paragénesis zeolíticas en el metamorfismo de muy bajo grado de las volcanitas paleógenas al sur de Confluencia, Neuquén, Argentina. *Revista Geológica de Chile*. **28**, 3-22.

The authors wish to acknowledge the support provided by PIP CONICET 5062 and UBACyT X840.

DISORDERED NATROLITE OF NEUQUEN, PATAGONIA ARGENTINA

María E. Vattuone^{1,2}, Sabrina Crosta¹, Janina Berbeglia¹, Carlos Latorre,^{1,2}, Carmen I. Martínez Dopico¹, and Ernesto Gallegos¹

¹ Depto de Geología, FCEyN, Universidad de Buenos Aires, Argentina. elena@gl.fcen.uba.ar

² INGEIS, CONICET, Buenos Aires, Argentina.

Natrolite has been found in an alkaline zeolite assemblage in an amygdaloid basalt in Junín de los Andes, Neuquén province, Argentina, as noted Vattuone *et al.* (2005).

Following Gaines *et al.* (1997) and Deer, *et al.* (2004), the degree of ordering in the structure of natrolite is estimated using the difference between the *b* and *a* unit cell dimensions. In “fully ordered” natrolite *b-a* = 0.35 Å, and in the disordered type, “Na-rich gonnardite (ex tetranatrolite)” *b-a* = 0 Å (completely disordered type) to 0.175 Å (50% disorder).

XRD analyses were performed by the Debye Scherrer method on a goniometer using 1.5418 Å Cu K_α radiation and a Ni filter. The XRD data of the natrolite samples analyzed (JU1-4 and JU1-7N) correspond to the 20-0759 and 19-1185 files of JCPDS Mineral Powder Diffraction File Data Book (Bayliss *et al.* 1986). Based on this, the cell parameters were calculated for each sample (table 1) and *b-a* = 0.232 (JU1-4) and 0.183 (JU1-7N). The cell parameters listed in Table 1 indicate that Junin natrolite exhibits 50% Si/Al disorder.

Parameter	File 20-0759	JU 1-4	sigma	File 19-1185	JU 1-7N	sigma
<i>a</i> ₀	18.295	18.294	0.022	18.284	18.527	0.358
<i>b</i> ₀	18.615	18.526	0.029	18.620	18.710	0.293
<i>c</i> ₀	6.603	6.602	0.011	6.601	6.601	0.155

Table 1. Cell parameters for JU1-4 and JU1-7N. Values expressed in Å units.

Chemical analyses indicated: T_{Si} ≥ 0.63, Si/Al ≥ 1.70, and Ca = 0-0.55. This composition combined with the disorder in the structure are indicative of tetranatrolite/Na-rich gonnardite.

Bayliss, P., Erd, D. C., Mross, M. E., Sabina, A. P. and Smith, D. K. (1993) Mineral Powder Diffraction File. Compiled for the JCPDS. Pasadena, USA. 1396p.

Deer, W., Howie, R., Zussman, J., and Wise, W. (2004) Rock Forming Minerals - Framework Silicates: The Geological Society, London, England. 982p.

Gaines, R., Skinner, H., Foord, E., Mason, B. and Rosenzweig, A. (1997) Dana's New Mineralogy. John Wiley & Sons Inc., New York. 1819 p.

Holland, T. and Redfern, S. (1997) Unit cell refinement from powder diffraction data: the use of regression diagnostics. *Mineralogical Magazine*, **61**, 65-77.

Vattuone, M., Crosta, S., Martínez Dopico, C., Gallegos, E., Berbeglia, Y., Lagorio, S. and Latorre, C. (2005) Zeolitas alcalinas en basaltos amigdaloides de las cercanías de Junín de los Andes, Neuquén. XVI Congreso Geológico Argentino, Vol. II: 601-602. La Plata.

The authors wish to acknowledge the support provided by PIP CONICET 5062 / UBACyT X840

PAULINGITE FROM JUNIN DE LOS ANDES, PATAGONIA, ARGENTINA

María E. Vattuone^{1,2}, Sabrina Crosta¹, Carlos Latorre^{1,2}, Pablo R. Leal^{1,2} and Janina Berbeglia¹

¹Depto de Geología, FCEyN, Universidad de Buenos Aires, Argentina; elena@gl.fcen.uba.ar

²CONICET, Buenos Aires, Argentina

Paulingite in assemblage with Ca-K-Na phillipsite and chabazite was found on the border of amygdales of Tertiary amygdaloidal, alkaline basalts located near Junin de los Andes, Patagonia. The outcrop is located at 39°54'57" south and 71°03'10" west. The zeolites were studied by SEM, EDS and XRD.

Analcime, natrolite, thomsonite, mesolite and scolecite also occur filling different amygdales. In the matrix of these rocks, albite, interestratified chlorite/smectite, pumpellyite, and very scarce yugawaralite are present. Altered olivine and fresh pyroxene are the primary minerals that remain in few samples of these rocks (Vattuone et al., 2006).

Paulingite is isotropic with dodecahedral, trapezohedral and cubic forms (Fig. 1). The XRD spacings are coincident with 39-1378 JCPDS-ICDD (1994). The cubic unit cell parameter is $a_0 = 35.10$ Å, according to Armbruster and Gunter (2001). Table 1 shows the chemical composition that exhibits a low $T_{Si} = 0.71-0.72$. The amount of Ca and K indicate that this paulingite is in the range proposed by Passaglia and Sheppard (2001) for this species. The paulingite-phillipsite assemblage indicates that temperature of formation occurs in 60-80°C range (Deer et al., 2004). On the other hand their crystallization in basalt amygdales suggests deuteritic processes.

Arnbruster, T. and Gunter, M. (2001) Crystal structure of natural zeolites. In: Natural Zeolites (Bish, D. and Ming, D., editors). *Reviews in Mineralogy and Geochemistry*, **45**, 1-67 pp.

Deer, W., Howie, R., Zussman, J., and Wise, W. (2004) *Rock Forming Minerals. Framework Silicates*. 4B. The Geological Society. 2nd Edition, London, 982 pp.

Passaglia, E. and Sheppard, R. (2001) The crystal chemistry of zeolites. In: Natural Zeolites (Bish, D. and Ming, D., editors). *Reviews in Mineralogy and Geochemistry*, **45**, 69-115 pp.

Vattuone, M. E., Martínez Dopico, C., Berbeglia, Y., Gallegos, E. and Crosta, S., (2006).

Chabazite, Ca-Na-K- phillipsite, analcime and natrolite: alkaline zeolites filling amygdales in tertiary basalts of Patagonia, Argentina, South America. *Zeolite '06-7th International Conference on the Occurrence, Properties, and Utilization of Natural Zeolites*, Socorro, New Mexico USA. Bowman and S. Delap (Eds). 242-243.

The authors wish to acknowledge the support provided by PIP CONICET 5062 and UBACyT X840.

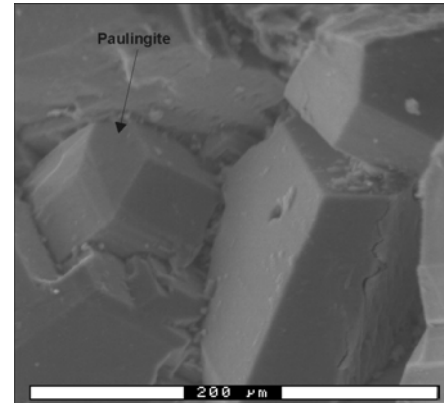


Figure 1: Dodecahedral crystals of paulingite.

Table 1: Chemical composition

Mineral	Paulingite		
SiO ₂	52,40	52,89	52,42
Al ₂ O ₃	17,91	17,57	17,68
MgO	0,00	0,00	0,00
BaO	0,00	0,00	0,00
CaO	6,77	6,68	6,77
Na ₂ O	0,00	0,00	0,00
K ₂ O	4,92	4,86	5,12
84 O			
Si	29,97	30,20	30,03
Al	12,07	11,83	11,94
Mg	0,00	0,00	0,00
Ba	0,00	0,00	0,00
Ca	4,15	4,08	4,16
Na	0,00	0,00	0,00
K	3,59	3,54	3,74
Tsi=Si/(Si+Al)	0,71	0,72	0,72
*E%	1,51	1,11	-1,00

CONVENTIONAL AND LOW-VOLTAGE CRYO-FIELD EMISSION SCANNING ELECTRON MICROSCOPY OF PYROXENE WEATHERING TO SMECTITE, KOUA BOCCA ULTRAMAFIC COMPLEX, IVORY COAST

Michael A. Velbel¹, and William W. Barker²

¹Department of Geological Sciences, Michigan State University, East Lansing, MI 48824-1115
U.S.A. velbel@msu.edu

²Department of Geology and Geophysics, University of Wisconsin-Madison, Madison, WI, 53706 U.S.A.

Air dried and freeze dried samples of clinopyroxene and smectite in a saprolitized clinopyroxenite from Koua Bocca, Ivory Coast, West Africa were examined by conventional and field-emission (FE) scanning electron microscopy (SEM) to characterize textures developed during natural weathering. Comparison with air-dried material allowed evaluation of high pressure cryofixation as a technique for preserving textures of hydrated clay minerals.

Air-dried samples have elongate etch pits, and denticulated terminations on pyroxene remnants, similar to those of other naturally weathered chain-silicates. Both product-free and thinly coated denticles are visible in conventional SEM images of air-dried pyroxene. Denticles on air-dried pyroxenes imaged with FE-SEM appear clean in some instances, and thinly coated with vermiciform or wispy textured products on others. Small, flat lamellae, oriented parallel to the C-axis, lend a distinct splintery appearance to pyroxene surfaces in fully hydrated samples. These lamellae often display a combination of straight (110) pyroxene edges and a crinkled border suggestive of smectite. Narrow lenticular (110) open cleavages occur in both preparations and are not a pressurization artifact. Most often these openings contain no secondary minerals.

Denticulated pyroxene remnants are separated from boxwork smectite in air-dried samples by peripheral voids similar to those previously reported from optical petrography and, in some instances, by narrow voids apparently created by shrinkage of smectite. Air-dried smectite boxworks consist of stacks of wavy layers commonly exhibiting vermiciform edges. In contrast, weathering products appear porous, wispy and variously cobweb- or cornflake-like in freeze-dried preparations. Pyroxene denticles in freeze-dried samples are thinly coated with cobweb- or cornflake-textured products, some of which partly fill small etch pits on the larger denticles.

Intergranular spaces between pyroxene denticles, lined with collapsed smectite in air dried samples, are filled with thin packets of anhedral smectite crystallites oriented face to face when hydrated. Regions of edge to face "house of cards" texture also occur locally. Unlike the large, continuous pores that appear to result from shrinkage of smectite and consequent pulling away of the smectite from the denticulated pyroxene-smectite interface in air-dried samples, pore space in freeze-dried samples is much smaller in scale. Pores actually present during a weathering episode thus are smaller and more numerous than would be inferred from examining air-dried materials. Improved insight into the microtextures of naturally formed clay minerals made possible by improved sample preparation methods may shed new light on the role of clays, their microtextures, and the chemical microenvironments the microtextures produce, on reactions and rate-processes of importance in environmental geochemistry and global geochemical cycling.

IONIC DIFFUSION IN 2:1 PHYLLOSILICATES

Michael A. Velbel

Department of Geological Sciences, Michigan State University, East Lansing, MI 48824-1115
U.S.A. velbel@msu.edu

Ionic diffusion coefficients for clay materials vary with mineralogy, porosity, and (in the case of mixtures of clay and non-clay minerals), the proportion of clay in the mixture. The influence of clay mineralogy on ionic diffusion coefficients in clay materials is examined here by compiling several hundred published ionic diffusion coefficients for 2:1 phyllosilicates.

Published ionic diffusion coefficients for 2:1 phyllosilicates vary over approximately six orders of magnitude. Within-group variation in reported values of ionic diffusion coefficients for individual groups of phyllosilicates (smectite, vermiculite, mica) is up to four orders of magnitude. In general, materials reported as smectite or bentonite have the highest diffusion coefficients and micas the lowest, with vermiculite in between.

Arrhenius activation energies for cation diffusion in 2:1 phyllosilicates vary with the layer charge of the phyllosilicate and the ionic potential (z/r , where z and r are the valence and crystal ionic radius of the diffusing cation) of the diffusing cation. Arrhenius activation energies for cation diffusion are lowest for monovalent cations in 2:1 clays with low layer charge, and highest for divalent cations in mica interlayers, with intermediate values for divalent cations in low layer-charge clays.

Both cation diffusion coefficients and Arrhenius activation energies for diffusion in 2:1 phyllosilicates can be thought of as scaling with simple Coulomb's Law electrostatic attraction between the charged phyllosilicate surface and the charged diffusing ion; the stronger the electrostatic attraction between the diffusing cation and the charged phyllosilicate, the lower the diffusion coefficient and the higher the Arrhenius activation energy for diffusion. Empirical relationships based on these previously published data allow estimation of cation diffusion coefficients and Arrhenius activation energies for diffusion through 2:1 phyllosilicate materials.

PHYLLOSILICATES FORMED BY OLIVINE HYDRATION IN CARBONACEOUS CHONDRITES: AQUEOUS ALTERATION IN THE EARLY SOLAR SYSTEM

Michael A. Velbel¹, Eric K. Tonui², and Michael E. Zolensky³

¹Department of Geological Sciences, Michigan State University, East Lansing, MI 48824-1115 U.S.A.; velbel@msu.edu

²Department of Earth and Space Sciences, UCLA, Los Angeles, CA, U.S.A.

³Astromaterials Research & Exploration Science Office, NASA Johnson Space Center, Houston, TX 77058 U.S.A.

Some phyllosilicates in CM carbonaceous chondrites formed by aqueous alteration of anhydrous precursor phases, most likely on CM parent-bodies (outer-Main-Belt asteroids). Consequently, these meteorites record the characteristics of water as it occurred in the early solar system. Broad trends in the compositions of hydrous phyllosilicates have been suggested to be related to degree of alteration, but details of the reactions that formed secondary minerals remain obscure.

Olivines (Fo_{77-99}) are partially replaced by serpentine in the minimally brecciated CM2 QUE93005. Despite the broad range of reactant olivine compositions, serpentine replacing olivine in QUE93005 has a narrow range of $\text{Fe}/(\text{Fe}+\text{Mg})$ (molar) ratios. Nogoya is extensively brecciated and contains olivine (Fo_{65-99}). Serpentine replacing olivine in Nogoya has a narrow range of $\text{Fe}/(\text{Fe}+\text{Mg})$ (molar) ratios. The composition of replacement serpentine in Nogoya is identical to previously reported Nogoya replacement Mg-serpientes, and to the previously reported mode in the large range of serpentine compositions in Nogoya matrix and rim material. Replacement serpentines in QUE 93005 and ALH81002 are more Fe-rich than those in Nogoya.

Implications: (1) Importation of Fe is required for serpentines replacing some olivine compositions in each of the three CM chondrites, and Fe exportation is required for others in the same sample, suggesting that secondary-mineral composition depended little on elements supplied locally by the reactant mineral and more strongly on external factors such as solution composition. (2) Intrameteorite homogeneity of replacement serpentine exists in each CM chondrite, regardless of the composition of the reactant olivine. This suggests that the aqueous medium driving the replacement reaction was compositionally uniform on scales much larger than individual olivine crystals, chondrules, or clasts. (3) QUE93005 and ALH81002 olivines were altered to serpentine in geochemically similar environments; Nogoya altered in a geochemically different setting. (4) If pervasive aqueous alteration of all fragments took place largely after assembly of reactant materials into the present rock, and subsequent to most major brecciation and mixing of clasts (i.o.w., on the parent body), the aqueous medium may have been homogenous on the 1-10 cm scale. Intrameteorite homogeneity militates against pre-assembly alteration. (5) Intermeteorite heterogeneity of both replacement and chondrule-rim/matrix serpentine compositions between different CM2 chondrites implies larger-than-meteoroid-scale heterogeneity of the CM aqueous alteration environment. It remains to be established whether larger-than-meteorite-scale heterogeneity in the alteration environment was due to different CM chondrites sampling (a) different spatial regions of a large spatially heterogeneous alteration environment, (b) a single temporally evolving aqueous alteration system at different stages of its chemical evolution, or (c) different discrete and isolated aqueous alteration environments.

ALTERING THE HYDROPHOBICITY OF IRON(III) EXCHANGED CLAY CATALYSTS TO IMPROVE SUBSTRATE SPECIFICITY

Philip J. Wallis², Will P. Gates^{1,2,3}, Antonio F. Patti^{2,4}, and Janet L. Scott^{2,5}

¹Department of Civil Engineering, Monash University, Clayton, Vic, Australia

²Centre for Green Chemistry, Monash University, Clayton, Vic, Australia.

³SmecTech Research Consulting, Bentleigh East, Vic, Australia; gateswp@smectech.com.au

⁴School of Applied Sciences and Engineering, Monash University, Churchill, Vic, Australia.

⁵Unilever Home and Personal Care R&D, Bebington, Wirral, UK.

Mixed cation clay (MCC), containing either Fe^{3+} and hexadecyltrimethylammonium (HDTMA⁺) or Fe^{3+} and choline, were prepared to demonstrate how the catalytic activity of clays in oxidative coupling reactions could be enhanced based on the properties of the starting materials. The overall aim was to develop *in situ* materials to enhance organic matter conversion and stabilization. A series of MCC were prepared using purified SWy-2, with Fe^{3+} being loaded first followed by the organic cation ($\text{Fe}^{3+}/\text{choline}^+ - \text{MCC}$, $\text{Fe}^{3+}/\text{HDTMA}^+ - \text{MCC}$). An increasing amount of organic cations were exchanged to produce series of MCC with a range of organic content. The MCC were tested to determine the optimum loading composition effective in oxidative coupling of 2-naphthol to binol and of anthrone to bianthrone (a more hydrophobic substrate).

For the $\text{Fe}^{3+}/\text{choline}^+ - \text{MCC}$ series, optimal conversion of 2-naphthol to binol occurred when the Fe^{3+} -clay was exposed to choline^+ corresponding to 20-40 % of the cation exchange capacity (CEC). For the $\text{Fe}^{3+}/\text{HDTMA}^+ - \text{MCC}$ series, optimal conversion of 2-naphthol occurred when the Fe^{3+} -clay was exposed to HDTMA⁺ corresponding to only 5% of CEC, and conversion decreased with further organophilicity of the MCC. This result demonstrated that MCC organophilicity inhibited catalytic activity, either due to exclusion of the reactive substrate, or from lack of available Fe^{3+} cations due to displacement by HDTMA⁺. In contrast, optimum conversion of anthrone to bianthrone by the $\text{Fe}^{3+}/\text{HDTMA}^+ - \text{MCC}$ series was achieved by exposure of the Fe^{3+} -clay to HDTMA⁺ corresponding to 80% of the CEC, demonstrating the importance of clay organophilicity for the reaction of more hydrophobic substrates.

BEHAVIOR OF H_2O MOLECULES IN THE CHANNELS OF NATROLITE: A THERMAL ANALYSIS AND X-RAY POWDER DIFFRACTION STUDY

Hsiu-Wen Wang and David L. Bish

Department of Geological Sciences, Indiana University, 1001 East 10th Street, Bloomington, IN 47405 USA; hw7@indiana.edu

The thermal behavior of natrolite ($\text{Na}_{16}\text{Al}_{16}\text{Si}_{24}\text{O}_{80} \cdot 16\text{H}_2\text{O}$) and the interplay between dehydration/rehydration and crystal structural changes were studied by thermogravimetric analysis (TG) and temperature- and atmosphere-controlled X-ray powder diffraction (XRD). Natrolite dehydration occurred as a discrete reaction with an abrupt and single-stage weight loss in the TG curve. The dehydrated phase, α -metanatrolite ($\text{Na}_{16}\text{Al}_{16}\text{Si}_{24}\text{O}_{80}$), formed during dehydration and the reaction was accompanied by a structural phase transition. The dehydration reaction is inhibited by the build-up of $\text{P}_{\text{H}_2\text{O}}$ in intercrystallite pore spaces, with a dehydration onset temperature of $\sim 255^\circ\text{C}$ with a 4-mg sample, increasing to $\sim 295^\circ\text{C}$ with an 18-mg sample. The positions of H_2O , located at the centers of the zigzag channels along the a and b axes, also limit H_2O diffusion and give rise to an apparent kinetic effect. Rietveld refinements with XRD data collected from 22.5°C to 400°C at ~ 0.15 mbar suggested that the $(\text{Al},\text{Si})_5\text{O}_{10}$ chains begin to twist at temperatures $>200^\circ\text{C}$ (Fig. 1). The temperature-induced structural changes lead to breakage of H-bonds between protons and framework O anions, causing H_2O to be held more loosely by the framework. The occurrence of a steep weight loss in the TG curve and an asymmetric derivative TG peak after twisting of the chains results from the breakage of H-bonds and more energetic H_2O molecules at higher temperatures. The natrolite-to- α -metanatrolite-to-natrolite reaction is strongly hysteretic, especially after complete dehydration (Fig. 2). When heating was switched to cooling halfway through the dehydration reaction, a smaller hysteresis effect was observed, with the TG curve showing minor further dehydration and then remaining at constant weight until the structure gradually reequilibrated to natrolite, causing rehydration (Fig. 2). Evidence for a solvus was observed during dehydration/rehydration cycles (Fig. 1), indicating that the H_2O site occupancy changed from 1 to 0 without any partially hydrated intermediate. Structure refinements indicate that the extra-framework Na cations move towards the framework O after loss of H_2O . Hysteresis appears to be a result of framework twisting and concomitant changes in H-bonding, occurring $>200^\circ\text{C}$.

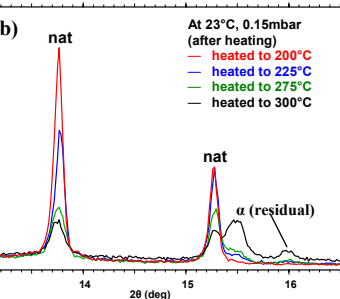
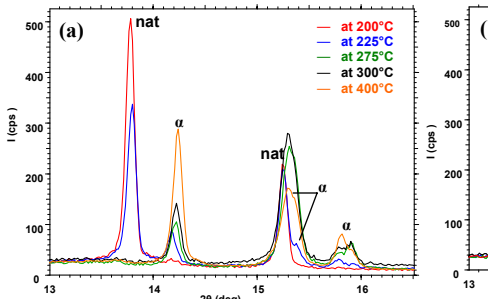


Figure 1. (a) XRD patterns of natrolite (nat) showing changes in peak positions and intensities from $200\text{--}400^\circ\text{C}$; α -metanatrolite (α) occurs $>200^\circ\text{C}$. (b) XRD patterns of natrolite (nat) after cooling to 23°C from $200, 225, 275$, and 300°C at 0.15 mbar. Rehydration is much slower from α -metanatrolite than from natrolite.

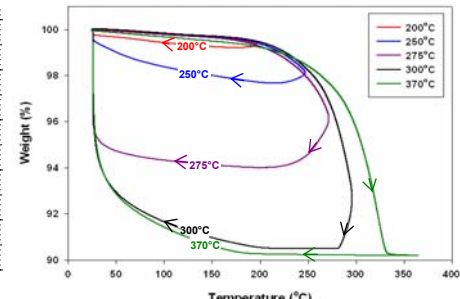


Figure 2. Natrolite TGA curves, showing the occurrence of hysteresis. Sample mass for all measurements is $\sim 13 \pm 1$ mg.

THERMODYNAMIC MODEL OF ANALCIME DEHYDRATION

Jie Wang and Philip S. Neuhoff

Department of Geological Sciences, University of Florida, 241 Williamson Hall, Gainesville, Florida 32611-2120, USA; jiewang@ufl.edu

Analcime is one of the most common rock-forming zeolites. It appears to be stable over a considerable range of temperature (T) and pressure (P) conditions that span geologic environments ranging from surficial alkaline lakes to primary igneous occurrences in lavas and alkaline pegmatites. The hydration state of analcime as a function of T, P, and the chemical potential of water is an important consideration in its stability. Detailed studies of thermodynamics of de/hydration of analcime allow evaluation of the changes in environmental conditions that ultimately lead to the structural modification.

In order to evaluate the hydration state of analcime in geologic and engineered environments, a thermodynamic model of analcime dehydration was developed. Equilibrium observations of analcime dehydration at ten different temperatures between 573 and 750 K and controlled humidity were conducted by thermogravimetry. The equilibrium constant calculated from mass loss of analcime during the dehydration were used in conjunction with heat capacities of hydrated and dehydrated analcime determined by differential scanning calorimetry (DSC) to determine the Gibbs energy ($\Delta G_{r,298K,1bar}^o$) and entropy ($\Delta S_{r,298K,1bar}^o$) of the dehydration (to water vapor) reaction at 298.15 K, 1 bar. The calculations employed an ideal solution model, as suggested by heat of dehydration measurements on analcimes of different hydration states. The results of $\Delta G_{r,298K,1bar}^o$ and $\Delta S_{r,298K,1bar}^o$ are 47.58 kJ/mol_{H₂O} and 125.97 J/(mol_{H₂O}K), respectively. The standard enthalpy of reaction derived from $\Delta G_{r,298K,1bar}^o$ and $\Delta S_{r,298K,1bar}^o$ is 85.14 kJ/mol_{H₂O}, which is consistent with heat of vapor adsorption measurements by DSC.

The thermodynamic model derived above was used to evaluate the hydration state of analcime as a function of T and P. Geologic observations of analcime formation in diagenetic and igneous environments suggested that it formed *in situ* T from ~20 °C to 650 °C and P up to 2 kbar (e.g., Iijima, 1978). Under these conditions, our model predicts that analcime is almost fully hydrated (water fraction > 99%) if provided liquid or supercritical water is stable (i.e., above and beyond the liquid-vapor saturation curve). However, analcime dehydrates significantly at conditions below the liquid-vapor saturation curve. Thus, the hydration state of analcime can be determined by this model if the T-P condition is available. For instance, in Yucca Mountain the emplacement of radioactive waste will change the geological environment of large volume of rocks containing analcime. Thermal energy released by the nuclear waste may increase T in the repository up to the regulatory limit of 250 °C. Assuming a constant water vapor pressure of 33 mbar (100% relative humidity at 25 °C), our model predicts that analcime will lose ~23.4% of water at 250 °C, with a heat consumption by the dehydration process of about 19.2 kJ/mol_{analcime}.

Iijima, A. (1978) Geological occurrences of zeolite in marine environments, Pp. 175–198 in: *Natural Zeolites: Occurrence, Properties, Applications* (B.L. Sand and F.A. Mumpton, editors). New York, Pergamon Press.

PREPARATION AND APPLICATION OF SURFACTANT-MODIFIED ZEOLITIC MATERIALS FOR REMOVAL OF CHROMATE SPECIES FROM WATER

Jolanta K. Warchol¹, Robert S. Bowman², and Panagiotis Misaelides³

¹Rzeszów University of Technology, Department of Civil and Environmental Engineering, 6 Powstańców Warszawy Str., 35-959 Rzeszów, Poland, jwarchol@prz.rzeszow.pl

²New Mexico Institute of Mining and Technology, Department of Earth and Environmental Science, 801 Leroy Place, Socorro, New Mexico 87801, USA

³Aristotle University, Department of Chemistry, GR-54124 Thessaloniki, Greece

Chromium is among the elements absolutely necessary for living organisms. However, despite chromium's relatively high abundance in nature (average concentration in the earth's crust: ca 100 mg/kg), it is considered as a high-priority environmental pollutant. Chromium is present in aqueous solutions in various anionic forms (CrO_4^{2-} , $\text{Cr}_2\text{O}_7^{2-}$, HCrO_4^-), which can be toxic to living organisms even at $\mu\text{g/L}$ concentrations. Among the different techniques proposed for chromate removal (e.g., reduction/precipitation, biosorption, and nano- and ultrafiltration), adsorption on natural and synthetic sorbents is attractive. Natural zeolitic materials possess a negatively charged surface and therefore mainly cation exchange properties. However, recent investigations have shown that chemical treatment and modification of the natural zeolite surface can provide them with an affinity for inorganic anions and non-polar organic species, while retaining much of their sorption capacity for metal cations.

The removal of chromate species from aqueous solutions by surfactant-modified zeolitic tuffs from the Pentolofos area (Thrace, Greece) and the Winston area (New Mexico, USA) was studied under batch conditions. The zeolitic material was modified by the cationic surfactants hexadecyltrimethylammonium bromide (HDTMA-Br), octadecyltrimethylammonium bromide (ODTMA-Br) and hexadecyltrimethylammonium chloride (HDTMA-Cl), and characterized by scanning electron microscopy, FT-IR spectrometry and zeta potential measurements. The experimental data for chromium uptake by surfactant-modified zeolites was used for sorption equilibrium calculations by employing the Freundlich and Langmuir sorption equation.

The experimental study and modeling calculations indicated that chromium uptake was not strongly influenced by the type of surfactant but showed, as expected, a dependence on the solution pH. The maximum sorption capacity (2.27 mg/g) of Cr(VI) was achieved at a solution of initial pH = 4. The variation of adsorption with pH was primarily a function of changes in Cr(VI) speciation.

PROBING CLAY SURFACES WITH NMR: COMPUTING ^{27}Al AND ^{29}Si CHEMICAL SHIFTS

Nancy A. Washton¹, Karl T. Mueller¹, and James D. Kubicki²

¹Dept. of Chemistry, The Pennsylvania State University, University Park, PA 16802 USA
nam@chem.psu.edu

²Dept. of Geosciences, The Pennsylvania State University, University Park, PA 16802 USA

Absorption concentrations of the compound 3,3,3-(trifluoropropyl)dimethylchlorosilane (TFS) onto natural aluminosilicates have been shown to correlate with dissolution and weathering rates (Washton et al., 2007). Based on the preponderance of layered silicates in the environment, this work is expanded to examine the binding of TFS to the edge-sites on kaolinite clays, where dissolution and precipitation are known to occur (Casey and Bunker, 1990; Fitzgerald et al., 1997; Nagy et al., 1999; Bickmore et al., 2001). In this talk, the TFS adsorption experiments and subsequent NMR spectra will be discussed, but the main focus will be on the modeling of clay edge sites and the ability of quantum mechanical calculations to reproduce the observed ^{27}Al and ^{29}Si NMR chemical shifts. The ability to match calculated chemical shifts to the experimentally obtained values is a critical step toward elucidating the chemical speciation of the surface sites participating in binding reactions with TFS. Furthermore, the computational chemistry approach allows for further investigation of reaction mechanisms of the TFS adsorption process, which may subsequently be applied to study clay weathering processes. Clusters of three silica tetrahedron and two Al octahedron extracted from the kaolinite crystal structure are capable of reproducing ^{27}Al and ^{29}Si chemical shifts for atoms in the kaolinite structure and the TFS probe molecule. With this combination of NMR spectroscopy and computational chemistry, a method for identifying and quantifying reactive surface areas on aluminosilicates is available. With quantified reactive surfaces areas and realistic pictures of the dissolution mechanisms, we posit that scaling weathering kinetics from the molecular to the field scales will become approachable.

Washton N. M., Brantley S. L., and Mueller K. T. (2007) Probing the molecular-level control of aluminosilicate dissolution: A sensitive solid-state NMR proxy for reactive surface area. *Geochimica et Cosmochimica Acta*, submitted.

Bickmore B. R., Bosbach D., Hochella M. F., Charlet L., and Rufe E. (2001) In situ atomic force microscopy study of hectorite and nontronite dissolution: Implications for phyllosilicate edge surface structures and dissolution mechanisms. *American Mineralogist* **86**, 411-423.

Casey W. H. and Bunker B. (1990) Leaching of mineral and glass surfaces during dissolution. *Reviews in Mineralogy* **23**, 397-426.

Fitzgerald J. J., Hamza A. I., Bronnimann C. E., and Dec S. F. (1997) Studies of the solid/solution "ineterfacial" dealumination of kaolinite in HCl(aq) using solid-state ^1H CRAMPS and SP/MAS ^{29}Si NMR spectroscopy. *Journal of the American Chemical Society* **119**, 7105-7113.

Nagy K. L., Cygan R. T., Hanchar J. M., and Sturchio N. C. (1999) Gibbsite growth kinetics on gibbsite, kaolinite, and muscovite substrates: Atomic force microscopy evidence for epitaxy and an assessment of reactive surface area. *Geochimica et Cosmochimica Acta* **63**, 2337-2351.

VOLATILE LIGHT ELEMENT DISTRIBUTIONS IN BALTIC BASIN BENTONITES: A POTENTIAL CONNECTION TO HYDROCARBON SOURCES

Lynda B. Williams¹, Jan Środoń,² Warren D. Huff³, and Richard L. Hervig⁴

¹Lynda B. Williams, SESE, Arizona State University, Tempe, AZ 85287-1404 USA;
Lynda.Williams@asu.edu

²Jan Środoń, Inst. Geol. Sci PAN, Senacka 1, PL-31 002 Krakow, Poland

³Warren D. Huff, Dept Geol., University of Cincinnati, Cincinnati, OH 45221-0013 USA

⁴Richard L. Hervig, SESE, Arizona State University, Tempe, AZ 85287-1404 USA

Nitrogen, boron and lithium distributions were studied in Ordovician-Silurian bentonites from the Baltic Basin. The bentonites were deposited in different paleogeographic settings from carbonate platform in the NE (Estonia) grading SW toward deep basin shales (Denmark, Poland).

The N content of illite-smectite (I-S) is commonly high where organic matter has matured to release hydrocarbons and NH_4^+ . Bentonites in black shales show NH_4^+ substitution for K^+ with increasing illitization (Williams and Ferrell, 1991). Kerogen also releases B that is distinctly ^{10}B -enriched; therefore light $\delta^{11}\text{B}$ values in illite may reflect organic sources (Williams and Hervig, 2004). Lithium has elevated concentrations in oilfield brines (Collins, 1975) indicating another link to organic sources.

Three size fractions of authigenic illite were considered ($<0.02\mu\text{m}$; $0.02\text{--}0.05\mu\text{m}$; $0.05\text{--}0.2\mu\text{m}$). I/S ratios and fission track data indicate temperatures of $185\text{--}200^\circ\text{C}$ along the Norwegian and Polish Caledonides, decreasing to $120\text{--}130^\circ\text{C}$ in the central trough (Sweden to Estonia). K-Ar dates of bentonites in the central trough (Denmark to Estonia) are between 363-426 Ma, while bentonites in sediments to the N (Norway) and S (Poland) are 294-390 Ma.

Illite shows high values of N (>1000 ppm) in the SW Baltic Basin where deep water-shales reached 200°C . The central trough (Sweden) has elevated B (>250 ppm), while high Li concentrations (>100 ppm) are found in the carbonate platform sediments to the NW (Estonia). The $\delta^{11}\text{B}$ of different illite size fractions vary by several ‰, reflecting changes in the fluid $\delta^{11}\text{B}$ during crystal growth. Generally the coarser (youngest) fractions are ^{10}B -enriched. The oldest illites (central trough) precipitated from positive $\delta^{11}\text{B}$ waters, while the younger illites (Norway and Poland) precipitated from negative $\delta^{11}\text{B}$ waters.

Fluid chemistry may change in response to a thermal pulse (tectonic related) releasing trace elements from organic-rich sediments. The regional pattern of elevated N, B and Li concentrations, if not related to local stratigraphy, could reflect differential mobilization of these elements along a thermal gradient. The most volatile element (Li) would travel farthest from the heat source, producing basin scale segregation of hydrocarbon-sourced volatiles. This element distribution could be useful in tracing other volatiles (e.g. CH_4) through black shales.

Collins, A.G. (1975) *Geochemistry of Oilfield Waters*, New York, Elsevier, 496p.

Williams, L.B. and Ferrell, R.E., Jr. (1991) Ammonium substitution in illite during maturation of organic matter. *Clays and Clay Minerals*, **39**, 400-408.

Williams, L.B. and Hervig, R.L. (2004) Boron isotope composition of coals: A potential tracer of organic contaminated fluids. *Applied Geochemistry*, **19**, 1625-1636.

DIAGENETIC MINERALS AND TEXTURES IN OIL SHALE SAMPLES FROM THE PICEANCE BASIN, COLORADO

Giday WoldeGabriel¹, Steve J. Chipera¹, Marcus Wigand², Melissa Fittipaldo¹, J. William Carey¹, and John P. Kaszuba¹

¹Earth & Environmental Science, Los Alamos National Laboratory, Mail Stop D469, Los Alamos, NM, USA; wgiday@lanl.gov

²Chemistry Division, Los Alamos National Laboratory, Los Alamos, NM, USA

In the last few years, research and development efforts in oil shales have significantly increased as a result of the drastic increase in crude oil prices. Although most oil shale explorations are focused on technology-driven processes, basic research to understand the geological processes that were responsible for the partial differentiation of organic matter from the inorganic primary and secondary mineral assemblages during diagenesis is crucial to determine innovative and cost-effective extraction methods for shale oil. We present optical and scanning electron microscopy results of preliminary investigations of oil shale samples from the Green River Formation of the Piceance Basin in Colorado. According to size and grade, the Devonian-Mississippian black shales and the Eocene Green River Formation oil shale deposits of the eastern and western United States, respectively, are considered to contain the largest shale oil reserves in the world.

Distinct textural features and at least two dominant types of mineral assemblages were recognized in the oil shale samples from the Green River Formation in the Piceance Basin of Colorado. One group of samples consists of alternating laminations of foliated black to orange organic matter and light brown crystal-rich inorganic minerals in a clay matrix with disseminated organic matter. Another group of samples is characterized by tightly folded and sheared laminations of alternating black to orange organic matter and a light to medium brown crystal-rich inorganic mineral assemblage. The folding and faulting of the organic and inorganic layers are post-diagenetic features probably related to local soft-sediment deformation because underlying sediments do not show these kinds of structures. For most oil shale samples, the black to orange organic matter in the matrix generally wraps around coarse detrital and diagenetic minerals grains, implying flowage. The organic matter probably retarded inorganic mineral diagenesis.

Two distinct types of inorganic mineral assemblages characterize the oil shale samples. The dominant authigenic mineral assemblage consists of dawsonite, dolomite, clays, calcite, quartz, feldspar, and pyrite. Dolomite predates dawsonite, and pyrite crystallized on coarse dolomite grains. Pyrite is closely associated with organic matter. Dolomite, clay, quartz, feldspar, and pyrite were noted in some of the oil shale samples with trace amounts or no dawsonite. Although pyrite postdates dolomite, both minerals are closely associated with organic matter. The paragenetic relation of fine-grained feldspar and quartz grains with the other minerals was not apparent and more work is being done to understand the diagenetic processes.

USING CLAYS AND NANO-PHASE MINERALS TO REVEAL LATE TERTIARY PALEOCLIMATE CHANGES IN CENTRAL CHINA

Huifang Xu¹, Tianhu Chen^{1, 2}, Junfeng Ji³, Jun Chen³, Qiaoqin Xie², Huayu Lu^{3, 4}, and Xiaoyong Wang⁴

¹Department of Geology and Geophysics, University of Wisconsin Madison, 53717, USA

²School of Natural Resource and Environmental Engineering, Hefei University of Technology, Hefei, 230009, P.R. China

³Department of Geoscience, Nanjing University, Nanjing, Nanjing 210093, P.R. China

⁴Institute of Earth Environment, Chinese Academy of Sciences, Xi'an, 710075, China

Paleosols in loess deposits of central China can provide a good opportunity to reconstruct the long-term monsoon changes in China and East Asia. The eolian record in the Chinese Loess Plateau can be extended from 2.6 Ma back to about 7.0 Ma, because it has been demonstrated that the late Tertiary red clay deposits underlying the Pleistocene loess and paleosol sequence in the Chinese Loess Plateau are also of eolian origin. Many important nanophase minerals such as hematite, dolomite, calcite nano-fibers, smectite and palygorskite, which can act as indicators of the paleoclimate and paleoenvironment changes, were found in the red clay of the Chinese Loess Plateau. Results from X-ray diffraction (XRD), scanning electron microscopy (SEM) and transmission electron microscopy (TEM) indicate that large amounts of nano-phase and poorly-crystalline hematite were formed due to chemical weathering of Fe-bearing silicates. Dolomite and palygorskite were crystallized from interstitial soil solutions and/or transformed from calcite and illite-smectite, respectively. We propose that the calcite nano-fibers resulted from crystallization in bioorganic-bearing solutions. The dolomite and palygorskite assemblage indicates a dry and hot environment, because it is widely known to occur in modern desert soils. Preservation of calcite nano-fibers also indicates a dry environment. All characteristics of authigenic nano-phase minerals occurring in the red clay indicate a paleo-environment with strong evaporation and chemical weathering, and much drier and hotter than the overlying Pleistocene loess and paleosols. Low magnetic susceptibility (MS) in the red clay layers is produced by the strong oxidation of eolian magnetite as a combined result of strong chemical weathering and low pedogenic magnetite formation due to weak microbial activity. Based on our results, it can be inferred that strong chemical weathering and weak microbial activity under dry and hot climate is the main reason for low magnetic susceptibility in the red clay layers, which is different from the paleoclimate for the overlying Pleistocene loess (indicating cold and dry paleoclimate) and paleosols (indicating warm and humid paleoclimate).

TRACE MINERAL COMPONENTS IN THE CHETO, ARIZONA, BENTONITE

Hongji Yuan and David L. Bish

Department of Geological Sciences, Indiana University, Bloomington, IN 47405 USA;
honyuan@indiana.edu

The source of the economically important Cheto, Arizona, bentonite has been analyzed by Kiersch and Keller (1955) and Sloane and Guilbert (1967) who concluded the deposit formed via the alteration of a Pliocene vitric quartz-latite ash. Other studies have evaluated the potential of trace element geochemistry to clarify source materials and mode of formation of clay deposits. Although the potential is great, it is often necessary to know the distribution of the trace elements within a rock (in this case a bentonite) in order to interpret source and formation mechanism. The trace element composition of the SAz-1 source clay was presented by Kogel et al. (2001), but little work has been done on the nature of the trace element distribution in this bentonite.

Cheto bentonite samples were collected by the second author, and when sampled in-place, the bentonite was bright white and waxy, with no visual evidence of any impurities. After several months in the laboratory, bentonite surfaces showed randomly distributed black dendritic spots. Sloane et al. (1967) showed scanning electron microscope (SEM) images of these spheroids but did no chemical analysis. We studied the nature of these growths and the texture of the bentonite using SEM and X-ray powder diffraction (XRD). SEM study of fractured surfaces showed that Mn oxides and Ce-phosphates are highly concentrated in the spots (Fig. 1). Mn oxides outline the dendritic shape of the spots, whereas the Ce-phosphate appears as spheres embedded in the Mn oxides. SEM study of a water-settled separate suggested that the smectite is coated by the Mn oxides. Energy dispersive spectra of Ce-enriched regions shows that they are enriched Zr and V, in addition to Ce and P. XRD analysis of the separate showed the Mn-oxide mineral rancieite $[(\text{Ca},\text{Mn})\text{Mn}_4\text{O}_9 \cdot 3\text{H}_2\text{O}]$, but the Ce-phosphate mineral could not be identified by XRD, perhaps due to its low concentration. Local enrichment of Mn, Ce, Zr and V may be due to their immobility during alteration from a vitric quartz-latite ash to bentonite, and these concentrations in trace phases will likely dominate the trace-element geochemistry of the bentonite. The process responsible for local enrichment of Mn remains unclear but may have involved oxidation of Mn.

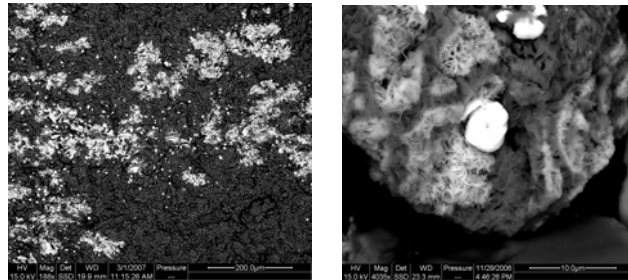


Figure 1. Back-scattered electron image of a) dendritic morphology of back spots; b) spherical Ce-phosphate embedded in Mn oxides

Kiersch, G.A. and Keller, W.D. (1955) Bleaching clay deposits, Sanders-Defiance Plateau District, Navajo Country, Arizona. *Economic Geology*, **50**, 469-494.

Sloane, R.L. and Guilbert, J.M. (1967) Electron-Optical Study of Alteration to Smectite in the Cheto Clay Deposit. *Clays and Clay Minerals*, **15**, 35-44.

Kogel, J.E. and Lewis, S.A. (2001) Baseline studies of The Clay Minerals Society Source Clays: Chemical analysis by ICP-MS. *Clays and Clay Minerals*, **49**, 387-392.

ORIENTED SMECTITE DEPOSITS AS MODEL SHALES

Mokhtar Zabat and Henri Van Damme

Ecole Supérieure de Physique et Chimie Industrielles – PPMD, ESPCI-UPMC-CNRS, 10 rue Vauquelin, 75231 Paris cedex 05, France; Henri.vandamme@espci.fr

Thin oriented smectite deposits (or films) intercalated or interstratified with polyelectrolytes have recently attracted attention as possible nanocomposite model materials for artificial nacre. The main property looked for is a high fracture energy. On the other hand, neat (polymer-free) oriented smectite deposits may also be considered as good models for shale rocks. In this respect, their mechanical and transport properties are important for the tightness of gas (including carbon dioxide) reservoirs. So far, little attention has been paid to the influence of the interlayer cations on the mechanical properties of smectite deposits. In the present work, we investigated the mechanical and textural properties of self-supported and oriented homoionic montmorillonite films, casted by evaporation or by filtration from ion-exchanged colloidal suspensions. Eight different interlayer cations were studied: Li, Na, Mg, Ca, Ba, Al, La and Cs. The mechanical properties (modulus, ultimate strength, ultimate strain, strain hardening, creep, visco-plastic effects) of the films were investigated in pure tensile loading and compared to Monte-Carlo simulations of the cohesion forces between individual montmorillonite platelets. The texture of the deposits was characterized by XRD, atomic force microscopy and optical microscopy. The deformation mechanism was investigated by monitoring and analyzing the textural changes during strain.

The main result is that the macroscopic strength, modulus and ultimate strain are anti-correlated to the strength of the interlayer cohesion within the “quasi-crystalline” aggregates. Rather, the macroscopic properties are controlled by defects between the “quasi-crystals”. The strongest and most deformable samples, and also the less permeable, are those in which the platelets form thin and highly deformable aggregates (Na, Li) in an entangled arrangement akin to the structure of polymer melts. Conversely, the weakest samples are those in which the individual platelets form the thickest and most rigid aggregates.

Finally, an attempt will be made to reconcile this picture with the nano-granular mechanical behaviour of shales, as recently evidenced by nanoindentation (Bobko and Ulm, 2007).

AN INTEGRATED PROCESS USING WYOMING ZEOLITE FOR TREATING SALINE-SODIC WATERS PRODUCED FROM COALBED NATURAL GAS OPERATIONS

Hongting Zhao¹, George F. Vance¹, Mike A. Urynowicz², Girisha K. Ganjegunte³ and Robert W. Gregory⁴

¹Department of Renewable Resources, 1000 E. University Ave., University of Wyoming, Laramie, WY 82071, USA; hzhao@uwyo.edu

²Department of Civil & Architectural Engineering, 1000 E. University Avenue, University of Wyoming, Laramie, WY 82071, USA

³Department of Soil and Crop Sciences, Texas Agricultural Experiment Station, Agricultural Research & Extension Center, Texas A&M University System, 1380 A&M Circle, El Paso, TX 79927, USA

⁴Wyoming State Geological Survey, P.O. Box 1347, Laramie, WY 82073, USA

Fast development of the coalbed natural gas (CBNG) industry in many parts of the western U.S., including the Powder River Basin in Wyoming and Montana, has resulted in the co-production of potentially saline-sodic waters, hereafter referred to as CBNG water. Management of CBNG water is a major environmental challenge because of its quantity and quality. In this study, the potential utilization of natural zeolites was examined for removal of sodium (Na^+) from CBNG waters. Zeolite samples studied included a natural Na-rich zeolite from Wyoming as well as naturally Ca-rich zeolites from New Mexico and Idaho. Surrogate CBNG water that simulated the water chemistry of CBNG waters was used. Wyoming zeolite was pretreated in 0.1 M CaCl_2 solution and converted to a Ca-rich zeolite before use. Column studies indicated that one metric tonne (1000 kg) of the Ca-Wyoming zeolite can treat $\sim 1.2 \times 10^5$ L ($\sim 3.2 \times 10^4$ gallons) CBNG water to reduce its sodium adsorption ratio (SAR, $\text{mmol}^{1/2} \text{L}^{-1/2}$) from 30 to an acceptable level of 10. Compared to results of the other zeolites ($\sim 1.6 \times 10^4$ and 6.0×10^4 L, respectively), it is suggested that water treatment with locally available Wyoming zeolite appears to be more effective and may be a promising and feasible treatment technology for maximizing the beneficial use of poor-quality CBNG in the Powder River Basin, Wyoming. Ongoing studies are evaluating water treatment techniques involving the direct application of zeolite to CBNG waters and development of a field scale prototype.

RHEOLOGY OF THE SONICATION-INDUCED SOL-GEL TRANSITION OF STEAM-TREATED DODIUM SMECTITE

Liming Zhu and David L. Bish

Department of Geological Sciences, Indiana University, 1001 East 10th Street, Bloomington, IN 47405, USA; limzhu@indiana.edu

Sol-gel transitions have been studied to deduce the nature of particle-particle and particle-water interactions in the smectite-water system. Past studies focused on the gel-to-sol transitions induced by variables such as ionic strength, pH, and solid volume fraction. As a result, the transitions are usually interpreted as the net result of multiple variables, complicating our understanding of underlying mechanisms. In this study, different degrees of ultrasonication were applied as the only variable to control the sol-gel transition in a smectite sol, and we measured rheological properties through the sol-to-gel transition. Complex (G^*), storage (G'), and loss (G'') moduli as well as yield stress (σ_y) were used to evaluate the sol-gel transition and the strengths of gels. Flow viscosity (η) was determined to evaluate the behaviors of sols. The sol was obtained from a 7.8 wt % suspension of the $<6\text{-}\mu\text{m}$ fraction of steam-treated SWy-1. Steam treatment was accomplished by reacting 4.84g of SWy-1 with 0.34g of deionized water in a Parr reaction vessel at 250°C for 8 days. Ultrasonication at 20 kHz was applied at 58 watts for 10s, 30s, 60s, and 90s, at 14 watts for 5s, and at 10 watts for an equivalent of 1.1s. The viscoelastic behavior of the gels and the flow properties of sols were studied by stress and frequency sweeps and viscometry, respectively, using an ATS Rheologica parallel-plate system with a 0.2-mm gap at 24°C. Results of stress sweeps of 0.1-100Pa at 1Hz showed that a typical gel began to form after 10s of 58-watt sonication. Specifically, the 10s gel had a G' value of 10 Pa in the linear viscoelastic region (LVR) and a σ_y of 2.2 Pa. The 30s, 60s, and 90s gels had G' values of 222 Pa, 377 Pa, and 692 Pa and σ_y values of 7 Pa, 19 Pa, and 30 Pa, respectively. The presence of higher G' and σ_y values as a function of sonication time indicated that gel strength increased with sonication. In addition, the yield behavior of the 10s gel was more gradual than the other gels, indicating the existence of different microstructures for the weaker gel (i.e., 10s gel) vs. the stronger gels (i.e., 30s, 60s, and 90s gels). Instead of forming a typical gel, the 5s suspension exhibited transitional behavior, with the presence of only the LVR and the lack of a well-defined σ_y . Frequency sweeps were applied to evaluate further the transitional nature of the 5s suspension as well as to characterize thoroughly the other suspensions. All gels showed considerably larger G' than G'' values with increasing differences between G' and G'' in the stronger gels. G^* values also increased with gel strength. The 5s suspension had more characteristics of a gel than a floc, with $G' > G''$ and a clear separation between them. Both stress and frequency sweeps indicated that the 1.1s suspension was similar to the original sol, with the absence of the LVR and σ_y values and comparable G' and G'' values that contributed to a very low G^* . Further viscometry study showed that the two were indistinguishable in terms of η . These rheological studies showed that steam treatment led to the formation of a smectite sol, and a detectable sol-to-gel transition was achieved by sonication. This transition was unidirectional with stronger gels forming after higher degrees of sonication.

Author Index

A

Aagaard, P., 30, 76
Adame, D., 24, 39
Adler, P. M., 24, 40
Akdeniz, Y., 36, 41
Akob, D. M., 25, 42
Allen, B. L., 28, 147
Alles, S., 31, 154
Amblès, A., 26, 138
Anastácio, A. S., 25, 42
Aparicio, P., 36, 43
Aplin, A. C., 30, 75
Arnold, D. E., 29, 44
Arnórsson, S., 34, 92
Aronson, J. L., 26, 127
Asgar-Deen, M., 26, 127
Atalan, G. S., 34, 45, 128
Austin, G. S., 29, 55
Austin, J. C., 23, 46
Ayonghe, S. N., 28, 130

B

Banaś, M., 33, 79
Barker, W. W., 30, 161
Bathija, A. P., 24, 47
Bauer, A., 25, 48
Baugh, K. M., 31, 49
Beall, G. W., 24, 39, 140
Belviso, C., 32, 50
Bender Koch, C., 28, 112
Berbeglia, J., 31, 32, 159, 160
Berger, J. N., 25, 51
Bergström, S. M., 33, 100
Bhattacharyya, S., 36, 84
Bian, J., 26, 117
Bibring, J. P., 34, 53
Bird, D. K., 34, 92
Bish, D. L., 30, 32, 34, 52, 165, 172, 175
Bishop, J. L., 29, 34, 53, 87
Blinman, E., 29, 54, 55
Bloch, J. D., 35, 56
Blum, A., 36, 57
Bobos, I., 28, 58
Boccaccini, A. R., 28, 64
Bonch-Osmolovskaya, E., 35, 149
Bourg, A. C. M., 27, 59
Bourg, I. C., 27, 59
Bowers, G. M., 29, 30, 37, 60, 61, 105
Bowman, R. S., 32, 36, 62, 152, 167
Boyd, S. A., 30, 142
Brady, P. V., 25, 145
Bristow, T. F., 26, 33, 63, 78
Brito, S., 24, 108

Brophy, J. G., 29, 150
Brown, A. J., 34, 53
Brown, A. P., 30, 75
Burgess, E., 35, 149
Busch, A., 31, 154

C

Calabria A., 28, 64
Carey, J. W., 23, 26, 34, 52, 65, 66, 69, 170
Carruyo, G., 24, 125
Cashion, J. D., 35, 93
Caulfield, J. A., 25, 31, 123, 124
Cavalcante, F., 32, 50
Cervini-Silva, J., 23, 24, 31, 67, 72, 99
Chang, Y. N., 31, 155
Chen, J., 28, 171
Chen, T., 28, 171
Chenu, C., 26, 138
Chipera, S. J., 26, 28, 34, 52, 65, 68, 69, 170
Choi, S., 27, 132
Chorover, J., 27, 132
Christidis, G. E., 29, 150
Chung, K. S., 30, 31, 70, 155
Ciminelli, V. S. T., 36, 97
Clark, R. N., 34, 53
Colman, A., 35, 149
Constan, C. I., 29, 71
Cornejo Garrido, H., 23, 72
Cox, J., 23, 46
Criscenti, L. J., 34, 37, 73, 131
Crosta, S., 31, 32, 159, 160
Crowe, D., 35, 148, 149
Cygan, R. T., 34, 37, 119, 131

D

Daemen, L. L., 34, 131
Davis, M. C., 29, 60
Day-Stirrat, R. J., 30, 31, 74, 75
Declercq, J., 30, 76
Deng, Y., 33, 77
Derkowski, A., 26, 33, 63, 78, 79
Destaillets, H., 24, 67
Detellier, C., 24, 120
Diacò, T., 24, 120
Díaz, M. E., 31, 157
Dietiker, M., 22, 139
Dikmen, S., 36, 80
Dikmen, Z., 36, 81
Dipple, G. M., 23, 82
Dixon, J. B., 23, 106
Dogan, A. U., 36, 83
Dogan, M., 36, 83
Dohrmann, J. R., 24, 108
Donahoe, R. J., 36, 84

Donahue, K., 35, 85
Dong, H., 25, 102, 110
Drits, V. A., 23, 113
Droser, M., 23, 109
Drummy, L. F., 22, 86
Dunbar, N., 35, 56, 85
Dyar, M. D., 29, 34, 53, 87
Dypvik, H., 30, 76

E

Eberl, D. D., 25, 33, 36, 57, 88, 110
Ehlmann, B. L., 34, 53
Elsass, F., 28, 137
Elswick, E. R., 29, 151

F

Farmer, B. L., 37, 98
Fernández, P., 23, 72
Fernández-Lomelin, P., 31, 99
Ferrell, R. E., 23, 89
Fialips, C., 34, 52
Fiehn, B., 25, 48
Finger, K. L., 29, 150
Fiore, S., 32, 50
Fiser, J., 35, 149
Fishman, N., 36, 57
Fittipaldo, M., 26, 170
Fowler, M., 26, 127
Frantzen, A. S., 30, 31, 36, 49, 90, 91
Franus, W., 33, 79
Fridriksson, T., 34, 92

G

Galán, E., 36, 43
Gallegos, E., 31, 159
Ganjegunte, G. K., 32, 174
Gates, W. P., 26, 35, 93, 164
Ghalavand, A., 31, 94
Gholamhoseini, M., 31, 94
Giannelis, E. P., 22, 95
Giese, R. F., 25, 116
Giffaut, E., 37, 144
González, E., 24, 125
Görtzen, A., 25, 48
Graham, E. Y., 36, 84
Grasset, L., 26, 138
Greathouse, J. A., 37, 119
Greenhalgh, B. R., 26, 117
Gregory, R. W., 32, 174
Grover, K., 25, 115
Gubulin, J. C., 31, 156
Guggenheim, S., 31, 35, 96, 146
Guimarães, A. M. F., 36, 97
Guthrie, Jr., G. D., 23, 66
Guzmán, J., 23, 72

H

Hartl, M. A., 34, 131
Heald, S., 25, 102
Heinz, H., 37, 98
Heizler, L. L., 35, 56
Hernández-Pineda, J., 31, 99
Hervig, R. L., 33, 169
Hill, R., 36, 57
Hillier, S., 26, 127
Hodges, M., 35, 149
Hollingsworth, E., 35, 149
Hooper, R. L., 35, 143
Hudnall, W. H., 23, 28, 103, 147
Huertas, F. J., 25, 145
Huff, W. D., 33, 100, 169
Hugget, J., 35, 101
Hwang, K. K., 30, 70

J

Jahren, J., 30, 76
Jaisi, D. P., 25, 102
Jamshidi, E., 31, 94
Jaynes, W. F., 23, 103
Ji, J., 28, 171
Joeckel, R. M., 30, 129
Johnston, C. T., 24, 30, 104, 141, 142
Jones, S. E., 22, 86
Junaid, A. S. M., 26, 117

K

Kalinichev, A. G., 37, 105, 111
Kannewischer, I., 23, 106
Karpov, G., 35, 149
Kaszuba, J. P., 26, 65, 69, 107, 170
Katz, L. E., 36, 62
Kaufhold, S., 24, 108
Kazan, O., 36, 135
Kennedy, M. J., 23, 26, 33, 63, 78, 109
Kibanova, D., 24, 67
Kienzler, B., 25, 48
Kil, D. S., 30, 31, 70, 155
Kim, J., 25, 110
Kinaci, G., 36, 135
Kinney, K. A., 36, 62
Kirkpatrick, R. J., 30, 37, 61, 105, 111
Kliem, B. K., 28, 112
Koenig, A., 26, 117
Kogure, T., 23, 113
Kohler, E., 26, 29, 114, 136
Komarneni, S., 25, 29, 60, 115
Koster van Groos, A. F., 35, 96
Kostka, J. E., 25, 42
Krooss, B. M., 31, 154
Kubicki, J. D., 37, 168
Kublanov, I., 35, 149
Kulshrestha, P., 25, 116
Kumar, P., 37, 111
Kurtev, K. D., 30, 75

Kuznicki, S. M., 26, 117
Kyle, J., 35, 149

L

Landais, P., 25, 118
Larentzos, J. P., 37, 73, 119
Latorre, C., 31, 32, 158, 159, 160
Leal, P. R., 31, 32, 158, 160
Lee, H., 30, 70
Lee, S., 31, 155
Letaief, S., 24, 120
Lett, M. C., 25, 51
Li, H., 30, 142
Li, Q., 37, 111
Liang, H., 24, 47
Liewig, N., 28, 137
Lok, J., 24, 104
López-Santiago, N. R., 31, 99
Loucks, R. G., 31, 74
Lu, H., 28, 171
Lu, N., 24, 47
Lucas, S. G., 33, 121

M

Malikova, N., 37, 144
Mamba, B., 34, 126
Marquardt, C., 25, 48
Marry, V., 37, 144
Martínez Dopico, C. I., 31, 159
Maurice, P. A., 25, 122
Mayer, L., 23, 109
McCaffrey, W. C., 26, 117
McDonald, E., 33, 77
McLemore, V., 35, 85
Meyer, E. E., 26, 127
Michel, A., 29, 114
Mikula, R. J., 23, 134
Miller, K. E., 25, 31, 123, 124
Milliken, K. L., 31, 74
Milliken, R. E., 34, 53
Mills, G., 35, 149
Misaelides, P., 32, 167
Moore, D. M., 29, 54
Morán, C., 24, 125
Moro, D., 36, 43
Moronta, A., 24, 125
Mueller, K. T., 27, 29, 37, 60, 132, 168
Mulaba-Bafubandi, A. F., 34, 126
Mundil, R., 33, 100
Murchie, S. L., 34, 53
Murray, H. H., 29, 150, 151
Mustard, J. F., 34, 53

N

Nadeau, P., 26, 127
Naik, R. R., 22, 37, 86, 98
Neal, A., 35, 149
Nenoff, T. M., 34, 131

Neuhoff, P. S., 34, 45, 92, 128, 166
Nicklen, B. L., 30, 129
Ntasin, E. B., 28, 130

O

O'Day, P. A., 27, 132
Ockwig, N. W., 34, 131
Okada, A., 22, 133
Omotoso, O., 23, 134
Orhun, O., 36, 81, 135

P

Pachter, R., 37, 98
Parra, T., 26, 29, 136
Patti, A. F., 26, 164
Pelkey, S. M., 34, 53
Perdrial, N., 25, 28, 51, 137
Pérez, A. I., 31, 157
Pevear, D., 23, 109
Pimenov, N., 35, 149
Plante, A. F., 26, 138
Plötze, M., 22, 139
Powell, C. E., 24, 140
Power, I. M., 23, 82
Prasad, M., 24, 47
Premachandra, G. S., 24, 30, 104, 141, 142
Puzrin, A., 22, 139

R

Rana, K., 30, 142
Ranst, E. V., 28, 130
Raudsepp, M., 23, 82
Ravella, R., 29, 60
Reinholdt, M. X., 37, 111
Riediger, C., 26, 127
Righi, D., 26, 138
Robb, F., 35, 149
Romanek, C., 35, 148, 149
Römer, J., 25, 48
Rosenberg, P. E., 35, 143
Rotenberg, B., 37, 144
Rozalen, M. L., 25, 145
Rule, A. C., 31, 146
Russell, D., 28, 147

S

Sánchez, J., 24, 125
Schaefer, M. W., 29, 87
Schoonheydt, R. A., 24, 104
Schroeder, P. A., 22, 23, 35, 46, 148, 149
Scott, J. L., 26, 164
Sedov, S., 23, 72
Shriner, C. M., 29, 150, 151
Simpson, J. A., 32, 152
Skiba, M., 27, 153
Sklute, E. C., 29, 87
Slepova, T., 35, 149

Smith, D. B., 33, 88

Soko, L. T., 34, 126

Sokolova, T., 35, 149

Solano, R., 24, 125

Southam, G., 23, 82

Spencer, E., 35, 149

Spilde, M., 35, 56

Spolenak, R., 22, 139

Sposito, G., 27, 59

Środon, J., 33, 79, 169

Stanjek, H., 31, 154

Stucki, J. W., 25, 42

Suh, E. C., 28, 130

Suh, Y. J., 30, 31, 70, 155

Sullivan, E. J., 36, 62

Swayne, G., 34, 53

T

Techtmann, S., 35, 149

Tenorio Arvide, M. G., 23, 106

Teppen, B. J., 30, 142

Thom, J. M., 23, 82

Timm, H. L., 29, 151

Tonui, E. K., 34, 163

Toprak, F. O., 33, 100

Torres, J. C., 31, 156, 157

Trejo, M., 24, 67

Turq, P., 37, 144

U

Ülkü, S., 36, 41

Upamanyu, M., 24, 47

Urynowicz, M. A., 32, 174

Usuki, A., 22, 133

V

Vaia, R. A., 22, 37, 86, 98

Valdrè, G., 36, 43

Van Damme, H., 24, 173

van der Pluijm, B. E., 31, 74

Vance, G. F., 32, 174

Vaniman, D. T., 28, 34, 52, 68

Vasconcelos, W. L., 28, 36, 64, 97

Vattuone, M. E., 31, 32, 158, 159, 160

Velbel, M. A., 30, 34, 161, 162, 163

Vertlib, V., 22, 139

Vuilleumier, R., 37, 144

W

Wagner, I., 35, 149

Wallis, P. J., 26, 164

Wang, H. W., 32, 165

Wang, J., 34, 128, 166

Wang, X., 28, 171

Warchał, J. K., 32, 167

Warr, L. N., 25, 51

Washton, N. A., 37, 168

Wells, T. A., 31, 124

White, G. N., 23, 106

Wiegel, J., 35, 149

Wigand, M., 26, 69, 107, 170

Williams, L. B., 33, 169

Wilson, S. A., 23, 82

Wittman, N., 35, 149

WoldeGabriel, G., 26, 69, 170

Wood, T. D., 25, 116

X

Xie, Q., 28, 171

Xu, H., 28, 171

Y

Yörükogulları, E., 36, 80

Yuan, H., 30, 172

Z

Zabat, M., 24, 173

Zartman, R. E., 23, 103

Zeisig, A., 24, 108

Zhang, C., 35, 149

Zhang, G., 25, 110

Zhang, J., 25, 115

Zhao, H., 32, 174

Zhao, W., 35, 149

Zhu, L., 30, 175

Ziock, H. J., 23, 66

Zolensky, M. E., 34, 163

45TH ANNUAL MEETING OF THE CLAY MINERALS SOCIETY



WORKSHOP: *Clay Surface Redox Processes and Characterization Techniques*, April 5

TECHNICAL SESSIONS: April 7-9

FIELD TRIP: *New Orleans, Clay, and the Future*, April 10

Joint Meeting with the Geo-chemistry Division of the American Chemical Society · 235th - ACS National Meeting and Exposition

CONTACT: Brenda Ross
bross@cottey.edu

www.cottey.edu/clay



“CLAYS OF DEMETER”
APRIL 5-10, 2008 • NEW ORLEANS, LOUISIANA, USA